# *Schistosoma mansoni* extracellular vesicles:

# immunobiology and vaccine efficacy

Thesis submitted by:

**Desalegn Woldeyohannes Kifle (DVM, MSc)**

College of Public Health, Medical and Veterinary Sciences

Centre for Molecular Therapeutics

Australian Institute of Tropical Health and Medicine

**James Cook University**

**This dissertation is submitted for the degree of Doctor of Philosophy**

**Supervisors:**

Distinguished Professor Alex Loukas

Doctor Javier Sotillo

Doctor Mark Pearson

May 2020

# Statements on the contribution of others

I acknowledge the help of the following individuals and institutions:

| Nature of assistance | Contributions | Name | Affiliation |
|---|---|---|---|
| Intellectual support | Project plan and development | Prof Alex Loukas | James Cook University |
| | | Dr Javier Sotillo | James Cook University |
| | | Dr Mark Pearson | James Cook University |
| | Editorial support | Prof Alex Loukas | James Cook University |
| | | Dr Javier Sotillo | James Cook University |
| | | Dr Mark Pearson | James Cook University |
| | Lab facility support | Prof Alex Loukas | James Cook University |
| Financial support | Research | Prof Alex Loukas | James Cook University |
| | | NHMRC program grant | |
| | Stipend | JCU International Post Graduate Research Scholarship | James Cook University |
| | Conference support | Australian Society of Parasitology | Australian Society of Parasitology |
| | Write up support | College of Public Health, Medical and Veterinary Sciences | James Cook University |
| Technical support | EV internalisation | Dr Thewarach Laha | Khon Kaen University |
| | | Dr Sujjitra Chaiyadet | Khon Kaen University |
| | Mice necropsy | Mr Darren Pickering | James Cook University |
| | | Mr Luke Becker | James Cook University |
| | RNAseq data analysis | Dr Ashley Waardenberg | James Cook University |
| | | Dr Ingrid Wise | James Cook University |

# Acknowledgements

First of all, I would like to offer my deepest gratitude and appreciation to my principal supervisor, Distinguished Prof Alex Loukas, an inspiring scientist, for taking a chance to accept me as his student, supporting my scientific career through the supervision, encouragement and advice he has provided to me despite his busy schedule throughout my PhD study. Thank you for facilitating for me to travel overseas and visit his collaborator's lab in Thailand to undertake experiments which have significantly contributed to the successful completion of this thesis. Without his guidance and leadership, this project would not have been possible.

I also would like to extend my sincere gratitude to my co-supervisors, Dr Javier Sotillo and Dr Mark Pearson for their supervision, technical and scientific support. Thank you for the many constructive and inspiring discussions we have had, and how you helped me to solve all the everyday problems in the lab; without their assistance many of the experiments would not be realized.

I would like to thank all Loukas Lab members especially Luke Becker, Darren Pickering and Ramon Eichenberger for their assistance in the laboratory at different times during the study period. I have learned a lot from them.

I'm so grateful and thankful to James Cook University for the admission to and scholarship opportunities for the PhD Program, the AITHM for the financial support and laboratory resources, Graduate Research School, and my College-PHMVS. I feel privileged.

Special thanks go to Associate Professor Thewarach Laha and Dr Sujjitra Chaiyadet at Khon Kaen University in Thailand for the fruitful collaboration and access to their laboratory space, equipment and expertise in experiments involving *S. mansoni* extracellular vesicle internalisation and blocking assay, without which this work would have been left unfinished. I would also like to thank Drs Ashley Waardenberg, Ingrid Wise and Ms Martha Cooper for assistance with bioinformatics.

Next, I would like to thank Ms Mel Campbell, the Biotech Project Manager for the Loukas Lab at JCU, who facilitated the administrative issues related to my PhD project.

Finally, I would like to thank my loving and caring wife Dagmawit Werha, for always being there and providing me with her unconditional support, she was a constant source of encouragement and reassurance, especially on the toughest days of my PhD study. Thank you for understanding, and the sacrifice you have paid in raising our adorable kids with more love than one could ever imagine a mother can give to her children. My son Elmar, I know you were too young to recognize me as your dad by the time you left for Ethiopia for the better, but for me it was like an irresistible feeling. Moreover, we could not celebrate together the arrival of our little blessing, my daughter Nolawit, I cannot wait to give you a big hug and kiss. They all are so inspirational to me.

# Publications by the candidate relevant to the thesis

1. **Desalegn Woldeyohannes Kifle**, Javier Sotillo, Mark S. Pearson and Alex Loukas. **Extracellular vesicles as a target for the development of anti-helminth vaccines.** *Emerging Topics in Life Sciences,* 2017, (1) 659–665. Incorporated as part of Chapter 1.

2. **Desalegn Woldeyohannes Kifle**, Mark S. Pearson, Luke Becker, Darren Pickering, Alex Loukas, Javier Sotillo. **Proteomic analysis of two populations of *Schistosoma mansoni*-derived extracellular vesicles: 15k pellet and 120k pellet vesicles.** *Molecular and Biochemical Parasitology*, 2020, 236, 111264. Adopted for publication from Chapter 2.

3. **Desalegn Woldeyohannes Kifle**, Sujittra Chaiyadet, Ashley J. Waardenberg, Ingrid Wise, Martha Cooper, Luke Becker, Denise L. Doolan, Thewarach Laha, Javier Sotillo, Mark S. Pearson, Alex Loukas. **Uptake of *Schistosoma mansoni* extracellular vesicles by human endothelial and monocytic cell lines and impact on vascular endothelial cell gene expression.** ''Accepted for publication in *International Journal for Parasitology* on 22 May, 2020.

# Abstract

Schistosomiasis is a chronic disease caused by infection with trematode parasites of the genus *Schistosoma*. Currently, there is no vaccine available to limit the global burden of this disease, and treatment depends on a single drug, praziquantel, which warrants concern about emerging drug resistance and emphasises the need for rigorous research into discovery of new drug targets and vaccine antigens. Various strategies are employed by parasites to manipulate their hosts, one of which is the secretion by parasites of extracellular vesicles (EVs). EVs are membrane-encapsulated vesicles secreted by different types of cells and can be grouped into exosome-like vesicles (ELVs) and microvesicles (MVs). The parasitic blood fluke *Schistosoma mansoni* secretes EVs. However, the sub-vesicular composition of these EV proteins and their roles in molecular host-parasite communication, as well as their vaccine efficacy has not been studied before.

Chapter 2 (first data chapter) of this thesis provides the first comprehensive proteomic analysis of *S. mansoni* EVs – ELVs and MVs. To achieve this, I isolated and purified EVs from *S. mansoni* ES products using an Optiprep iodixanol gradient and fractions containing vesicles were confirmed by tunable resistive pulse sensing using a qNano instrument for both ELVs and MVs. Trypsin shaving as well as sequential extraction techniques were used to obtain samples of integral membrane, peripheral membrane and cargo components for proteomic analysis of *S. mansoni* EVs using quantitative liquid chromatography-tandem mass spectrometry. A total of 286 and 716 proteins were identified in *S. mansoni* ELVs and MVs, respectively. Among the proteins identified were previously described and new potential vaccine candidates. Moreover, proteins of relevance in host-parasite communication were identified from both vesicle types, including proteases, antioxidants, EV biogenesis/trafficking proteins.

The role of *S. mansoni* EVs in host-parasite communication and their impact on host cell gene expression was presented in Chapter 3 of this thesis. Using confocal fluorescence microscopy, I confirmed that *S. mansoni* ELVs and MVs are internalised by Human Umbilical Vein Endothelial Cells (HUVEC) as well as the THP-1 human monocyte cell line, implying roles in host-parasite communication in distinct cell types. To investigate the biological effects of uptake of *S. mansoni* ELVs by HUVEC cells, RNA was extracted and submitted to Next Generation RNA sequencing, and revealed 59 differentially expressed genes (DEGs) compared with control ELVs from untreated HUVEC cells. Of the DEGs, 17 and 42 genes were downregulated and upregulated, respectively. Significantly downregulated genes in HUVEC cells treated with *S. mansoni* ELVs encoded proteins involved in complement and coagulation cascades and glycolysis. DGEs that were upregulated in HUVEC cells treated with *S. mansoni* ELVs encoded proteins involved in inhibition of platelet aggregation and vasodilation, inflammation and immune-regulation, and vascular smooth muscle contraction. String analyses of DEGs revealed numerous axes of interacting genes, notably arachidonic acid metabolism and glycolysis pathways.

Tetraspanins (TSPs) are abundant transmembrane proteins that are diagnostic features of most eukaryotic ELVs. TSPs are known to be efficacious vaccine antigens for schistosomiasis, so I expressed selected *S. mansoni* EV TSP proteins in recombinant form, produced antibodies against them, and used those antibodies to disrupt EV uptake by host cell lines, and therefore EV-mediated parasite-host communication.

Chapter 4 of this thesis explored the vaccine potential of adjuvanted *S. mansoni* MVs in a mouse model of schistosomiasis over two independent trials. In one trial, mice vaccinated with *S. mansoni* MVs showed a modest reduction in the number of eggs in the liver (28%, $P<0.01$) and intestine (35%, $P<0.01$) compared to mice that were immunised with murine fibroblast MVs as a control. Adult worm burden and egg viability, as determined by egg hatching from liver homogenates, were not

significantly decreased. In a second trial, similar trends were observed but the worm and egg burden data did not reach statistical significance. To identify the antigenic targets from EVs, sera collected from mice immunised with *S. mansoni* ELVs and MVs were used to probe a *S. mansoni* protein array consisting of ~1,000 recombinant proteins. Antigens for which the strongest immune responses were detected included proteins that were predicted and/or proven to be located on the tegument membrane, intracellular proteins, and metabolic enzymes that have key roles in parasitism.

Selected *S. mansoni* EV recombinant TSPs – *Sm*-TSP-1, *Sm*-TSP-2, *Sm*-TSP-4, and *Sm*-TSP-1 + *Sm*-TSP-2 + *Sm*-TSP-4 – were assessed for vaccine efficacy over two independent trials in Chapter 5 of this thesis. Anti-TSP IgG antibodies bound and hence recognised their cognate TSPs, particularly *S. mansoni* TSP-2, on the tegument of adult worm sections, implying that their surface accessibility renders schistosomes vulnerable to antibody-mediated killing. Vaccination of mice with *Sm*-TSP-2 and the cocktail of TSPs (including TSP-2) showed a significant reduction in adult worm counts (30-36%, $P<0.01$) and liver egg burdens (26-36%, $P<0.01$, $P<0.05$) in one but not both of the trials. Intestinal egg burdens were significantly decreased (31%, $P<0.05$) in mice vaccinated with the cocktail of TSPs. Egg viability was significantly decreased in mice vaccinated with Sm-TSP-2 and the cocktail of TSPs. There was no significant reduction obtained for any of the parasitological data assessed for mice vaccinated with either *Sm*-TSP-1 or *Sm*-TSP-4.

Altogether, this thesis has provided a comprehensive molecular characterisation of two distinct populations of adult *S. mansoni* EVs. The role of these EVs in host-parasite communication and host cell gene regulation *in vitro* has been assessed in HUVEC cells. Vaccine efficacy of *S. mansoni* EVs and recombinant forms of EV surface proteins was assessed in a mouse model of schistosomiasis, providing a foundation upon which to select key antigenic targets for an ultimate subunit vaccine.

# Table of contents

# List of Figures

# List of Tables

# List of abbreviations

| | |
|---|---|
| °C | Degrees Celsius |
| 2YT | 2X YT (two times yeast and tryptone) |
| ABs | Apoptotic bodies |
| Alum | Aluminium hydroxide |
| ART | Artemether |
| BCA | Bicinchoninic acid |
| BLAST | Basic local alignment search tool |
| BSA | Bovine serum albumin |
| CAA | Circulating anodic antigen |
| CCA | Circulating cathodic antigen |
| cDNA | Complementary Deoxyrobonucleic acid |
| $CO_2$ | Carbon dioxide |
| DALYs | Disability adjusted life years |
| DGE | Differential gene expression |
| DNA | Deoxyribonucleic acid |
| EDTA | Ethylenediaminetetraacetic acid |
| ELISA | Enzyme linked immunosorbent assay |
| ELVs | Exosome-like vesicles |
| EPG | Egg per gram |
| ES | Excretory-secretory |
| ESCRT | Endosomal sorting complex responsible for transport |
| EVs | Extracellular vesicles |
| *g* | Relative centrifugal force |

| | |
|---|---|
| g | Gram |
| GO | Gene onthology |
| GST | Glutathione S-transferase |
| HPR | Horseradish peroxidase |
| HSP | Heat shock protein |
| HUVEC | Human umbilical vein endothelial cells |
| IFN | Interferon |
| IgA | Immunoglobulin class A |
| IgE | Immunoglobulin class E |
| IgG | Immunoglobulin class G |
| IgM | Immunoglobulin class M |
| IL | Interleukin |
| ILVs | Intraluminal vesicles |
| IMPs | Integral membrane proteins |
| IPTG | Isopropyl β-D-1-thiogalactopyranoside |
| kDa | Kilodalton |
| L | Litre |
| LC-MS/MS | liquid chromatography-tandem mass spectrometry |
| LEL | Large extracellular loop |
| m | Milli |
| M | Molar |
| MDA | Mass drug administration |
| MHC | Major histocompatibility complex |
| miRNA | Micro ribonucleic acid |

| | |
|---|---|
| mRNA | Messenger RNA |
| MVs | Microvesicles |
| MVBs | Multivesicular bodies |
| MVE | Multivesicular endosome |
| n | Nano |
| NCBI | National Centre for Biotechnology Information |
| OD | Optical density |
| ORF | Open reading frame |
| PAGE | Polyacrylamide gel electrophoresis |
| PBS | Phosphate buffered saline |
| PBST | phosphate buffered saline with 0.05% Tween 20 |
| PCR | Polymerase chain reaction |
| pH | Power of hydrogen |
| PM | Plasma membrane |
| PMP | Peripheral membrane protein |
| POC | Point-of care |
| PZQ | Praziquantel |
| RA | Radiation-attenuated |
| RDT | Rapid diagnostic test |
| RNA | Ribonucleic acid |
| RNAi | RNA interference |
| rpm | Revolution per minute |
| RT | Room temperature |
| SD | Standard deviation |

| | |
|---|---|
| SDS | Sodium dodecyl sulphate |
| SEM | Standard error of the mean |
| TBST | Tris-buffered saline with 0.05% Tween |
| TGF | Transforming growth factor |
| Th1 | T helper type 1 |
| Th2 | T helper type 2 |
| TLPs | Trypsin liberated proteins |
| TNF | Tumour necrosis factor |
| tRNA | Transfer RNA |
| TRPS | Tunable resistive pulse sensing |
| TRX | Thioredoxin |
| TSP | Tetraspanin |
| WHO | World Health Organization |
| µ | Micro |

# Chapter 1

# Introduction and Literature review

## 1.1. Introduction

### 1.1.1. Schistosomiasis

Schistosomiasis is a common neglected disease caused by blood fluke parasites of the genus *Schistosoma.* Nearly 190 million people are infected in developing countries in the tropics and sub-tropics, with more than 70 million new infections (GBD 2016 DALYs and HALE Collaborators, 2017), and nearly 300,000 deaths every year (Colley et al., 2014). Most infected and vulnerable individuals are found in sub-Saharan Africa, and close to 800 million people are at risk (Utzinger et al., 2009, Cai et al., 2016). Based on the 2016 Global Burden of Disease Study, the global burden of schistosomiasis is estimated to be 1.9 million disability-adjusted life years (GBD 2016 DALYs and HALE Collaborators, 2017). Three main species of schistosomes infect human beings: *Schistosoma mansoni*, *Schistosoma haematobium* and *Schistosoma japonicum*. *S. mansoni* and *S. haematobium* both occur in Africa and the Middle East; *S. mansoni* is also present in the Americas. *S. japonicum* is localised to Asia, primarily the Philippines and China. *S. mansoni* is responsible for one-third of schistosomiasis infections globally (van der Werf et al., 2003). *Schistosoma* species have complex life-cycles involving infection of a freshwater snail intermediate host in which they multiply asexually as well as a definitive vertebrate host where adult male and female worms grow and sexually reproduce (McManus et al., 2018). The *S. mansoni* and *S. japonicum* egg stages are excreted from the host within faecal material (or urine in the case of *S. haematobium*) whereupon the eggs hatch to release free swimming miracidia that infect snails. Eggs trapped in the vasculature of the liver, intestines or bladder, depending on the species, cause the majority of disease-associated clinical signs and

pathology (McManus and Loukas, 2008). Because of the suite of immune-evasion pathways utilized by the adult flukes, they can live for up to 10 years in the portal blood vessels of the mesenteric plexus (Collins et al., 2013). The unique tegumental bilayer of the outer surface of the parasite is endowed with a population of stem cells, undergoes frequent regeneration and turnover, and is instrumental in immune escape pathways by making *S. mansoni* surface proteins inaccessible to host immune cells (Collins et al., 2016).

Research in schistosomiasis has contributed substantially to better understand the mechanisms of parasitism (Zhu et al., 2014, Driguez et al., 2016a). In studies carried out to assess the molecular basis of host-parasite interactions, the identification of schistosome tegument proteins has been targeted for the development of new diagnostics and their potential as vaccine candidates (Wilson, 2012). Schistosome antigen discovery for vaccine development has been assisted by major advances in molecular biology, specifically the sequencing of the genomes, the tegument proteomes and the transcriptomes of different schistosome species (Sotillo et al., 2019b). The availability of this information, together with improving post-genomic tools has the potential to reveal many new vaccine candidate antigens (Sotillo et al., 2016a). The most relevant targets are the excretory-secretory (ES) products as well as molecules on the surface of the worm. These are the molecules that directly interact with the host immune system (Hotez et al., 2010).

In addition to secreting soluble proteins, schistosomes secrete extracellular vesicles (EVs). EVs are membrane-encapsulated vesicles that can be grouped into exosomes and microvesicles (MVs) based on their size and cargo content such as protein and RNA (Meldolesi, 2018). Parasite EVs can play roles in host-parasite and parasite-parasite communication, and have also been implicated in pathogenesis of helminth infections, such as the carcinogenic liver fluke *Opisthorchis viverrini* (Chaiyadet et al., 2015a). Furthermore, EVs from the parasitic nematode *Heligmosomoides polygyrus* suppress inflammation by downregulating T helper type 2 (Th2) immune responses in

mice. *H. polygyrus* EVs contain micro-RNAs (miRNAs) that regulate inflammation (Buck et al., 2014), suggesting a mechanism by which these vesicles exert their immunomodulatory properties and highlighting their potential as diagnostic tools and therapeutic agents. In this thesis, I focus on presenting the available information based on recent literature about the roles of EVs in schistosomiasis and other helminth infections in communication, gene regulation, immune modulation and pathogenesis, and further highlight their importance as targets for therapeutics and diagnostics.

### 1.1.2. Life-cycle

Adult male and female *S. mansoni* reside and mate in the portal veins of the liver. They migrate to the mesenteric veins draining the large intestine where the female lays fertilized eggs. The eggs are shed into the environment through the faeces. Those eggs that remain trapped in the host tissues elicit an inflammatory response and then die, becoming encapsulated by immune granulomas. Eggs that are released in the faecal stream into freshwater hatch and release ciliated miracidia, a free-living stage that infects a suitable snail intermediate host (*Biomphalaria* species) (Utzinger et al., 2009). Once in the snail the parasite undergoes asexual replication and the infective cercariae leave the snail into the water (Collins et al., 2011). This asexual reproductive cycle in the snail requires 4 to 6 weeks to complete. Cercariae deplete their energy reserves significantly within a few hours of being released from snails (Lawson and Wilson, 1980), but can remain infective for 1-3 days, during which they locate a mammalian host in the water, penetrate the skin and lose their tail to become the schistosomulum stage. Schistosomula reach the circulation, pass through the lung vasculature and finally reach the mesenteric plexus in the portal veins (Figure 1-1). Schistosomula require on average 6 weeks (5–7 weeks) to mature to full adulthood whereupon the dioecious adult flukes pair, copulate and the female releases eggs to continue life cycle (Ross et al., 2002).

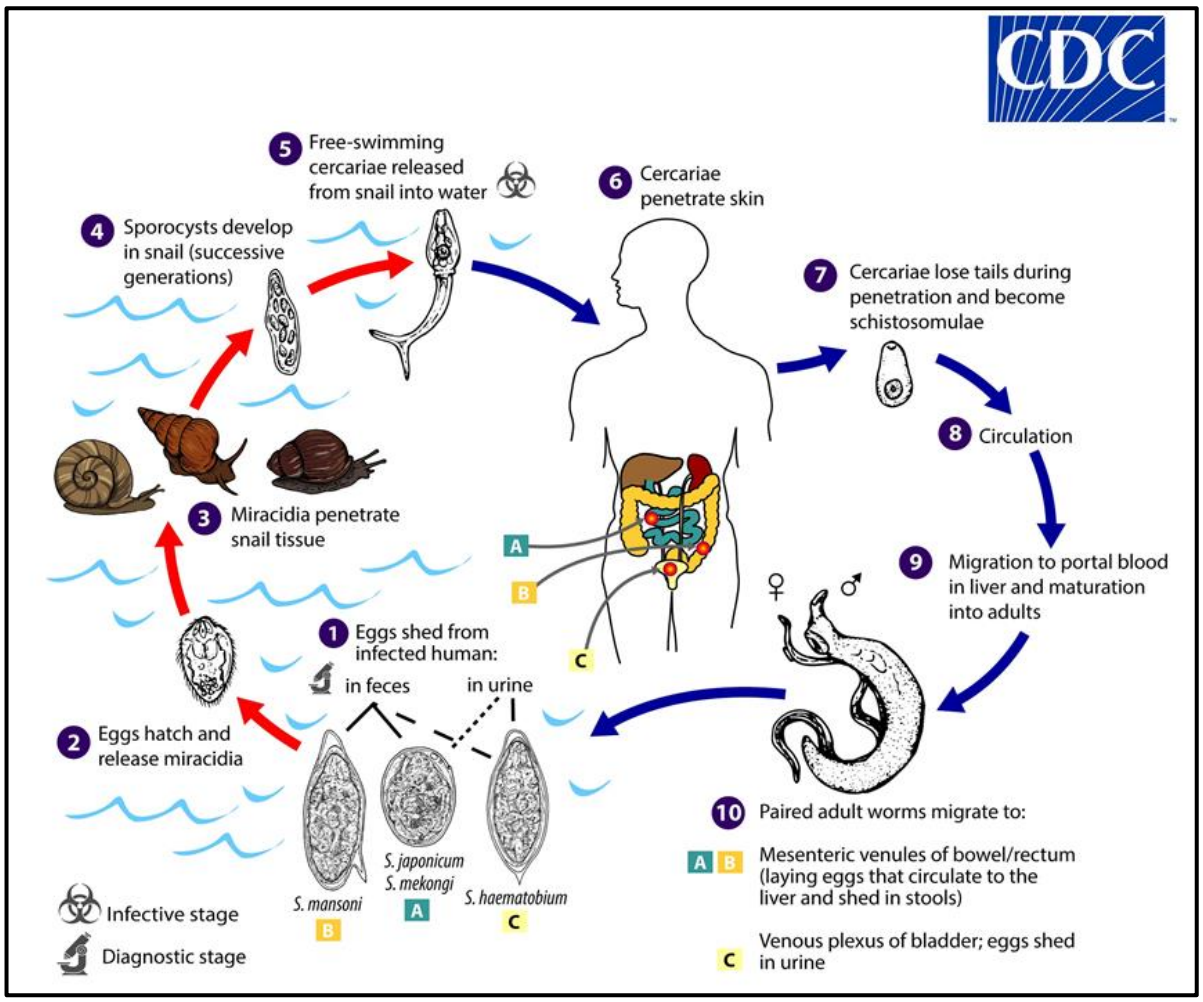


**Figure 1. 1. The life cycle of the schistosome parasite.**

(https://www.cdc.gov/parasites/schistosomiasis/biology.html)

**Steps 1–3:** When individuals infected with *S. mansoni* defaecate in freshwater, parasite eggs are shed in the faecal stream. The eggs hatch and infect freshwater snails (*Biomphalaria* spp.). The parasites then develop and replicate asexually within the snails. **Steps 4–5:** The cercarial stage of the parasite emerges from the infected snails into freshwater, where they can live for up to two days. **Step 6:** Upon contacting a mammalian host, cercariae infect individuals through skin penetration. **Steps 7–10:** In the body, the larvae get access to the circulatory system and ultimately reach the portal blood vessels (mesenteric plexus) where they develop into adult male and female parasites which then pair, mate, and remain coupled for up to seven years. Female parasites release hundreds of eggs daily, some of which are excreted in the faeces whereas others are retained in the

tissues and cause the granulomatous reactions that drive the pathology associated with schistosomiasis.

### 1.1.3. Epidemiology

Schistosomiasis, affecting > 200 million people worldwide (Colley et al., 2014), particularly in developing and tropical regions, is one of the most important parasitic diseases. The eggs of *S. mansoni* and *S. japonicum* when trapped in the portal system elicit hepatosplenic inflammation and liver fibrosis (Gryseels et al., 2006). Eggs of *S. haematobium* can promote bladder cancer in chronically infected individuals (Mayer and Fried, 2007). In Africa and the Middle East both *S. haematobium* and *S. mansoni* occur, whereas only *S. mansoni* exists in the Americas. Primarily located in the Philippines and China, *S. japonicum* is localised throughout Asia (Figure 1.2). The distribution of each species of schistosome depends on the existence of a specific suitable snail host. Aquatic freshwater *Biomphalaria* and *Bulinus* snails serve as intermediate hosts for *S. mansoni* and *S. haematobium*, respectively, and *Oncomelania,* which is an amphibious freshwater snail, serves as an intermediate host for *S. japonicum.*

Several physical and biological factors influence the distribution of the snails. Temperature - affecting the development of larval snails, their growth and rate of transmission - is one of the major determining factors for their distribution and survival (Gryseels et al., 2006, Kalinda et al., 2017). As a result, snail intermediate hosts for *Schistosoma* species are geographically restricted to the relatively warm tropical and subtropical regions, especially in Africa, Asia, Middle East, South America, and the Caribbean; snails do not exist in locations with extreme temperatures, i.e. at high altitudes or in temperate regions (Gryseels et al., 2006, Kalinda et al., 2017).

Despite mass administration of the drug praziquantel to treat schistosomiasis for the last two decades, the infection still causes a loss of 1.9 million DALYs (GBD 2016 DALYs and HALE Collaborators, 2017). The DALYs attributed to schistosomiasis is a conservative estimate as it doesn't

take into consideration the morbidity associated with infections that were conventionally regarded as ‘‘asymptomatic’’ (King, 2015).

Chronic schistosomiasis is the most prevalent form of the disease in endemic areas. In such areas, children can get their first infection as early as two years of age, after which the intensity of infection increases with exposure over the first 10 years (Colley et al., 2014). The occurrence of schistosome infections in infants and young children is being progressively noticed. This situation did not attract due attention in the past, partly because more emphasis is given to treatment of school-aged children, because of the age-related low parasite egg output, and because of the poor sensitivity of standard diagnostic tests that quantify egg burdens microscopically. Infection that occurs in early childhood in endemic regions will likely have a major role the establishment of chronic inflammation due to schistosome eggs trapped in the tissues and the subsequent formation of immune granulomas (Colley et al., 2014, Schwartz and Fallon, 2018).

Furthermore, there is a high prevalence of schistosomiasis in young adolescents, although this prevalence is generally reduced in adulthood (McManus et al., 2018). However, as long as adults have frequent contact with water bodies harbouring cercariae, high prevalence can persist in adults (Colley et al., 2014, McManus et al., 2018). Schistosomiasis sero-surveillance carried out in endemic areas has shown that nearly all long-term residents become infected at least once in their lifetime. In settings with typical transmission trends, 60-80% of school-age children and 20-40% of adults are actively infected (Colley et al., 2014). However, age-associated infection patterns are unpredictable in populations with recent exposure to transmission compared to those in long-standing endemic conditions. Hence, some type of age-associated innate resistance could have a major contribution in the epidemiology of schistosomiasis, as slowly developing adaptive immunity is not relevant in such circumstances (Gryseels et al., 2006).

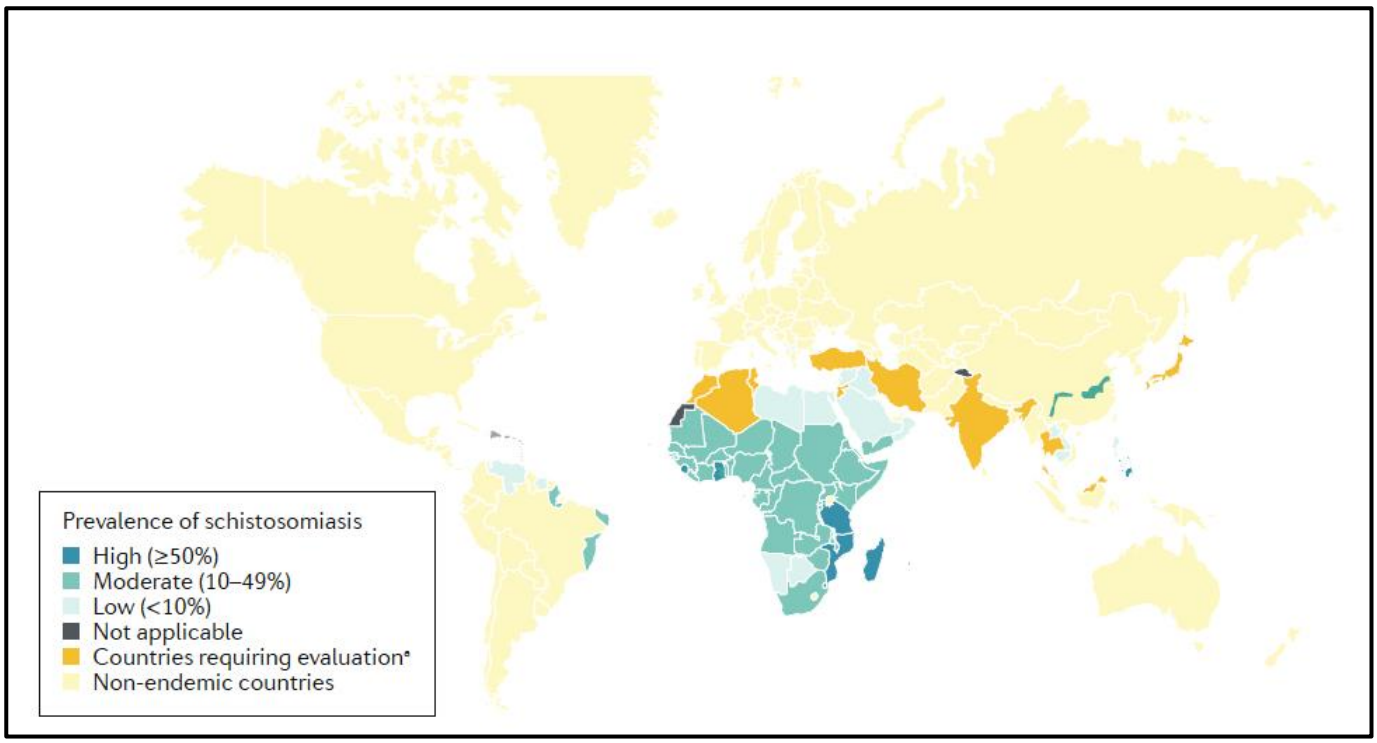


**Figure 1. 2. Worldwide distribution of schistosomiasis** (McManus et al., 2018).

### 1.1.4. Immunopathogenesis

The different life cycle stages of *S. mansoni* express hundreds, if not thousands, of antigenic moieties. Many of these antigens elicit intense and easily detected humoral and cellular immune responses (Gaze et al., 2014). It is well documented from clinical and epidemiological studies that individuals residing in schistosome endemic settings develop some form of acquired immunity after multiple exposures (Gryseels et al., 2006, Schwartz and Fallon, 2018). Regarding immunity developed by mammalian hosts to schistosome infection, innate or acquired immune responses are likely to have an important role in limiting the reproductive capacity of schistosomes (Gryseels et al., 2006, Costain et al., 2018). Because the decrease in infection rates after adolescence can also be explained by reduced water contact, proving the existence of effective (albeit non-sterilizing) acquired immunity in these groups is challenging (Gryseels et al., 2006).

Studies using comparative models of reinfection after curative therapy have demonstrated that children are more susceptible to schistosome infection than adults, and that these discrepancies cannot be explained by water contact patterns (McManus et al., 2018). Findings from studies in humans and livestock suggest that adaptive immunity is mediated by IgE against larval and adult parasite antigens, which in turn generates eosinophil-mediated attack of the larval stage parasites. Blockade of IgE receptors by excess anti-schistosome IgG4 and possibly other immunoglobulin isotypes in the first years of infection is thought to be the cause for the slow development of acquired immunity. Some researchers report the role of schistosome-specific IgA, for example anti-Sm28GST, for the slow release of somatic antigens from dying worms or for mediating protective immunity in people (Capron et al., 2005). The former hypothesis has been used to support the presence of increased immunity after drug therapy; however, these observations need to be further confirmed by additional studies (Mutapi et al., 2013).

Cell mediated immunity is responsible for most schistosomiasis-associated pathology during chronic infection. Most chronic responses in schistosomiasis are not due to the adult worms but to the T cell-dependent immune response of the host, which is directed against schistosome eggs trapped in tissues, mainly in the liver and intestines (McManus and Loukas, 2008, Schwartz and Fallon, 2018).

In general, the immune response to schistosomiasis at early stages of infection in mice shows a predominantly T helper type 1 (Th1) cellular response but shifts to an egg-induced Th2 response as the infection becomes chronic (Alves et al., 2016). The Th1 response is characterised by an increase in proinflammatory cytokines such as interleukin IL-1, IL-12, IFN-γ and TNF-α that further activate macrophages to generate nitric oxide targeting schistosomula and immature adult worms (Pearce, 2002, Wilson et al., 2007, Torben et al., 2012). After the deposition of eggs the immune response switches to a pronounced Th2 response with the formation of granulomatous lesions characterised by high levels of IL-4, IL-5, IL-10, IL-13 and IgE, facilitated by dendritic cells (Pearce,

2002, Ndlovu and Brombacher, 2014), connecting the innate with the adaptive immune response (Colonna et al., 2006). The granulomas formed wall-off the egg and its liberated proteolytic enzymes which otherwise cause tissue necrosis. However, the granuloma formation process induces prolonged chronic inflammation that is responsible for the clinical signs of schistosomiasis (Colley et al., 2014, Fairfax et al., 2012). Moreover, there is evidence from studies in mice indicating that, in addition to Th1 and Th2 immune responses against schistosomiasis, there is a relationship between severe pathology and IL-17-producing CD4+ T helper (Th17) cells (Larkin et al., 2012, Chen et al., 2013a).

Studies conducted on the human immune response to schistosomiasis suggest that acquired anti-schistosome protective immunity after curative drug therapy is mediated by a Th2 immune response and the generation of protective IgE antibodies mounted against larval antigens and adult worms (Gryseels et al., 2006). Indeed, repeated rounds of praziquantel treatment and the ensuing protective immune response observed in some indivduals has been touted by some researchers as a vaccination approach (Mutapi et al., 2013). Another group of subjects called putatively resistant ( PR) individuals are constantly exposed to schistosomes but never get infected and have not been treated with praziquantel (Viana et al., 1994). This group is thought to mount a protective response aimed at the schistosomula stage of the parasite and is characterised by both Th1 cytokines such as IFN-γ as well as Th2 responses typified by IgE against schistosomula tegument antigens (Viana et al., 1995). Moreover, levels of IgG4 against soluble worm antigen preparation, soluble egg antigen and Sm 22.6 were higher in susceptible subjects compared with PR subjects (Oliveira et al., 2012).

In the long term, schistosomiasis usually progresses to the chronic intestinal form because immune responses to the granulomatous tissue are suppressed by several mechanisms. The occurrence of clinical signs is usually linked to the intensity of infection but often the intestinal form of the disease

manifests as non-specific recurrent abdominal ache and diarrhoea with rectal bleeding (Mohamed AR et al., 1990, McManus et al., 2018). Symptoms like these are usually not systemic in nature, but rather characterized by isolated polyposis, pseudopolyposis and mucosal hyperplasia interspersed with apparently normal intestinal tissue (Cao et al., 2010). Some individuals infected with *S. mansoni* present with massive fibrosis followed by hepatosplenic syndrome with periportal fibrosis, mainly due to their poor regulatory responses to parasite egg antigens (Colley et al., 1986, McManus et al., 2018). Clinical signs include upper quadrant abdominal distress with enlarged palpable and hard liver and spleen. As a complication of portal hypertension, ascites and haematemesis from oesophageal varices can follow, and frequently result in death (Richter et al., 1998). In patients with chronic hepatic fibrosis, complicated by granulomatous pulmonary arteritis, substantial pulmonary hypertension can occur (Lambertucci et al., 2000, McManus et al., 2018). It usually takes 5-15 years for advanced fibrosis to occur (Gryseels, 1992); however, it can occur in children as young as 6 years (Doehring-Schwerdtfeger et al., 1990), urging the necessity for examination and treatment of preschool children (Stothard et al., 2011).

Acute schistosomiasis occurs usually in travelers or immigrants to endemic areas that have no previous exposure to schistosome antigens. It follows weeks to months after the first infection, as a result of worm maturation, release of egg antigen, and the host's immune complex responses and granuloma formation. In acute schistosomiasis (sometimes referred to as Katayama syndrome) the typical clinical signs lasting 2-10 weeks include an abrupt onset of fever, myalgia, headache, malaise, abdominal pain, eosinophilia and fatigue. These are not commonly seen in individuals from endemic settings and this may be as a result of *in utero* priming of T and B lymphocyte responses of babies born to mothers with parasitic infections (Pearce, 2002, McManus et al., 2018).

### 1.1.5. Diagnosis

The standard diagnostic method for active schistosomiasis due to *S. mansoni* is the detection of viable eggs in faeces (or urine for *S. haematobium*). Currently however, due to the low sensitivity of microscopy-based examination of faeces or urine, the absence of schistosome infection cannot be reliably concluded. For the diagnoses of mild and light infections, concentration techniques, for example, sedimentation using glycerine solution or centrifugation in formol-ether are required. In field conditions, thick smear or Kato-Katz technique is usually used, as it also allows for a quantitative measure of infection intensity, commonly presented as parasite eggs per gram of host faeces (Gryseels et al., 2006).

Schistosome DNA can be identified using molecular methods that have greater sensitivity and specificity than microscopic examination. However, these methods still have limitations due to sampling following uneven distribution of eggs in the faeces and sub-optimal use in field conditions (Meurs et al., 2015). Multiplex polymerase chain reaction (PCR), which includes detection of several intestinal parasites in a single stool sample, can be an advantage when diagnosing infections in travelers (Cnops et al., 2012). Serum assessment can also be used to detect parasite DNA (Colley et al., 2014).

In addition, diagnosis of schistosomiasis is also often based on the detection of antibodies against crude parasite antigen extracts. The main limitation of this type of assay is its inability to differentiate previous recent exposure from current infection in people living in a schistosomiasis-endemic area, where people remain seropositive for several years after treatment (Doenhoff et al., 2004); moreover, some antibodies can cross-react with other helminths antigens, which makes its use under field conditions difficult. However, such assays are relevant for the diagnosis of migrants and travelers who are occasionally exposed. In addition, they can be important for new cases that involve children and in low-transmission or post-control settings. Antibody detection assays such as

rapid diagnostic point-of care (POC) tests (Nausch et al., 2014) may prove useful as infection intensities decline following control programmes, as has been the case in the People's Republic of China (Cai et al., 2014). Frequently applied methods identify IgG and/or IgM against antigens from different stages of the parasite such as cercariae, schistosomula, adult flukes and eggs. Moreover, detection of parasite antigens in infected host tissues/fluids has been used in the diagnosis of schistosomiasis using techniques including enzyme linked immunosorbent assay (ELISA), rapid diagnostic test (RDT), indirect immunofluorescence assay (IIFA), or indirect haemaglutination assay (IHA), luminex multiplex immunoassay (LMI), and immunomagnetic separation (IMS).

Somatic parasite antigens, such as the circulating cathodic antigen (CCA) and the circulating anodic antigen (CAA) in blood of infected individuals, can be identified and quantified with tagged monoclonal antibodies in serum. These genus-specific proteoglycan antigens of the schistosome gut epithelium are released in the excretory/secretory products of worms. Both antigens can be demonstrated in blood at around 3 weeks post-infection. CAA and CCA are also excreted in host urine and can be detected in serum and urine with a commercially available POC assay that detects *S. mansoni* CCA. It is now applied for screening of *S. mansoni*- infected communities in relation to mass drug administration (MDA) programmes (Ochodo et al., 2015). Concentration of urine samples can enhance the sensitivity of the POC- CCA assay (Grenfell et al., 2018). Antigen detection in serum and urine, however, cannot be used widely for clinical applications because in light infections its sensitivity decreases and the costs of POC- CCA screening may be prohibitive. However, it is a useful research tool for therapeutic and epidemiological studies for a direct, specific and stable measure of parasite loads (Weerakoon et al., 2015).

Ultrasonography assists as a rapid, safe and non-invasive tool for examining the pathology due to chronic hepatosplenic disease. According to WHO clinical guidelines, the severity of hepatic fibrosis can be graded based on the image pattern of liver appearance and by objectively measuring the size

of the main portal vein diameter and the wall thickness of a peripheral segmental portal vein. The degree of fibrosis is again used to predict portal hypertension development and bleeding in the gastrointestinal tract. Ultrasonography may also be applied to monitor the success of treatment against schistosomes in advanced cases. Magnetic resonance imaging (MRI) has provided a higher specificity and sensitivity for differentiating chronic hepatosplenic schistosomiasis and cirrhosis (Burke et al., 2009, McManus et al., 2018). Biomarkers of liver fibrosis including the P1 fragment of laminin, pro-collagen peptides type III and IV, fibrosin, hyaluronic acid, TNF-α R-II and sICAM-1 have the capacity to give a highly sensitive and cost effective method for examining fibrosis due to schistosomiasis, but they are still under investigation. IL-13 secretion by peripheral blood mononuclear cells (PBMCs) may be an important cytokine revealing the persistence of fibrosis after treatment (Burke et al., 2009). Acute schistosomiasis, in addition, is clinically characterized by finding diffuse pulmonary infiltrates on chest X-ray films and almost all cases are diagnosed with eosinophilia and a history of recent contact with water bodies (Burke et al., 2009, McManus et al., 2018).

Improved diagnostic tools for schistosomiasis are still required (both in the clinic and in the field) and novel techniques are being investigated. For instance, positron emission tomography (PET) scans have been applied experimentally to identify adult worms in the body (Salem et al., 2010). Moreover, microfluidics is currently offering assays that have the capacity to detect antibody and worm antigen (Chen et al., 2013b). However, currently there is no true gold standard tool for quantifying and correlating the outputs with actual parasite load, and this remains a significant hurdle (Colley et al., 2014).

### 1.1.6. Treatment

Praziquantel (PZQ) is the drug of choice for treating schistosomiasis. Its mode of action is by paralyzing the parasites and causing damage to the tegument of the fluke (Colley et al., 2014). A study in mice has demonstrated that PZQ treatment disrupts the tegument, exposing tegumental antigens to the host immune attack (Mehlhorn et al., 1981) which results in significant change of parasite-host-specific immune responses (Mutapi et al., 2007). PZQ is effective at killing all *Schistosoma* species, and for full efficacy its mode of action requires an intact host immune response. It is effective against adult schistosome parasites, but has poor activity against immature worms, and cannot prevent reinfection. PZQ can be administered with and without anti-inflammatory drugs at a standard single dose of 40 mg/kg of bodyweight (Bergquist et al., 2017). After this dose is given, 70-100% of subjects do not excrete eggs. In many subjects that are not fully cured, antigen concentrations and egg counts are decreased by greater than 95% (Utzinger et al., 2000). Clinical, sonographic and radiographic reports have indicated that from weeks to months following treatment, there is a decrease in intestinal lesions, abnormal liver growth, and or hepatic fibrosis (Richter, 2003). This dose is therefore applied and recommended for most community-based mass treatment programs. However, cure rates can be much lower in communities with high initial egg counts and in those exposed to rapid reinfection (Zwang and Olliaro, 2017). In such cases, the regimen can be increased up to 60 mg/kg, but to avoid side effects from the drug, when possible, it is split in two and taken several hours apart. This regimen is also recommended for individual case management or in individuals who have left the endemic regions, to reach complete cure. After initial treatment, particularly if there is high antibody titres, eosinophilia, or clinical signs persisting 6-12 weeks, a repeat dose can be important to completely cure people with sub-patent infections (Gryseels et al., 2006). Research reported that treatment of young children with PZQ resulted in satisfactory cure rates, and marked reduction in egg-output, with only mild and transient reported side-effects (Sousa-Figueiredo et al., 2012, McManus et al., 2018).

Moreover, combination treatment with PZQ and Artemether (ART) has been reported to be safe and to have an added advantage because ART also kills larval forms of the worm (Colley et al., 2014, McManus et al., 2018). It was suggested that schistosomes ingest ART and in the presence of haemin or other iron-containing molecules cleave it in their gut where a free radical reaction takes place which is toxic to the worms and eventually kills them (Xiao et al., 2003). A meta-analysis has reported twice as many cure rates after treatment with PZQ and ART together compared with PZQ alone (Perez del Villar et al., 2012). The use of ART for multi-drug resistant malaria, however, precludes its widespread use for treating schistosomiasis (Bergquist et al., 2017).

Oxamniquine acts only on *S. mansoni* and was the first-line drug in Brazil until the late 1990's and remained in use until 2010 (Valentim et al., 2013). It is as effective as PZQ but can have more marked side-effects, most noticeably sleep induction, epileptic seizures and drowsiness. PZQ-resistant schistosomes were isolated from Brazilian patients in the 1970's and also selected in the laboratory settings from sensitive parasite lines (Valentim et al., 2013). Under selective pressure, PZQ-tolerant schistosome strains can be very easily identified in animals. Under field conditions, low cure rates have been reported for PZQ in northern Senegal, but these could be explained by very high transmission rates, reinfection, pre-patent infections maturing, and perhaps the epidemic nature of the focus (Gryseels et al., 2001). Tolerant strains to PZQ have been identified in Egypt from patients who did not originally respond well to therapy, but these findings need to be supported by further studies to confirm whether true drug resistance is emerging. The disastrous case in cattle, with extensive resistance developed to anthelmintic drugs because of population mass treatment, implies that attention is required (Shalaby, 2013). These warrant monitored and careful drug usage, and underscore the urgent need for new drugs and other tools to control schistosomiasis.

### 1.1.7. Control

From the 1920's to 1980's snail control was the most popular method employed to avoid infection, since no drugs were suitable for mass supply (Gryseels et al., 2006). Although predators, biological competitors, chemicals and habitat change have been applied to decrease snail populations, efforts currently mainly use niclosamide, which is a molluscicide that kills snails at low concentrations and is safe to people. However, niclosamide is toxic to some freshwater fish and to amphibians and at the same time, is expensive and logistically difficult to deploy (Colley et al., 2014). In addition, large material and human resources are required for effective application, plus rigorous malacological and epidemiological surveillance are needed (Gryseels et al., 2006, McManus et al., 2018).

Behavioral change is a likely, but challenging means to the management of any health problem. However, with proper community participation, it could be beneficial for decreasing both contamination of water bodies (snail habitat) by faeces containing schistosome eggs, and people contact with water containing schistosomes. Behavioral changes in the population, together with improvements in sanitation and water supply, could be effective for control. The supply of schistosome-free water for bathing, washing, and recreation is successful in reducing transmission but is expensive and economically unrealistic in most regions where schistosomiasis exists (Colley et al., 2014, Grimes et al., 2015).

Mass community-based treatment with PZQ is currently the primary element of most national control programmes in many countries, and is also advocated by WHO (Ross et al., 2017, Turner et al., 2017). However, in terms of morbidity prevention and control, the advantage of shifting to MDA was largely variable among the different circumstances analysed. For regions where the target is to stop transmission, however, the projected advantage of MDA was relatively consistent (Turner et al., 2017). A number of strategies can be implemented, for example treatment of particular risk groups such as school-aged children, indiscriminate population-based treatment, and active case

detection. Complicating these strategies however is that the global long-term control of the disease demands intersectorial and integrated approaches that go beyond simply deworming (McManus et al., 2018), including ecological and behavioral changes. Such changes require sustainable financial input that must largely be supported by national governments. In addition, limited donor funding needs to be better allocated to sustainable development activities such as poverty reduction and schistosomiasis control measures (Ross et al., 2017, McManus et al., 2018).

## 1.2. *Schistosoma* vaccine development

### 1.2.1. History of schistosomiasis vaccine development

The development of successful viral and bacterial vaccines in the early 20$^{th}$ century led to the first attempts to develop a schistosomiasis vaccine in the late 1950s, which involved vaccination of mice with crude worm extracts or purified components (Sadun and Lin, 1959). The results obtained, however, were ambiguous with lack of consistency in worm burden reduction, even in the same laboratory. It appeared therefore that crude extracts alone were inadequate vaccines, and perhaps there were a few key protective antigens that needed to be identified.

Smithers and Terry then proposed the concomitant immunity hypothesis in schistosomiasis (Smithers and Terry, 1969), and this impacted heavily on vaccine development and immunology. They reported that when the rhesus macaque was challenged with cercariae, the primary worm load persisted but the animals were resistant to a secondary infection. These findings were regarded as fundamental for vaccine development and led to a paradigm shift for schistosomiasis vaccine discovery. In addition, the observation of *in vitro* killing of transformed schistosomula by the immune system involving antibodies, eosinophils and complement (Butterworth et al., 1974), known as antibody-dependent cellular cytotoxicity, offered an explanation of how concomitant immunity might work (Butterworth, 1984).

While skepticism was dominating about the possibility of developing a schistosomiasis vaccine guided by immune profiles elicited by hosts with a chronic infection, studies on the mechanism of immunity induced by attenuated cercariae using gamma, X-ray and/or UV radiation was gaining impetus. Using attenuated cercariae as a schistosomiasis vaccine was first attempted in the early 1960s, and rigorous analysis were conducted from the late 1970s onwards (Minard et al., 1978). Significant levels of reduction in worm burdens in mice (> 90%) and primates (86%) (Mountford et al., 1996, Kariuki et al., 2004, Wynn et al., 1995) were observed, and demonstrated proof of principle that a vaccine for schistosomiasis was attainable. The concept of attenuated cercariae as a vaccine has been assessed for multiple species of schistosomes in different host species (Agnew et al., 1989, Anderson et al., 1998, Dean et al., 1996, Ruppel et al., 1990). More recent studies undertaken with UV-attenuated cercariae given once or, more effectively, multiple times to C57BL/6 mice have confirmed earlier findings with significant reductions in worm and hepatic and intestinal egg numbers 38%, 52%, 26%, respectively, in vaccinated animals (El-Shabasy et al., 2015, Reda et al., 2012). The same study reported tegumental changes in the adult worms (swelling, fusion of tegumental folds, vesicle formation and loss or shortening of spines on the tubercles). Further, another study demonstrated that single immunization with radiation-attenuated cercariae can confer protective immunity levels of 60-70% ( Ricciardi and Ndao, 2015) in animal models, and these levels can be increased with booster doses. Notably, radiation-attenuated cercariae of *S. mansoni* have been demonstrated to confer protection, 52% - 84% reduction in worm counts, in non-human primates, including chimpanzees and baboons (Soisson et al., 1993, Yole et al., 1996). In addition, radiation-attenuated larvae of *S. haematobium* induce protection (85-90%) in baboons (Harrison et al., 1990).

These findings provided hope for the development of subunit vaccines against schistosomes. Nearly two-and-half decades ago, the WHO kicked-off an independent trial by taking into account the six most promising *S. mansoni* vaccine candidates at that time (Hotez et al., 2019).

The first schistosome antigen that entered human clinical trials consisted of a recombinant glutathione-S-transferase from *S. haematobium* (rSh28GST) (Bilhvax) formulated with aluminum hydroxide adjuvant (Riveau et al., 2012). Cytokine production triggered by this vaccine candidate was shown to be influenced by factors such as schistosome infection status, host age and PZQ treatment history and this has provided an indication as to the features which should be considered for determining the efficacy of the GST-based vaccine during its testing in targeted endemic communities (Bourke et al., 2014). The vaccine was immunogenic and well-tolerated in phase 1 (Riveau et al., 2012) and phase 2 clinical trials in healthy adults in non-endemic Europe and *S. haematobium* endemic areas of West Africa (Niger and Senegal), and has completed a phase 3 efficacy trial in Senegalese school-age children in 2012 and was not found to be efficacious (Riveau et al., 2018). At preclinical stage, the enzyme present in *S.mansoni* homologue (Sm28GST) has been tested extensively as a recombinant protein vaccine in various experimental models and has shown partial protection in terms of reduced worm burdens, inhibition of female worm fecundity and a reduction in egg viability (Capron et al., 2002).

Advances in systems biology have made the discovery, selection and testing of novel schistosomiasis vaccine candidates possible as a key strategy for controlling the disease (Mo et al., 2014, Sotillo et al., 2016a). Immunological profiles of human sera from putatively resistant individuals in schistosomiasis endemic areas has been conducted (Pearson et al., 2015, Gaze et al., 2014) and has resulted in the identification of numerous known and novel antigens, including the *Sm*-TSP-2 vaccine antigen for human schistosomiasis.

*Sm*-TSP-2 is a member of the tetraspanin (TSP) family. TSPs contan four transmembrane domains and two extracellular loops. The large extracellular loop 2 domain of *Sm*-TSP-2 when expressed in recombinant form provided high levels of protection, with 40-57% and 64-65% reduction in the number of adult worms recovered and egg burden, respectively in a murine model of schistosomiasis (Tran et al., 2006), even when formulated with alum/CpG (Pearson et al., 2012). Furthermore, IgG1 and IgG3 antibodies from putatively resistant human subjects uniquely recognized TSP-2 compared to chronically infected subjects (Tran et al., 2006). The *Sm*-TSP-2 schistosomiasis vaccine was selected for process development and scale-up manufacture according to current good manufacturing practices (cGMP) in the *Pichia Pink* yeast expression system (Curti et al., 2013). Through a product development partnership led by The George Washington University and Texas Children's Hospital Center for Vaccine Development, the recombinant *Sm*-TSP-2 protein was adjuvanted with Alhydrogel® to be given together with an aqueous formulation of the Toll like receptor-4 agonist AP 10-701. A phase 1 clinical trial assessing the immunogenicity and safety of *Sm*-TSP-2/Alhydrogel® with or without AP 10-701 was recently concluded in Houston at the National Institute of Allergy and Infectious Diseases (NIAID), National Institute of Health (NIH)-sponsored Vaccine and Treatment Evaluation Unit of the Baylor College of Medicine. Another NIAID/NIH-funded phase 1 trial of *Sm*-TSP-2 vaccine is ongoing in a schistosomiasis endemic area of Brazil, and a phase 2 clinical trial of the same vaccine is currently being planned in Uganda, as reviewed in (Hotez et al., 2019).

A 14 kDa fatty acid-binding protein known as r*Sm*14 when expressed in *Pichia pastoris* was shown to be immunogenic and well-tolerated in healthy, adult males from a non-endemic area when formulated with a stable oil in-water emulsion of glucopyranosyl lipid A (GLA-SE) in a phase 1 trial (Santini-Oliveira et al., 2016). Vaccination induced IgG antibodies against *Sm*14 as well as a strong Th1 cellular response as shown by IFN-ɣ secretion upon re-stimulation of peripheral blood

mononuclear cells from study subjects (Tendler et al., 2015). The Fundação Oswaldo Cruz in Brazil has led to the development of this vaccine. A second trial was recently finalised in male adults in an endemic region of Senegal but the outcomes have not yet been reported. Preclinical studies reported that immunizing with r*Sm*14 vaccine protected mice against *S. mansoni* infection with 67% reduction in the number of adult worms recovered, and encouragingly, no autoimmune response was observed even though its structure is identical in basic form with mammalian host homologues (Tendler et al., 1996). Recombinant Sm14 is being developed as an anthelmintic vaccine for use against both fascioliasis of livestock and human schistosomiasis caused by *S. mansoni* (Tendler et al., 2018).

Sm-p80, a calcium-dependent neutral protease known as calpain, is another *S. mansoni* vaccine antigen that is scheduled to enter phase 1 clinical trials (Siddiqui et al., 2018). *Sm*-p80, was expressed in *Escherichia coli*, has been demonstrated to confer high levels of protection in a range of animal models, including hamsters (*S. haematobium*) and non-human primates (*S. mansoni*), with evidence that the vaccine elicits high levels of antibody in baboons for several years (Siddiqui and Siddiqui, 2017). Clinical trials with the recombinant protein formulated with GLA-SE or with a CpG oliogodeoxynucleotide adjuvant is led by Texas Tech University, PAI (Preparing for Successful Pre-Approval Inspections) Life Sciences, and Infectious Diseases Research Institute (IDRI) (Siddiqui et al., 2018). Of note, *S. japonicum* vaccines are also under development for use in animals in endemic areas of the Philippines and China that would interrupt it's transmission to humans from water buffalo and other mammals (Hotez et al., 2019). In preclinical studies, for instance, compared to control animals, 70% and 75% reduction in worm and hepatic egg burden, respectively, were shown in mice immunized with a formulation of recombinant *Sm*-p80 and CpG dinucleotides (Ahmad et al., 2009b). In a non-human primate model, immunized baboons had a 58% reduction in parasite burden compared to controls (Ahmad et al., 2011). Furthermore, different *Sm*-p80 vaccine

formulations were able to reduce established adult worm burdens in a chronic infection/vaccination model in baboons, and decrease retention of eggs in tissues and reduce egg excretion in faeces (Karmakar et al., 2014c). Moreover, in addition to its prophylactic efficacy, *Sm*-p80 immunization could also confer killing of already established adult parasites and protect against urinary schistosomiasis caused by *S. haematobium* (Karmakar et al., 2014c). Similarly, in a schistosome cross-species protection experiment, the *Sm*-p80 vaccine generated 25% and 64% reductions in *S. haematobium* adult worms and eggs load, respectively, in the urinary bladder of vaccinated baboons (Karmakar et al., 2014a). Moreover, *Sm*-p80 is the first single vaccine (Molehin et al., 2016) to have shown substantial protection against the three major schistosome species which infect humans. A recent study in baboons demonstrated that rSm-p80 with GLA-Alum as adjuvant provided 33–53% and 38% reductions in worm burden in mice and baboons, respectively, compared to those immunized with adjuvant only (Zhang et al., 2018b). In another related study, Sm-p80 showed potent prophylactic efficacy against transmission of *S. mansoni* infection and was correlated with a significant decrease in egg-induced pathology in vaccinated animals, compared to controls (Zhang et al., 2018c). The same study reported a 93% reduction of female worms and significantly less clinical manifestations of hepatic or intestinal schistosomiasis by reducing the tissue egg-load by 90%. Further, a 35-fold and 81% reduction in faecal egg counts and in hatching of eggs into miracidia, respectively, were reported compared to unvaccinated controls, demonstrating the parasite transmission-blocking potential of the vaccine. In a simulated filed condition of human schistosomiasis, Siddiqui and collogues showed a moderate reduction in worm burden but a significant reduction in tissue egg burdens in baboons immunized with recombinant Sm-p80 + CpG-ODN, compared with adjuvant-treated control baboons (Siddiqui et al., 2018). Sm-p80-based vaccine formulations have many salient futures: (1) egg induced pathology resolution both in rodents and baboons; (2) prophylactic efficacy against intestinal schistosomiasis; (3) cross-protection against intestinal and urinary schistosomiasis; (4) longevity of immune response - robust

antibody titres for 5-8 years in baboons and up to 60 weeks in mice; (5) post-exposure therapeutic effect via killing of established adult worms in chronic infections; (6) transplacental transfer of Sm-p80-specific antibodies in baboons. Moreover, the Sm-p80-based vaccine has multifaceted effectiveness against several stages of the parasite's life cycle (Ahmad et al., 2009b, Ahmad et al., 2009a, Ahmad et al., 2011, Karmakar et al., 2014a, Karmakar et al., 2014b, Zhang et al., 2014, Zhang et al., 2010). Additionally, Sm-p80-specific IgE has not been detected in infected or high risk populations from South America (Gaze et al., 2014) and Africa (Ahmad et al., 2011), thus lessening the risk of hypersensitivity reaction following vaccination in humans.

Other key schistosome surface proteins located in the apical surface or tegument of the parasite have been characterised and could be potential alternative vaccine antigens. None of these, however, are currently being developed for trials. As a way forward, an optimal vaccine development strategy for clinical trials moving forward should consider such aspects as (i) evaluating the existing candidates alone and in combination, together with several different adjuvants and immunostimulants; (ii) coordinating and financing of schistosomiasis vaccine clinical development efforts; (iii) evaluating how to best introduce a schistosomiasis vaccine, for example through existing health systems and/or its integration into programs - expanded program on immunisation - could be considered in tackling bottlenecks in clinical development of vaccine against schistosomiasis. Finally, those candidate vaccines that have advanced to clinical trials, if eventually licensed, will require a great deal of innovative thought and intersectorial cooperation for financing to realise their full benefit.

### 1.2.2. Feasibility of vaccine development

There is currently no available vaccine for schistosomiasis, and rigorous research efforts are required to progress early stage discoveries towards a clinically validated and approved vaccine to prevent this disease. The feasibility of generating an effective vaccine for the prevention and control

of schistosomiasis exists, and is supported by robust immunologic data in both humans and animal models (Fonseca et al., 2015, Wilson et al., 2017). In general, immune responses against schistosomes have two different phases: (a) immune-pathogenesis as a result of host immune responses towards egg antigens which are trapped in host tissues and (b) age-related resistance to reinfection which confers protective mechanisms over many years. Research shows that incomplete protective innate immunity can develop in endemic regions, and acquired immunity is boosted by repeated treatment with PZQ in response to antigens released by dying adult flukes (McManus and Loukas, 2008). Moreover, in studies involving animal challenge models, immunisation with irradiated schistosome cercariae can confer upwards of 80% protection against challenge infection (Hotez et al., 2010). Studies using irradiated schistosome larvae showed that they were killed in the lungs by a protective immune response. A small proportion of the larvae enter and persist in the skin-draining lymph nodes where they elicit an immune response greater in intensity and differing in quality from that induced by non-irradiated parasites. Other larvae travel only as far as the lungs where they recruit lymphocytes to arm that organ (Coulson and Wilson, 1997). Lung stage schistosomula were the main target of the immune response and Th1 polarised immunity is prominent in the spleen at this time (Bickle, 2009). With multiple exposures of mice to attenuated cercariae, the immune response progressively develops a Th2 profile, and protection is passively transferable to naïve recipients with immune serum (Kariuki et al., 2004). The immune responses of primates to the attenuated vaccine illustrate this switch, with the cytokine profile changing from Th1 to Th2 with successive exposures to attenuated cercariae (Eberl et al., 2001). While offering in some cases high levels of protection, irradiated cercarial vaccines are impractical for wide-scale deployment. In another related study, mice vaccinated with irradiated cercariae mounted both humoral and cellular immune responses to lung-stage worms (Wilson et al., 1999), and under some conditions, the administration of the cercarial vaccine together with IL-12 enhanced protective immunity (Wynn et al., 1995). However, in a natural infection, due to the fact that the parasite

evades the immune response, it can survive for many years in the host (Colley and Secor, 2014). Moreover, animal field trials with subunit vaccines for platyhelminth infections in pigs like cysticercosis caused by *Taenia solium* and echinococcosis in sheep caused by *Echinococcus granulosus* have shown significant efficacy (Molehin et al., 2016), which enhances the likelihood of developing an effective vaccine for schistosomiasis.

### 1.2.3. New vaccine candidates and future directions

Current vaccine development endeavors target the prevention of schistosome infection and/or decrease egg burden through attenuation of parasites and their subsequent egg laying capacity. Major advances in schistosome molecular biology such as genomics, transcriptomics, proteomics and immunomics have aided new antigen discovery (Loukas et al., 2011, Gaze et al., 2012, Driguez et al., 2016b). Access to this information in conjunction with improving postgenomic technologies has the capacity to facilitate the discovery of many new vaccine candidates. Molecules exposed to host antibodies, notably ES products and proteins anchored to the outer tegument of the worm are the most important candidates (El Ridi and Tallima, 2013).

One major reason for the lack of advanced schistosomiasis vaccines to date is the early stage selection of inappropriate vaccine candidates. In order to develop a suitable vaccine, a series of parameters need to be considered, which include: knowledge of key elements of the protective immune response in humans; identifying and characterising the best target antigens; determining the efficacy of the vaccine candidate by taking into account the reduction of parasite burden and reductions in immunopathology; assessing its safety; and ensuring an appropriate level of funding is available for infrastructure and qualified manpower to perform clinical trials (El Ridi et al., 2015). Over 100 schistosome vaccine antigens have been identified, of which about one-quarter have shown some level of protection in the murine model of schistosomiasis (Siddiqui et al., 2011). Many candidate antigens are not exposed on the surface of live parasites, and as such,

it is difficult to conceive how they would be targets of protective immunity (Tebeje et al., 2016). As a result, it is not apparent how the host immune pathways can be rid of parasites through interactions with cytosolic and internal proteins such as fatty acid binding protein, paramyosin, triose-phosphate isomerase (TPI), schistosome glyceraldehyde 3-phosphate dehydrogenase (SG3PDH), or glutathione S-transferase (GST) (McManus and Loukas, 2008). Moreover, vaccine trials in mice indicated that none of the above vaccine candidate antigens induced >40% reduction in challenge worm burden, the benchmark set by the WHO for progression of schistosome vaccine antigens into clinical trials (El Ridi and Tallima, 2013). Further, surface membrane proteins are protected in the immature larvae and adult parasites and unless the parasite is suffering excessive loss of tegument integrity and poised to die (eg. after PZQ treatment), they generally cannot be accessible to the host immune effector mechanisms (Loukas et al., 2007). Conversely, lung schistosomula ES products are ideal potential vaccines targets. ES products elicit primary and memory immune responses, and are accessible targets to toxic radicals, effector cells through cytokine productions and cells that would directly target schistosomula in the lung capillaries (El Ridi and Tallima, 2009). Similarly, skin-stage schistosome ES directs DCs to drive Th2 responses *in vivo* (Jenkins and Mountford, 2005). This ES contains proteases, including several elastases that facilitate parasite skin penetration (McKerrow et al., 2006), and can cleave host IgE antibodies (Pleass et al., 2000). The presence of multiple isoforms of cercarial elastase and a metalloprotease was identified using proteomic analysis of cultured parasites (Knudsen et al., 2005, Curwen et al., 2006), and by proteomics of human skin traversed by invading cercariae (Hansell et al., 2008). Proteomic analysis on egg ES identified two abundant proteins, a ribonuclease omega-1 and alpha-1 (Dunne et al., 1991, Cass et al., 2007). Moreover, schistosomula in skin were shown to secrete glycolytic enzymes, such as GADPH, TPI, enolase and aldolase, as well as several homologues of the venom allergen-like family. Cercarial ES also contains the immunomodulator Sm16 that can inhibit toll-like receptor signalling in monocytes (Brännström et al., 2009). Further, calpain, TPI, GST, SG3PDH, aldolase, TPX,

and 14-3-3 protein homolog1 were detected among soluble proteins of *in vitro*-grown 8-day *S. mansoni* schistosomula (Curwen et al., 2004) and secretions of *S. mansoni* cercariae (Knudsen et al., 2005, Curwen et al., 2006). In addition, vaccine candidates such as 14-3-3, aminopeptidase, and SG3PDH have been identified from adult *S. japonicum* ES products (Liu et al., 2009), and TPI and GST in ES products of both egg and adult *S. haematobium* (Sotillo et al., 2019a). Thus, targeting these specific molecules may allow the development of vaccines that promote worm clearance.

In view of new antigen discovery efforts, emphasis has been placed on proteomic analyses of the tegument surface proteome as a source of host-accessible antigens (Sotillo et al., 2015, Wilson, 2012). Several hundred schistosomula tegument proteins have been identified using mass spectrometry approaches and proposed as a reservoir of potential vaccine antigens (Sotillo et al., 2015). This group of tegument surface proteins includes previously identified prominent proteins such as *Sm*-p80, *Sm*-TSP-2, Sh28GST, Sm14 and Sm29, and a host of other antigens that have shown varying levels of efficacy in mouse models (Tebeje et al., 2016). Furthermore, it is suggested that surface membrane proteins of newly transformed schistosomula are prime targets for effective vaccines against schistosomiasis (Sotillo et al., 2015). This is attributed to observations that vaccine-mediated killing of juvenile worms occurs primarily in the lungs (Hewitson et al., 2005). Moreover, recent reports have shown that in addition to elimination of schistosomula from lungs, vaccine-mediated killing can also be achieved for established adult parasites in the mesenteries as seen in mice and chronically infected non-human primates (Molehin et al., 2016).

Much of our current understanding of immunity and immune mechanisms against schistosomiasis relies on studies conducted in mice, but vaccines based on studies performed only in the mouse model could have undesirable effects if taken prematurely to human clinical trials. In addition, it has been reported that a large proportion of penetrating cercariae fail to mature

in the mouse because its pulmonary capillaries are fragile, raising the question as to whether this model is appropriate for vaccine efficacy studies. This reinforces the argument that further critical examination of any identified candidate vaccine antigen, whether it has foundation in acquired immunity, or not, is critical, and that moving to studies using larger models such as rabbits, pigs or bovines in the case of *S. japonicum,* or non human primates for *S. mansoni* and *S. heamatobium,* is clearly necessary.

Further, selection of recombinant protein expression system is another important point to consider. Extracellular vaccine candidates need to be expressed in bacteria or eukaryotic expression systems. Many of the selected antigens are likely to require processing through the endoplasmic reticulum by virtue of their expression sites in the parasite, and this may prove challenging. Difficulties in obtaining good expression levels and in scaling up production according to good laboratory practice/GMP standards for the limited number of antigens selected have turned out to be another major hurdle. Some of the vaccine candidates have encountered challanges in scale-up production and have been halted (Bergquist et al., 2005, McManus and Loukas, 2008).

In addition to searching for new vaccine antigens, suitable adjuvants, formulation methods and delivery routes are essential for generating optimal immune responses. Types of adjuvants selected can skew the immune response to a vaccine, and can potentiate the strength of the immune response to immunogens, enable dose and dosage sparing, and help to avoid and complement immune deficiencies in the elderly and young (Karmakar et al., 2014c, Wilson et al., 2017). However, appropriate antigen and adjuvant choice, effective immunogen design using potential immune correlates, and strong efficacy in experimental animal models will not be sufficient for a successful vaccine unless cGMP manufacturing of the vaccine product is feasible (McManus and Loukas, 2008).

Key features of an ideal vaccine for human schistosomiasis include: 1) it should preferably target the two major human schistosomes, *S. mansoni* and *S. haematobium*, which are often co-endemic in the Middle East and Africa. 2) it should prevent the immunopathology seen in the intestine and liver (*S. mansoni*) and the bladder and female genital tract (*S. haematobium*) during schistosomiasis by greatly reducing the number of eggs deposited in those tissues. 3) it should preferably have a prophylactic effect, which would be superior to MDA by preventing reinfection, which is key to preventing and controlling the infection in endemic areas and reducing parasite transmission.

## 1.3. Extracellular vesicles

### 1.3.1. What are Extracellular Vesicles?

Extracellular vesicles (EVs) are heterogeneous vesicles of membranous origin released by different types of cells. EVs comprise a complex mixture of genetic information, proteins, lipids, and glycans. EVs can broadly be categorised into three classes based on their cell of origin, contents, function, physical characteristics, specific protein markers and isolation techniques. These include (1) exosomes; (2) Micorvesicles (MVs) or ectosomes; and (3) apoptotic bodies (ABs), as depicted in Figure 1.3. A shared character in all of the three EV types is the surrounding lipid bilayer membrane with specific cargo molecules, such as, RNA, proteins, and lipids. However, their specific density and size vary considerably (Mathivanan et al., 2010); albeit that both measurement ranges for the different EV classes have been heterogeneously documented (Thery et al., 2001). Nevertheless, exosomes, first recognised in the 1980's (Kalra et al., 2016), are thought to range from 30-150 nm in diameter and with a specific density of 1.10–1.14 g/mL (Kalra et al., 2016) and pellet at 100,000 *g* (Raposo and Stoorvogel, 2013). They originate by inward invagination of endosomal membranes, resulting in the engulfment of cytosolic proteins and other components to the lumen of the vesicles (van Niel et al., 2018, Mathieu et al., 2019) within multivesicular endosomes (MVEs). Subsequent

fusion of MVEs with the plasma membrane (PM) then releases the vesicles into the extracellular space.

On the contrary, MVs, first discovered in the late 1960's (Hargett and Bauer, 2013) are relatively larger vesicles ranging from 150-1000 nm in diameter (van Niel et al., 2018, Mathieu et al., 2019) and pellet at 10,000 *g* (Raposo and Stoorvogel, 2013), and are ubiquitously packaged and originate from the PM by outward budding or protrusion (van Niel et al., 2018, Mathieu et al., 2019), as shown in Figure 1.3.

ABs (Figure 1.3) are released from both normal and cancerous cells undergoing apoptotic cell clearance or programmed cell death (Taylor et al., 2008), and are considered to range from 50-5,000 nm in diameter and hence are typically the largest of the three EV types (Mathivanan et al., 2010, Stremersch et al., 2016). Through a process of apoptosis the cell and cellular debris are dismantled in a coordinated fashion, which are again packed into apoptotic bodies. ABs have special features that elicit phagocytosis pathways, the ultimate fate in dying cells from which molecular building blocks will be recycled. Although some experiments have shown a biological function and role in communication for ABs (Bergsmedh et al., 2001), most current studies in the field of EVs focus on the smaller sized exosomes and MVs. Hence, ABs are not considered when referring to EVs throughout this thesis. And, because the methods used to isolate and purify membrane vesicles differ significantly between studies, I will not strictly distinguish exosomes from MVs throughout this literature review, and instead will refer to them collectively as EVs, unless specifically mentioned as it appears in the sourced literature.

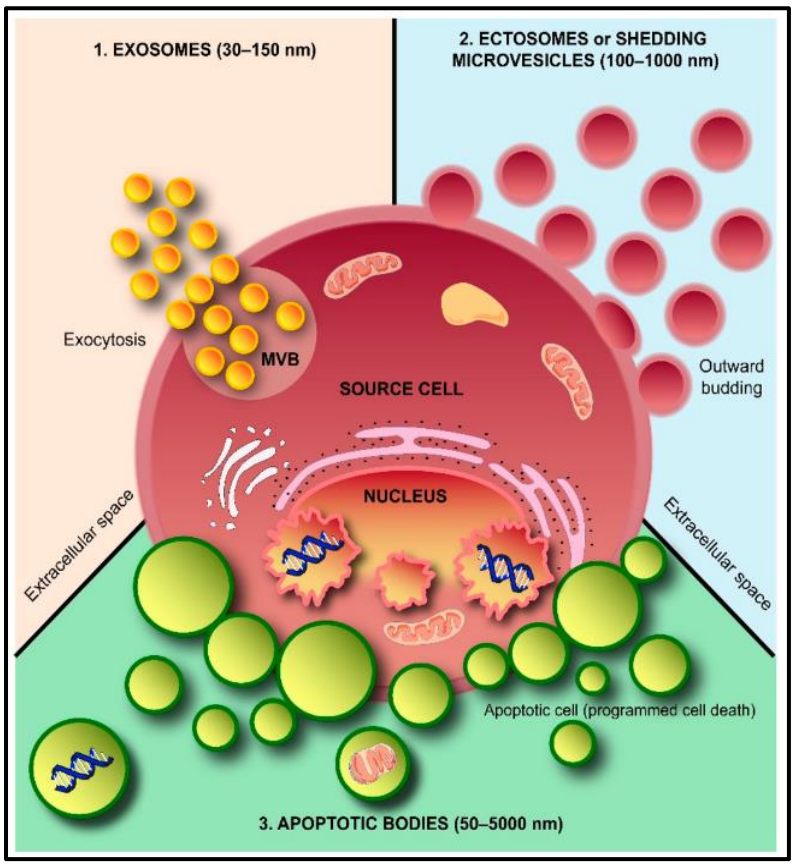


**Figure 1. 3. The different types of eukaryotic extracellular vesicles** (Kalra et al., 2016).

The mechanisms involved for selective packaging of cargo destined for intercellular communication and internalisation of these into recipient cells is likely to vary between different cells or organisms (Shifrin et al., 2013, Jeppesen et al., 2019). Among EV cargo, there is clear evidence that certain miRNA, lipid and protein species are found enriched in certain vesicle types.

The protein profiles of EVs from many cell lines and eukaryotic organisms have been examined by sodium dodecyl sulfate polyacrylamide gel electrophoresis (SDS-PAGE), immunoblotting, or proteomic analysis. EVs with high purity should be free of contamination, for example, from serum proteins and proteins of intracellular compartments (such mitochondria or the endoplasmic reticulum). Development of ExoCarta (http://www.exocarta.org), a manually curated database that contains information on proteins, RNA and lipids located in exosomes (Simpson et al., 2012,

Keerthikumar et al., 2016), and Vesiclepedia (http://microvesicles.org), a community annotation compendium for all EVs (Kalra et al., 2012), has helped researchers to appropriately add known constituents of exosomes and offer a broad highlight of their molecular composition (Simpson et al., 2012). Moreover, ExoCarta offers annotations with International Society of Extracellular Vesicles (ISEV) standards and hence supports researchers by swiftly updating the database with relevant literature (Lydic et al., 2015). Some of the proteins identified from larval and adult *S. mansoni* parasites are shown in Figure 1.4.

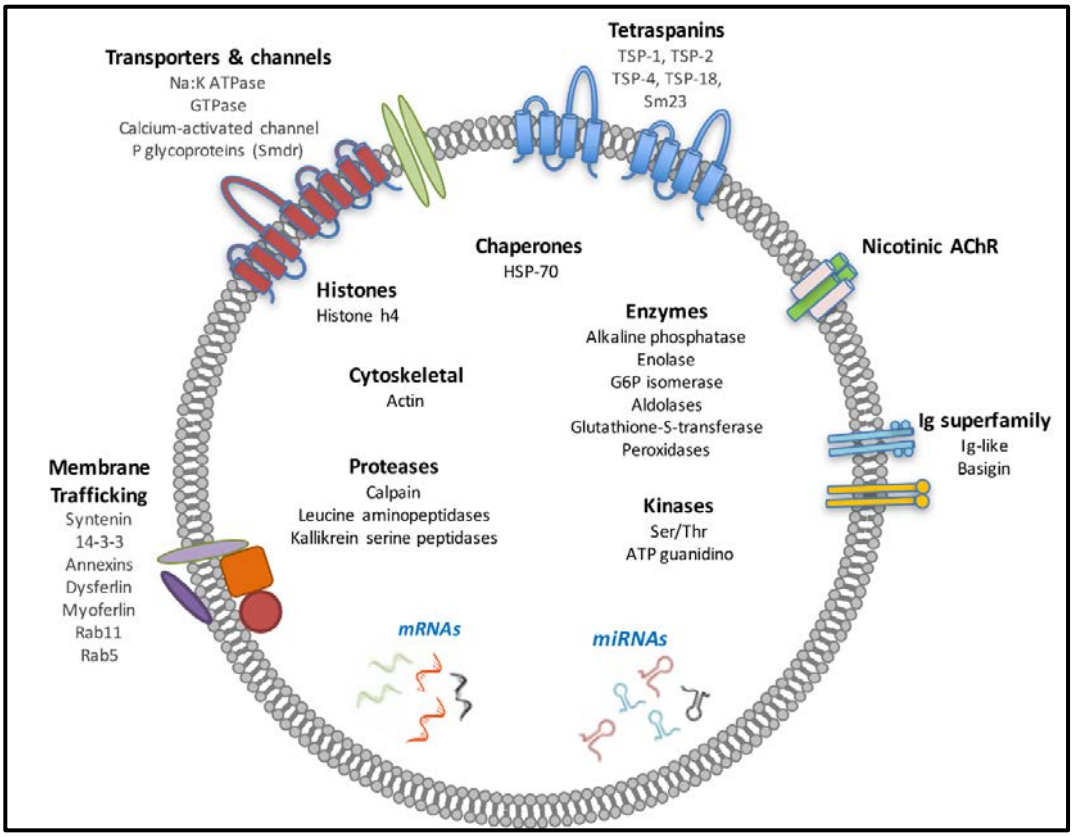


**Figure 1.4. Schematic representation of a schistosome extracellular vesicle** showing selective proteins of interest that were identified from larval (Nowacki et al., 2015) and adult flukes (Sotillo et al., 2016b). Adopted from (Kifle et al., 2017).

Among the EV subtypes, exosomes have been and continue to be extensively studied. Because exosomes comes from endosomes, proteins taking part in MVB formation (such as Alix and TSG101), adhesion (such as integrins), TSPs (e.g., CD9, CD63, CD81, CD82), membrane transport and fusion

(such as annexins, flotillins, GTPases), antigen presentation (MHC class molecules), heat shock proteins (Hsp70, Hsp90) and lipid-related proteins (Thery et al., 2009, Wu et al., 2019) are usually isolated from exosomes, and is independent of the cell of origin. Applying two different techniques, high resolution density gradient fractionation and direct immunoaffinity capture, studies with human colon (DKO-1) and glioblastoma (Gli36) cancer cell lines demonstrated separation and characterisation of small EVs from extracellular non-vesicular compartments (Jeppesen et al., 2019). While ALIX and syntenin-1 were among the most abundantly identified proteins in the density gradient-purified small EVs analysed, in the non-vesicular fractions the most abundant proteins identified were metabolic enzymes like ENO1, PKM, and GAPDH. Cytosolic proteins including tubulins and HSP90 were absent from classical exosomes expressing the TSPs CD63, CD81, and CD9 (van Niel et al., 2018, Zhang et al., 2018a). The same study surmised that some presumed exosome proteins were more likely to be associated with non-vesicular fractions than the EV fraction, highlighting a need for a reassessment of exosome composition. In another study, by employing asymmetric-flow field-flow fractionation, Zhang et al. identified two exosome subpopulations (small exosome vesicles, 60-80 nm and large exosome vesicles, 90-120 nm) and discovered a population of non-membranous nanoparticles termed “exomeres” (~35 nm) (Zhang et al., 2018a). Moreover, from five different cell lines, flotillins (FLOT1 and FLOT2) represented *bona fide* markers of small exosomes vesicles, while HSP90AB1 was preferentially associated with exomeres. Further, although CD63, CD9 and CD81 all exhibited specific association with both exosome subpopulations analysed, they all showed a cell type- and particle-dependent preferential expression, highlighting the necessity of combining CD9, CD63 or CD81 to isolate mammalian cell exosomes (Kowal et al., 2016).

Membrane proteins at endosomes or proteins that are identified to cluster into microdomains at the PM usually are also found on EVs. One of these protein families is the TSPs (Hemler, 2003). TSPs such as CD37, CD53, CD63, CD81 and CD82 were primarily discovered in exosomes secreted by B

cells and can be taken as a true marker for both the PM and early endosomes (Escola et al., 1998). Based on topological studies, TSPs have been defined as a superfamily of proteins with four transmembrane domains with some characteristic structural features. Despite their low sequence homology, TSPs contain four to six conserved extracellular cysteine residues, and polar residues within transmembrane domains. They also contain distinct palmitoylation sites and most members are also glycosylated (Stipp et al., 2003). TSPs are involved in a multitude of biological processes that imply roles in cell adhesion, motility, invasion, or membrane fusion as well as signaling and protein trafficking.

The role of TSPs in EV biogenesis and cargo selection have been reviewed by Andreu and Yanez-Mo (2014). These include their involvement as exosomes markers, in EV biogenesis and cargo selection, in EV targeting and uptake, and as an antigen presenter on EVs. For example, exosomes derived from B cells are enriched in all TSPs analysed (CD37, CD53, CD63, CD81, and CD82) by 7- to 124-fold (Escola et al., 1998). In addition, TSP membrane-spanning proteins are enriched on the surface of mammalian cell exosomes and are relevant for exosome release from parent cells (van Niel et al., 2011).

While several researchers have identified CD63, CD9, Alix, and TSG101 as exosomal markers (Mathivanan et al., 2010), it is becoming clear that these molecules can no longer be considered as “true markers”, but rather they are abundant in exosomes (Lotvall et al., 2014). Supporting these findings, Keerthikumar et al. showed an enrichment of CD63, CD9, Alix, and TSG101 in exosomes compared to MVs (Keerthikumar et al., 2015). Their research, moreover, assured that CD81 might uniquely be used as an exosomal marker, which was again confirmed by Minciacchi et al. (2015).

Unlike exosomes, MV molecular composition is still largely elusive, but glycoproteins (such as GPIb, GPIIb–IIIa and P-selectin) (Mezouar et al., 2015), integrins (such as Mac-1), matrix metalloproteinases (MMPs) (Li et al., 2013a), receptors (such as EGFRvIII) (Al-Nedawi et al., 2008),

and cytoskeletal components (such as β-actin and α-actinin-4) (Bernimoulin et al., 2009) appear to be enriched in MVs, and are cell type dependent. Proteomic analysis of MVs derived from monocytic THP-1 cells, mainly in the range of 0.78–0.99 μm, were shown to have unique protein expression patterns depending on the stimuli used, including cytoskeletal components, signaling molecules, adhesion receptors, and mitochondrial proteins (Bernimoulin et al., 2009). In like fashion, Keerthikumar and co-workers confirmed the enrichment of ribosomal, mitochondrial and centrosomal proteins in MVs (Keerthikumar et al., 2015). The study also assured the depletion of TSPs, ESCRT proteins, and proteins identified in attachment and transporting such as integrins, annexins and flotillins. Moreover, the same study mentioned an exclusive set of RAB GTPases that is identified in exosomes and MVs, at least in neuroblastoma cells. Research also suggests that MMP2 might be used as a marker of MVs (Keerthikumar et al., 2015). However, MV-identified proteins are mainly cell type dependent. For example, the marker of epithelial cells, CK18, was enriched in epithelial cell-secreted MVs and not in fibroblast-secreted MVs, (Keerthikumar et al., 2015, Minciacchi et al., 2015). A recent study, however, identified Annexin A1 as a specific marker of cells identified from mammalian MVs but not of exosomes (Jeppesen et al., 2019).

EVs are also composed of proteins that link with lipid rafts (including glycosylphosphatidylinositol-anchored proteins and flotillin) (Wubbolts et al., 2003, Raposo and Stoorvogel, 2013, Skotland et al., 2018). In comparison to the PM, exosomes from a variety of cells (Wubbolts et al., 2003, Raposo and Stoorvogel, 2013, Record et al., 2018) are highly enriched in sphingomyelin, cholesterol, and hexosylceramides at the expense of phosphatidylcholine and phosphatidylethanolamine. The fatty acids in exosomes are mostly monounsaturated or saturated. In conjunction with the high amount of cholesterol, this may be attributed to lateral segregation of these lipids into ILVs during their formation at MVEs. In comparison, not much is known about the protein and lipid composition of MVs and whether distinct elements are enriched on MVs compared to their originating PM.

Finally, different studies have also confirmed the presence of RNA contents in EV isolates from cell cultures and body fluids. The cargo of EVs is comprised of both mRNAs and miRNAs, and proteins can be synthesised by target cells from EV-associated mRNAs (Valadi et al., 2007). As a consequence of fusion with recipient cells, EVs from immune cells have been shown to selectively incorporate miRNA that can be functionally transferred (Montecalvo et al., 2012). Using unbiased deep sequencing of RNA from EVs demonstrated that, together with mRNA and miRNA, they also reveal many other small noncoding RNA types, for example RNA transcripts overlapping with protein coding regions, structural RNAs, tRNA fragments, vault RNA, yRNA, small interfering RNAs, and repeat sequences (Bellingham et al., 2012). Many RNAs that were identified in EVs were observed to be enriched compared to the RNA contents of the originating cells (Valadi et al., 2007, Nolte-'t Hoen et al., 2012), showing that RNA is selectively packed into EVs. It is worth mentioning here that several attempts have been unable to demonstrate whether isolated extracellular RNAs were genuinely linked with EVs or rather with RNA-protein complexes that may have been co-identified with EVs. Determining whether RNAs are within the cytosolic lumen or linked with the EV outer membrane can be carried out by measuring flotation in sucrose gradients and resistance to RNase digestion subsequent to protease treatment. Also, different RNA isolation techniques yield much variation in exosomal RNA level and patterns (Eldh et al., 2012), and the resulting variations in outcomes from several studies, and dearth of quantitative data, make it difficult to pursue a comparative inventory of the RNA profiles associated with EVs so far. Furthermore, a recent study showed that small EVs are not vehicles of active DNA release, and instead a new model for active secretion of extracellular DNA through an autophagy- and multivesicular-endosome-dependent but an exosome-independent mechanism (Jeppesen et al., 2019) has been proposed, suggesting the need for a reassessment of exosome composition.

### 1.3.2. Biogenesis and release of eukaryotic EVs

Exosomes are formed by inward budding of endosomal membranes, forming the progressive accumulation of ILVs within large MVBs. Although exosomes and MVs may share some contents (nucleic acid, proteins etc), because they follow different routes for their origin, the cellular machineries participating in their formation and release are most likely to vary. In the lysosomal route, MVEs bind to lysosomes for the breakdown of their contents, which is different from the pathway of secretory MVEs. There is morphological and biochemical evidence that these two different destinies depend on unique forms of MVEs that exist at the same time within a cell. Presence of cholesterol together with the toxin perfringolysin showed one cholesterol-rich MVE population for exosome formation and another, structurally similar, but cholesterol-poor population destined for the lysosomal pathway (Wiebke Möbius et al., 2002, Hessvik and Llorente, 2018). On the other hand, lysobisphosphatidic acid is clearly present in lysosome-destined epidermal growth factor-containing MVEs (White et al., 2006) but absent in exosomes (Wubbolts et al., 2003). Comprehensive reviews of the cell biology and function of EVs were recently published (van Niel et al., 2018, Latifkar et al., 2019).

The formation of MVEs comprises the lateral segregation of cargo at the defining membrane of an endosome and inward budding and scissing of vesicles into the lumen of the endosome. The molecular mechanisms involved in the biogenesis of MVEs or path for their degradation have been determined following the initial discovery of yeast mutants that had limitations in the transport to the vacuole, the yeast analogue of mammalian lysosomes (Raposo and Stoorvogel, 2013, Hessvik and Llorente, 2018).

The mechanisms for generation of ILVs within MVBs and the resulting binding with the PM to release exosomes into the extracellular space are not entirely known. One of the suggested molecular mechanisms associated with the biogenesis and release of exosomes is the ESCRT pathway. Studies

indicate that the ESCRT pathway may have unique functions in EV generation versus sorting for the lysosomal pathway. Though EV cargo selection may not be through ubiquitination, some ESCRT components have been identified in EV formation. For instance, the transferrin receptor, which in immature red blood cells is directed for exosome release, is linked with the ESCRT accessory protein Alix while sorting at MVEs. In addition, Alix was also indicated to be involved in exosome biogenesis and sorting of syndecans through an interaction with syntenin (Baietti et al., 2012, van Niel et al., 2018). The ESCRT machinery can be grouped into four multi-complex proteins: ESCRT-0, -I, -II, and –III. The first three ESCRT complexes help to recognize and sequester ubiquitinated membrane associated proteins at the endosomal defining membrane, and ESCRT III complex is key for budding and actual pinching of ILVs (Baietti et al., 2012); the accessory proteins, specifically the AAA-ATPase Vps4, are responsible for the dissociation and recycling of the ESCRT complex machinery. Most importantly, ESCRT-III in association with deubiquitinating enzymes, such as HD-PTP, helps deubiquitination of proteins. Alix was shown to promote intraluminal budding of vesicles in endosomes upon interaction with syntenin (Baietti et al., 2012, van Niel et al., 2018), which is the cytoplasmic adaptor of syndecan heparan sulphate proteoglycans. Moreover, the accumulation of luminal cargo seems to be triggered by the interaction of the ESCRT machinery with Alix (Bissig and Gruenberg, 2014).

The mechanisms by which RNA types are arranged and sorted into EVs are also still unresolved. Research suggests that RNAs in EVs share unique sequence motifs that may possibly work as cis-acting components for targeting to EVs (Batagov et al., 2011). Although it is speculative, the observation that ESCRT-II is a RNA-associated complex suggests that it may also be used to select RNA for assortment into EVs (Schorey et al., 2015). A recent study by McKenzie et al. using isogenic colon cancer cell lines showed that over-activity of KRAS as a result of mutation inhibits localization of Ago2 - RNA-induced silencing complex (RISC) component - to MVEs and decreases Ago2 secretion

in exosomes (McKenzie et al., 2016). The same study further showed inhibition of mitogen-activated protein kinases (MEKs) I and II, but not Akt, reverses the inhibitory effect of the activating KRAS mutation and leads to increased Ago2-MVE association as well as exosomal secretion of Ago2.

EV release is regulated in a number of cellular model systems. For instance, the activation of purinergic receptors with ATP can trigger MV release (Wilson et al., 2004). Following thrombin receptor activation, platelets are triggered to shed vesicles from the PM and to release exosomes (Heijnen et al., 1998). In response to activation by lipopolysaccharides, dendritic cells increase the release of MVs and change the protein composition (Obregon et al., 2006). Moreover, peptide-loaded immature dendritic cells were triggered to release exosomes following their interaction with T cells recognizing peptide-loaded MHC II (Buschow et al., 2009). Similarly, cross-linking of CD3 in T cells triggers exosome release by T cells, and PM depolarization increases the fast secretion of exosomes by nerve cells (Lachenal et al., 2011). The release of EVs is known to involve increasing intracellular $Ca^{2+}$ concentrations, as reported, for instance, for mast cells (Raposo et al., 1997) and a human erythroleukemia cell line (Savina et al., 2005), and also reviewed in (Taylor and Bebawy, 2019).

The primary evidence for the contribution of Rab GTPases, which need the function of Rab 11 for exosome secretion, comes from reports on immature red blood cell lines (Savina et al., 2002). Knockdown of Rab27a or Rab27b in an RNAi screen in HeLa cells targeting 59 members of the Rab GTPase family remarkably decreased the amount of exosomes secreted (Ostrowski et al., 2010). Rab27 functionally is linked with secretory lysosome-related organelles (Raposo et al., 2007, van Niel et al., 2018), but is clearly also directly implicated in strengthening endocytic compartments in secretion of exosomes. Similarly in other cell systems which host secretory endo/lysosomes, Rab27 might participate directly or indirectly in the transport and tethering at the cell surface of secretory MVEs. Indeed, silencing of two identified Rab27 effectors, Slac2b (EXPH5 (exophilin 5)) and Slp4

(SYTL4 (synaptotagmin-like 4)), prevented exosome secretion and phenocopied silencing of Rab27a and Rab27b, respectively (Ostrowski et al., 2010). On the other hand, targeting Rab GTPase-activating proteins, knockdown of the Rab GTPase-activating proteins TBC1D10A-C and interference with its effector, Rab35, decreased exosome secretion (Hsu et al., 2010). It should be noted that although Rab11, Rab27, and Rab35 are known to participate in exosome secretion and release, careful inactivation of one of these Rabs only incompletely affected this process. The functions of these GTPases could be either cell type dependent, complementary, or indirect by regulating pathways upstream of exosome secretion.

### 1.3.3. EVs as therapeutic targets

EVs contain proteins, nucleic acids and lipids, all of which are involved in the cell to cell communication process, including the transfer of virulence factors between cells (Deolindo et al., 2013). For example, a high concentration of tau protein, a feature of Alzheimer's disease, was demonstrated to be promoted through microglia-secreted EVs (Asai et al., 2015). In addition, disease causing organisms have been reported to use EVs to disseminate infection and evade the immune system (Schwab et al., 2015). Moreover, EVs from hepatitis C virus-infected cells were demonstrated to be effective in transmitting and establishing infection to normal human hepatocytes via RNA in secreted EVs (Ramakrishnaiah et al., 2013).

In relation to an increase in the number of EVs seen in advanced cancer and related disorders with poor outcomes (Silva et al., 2012), a therapeutic target is strategies to minimize the number of EVs in the circulation to optimal levels. In this regard, several studies are being undertaken to target exosome biology either by interfering with EV biogenesis and secretion mechanisms and/or by preventing their communication with host cells by targeting their surface molecules (Raposo and Stoorvogel, 2013). For instance, drugs such as fasudil, amiloride, or inhibitors of neutral sphingomyelinase can interfere with EV secretion as demonstrated both *in vivo* and *in vitro* to

occlude pathogenesis and disease progression (Trajkovic et al., 2008, Record et al., 2018). Comparable findings were also seen with other EV release inhibitors such as dimethyl amiloride, GW4869 and CYP2E1 inhibitor (Cho et al., 2017), highlighting that other small molecules could also regulate EV secretion and content. The actual limitation of these mechanisms would be to locate potential targets that would not hinder the physiological roles of normal cell-derived EVs. The main challenge here is specific inhibition mechanisms yet to be explored, although critical mechanisms in EV biogenesis and release are well documented. Furthermore, in addition to targeting EV biogenesis and release, blockage of EV internalisation by host cells represents a promising strategy in preventing disease progression via cell to cell communication. For instance, several molecular targets were investigated both on EVs and target cells in an effort to block or interfere with liver endothelial cell-secreted EV internalisation *in vivo* and subsequent hindering of fibrosis progression (Wang et al., 2015b).

EVs as therapeutic targets from different cells have been evaluated for managing liver diseases or cancers (Vlassov et al., 2012). Particularly, mesenchymal stem cells (MSCs) regulation of organ injury and its recovery could be attributed to EV-mediated communication between MSCs and tissue cells (Fatima et al., 2017). MSC-derived EVs have been shown to entail therapeutic potential in preclinical research in several types of tissues and conditions; this includes in the treatment of diseases and conditions targeting the central nervous system (Deng et al., 2017, Kim et al., 2016, Ruppert et al., 2018), kidney (Bruno et al., 2009, Eirin et al., 2017, Zou et al., 2016), lungs (Lee et al., 2012, Ahn et al., 2018, Khatri et al., 2018), heart (Lai et al., 2010, Liu et al., 2017), liver (Haga et al., 2017, Li et al., 2013b), bone (Furuta et al., 2016, Qi et al., 2016), and cartilage (Cosenza et al., 2017, Cosenza et al., 2018, Zhang et al., 2016). EVs have some benefits over cells as therapeutic targets and in tissue regulation; however, since they have a shorter half-life than cells, repeated application of EVs is required and poses a limitation for therapeutic purposes (Reiner et al., 2017).

A great utility of EVs is as a means by which to transfer bioactive molecules from the cell of origin to a target cell by crossing cellular barriers. These particular feature makes EVs potential therapeutic agents for delivery of small molecule drugs, therapeutic proteins and RNA species. In contrast to liposomes, EVs have lower toxicity and high intrinsic homing capacity, which can be inferred from their presence in all biological fluids (Lai et al., 2013). Moreover, EVs as therapeutic targets could be manipulated to express biologically active surface molecules that mediate a specific biological role or can interfere with bioactive molecules. Surface molecules can also be used to specifically target EVs towards recipient cell types, which can help crossing of physiologic barriers of cells such as in nerve cells (Alvarez-Erviti et al., 2011). In addition to interfering RNAs, EVs can also be loaded with other types of therapeutic cargo such as lipophilic small molecules. For example, anticancer agents doxorubicin (Tian et al., 2014) and paclitaxel (Yang et al., 2015), as well as the anti-inflammatory agent curcumin (Zhuang et al., 2011) have been successfully loaded into EVs and their efficacies were greatly potentiated over other delivery systems, and resulted in fewer unwanted effects on major organs.

Applying EVs as therapeutic targets is still in its infancy but offers huge potential. Studies to optimize EV isolation as well as resolve the complexities around EV biogenesis, composition and role are underway, including their use in clinical trials. In addition, the routes by which EVs are administered influences their bio-availability (Wiklander et al., 2015), so this needs to be taken into consideration when identifying any therapeutic strategy. Finally, in order to successfully use EVs as therapeutic targets in day-to-day clinical applications, hurdles must still be overcome. With these caveats in mind, it seems likely that EVs will become a platform for highly effective therapeutic targets against a range of diseases and disorders. In this review, I focus on presenting the available information based on recent literature about the roles of EVs in schistosomiasis and other helminth infections

in cellular communication, gene regulation, immune modulation and pathogenesis, and further highlight their importance as targets for therapeutics and diagnostics.

### 1.3.4. Helminth EVs and their roles during infections

Research on the interactions between EVs secreted from protozoan parasites and the cells in an infected host have provided data on new mechanisms of host-parasite communication (Regev-Rudzki et al., 2013, Twu et al., 2013, Meldolesi, 2018). Single celled parasite EVs can modulate pro-inflammatory immune pathways and in recipient cells induce production of regulatory cytokines (Silverman et al., 2010b). However, EV production by multicellular helminth parasites has received considerably less attention.

The identification of ELVs in the trematodes *Echinostoma caproni* and *Fasciola hepatica* was the first report of EVs secreted by parasitic helminths (Marcilla et al., 2012). Since this initial publication, helminth EVs have received increasing attention, particularly given the role of EVs in the transfer of RNAs and other signaling information to target cells, and as novel diagnostic markers of disease (Valadi et al., 2007). Further, *H. polygyrus* derived miRNAs and yRNAs were shown to be transferred into mammalian host cells using EVs, where they regulated host genes associated with immunity and inflammation (Buck et al., 2014, Eichenberger et al., 2018a, Zamanian et al., 2015), suggesting that this may be a shared characteristic for parasitic helminths (Montaner et al., 2014). Moreover, miRNAs were also identified in EVs from the parasitic trematodes *Dicrocoelium dendriticum* (Bernal et al., 2014), *F. hepatica* (Cwiklinski et al., 2015, Fromm et al., 2015, de la Torre-Escudero et al., 2019), *S. japonicum* (Wang et al., 2015a, Zhu et al., 2016a, Zhu et al., 2016b), *S. mansoni* (Nowacki et al., 2015, Sotillo et al., 2016b, Samoil et al., 2018), *O. viverrini* (Chaiyadet et al., 2015b), and *E. caproni* (Marcilla et al., 2012, Trelis et al., 2016). Published studies in the helminths EV field are summarized in Table 1.1.

#### 1.3.4.1. Role in communication

Cells often exchange information to keep cellular homeostasis or to respond to pathogens in the extracellular space. A universal method of communication is physical interaction by adhesion molecules, cell junctions, and soluble factors. However, increasing data are emerging that show EVs play significant roles in genetic cross-talk between cells by transferring proteins, nucleic acids, lipids, and other components, and in this way, cells can adjust the behavior of other cells (Deolindo et al., 2013, Meldolesi, 2018).

The observation that EVs from helminths are endocytosed by host cells implies a role in host-parasite communication. Marcilla and colleagues reported the release of EVs from the liver flukes *F. hepatica* and *E. caproni* and their subsequent internalisation into host cells *ex vivo* (Marcilla et al., 2012). Further, proteomic analyses showed that apart from being enriched in homologs of proteins that are widely found in mammalian EVs, these fluke EVs also contained species-specific protein cargo.

The existence of small RNAs in EVs from protozoan parasites (Pope and Lasser, 2013, Silverman et al., 2010a, Twu et al., 2013) suggests that RNA cargo in parasite EVs may regulate host cell gene expression by acting as miRNAs. The discovery of miRNAs with homology to mammalian miRNAs in the EVs from helminths such as *D. dendriticum* (Bernal et al., 2014), *H. polygyrus* and *Litomosoides sigmodontis* (Buck et al., 2014) strengthened this hypothesis. *H. polygyrus* EVs were shown to contain Argonaute, a protein involved in suppression of gene expression through miRNAs (Hutvagner and Simard, 2008). A direct role for EV-derived miRNA modulation of host cell pathways was demonstrated using microarrays, which showed the suppression of mouse genes predicted to be targets of the worm miRNAs upon incubation of mouse cells with *H. polygyrus* EVs *ex vivo* (Buck et al., 2014). Further, the authors identified a group of RNA species packed within exosomes of *H.*

*polygyrus*, including miRNAs such as let-7, miR200 and bantam, which could suppress expression of the gene encoding mouse phosphatase Dusp1 using a reporter assay.

*L. sigmodontis* miRNAs were demonstrated in sera of infected mice, pointing to the secretion of these miRNAs during infection. In addition to providing a possible mechanism for RNA transfer between parasites and host cells, a role for *H. polygyrus* EVs has been proposed in the down-regulation of Type 2 immune responses and eosinophilia in mice (Buck et al., 2014). Moreover, it was shown that exosome-like EVs secreted from adult *S. japonicum* play roles in regulating gene expression in macrophages (Wang et al., 2015a). Larval (schistosomula) *S. mansoni* secrete small non-coding RNAs (sncRNAs) found within and outside of EVs, including miRNAs and tRNA-derived small RNAs predicted to target host cell gene expression (Nowacki et al., 2015).

Chaiyadet et al. showed that *O. viverrini* secretes EVs that are endocytosed by human cholangiocytes *in vitro* and elicit a cascade of inflammatory and pro-tumorigenic changes within the cell (Chaiyadet et al., 2015b), thereby providing a plausible mechanism by which ES products are internalised by biliary cells of infected hosts (Chaiyadet et al., 2015a) and contribute to the progress of cholangiocarcinoma (Brindley and Loukas, 2017). Internalisation of *O. viverrini* EVs by human cholangiocytes and its effect on gene regulation led to dysregulated expression of proteins with proven roles in wound healing and cancer (Chaiyadet et al., 2015b). Among the proteins significantly regulated were different tropomyosin isoforms, PAK-2, a key kinase involved in tumor cell invasion (Coniglio et al., 2008), and the tight junction protein ZO-2, involved in cell-cell junction assembly and organization, and upregulated during cell proliferation and wound healing (Farkas et al., 2012). The same study further noted that PAK-2 could be involved in tumor progression by interacting with different components of the proteasome complex and with vimentin (a protein that plays a role in maitaining cellular integrity and offering resistance against stress in several epithelial cancers) (Coniglio et al., 2008). Cholangiocyte proteins that participated in the proteasome complex

underwent dysregulated expression upon internalising *O. viverrini* EVs (Chaiyadet et al., 2015b). The proteasome complex controls directly or indirectly many key cellular pathways and has been suggested as a therapeutic target in cancer (Frankland-Searby and Bhaumik, 2012, Rastogi and Mishra, 2012).

Zamanian et al. (2015) showed that EVs secreted by *Brugia malayi* contain let-7 and other key modulators of host gene expression. Let-7 plays an intricate role in macrophage polarization and response to pathogen challenge (Banerjee et al., 2013), and the authors proposed a role in macrophage gene regulation by parasite-derived let-7. Another study which compared the cellular expression levels of miRNAs from *F. hepatica* adult worms with *F. hepatica*-derived EVs reported that all miRNAs of these EVs were expressed and most of them were predicted to target genes involved in immuno-regulation, tissue growth and cancer, suggesting miRNAs are the molecular mediators of immune modulatory functions of EVs (Fromm et al., 2015). A study by Gu et al. demonstrated that both adult and larval (L4) stages of *Haemonchus contortus* secrete EVs packed with specific miRNAs with various suggested role in host-parasite interactions (Gu et al., 2017). Moreover, the same study suggested that only some helminth miRNAs might target host genes, and that their release is a selective process because the profile of released miRNAs in the ES products differed from that of somatic extracts of *H. contortus*.

A study on *B. malayi* L3 demonstrated that purified ELVs were endocytosed by a murine macrophage cell line (Zamanian et al., 2015). Another study by Zhu and co-workers demonstrated that mammalian cells could endocytose *S. japonicum* EVs and incorporate their miRNAs into host cells (Zhu et al., 2016a). Many helminth EVs contain proteins predicted to participate in vesicle biogenesis in mammalian cell EVs, such as Hsps 70/90 and members of the Rab GTPase family (Rab8, Rab10, and Rab11) (Zhu et al., 2016a). Rab proteins are important regulators of intracellular vesicle trafficking between different subcellular compartments using processes including vesicle budding,

membrane tethering and fusion and mobility along the cytoskeleton (Raposo and Stoorvogel, 2013). Further, the identification of RNA-binding proteins such as eukaryotic translation elongation factors 1 alpha (eEF1A) in *S. japonicum* EVs suggests a regulatory role of host gene expression and in host immune evasion (Zhu et al., 2016a).

Coakley et al. showed that *H. polygyrus* derived-EVs are internalised by macrophages whereupon they induce suppression of type 1 and type 2 immune-response-associated molecules – TNF, IL-6, RELMα and Ym1 - and downregulate expression of the IL-33 receptor subunit ST2 (Coakley et al., 2017).

A study which characterised EVs derived from *N. brasiliensis* (Eichenberger et al., 2018a) further highlighted the role of EVs in suppressing inflammation in a mouse model of inflammatory bowel disease. Furthermore, *N. brasiliensis* EVs were internalised by mouse gut organoid cells and contained miRNAs that are predicted to bind to mouse genes involved in immune processes, suggesting a potent anti-inflammatory role in the host gastrointestinal tract. While many immune cell subsets are absent from organoids, studies with cell lines have revealed that *E. granulosus* EVs were internalised by bone marrow derived dendritic cells (Nicolao et al., 2019), and two sub-populations of EVs secreted from adult *F. hepatica* were internalised by murine macrophages (de la Torre-Escudero et al., 2019).

**Table 1. 1. Summary of helminth-derived extracellular vesicles and their putative roles.**

| Taxonomic classification | Helminth | Type of vesicle | EV origin | Cargo composition characterized | EVs target | Applied | Putative Roles | References |
|---|---|---|---|---|---|---|---|---|
| **Trematodes** | *Fasciola hepatica* | Exosome-like vesicles (ELVs) | Adult worms | Proteins | Uptake by intestinal cells | *In vitro* | Not reported | (Marcilla et al., 2012) |
| | | ELVs | Adult worms | Proteins, miRNAs | Not reported | NA | Not reported | (Cwiklinski et al., 2015) |
| | | EVs | Adult worms | miRNAs | Not reported | NA | Not reported | (Fromm et al., 2015) |
| | | EVs | Adult worms | Not reported | Colon cells | *In vivo* | Immunomodulation | (Roig et al., 2018) |
| | | EVs | Adult worms | Proteins | mouse macrophage cells | *In vitro* | Facilitate internalisation | (de la Torre-Escudero et al., 2019) |
| | *Dicrocoelium dendriticum* | Exosomes | Adult worms | Proteins and miRNAs | Not reported | NA | Not reported | (Bernal et al., 2014) |
| | *Schistosoma japonicum* | ELVs | Adult worms | Proteins | Macrophage | *In vitro* | Polarization of host macrophage | (Wang et al., 2015a) |
| | | ELVs | Adult worms | Proteins, miRNA | Uptake by mouse liver cell | *In vitro* | Not reported | (Zhu et al., 2016a) |
| | | EVs | Eggs | miRNA | Uptake by Hepa 1-6, a murine liver cell line | *In vitro* | Not reported | (Zhu et al., 2016b) |
| | *Schistosoma mansoni* | ELVs | Adult worms | Proteins | Not reported | NA | Not reported | (Sotillo et al., 2016b) |
| | | EVs | Schistosomules | Proteins, miRNAs | Not reported | NA | Not reported | (Nowacki et al., 2015) |
| | | ELVs | Adult worms | Proteins, miRNAs | Not reported | NA | Not reported | (Samoil et al., 2018) |
| | | ELVs and MVs | Adult worms | Proteins | Not reported | NA | Not reported | (Kifle et al., 2020) |
| | | EVs | Adult worms | miRNAs | Th cells | *In vivo* and *in vitro* | Modulate Th-2 differentiations | (Meningher et al., 2020) |

| | | | | | | | | |
|---|---|---|---|---|---|---|---|---|
| | *Opisthorchis viverrini* | EVs | Adult worms | Not reported | Uptake by human cholangiocytes | *In vitro* | Inflammatory, liver cell proliferation; antibodies to EVs prevent EVs uptake | (Chaiyadet et al., 2015b) |
| | | EVs | Adult worms | Not reported | Primary bile duct cells | *In vivo and in vitro* | As vaccines | (Chaiyadet et al., 2019) |
| | *Echinostoma caproni* | Exosomes | Adult worms | Proteins | Uptake by intestinal cells | *In vitro* | Not reported | (Andresen et al., 1989, Marcilla et al., 2012) |
| | | Exosomes | Adult worm | Not reported | Systemic blood | *In vivo* | Immune-modulation | (Trelis et al., 2016) |
| **Cestodes** | *Echinococcus multilocularis* | Vesicles | Metacestodes | Not reported | Mononuclear cells/dendritic cells | *In vitro* | Immune-regulation | (Eger et al., 2003, Walker et al., 2004, Hubner et al., 2006) |
| | *Echinococcus granulosus* | Exosomes | Hydatid cyst | Proteins | Not reported | NA | Not reported | (Siles-Lucas et al., 2017) |
| | | ELVs | Hydatid cyst | Proteins | Uptake by dendritic cells | *In vitro* | Immuno-regulation | (Nicolao et al., 2019) |
| | | EVs | Hydatid cyst and protoscolex | Protein | T cells | *In vitro* | Immuno-regulation | (Zhou et al., 2019) |
| | *Taenia crassiceps Mesocestoides corti Echinococcus multilocularis* | EVs | Larvae | Protein and miRNAs | Not reported | NA | Not reported | (Ancarola et al., 2017) |
| **Nematodes** | *Heligmosomoides polygyrus* | Exosomes | Intestinal tract of adult nematode | Proteins, mRNAs, small RNAs and Y RNAs | Intestinal epithelial cells of the host | *In vivo and in vitro* | Immune-modulation in favor of parasite survival | (Buck et al., 2014) |
| | | Exosomes | Adult worms | Proteins | Not reported | NA | Not reported | (Simbari et al., 2016) |

| | | | | | | | | |
|---|---|---|---|---|---|---|---|---|
| | | EVs | Adult/larval worms | Not reported | Uptake by macrophage | *In vivo and in vitro* | Activates macrophages; Protective immunity | (Coakley et al., 2017) |
| | *Brugia malayi* | ELVs | Larval stage | Protein and miRNA | Uptake by macrophage | *In vitro* | Classical activation of macrophages | (Zamanian et al., 2015) |
| | | EVs | Microfilariae, larvae and adult worms | Proteins | Uptake by macrophage | *In vitro* | Immunomodulation | (Harischandra et al., 2018) |
| | *Trichuris suis* | EVs | Larvae | miRNA | NA | NA | Not reported | (Hansen et al., 2015) |
| | *Teladorsagia circumcincta* | ELVs | Larvae | Proteins | Immunoglobulins | *In vitro* | Recognized by IgA and IgG | (Tzelos et al., 2016) |
| | *Haemonchus contortus* | ELVs | Adult and larvae | miRNA | NA | NA | Not reported | (Gu et al., 2017) |
| | *Nippostrongylus brasiliensis* | EVs | Adult worm | Proteins, mRNAs and miRNAs | Uptake by mouse gut organoids | *In vitro and vivo* | Immunomodulation | (Eichenberger et al., 2018a) |
| | *Trichuris muris* | ELVs | Adult worms | Proteins, mRNAs and miRNAs | Uptake by murine colonic organoids | *In vitro* | Not reported | (Eichenberger et al., 2018c) |
| | | EVs | Adult worms | Proteins | Several antigens on EVs targeted by IgG | *In vivo* | vaccine | (Shears et al., 2018) |
| | *Ascaris suum* | EVs | Adult/larvae | Protein and miRNA | Not reported | NA | Not reported | (Hansen et al., 2019) |

*NA: Not applicable*

#### 1.3.4.2. Role in immune modulation

Many researchers have focused on characterizing the soluble ES products released by helminths that can modulate host immune responses. Less well characterised is the role of secreted helminth EVs in this process. A recent study showed the existence of ELVs secreted by *S. japonicum* adult flukes that were reported to elicit production of nitric oxide and other indicators of a Type 1 pathway by the murine macrophage-like cell line RAW264.7. While this study highlighted the potential immunomodulatory roles of *Schistosoma*-derived exosomes during infection, the molecular cargo of the vesicles was not characterized (Wang et al., 2015a). A more recent study by Meningher et al. demonstrated that adult *S. mansoni* parasites secrete miRNAs in EVs that are uptaken by Th cells *in vitro* and showed these EVs downregulate Th2 differentiation by modulating the Th2-specific transcriptional program (Meningher et al., 2020). The same study reported that schistosome miRNAs are found also in Th cells isolated from mesenteric lymph nodes and Peyer's patches of infected mice, where the schistosome miR-10 targets genes encoding MAP3K7 and consequently downregulates NF-κB.

EVs from *F. hepatica* were shown to contain peroxiredoxins and cathepsin cysteine proteases (Marcilla et al., 2012), and HDM-1/MF6p has been identified from *D. dendriticum* exosomes (Bernal et al., 2014). The above proteins have been shown to possess immunomodulatory activity as components of ES products prior to the discovery of helminth EVs (Dalton et al., 2013). In a murine model, *H. polygyrus* EVs were shown to have immunomodulatory effects (Coakley et al., 2016, Buck et al., 2014), supporting earlier findings with ES products from the same parasite (Maizels et al., 2012). Further, *H. polygyrus* exosomes could down-regulate an inflammatory airway response *in vivo*: during the first 24 h of an innate atopic 'danger' response to the fungus *Alternaria alternata in vivo*. *H. polygyrus* exosomes block activation of type 2 innate lymphoid cells and suppress eosinophilic recruitment into the lungs (Buck et al., 2014). In addition, *H. polygyrus* exosomes down-

regulate expression of IL1RL1/ST2 (the IL-33-specific receptor subunit) following co-culture with intestinal epithelial cells *in vitro* and during the allergic asthma response to *Alternaria in vivo* (Buck et al., 2014).

*B. malayi* exosome-like vesicles (ELVs) are internalised by, and induce a classically activated phenotype in host macrophages (Zamanian et al., 2015). Treatment with vesicles resulted in activation of J774A.1, a murine macrophage cell line, with significant increases in the levels of MCP-1, G-CSF, MIP-2 and IL-6 compared to macrophages treated with culture media alone (Zamanian et al., 2015).

The anti-helminth vaccine efficacy of exosomes from *E. caproni* was assessed using BALB/c mice. Development of the parasite was delayed in mice immunised with exosomes, and there was a decrease in symptom severity and increased survival following challenge infection with *E. caproni* (Trelis et al., 2016). Furthermore, exosomes elicited systemic antibody responses that specifically recognised exosome proteins. Following the immunisation with exosomes, elevated levels of IFN-γ, IL-4 and TGF-β were found in the spleen of experimental mice prior to infection. Infection with *E. caproni* induced a further increase in IL-4 and TGF-β, along with a rapid IL-10 overproduction, suggesting development of a Th2/Treg immune response (Trelis et al., 2016).

Coakley and co-authors showed that *H. polygyrus* derived-EVs are internalised by macrophages and they modulate their activation (Coakley et al., 2017). Moreover, EV uptake by macrophages resulted in suppression of type 1 and type 2 immune-response-associated molecules (TNF and IL-6, as well as RELMa and Ym1) and downregulated expression of the IL-33 receptor subunit ST2.

#### 1.3.4.3. Role in pathogenesis

There is growing evidence that EVs from some helminth parasites are involved in the progression of infections. For instance, while the mechanisms that facilitate chronic liver fluke infection to cause

cancer are multifactorial, a major involvement for fluke ES products in inducing a tumorigenic phenotype has been shown (Smout et al., 2011). Identification of *O. viverrini* ES proteins in cholangiocytes of infected hosts posed questions about the mechanisms by which parasite proteins are internalised by host cells, and its sequela for carcinogenic and pathologic changes (Smout et al., 2009, Smout et al., 2011). *O. viverrini* secretes ES products which are subsequently internalised by human cholangiocytes and drive cell proliferation and IL-6 production (Chaiyadet et al., 2015a). Chaiyadet and co-workers (Chaiyadet et al., 2015b) then showed that *O. viverrini* secretes EVs that are endocytosed by human cholangiocytes *in vitro* and elicit a cascade of inflammatory and pro-tumorigenic changes within the cell, thereby providing a plausible mechanism by which ES products are internalised by biliary cells of infected hosts and contribute to the progress of cholangiocarcinoma in infected hosts. The same study demonstrated that *O. viverrini* EVs elicit production of IL-6 from recipient human cholangiocytes, showing a role for these EVs in liver disease progression. Elevated IL-6 levels have been linked to chronic periductal fibrosis and cholangiocarcinoma in *O. viverrini*-infected individuals (Sripa et al., 2011). Furthermore, IL-6 has also been linked to the maintenance of chronic inflammation that could progress to tumor formation (Schafer and Werner, 2008). *O. viverrini* EVs were also involved in driving proliferation of cholangiocytes, a condition that has been reported in both infected human subjects and the hamster infection model (Sripa et al., 2012). This persistent cell proliferation, together with other carcinogenic factors such as chronic immunopathology and high intake of dietary nitrosamines (Sripa et al., 2007), triggers the establishment of malignant changes.

Recent characterisation of the miRNA content of EVs from *S. japonicum* revealed the presence of the Bantam miRNA, and its putative transfer to host liver cells (Zhu et al., 2016a). In *Drosophila*, Bantam miRNA has been reported to target a tumor-suppressor pathway (Hippo signaling), resulting in cellular growth and the suppression of cell death (Nolo et al., 2006). Consequently, schistosome-

specific miRNAs, such as Bantam, may have a role in liver pathology of schistosomiasis. In support of this concept, Zhu and colleagues assessed the mRNA expression of three potential target genes (Utp3, Gins4 and Tysnd1) of schistosome Bantam miRNA in mice. Both *in vitro* cell culture (liver cells treated with *S. japonicum* EVs) and *in vivo* animal studies (in the livers of *S. japonicum* infected mice) clearly showed conserved suppression of the same mRNAs in liver cells.

#### 1.3.4.4. Role as diagnostic markers

The application of exosomes to diagnose infectious diseases has not been intensively studied, but indicates great promise, as EV biomarkers could be of both pathogen and host origin. Strong immune reactivity towards *S. japonicum* EVs was identified when using sera from *S. japonicum*-infected rabbits. These findings act as a baseline for the identification of potential target molecules for the development of schistosomiasis biomarkers and vaccines (Zhu et al., 2016a). In addition, the protein MF6p, also known as MF6p/FhHDM-1, observed in *D. dendriticum* exosomes (Bernal et al., 2014) has been described as a potential marker for its use in diagnosis (Martinez-Ibeas et al., 2013). Moreover, the miRNA isolated in *D. dendriticum* exosomes could be employed as biomarker for the disease (Bernal et al., 2014). In the same analogy, three miRNAs (Bantam, miR-10 and miR-3479) have been described as schistosome-specific miRNAs in the plasma of schistosome infected rabbits (Cheng et al., 2013). Furthermore, Bantam and miR-3479 as well as *S. japonicum* miR-0001 have been verified by miScript PCR as schistosome specific, implicating that these molecules may have potential roles as novel biomarkers for the diagnosis of schistosomiasis (Cheng et al., 2013). A recent study detected schistosome miRNAs in EVs isolated from sera of schistosome infected individuals using qRT-PCR, suggesting that this may provide a new tool for diagnosing schistosomiasis in patients with a low parasite burden (Meningher et al., 2017). However, most of the reports to date that deal with EVs or EV molecules as biomarkers for different parasitic infections are only based on

preliminary observations and putative implications, and hence detailed characterization of EVs to this end is required.

#### 1.3.4.5. Role as vaccination platforms/therapeutic agents

The concept of applying EVs as vaccines has its origin in the cancer field. Exosomes secreted from dendritic cells pulsed with tumour antigens have been assessed in clinical trials as tumour 'vaccines'. The potential application of exosomes as vaccines for infectious diseases is beginning to garner attention. There are several potential benefits to using exosomes as vaccines against pathogens. These include: (1) more stable conformational conditions for the cargo; (2) more efficient interaction with the antigen presenting cells as a result of the expression of adhesion molecules on exosomes; (3) increased molecular distribution due to the capability of exosomes to circulate in bodily fluids and reach distal organs, and (4) because exosomes are one of the body's 'natural' mechanisms for transporting antigens between cells and one that likely has a potential role in cross-priming (Schorey et al., 2015). One way of applying helminth-derived EVs as vaccines is through synthetic vesicles containing the antigen of interest (Egesa et al., 2017).

There are emerging indications from studies done in murine models that EVs from parasites have a potential role as vaccine candidates. The administration of *E. caproni* exosomes to mice primed the immune response and reduced the severity of clinical signs in *E. caproni* infection (Trelis et al., 2016). Moreover, administration to mice of *H. polygyrus*-derived EVs formulated with alum generated protective immunity against larval challenge, further highlighting the potential of EVs as anti-helminth vaccine candidates (Coakley et al., 2017). This study, however, did not identify the specific protective EV antigens. The abundance of proteasome components in *S. japonicum* EVs (Zhu et al., 2016a) implicated the ubiquitin– proteasome system in a regulatory role during schistosome infection. Because of the vital role of the proteasome in parasite invasion (Mathieson et al., 2011), targeting proteasome molecules could be a candidate strategy for anti-schistosome vaccination.

Research has demonstrated the existence of numerous known vaccine candidates in EVs secreted by *S. mansoni* (Sotillo et al., 2016b, Samoil et al., 2018). For instance, *Sm*-TSP-2 is a member of the CD63 family of TSPs, a widely conserved exosome marker. *Sm*-TSP-2 is abundant in the *S. mansoni* EV membrane and is a candidate antigen for *Schistosoma* vaccine development (Tran et al., 2006, Sotillo et al., 2016b). There is a growing body of evidence that EV TSPs are good vaccine candidates. For example, blood-borne allogeneic exosome internalisation by dendritic cells could be interrupted with antibodies against EV TSPs (Morelli et al., 2004). In terms of helminth infections, Chaiyadet et al. (2015b) highlighted the involvement of *Ov*-TSP-1 in *O. viverrini* EV internalisation by cholangiocytes, whereby antibodies to the large extracellular loop blocked EV uptake by cholangiocytes. A more recent study by Chaiyadet et al. (Chaiyadet et al., 2019) demonstrated in a hamster vaccination-challenge model that vaccination with *O. viverrini* secreted EVs and recombinant EV TSPs induced protective antibodies that blocked EV uptake by target primary bile duct cells *in vitro.* Moreover, parasite challenge of hamsters after vaccination with both EVs and recombinant surface proteins significantly reduced adult worm loads compared to the control group administered adjuvant only. Indeed, TSPs are efficacious vaccine antigens in numerous helminth infections (Dang et al., 2012, Joseph and Ramaswamy, 2013, Tran et al., 2006, Loukas et al., 2007) and these data suggest that the mechanism of vaccine efficacy is associated with blockade of parasite EV internalisation by host cells *in vivo* and subsequent interruption of key physiological and pathological processes driven by EVs. These findings indicate that targeting exosomes and their surface proteins may provide a key anti-parasite vaccination strategy.

Sotillo et al. demonstrated the existence of several vaccine candidates, including TSPs, on EVs secreted by *S. mansoni* (Sotillo et al., 2016b). Adult *S. mansoni* release ELVs which are 50 – 130 nm in size, with over 80 identifiable proteins, 5 of which are TSPs as well as an abundant saposin-like protein. Some of these proteins are homologues of previously identified vaccine candidates for

helminth infections, and some are common to multiple life-cycle stages, including eggs, suggesting that vaccines based on these proteins could target different parasite stages. If EV internalisation by host cells plays a significant role in establishing parasitism, the disruption of this process via neutralizing antibodies may explain why vaccines directed against EV membrane proteins show efficacy.

The immunoregulatory properties of helminth EVs opens up another therapeutic strategy for their use, notably for the treatment of inflammatory diseases. Mice treated with EVs from *N. brasiliensis* prior to administration of a T cell-dependent colitis inducing agent, TNBS, were protected against colitic pathology and had reduced expression of IL-6, IFNγ IL-17a and IL-1β and elevated expression of IL-10 in the colon compared to mice that received a single intraperitoneal injection of control vesicles from grapes (Eichenberger et al., 2018a). Moreover, administration of *F. hepatica* EVs to mice prior to induction of T cell-independent colitis using dextran sulfate sodium ameliorated the pathological symptoms, suppressed pro-inflammatory cytokine expression and interfered with both MAPK and NF-kB pathways (Roig et al., 2018). These findings indicate that EVs from parasitic helminths can modulate inflammatory responses and exert a protective effect in the gut at least.

## 1.4. This project

Countless individuals are infected with schistosomes, and treatment depends on a single drug. After treatment, rapid reinfection occurs, precipitating the need for more rigorous practical control measures, such as vaccination. This PhD project focuses on identifying *S. mansoni* EV molecules that could be targeted for interruption of EV-mediated host-parasite communication and host cell gene regulation, with a specific focus on assessing the vaccine potential of these vesicles and their recombinant surface proteins in a mouse model of schistosomiasis.

The hypotheses underpinning this thesis are that:

1. EVs secreted from *S. mansoni* contain key surface molecules involved in their biogenesis, binding to and internalisation by host cells.
2. Vaccines against EV surface proteins will interrupt EV internalisation by host cells and could disrupt EV-mediated parasite-host communication.

My study is significant and novel given the impact it could potentially have on our understanding of schistosome biology and parasitic diseases in general. It will add vital new knowledge to- and fill the gap in- the field of molecular parasitology and significantly to the wider science community, and the findings could serve as a useful resource for future research, specifically in vaccine discovery and development against schistosomiasis.

# Chapter 2

## Molecular characterisation of *Schistosoma mansoni* extracellular vesicles

### Preamble

*Schistosoma* and other helminths secrete EVs with putative roles in host-parasite communication. In this chapter, I carried out a comprehensive proteomic analysis of two populations of *S. mansoni*-derived EVs – exosome-like vesicles (ELVs) and MVs. Several methods were implemented in order to undertake proteomic profiling of these EVs. Vesicles were isolated from the ES products of adult worms in culture medium using ultracentrifugation techniques. ELVs were purified by Optiprep iodixalon gradient, and fractions containing vesicles were confirmed by tunable resistive pulse sensing using a qNano instrument for both ELVs and MVs. I characterised proteins present in the membranes of the EVs (including external trypsin-liberated peptides, integral membrane proteins (IMPs) and peripheral membrane proteins (PMPs)), as well as cargo proteins, using LC-MS/MS. Database search and protein sequence analysis were carried out using different software. Sequences of the identified proteins were blasted and gene ontology annotations were obtained. Further, protein family analysis, signal peptide and transmembrane domain predictions were performed on the identified proteins using bioinformatics tools. The results provide the first report of a comprehensive compartmental proteomic analysis of adult *S. mansoni*-derived EVs. This chapter has been published as (Kifle et al., 2020).

## 2.1. Introduction

Schistosomiasis vaccine and diagnostic antigen discovery has focused on several developmental stages of the parasite with an emphasis on the tegument and ES proteomes (Knudsen et al., 2005, Liu et al., 2009, Perez-Sanchez et al., 2006, Mathieson and Wilson, 2010, Cass et al., 2007, Curwen et al., 2004, Wilson, 2012, Sotillo et al., 2019a). Despite advances in the characterisation of the secretome, substantially less is known about the molecular mechanisms involved in the release of these molecules. One such pathway is the release of EVs which has been recently described in *S. mansoni* (Sotillo et al., 2016b, Samoil et al., 2018) and other *Schistosoma* spp. (Wang et al., 2015a, Zhu et al., 2016a, Zhu et al., 2016b). Several studies have demonstrated that parasite-derived EVs play a key role during helminth infections. For example, EVs are capable of modulating host innate immune responses (Buck et al., 2014, Wang et al., 2015a). In addition, the administration of exosomes to mice primes the immune response and reduces the severity of clinical signs in *E. caproni* infection (Trelis et al., 2016). Further, EVs can carry and confer virulence factors to the host, producing biological effects (Buck et al., 2014, Barteneva et al., 2013, Silverman et al., 2010a). Internalisation of *O. viverrini* EVs by human cholangiocytes led to dysregulated expression of proteins involved in wound healing and cancer (Chaiyadet et al., 2015b). Moreover, immune reactivity towards *S. japonicum* EVs was identified when using sera from *S. japonicum*-infected rabbits (Zhu et al., 2016a). These findings serve as a baseline for the identification of potential target molecules for the development of schistosomiasis biomarkers and vaccines derived from EVs.

Protein composition of trematode-derived EVs has been characterised in several species using mass spectrometry approaches. Species studied include *F. hepatica* (Marcilla et al., 2012, Young et al., 2010, Cwiklinski et al., 2015, de la Torre-Escudero et al., 2019), *D. dendriticum* (Bernal et al., 2014), *S. japonicum* (Wang et al., 2015a, Zhu et al., 2016a, Zhu et al., 2016b), and *E. caproni* (Marcilla et al., 2012). While the protein composition of *S. mansoni* EVs has been characterized at a crude, whole-

vesicle level (Sotillo et al., 2016b, Samoil et al., 2018, Nowacki et al., 2015), the sub-vesicular distribution of those proteins has not been described. Herein, to my knowledge for the first time, I characterise the compartmental proteome content of *S. mansoni*-derived both ELVs and MVs.

## 2.2. Material and methods

### 2.2.1. Ethics statement

The study obtained ethical approval (A2004, A2391 and A2395) from the Animal Ethics Committee at James Cook University. All studies involving mice were performed at the animal facilities of the Australian Institute of Tropical Health and Medicine in accordance with guidelines and protocols approved by the Animal Ethics Committee.

### 2.2.2. Mice and parasite material

Male 6-8 week old BALB/c mice (Animal Resource Centre, WA) were used for the study. All animals were maintained under standard conditions with food and water *ad libitum*. *S. mansoni* (Puerto Rican strain)-infected *Biomphalaria glabrata* snails were provided by the National Institute of Allergy and Infectious Diseases Schistosomiasis Resource Centre for distribution through the Biodefense and Emerging Infections Research Resources Repository, NIAID, National Institutes of Health, USA: *S. mansoni*, Strain NMRI; exposed *B. glabrata*, NR-21962.

### 2.2.3. Snail shedding and infection of mice

Cercariae were shed from snails by exposure to light at 28°C for 1.5 h (Ramalho-Pinto et al., 1974). 1974). To obtain adult worms, 6-8 week old male BALB/c mice were infected with 120 cercariae via tail penetration and parasites harvested by vascular perfusion at 7-8 weeks post-infection (Lewis et al., 1986).

### 2.2.4. Parasite culture and collection of excretory/secretory products

To harvest ES products, *S. mansoni* adult worms were obtained from infected mice as described previously (Tucker et al., 2013). Briefly, mice were euthanized using an intraperitoneal injection of 0.2 ml pentobarbital/heparin solution followed by $CO_2$ gas administration and worms were perfused using perfusion solution (0.15 M sodium chloride with 0.03 M sodium citrate dehydrate in water) and collected in a container (Tucker et al., 2013). Worms were washed three times using serum-free Basch media (0.5 µM hypoxanthine (Sigma), 1 µM serotonin (Sigma), 1 µM hydrocortisone (Sigma), 0.2 µM triiodothyronine (Calbiochem), 8 mg insulin (Lifetech), 0.5× MEM vitamin (Invitrogen), 2× antibiotic/antimicotic (Invitrogen), 50 ml Schneider Drosophila medium (Invitrogen), 0.01 M HEPES (Invitrogen), and Eagle's basal medium (Invitrogen) to make 1 L final volume) (Basch, 1981) and cultured for 3 h at 37°C with 5% $CO_2$ in serum-free Basch media with a density of approximately 50 worm pairs in 5 ml of media. The culture media was discarded after 3 h, and replaced with fresh culture media. Worms were cultured for a further 10 days and ES products were collected every 24 h, centrifuged at 4°C (500 *g*, 2,000 *g* and 4,000 *g* for 30 min each) to pellet and discard parasite material such as tegumental debris and eggs, and kept at -80°C until further analysis. Worms were observed by microscopy daily to ensure that all were motile during *in vitro* culture. Immotile worms were removed as soon as they were detected.

### 2.2.5. EV isolation

EVs were isolated and purified following established methods previously described for *S. mansoni* (Sotillo et al., 2016b). After differential centrifugation, samples were concentrated using a 10 kDa spin concentrator (Merck Millipore), and centrifuged at 15,000 *g* for 1 h at 4°C to pellet MVs, which were washed with PBS three more times and kept at -80°C until use. To collect ELVs, supernatant was ultracentrifuged using an MLS-50 rotor (Beckman Coulter) at 120,000 *g* for 3 h at 4°C, and the resultant pellet was resuspended in 200 µl of PBS and subjected to Optiprep® discontinuous gradient

separation. One ml of 40%, 20%, 10% and 5% iodixanol solutions prepared in 10 mM Tris-HCl, 0.25 M sucrose, pH 7.2, was layered in decreasing density using an ultracentrifuge tube, and the 200 µl containing the resuspended EVs was added to the top layer and ultracentrifuged at 120,000 *g* for 18 h at 4°C. A control tube was prepared in a similar way, replacing EVs with PBS to calculate the density of fractions. A total of 12 sample fractions were collected from the Optiprep® discontinuous gradient, and the excess Optiprep® solution was buffer exchanged using PBS containing 1× EDTA-free protease inhibitor cocktail (Santa Cruz, Dallas, TX, USA) using a 10 kDa spin concentrator. The absorbance was measured at 340 nm for each fraction obtained from the control tubes, and their densities were calculated. Finally, protein concentration of all sample fractions was measured using a Bradford Protein Assay Kit (ThermoFischer).

### 2.2.6. Tunable Resistive Pulse Sensing analysis of EVs

The particle concentration and size distribution of each fraction was analysed for both *S. mansoni*-derived ELVs and MVs by tunable resistive pulse sensing (TRPS) using a qNano instrument (Izon) following the manufacturer's instructions. Nanopore NP150 and NP300 were used for ELVs and MVs, respectively. Pressure and voltage values were set to optimize the signal to ensure high sensitivity. Samples were diluted 1:5 in electrolyte (Izon) before applying to the nanopore. Calibration was performed using CP100 and CP400 carboxylated polystyrene calibration particles (Izon) for ELVs and MVs, respectively, at a 1:2,000 dilution. Size distribution and concentration of particles were analyzed using the software provided by Izon (version 3.2). Purity analysis of both ELVs and MVs (number of particles/µg of protein) was performed following methods described by Webber and Clayton (2013).

### 2.2.7. Trypsin shaving and sequential protein extraction of purified *S. mansoni* EVs

Peptides from surface-accessible proteins were released by trypsin hydrolysis of EVs using a protocol described previously (Robinson et al., 2013). Briefly, sequencing-grade trypsin (1 µg/µl) was added to purified EVs for 10 min at 37°C. Treated EVs were then centrifuged at 120,000 *g* at 4°C for 1 h, and surface peptides were obtained from the supernatant. EVs collected as a pellet were further processed to investigate proteins associated with the EV membrane and within the EV lumen. Briefly, EVs were resuspended in water and sonicated (3x) which resulted in the release of EV cargo content which was recovered from the supernatant by centrifugation at 120,000 *g* for 1 h at 4°C. Subsequently, the pellet was incubated with 0.1 M $Na_2CO_3$ (pH 11) on ice for 30 min and then centrifuged at 120,000 *g* at 4°C for 1 h to recover peripheral membrane proteins (PMPs) from the supernatant. Finally, integral membrane proteins (IMPs) were obtained by solubilizing the pellet in 1% Triton X-100/2% sodium dodecyl sulphate (SDS) at 37°C for 15 min.

### 2.2.8. In-gel digestion of proteins

For the proteomic analysis, each separated component of cargo, integral membrane and peripheral membrane proteins were electrophoresed on a 10% SDS-PAGE gel for 60 min at 140 V. Tryptic in-gel digestion was performed as described previously with minor modifications (Sotillo et al., 2014). In brief, the gel was stained with Coomassie blue (0.03%), destained overnight and each lane was cut into 7 slices (approximately 1 $mm^2$). Each band was destained by washing twice in 50% acetonitrile with 200 mM ammonium bicarbonate at 37°C for 45 min, reduced with 20 mM dithiothreitol (Sigma) in 25 mM ammonium bicarbonate for 1 h at 65°C, alkylated with 50 mM iodoacetamide (IAM, Sigma) in 25 mM ammonium bicarbonate at 37°C for 15 min and digested with 100 ng/µl trypsin (Sigma) at 37°C for 18 h. Peptides were extracted in 50% acetonitrile with 0.1% trifluoroacetic acid. The last step was performed three times to maximize peptide recovery. All peptides were finally dried in a vacuum concentrator. Samples were then resuspended in 10 µl of 0.1% trifluoroacetic acid and

tryptic peptides were desalted using a Zip-Tip® column (Merck Millipore) pipette tip according to manufacturer's protocol and dried in a vacuum concentrator before analysis using liquid chromatography-tandem mass spectrometry (LC-MS/MS). The experimental work-flow from sample collection to proteomic analysis is shown in Figure 2.1.

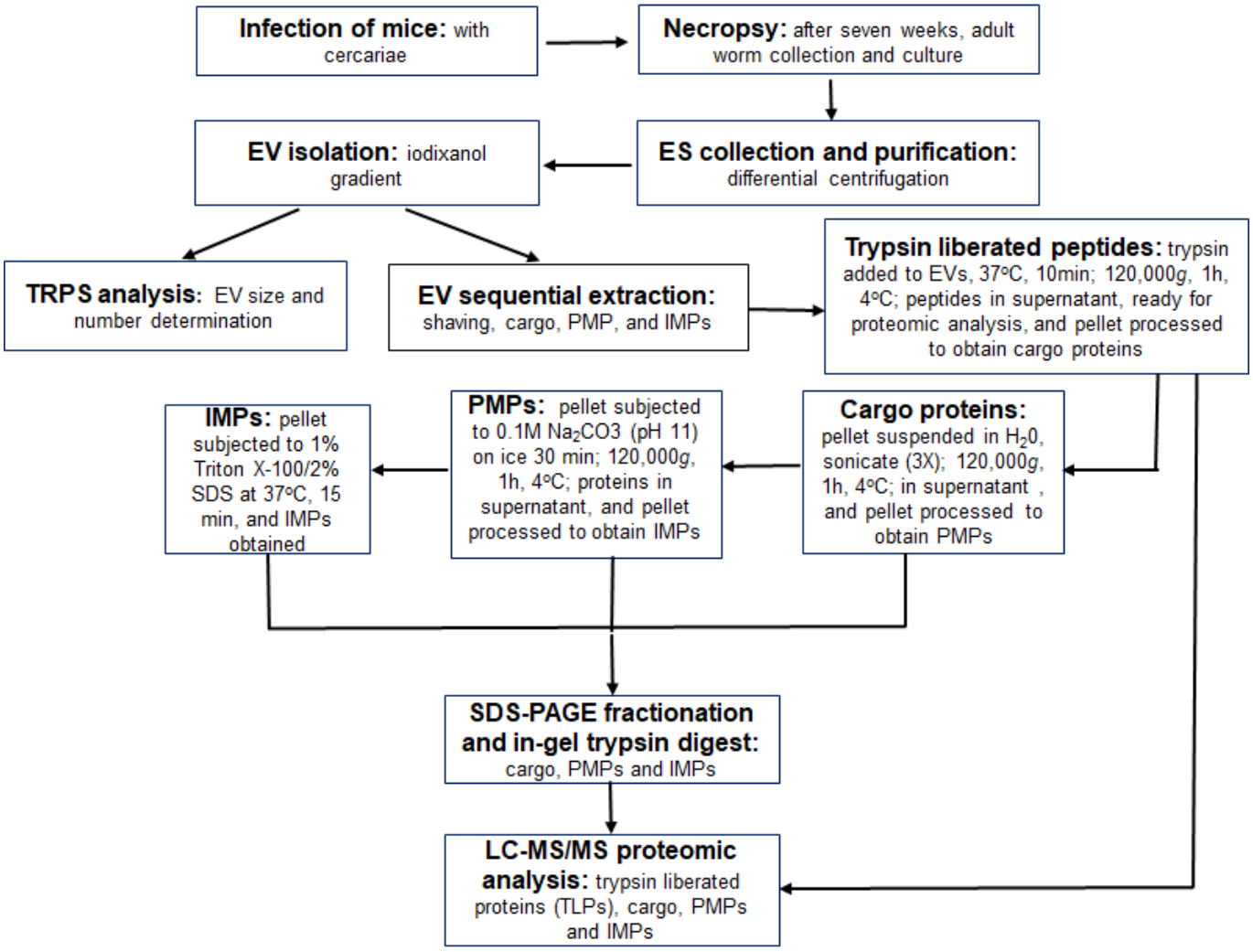


**Figure 2. 1. Overview of experimental workflow for proteomic analysis of *S. mansoni* extracellular vesicles.** Seven weeks after infection of mice with *S. mansoni* cercariae, adult worms were perfused and cultured. Excretory/secretory (ES) products were collected and purified from cell-conditioned media using differential centrifugation (500 *g*, 2,000 *g* and 4,000 *g* at 4°C, each for 30 min), followed by ultracentrifugation at 15,000 *g* at 4°C for 1 h to pellet MVs. The supernatant was then subjected to ultracentrifugation at 120,000 *g* at 4°C for 3 h to pellet the ELVs. The purity and concentration of

ELVs were enhanced using an Optiprep® gradient. Size and concentration of EVs were determined by tunable resistive pulse sensing using a qNano instrument. For the proteomic analysis, EV surface-exposed proteins were obtained using trypsin shaving, then, sequential extraction resulted in purification of cargo proteins, PMPs and IMPs. Proteins were submitted to in-gel trypsin digestion and LC-MS/MS for proteomic analysis.

### 2.2.9. LC-MS/MS protein analysis

Tryptic fragments from each sample were resuspended in 8 µl of 0.1 % formic acid in LC-MS/MS-grade water and separated chromatographically by an Eksigent nanoLC 415 system using a 15 cm long Eksigent column (C18-CL particle size 3 µm, 120 Å, 75 µm ID) and a linear gradient of 3-40% solvent B (100 acetonitrile/0.1% formic acid [aq]) for 45 min followed by 40-80 % solvent B in 5 min. A pre-concentration step (10 min) was performed employing an Eksigent Trap-column (C18-CL, 3 µm, 120 Å, 350 µm x 0.5 mm) before commencement of the gradient. A flow rate of 300 nl/min was used for all experiments. The mobile phase consisted of solvent A (0.1% formic acid [aq]) and solvent B. Eluates from the RP-HPLC column were directly introduced into the PicoView ESI ionisation source of a TripleTOF 6600 MS/MS System (AB Sciex) operated in positive ion electrospray mode. All analyses were performed using Information Dependant Acquisition. AnalystTF 1.7.1 (Applied Biosystems) was used for data analysis. Briefly, the acquisition protocol consisted of the use of an Enhanced Mass Spectrum scan with 15 sec exclusion time and 100 ppm mass tolerance. A cycle time of 1800 ms was used to acquire full scan TOF-MS data over the mass range 400–1250 m/z and product ion scans over the mass range of 100–1500 m/z for up to 30 of the most abundant ions with a relative intensity above 150 and a charge state of +2 − +5. Full product ion spectra for each of the selected precursors were then used for subsequent database searches.

### 2.2.10. Database search and protein sequence analysis

Data were searched against a database comprising the *S. mansoni* proteome obtained from WormBase ParaSite (http://parasite.wormbase.org/) appended to the common Repository of Adventitious Proteins (cRAP; http://www.thegpm.org/crap/) and their reversed decoy sequences using SearchGUI (v3.3.5). X!Tandem (vAlanin), Comet (v2018.01 rev.2), Tide (v3.2.x), MyriMatch (v2.1) and MS-GF + (v2016.01.02) were the search engines used, and the identification results were validated using PeptideShaker (v1.16.31). All searches were conducted employing the following search parameters: trypsin as digestion enzyme, maximum missed cleavages, 2; precursor ion mass tolerance ± 10 ppm, fragment ion tolerance ±0.1 Da; fixed modifications: carbamidomethylation of cysteine; variable modifications: deamidation of asparagine and glutamine, oxidation of methionine; Peptide Spectrum Matches (PSMs), peptides and proteins were validated at a 1.0% False Discovery Rate estimated using the decoy hit distribution. Reported results correspond to those proteins showing ≥ 2 distinct unique peptides. An estimate of the relative abundance of the predicted proteins was assessed using the spectrum counting abundance index (Milac et al., 2012). The mass spectrometry proteomics data have been deposited to the ProteomeXchange Consortium via the PRIDE partner repository with the dataset identifier PXD015857 and 10.6019/PXD015857.

### 2.2.11. Bioinformatic analyses

Gene ontology (GO) annotations were obtained using the Blast2GO software (Conesa et al., 2005), and GO terms were assigned as biological process or molecular function. Only children GO terms were used for subsequent analysis to avoid redundancy in GO terms. REViGO was used to summarize and plot GO terms (Supek et al., 2011). Protein family (Pfam) analysis was performed at the E-value <0.05 threshold using HMMER software (Conesa et al., 2005). Signal peptides and transmembrane domains were predicted using SignalP v4.1 and TMHMM v2.0, respectively (Emanuelsson et al., 2007, Krogh et al., 2001).

## 2.3. Results

### 2.3.1. EV size, concentration and purity

*S. mansoni* adult worm-derived ELVs were purified using an iodixanol density gradient as described previously for other helminths (Sotillo et al., 2016b, Eichenberger et al., 2018a, Eichenberger et al., 2018c). The density and protein concentration of all 12 fractions collected from the gradient were analysed. Fractions of ELVs from different batches with densities ranging from 1.09 to 1.22 g/ml (fractions containing *S. mansoni* ELVs) as described previously (Sotillo et al., 2016b) were combined and subjected to TRPS analysis using a qNano instrument to determine size and concentration of ELVs (Figure 2.2A). Likewise, MVs collected from different batches of EVs were combined, protein concentration was measured and TRPS analysis was performed to obtain size and concentration (Figure 2.2B) of the MV-enriched sample. Accordingly, purity analysis of both ELVs (4.1 X $10^8$ particles/µg protein) and MVs (1.6 X $10^7$ particles/µg protein) (Figure 2.2C) was also performed as described previously (Webber and Clayton, 2013).

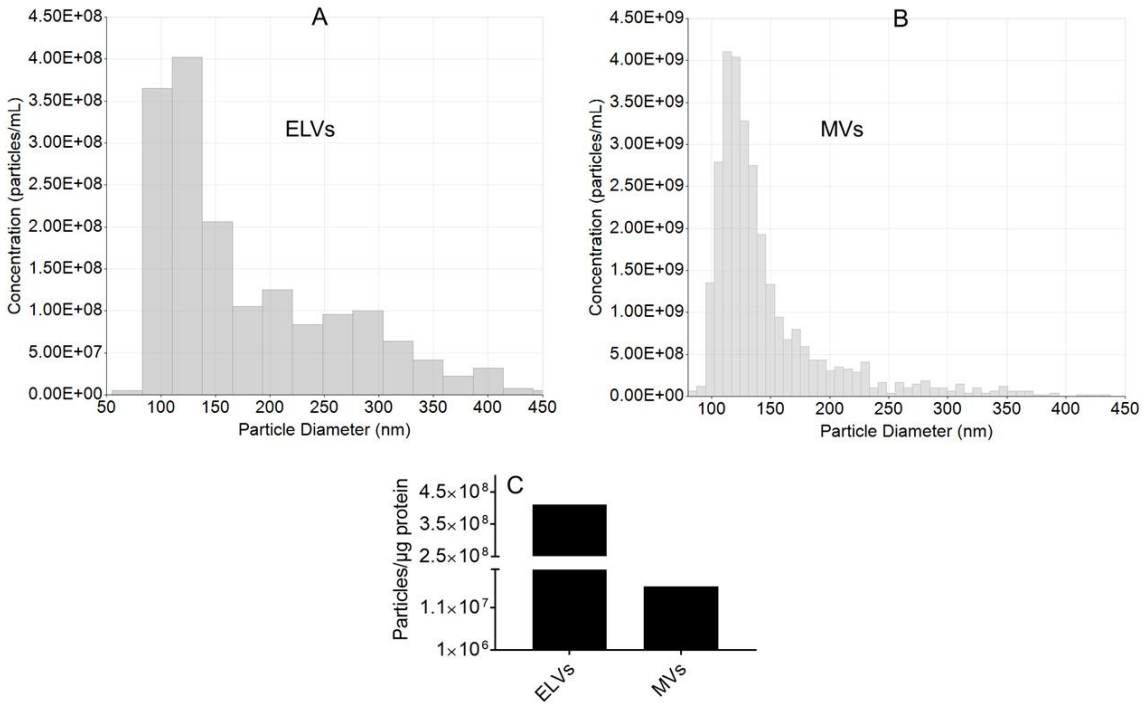

**Figure 2. 2. Tunable resistive pulse sensing (TRPS) analysis and purity of *S. mansoni* extracellular vesicles.** Particle size (x-axis) and number (y-axis) of ELVs (A) and MVs (B) after purification were analysed by TRPS using a qNano instrument (iZon). The purity of both ELVs and MVs (C) was determined according to Webber and Clayton (Webber and Clayton, 2013).

### 2.3.2. Proteomic analysis of *S. mansoni*-derived ELVs and MVs

A proteomic analysis on each of the four components - TLPs, cargo proteins, IMPs and PMPs - of both ELVs and MVs was performed. In total, 286 and 716 different proteins were identified from *S. mansoni*-derived ELVs (Figure 2.3A) and MVs (Figure 2.3B), respectively. Of these, 27 were specific to ELVs and 457 specific to MVs, while 259 proteins were identified in both types of EVs (Figure 2.3C). Antioxidants such as peroxiredoxin (Prx3) and proteins involved in exosome biogenesis or trafficking, such as vacuolar protein sorting-associated protein 28 homolog, were among the 27 ELV-specific proteins identified (Table 2.1, Figure 2.4). ELVs contained 72 TLPs, 52 cargo proteins, 238 proteins in the IMP component and 81 proteins in the PMP component, with the top 20 proteins identified from each compartment based on spectrum counting is presented as Supplementary Table 2.1, 2.2, 2.3 and 2.4, respectively. MVs, on the other hand, contained 218 TLPs, 138 cargo proteins, 576 IMPs and 142 PMPs, with the top 20 proteins identified from each compartment based on spectrum counting is presented as Supplementary Table 2.5, 2.6, 2.7 and 2.8, respectively. Some of the most abundant proteins identified, based on spectrum counting, in both *S. mansoni*-derived ELVs (Supplementary Table 2.1-2.4) and MVs (Supplementary Table 2.5-2.8), included the TSPs TSP-2 and TSP-4, glutathione-S-transferase (GST), saponin B domain-containing protein, DM9 domain-containing protein, cathepsin domain-containing proteins, 13 kDa tegumental antigen, and histone H4-like protein. However, the TSP Sm23 was only identified in MVs.

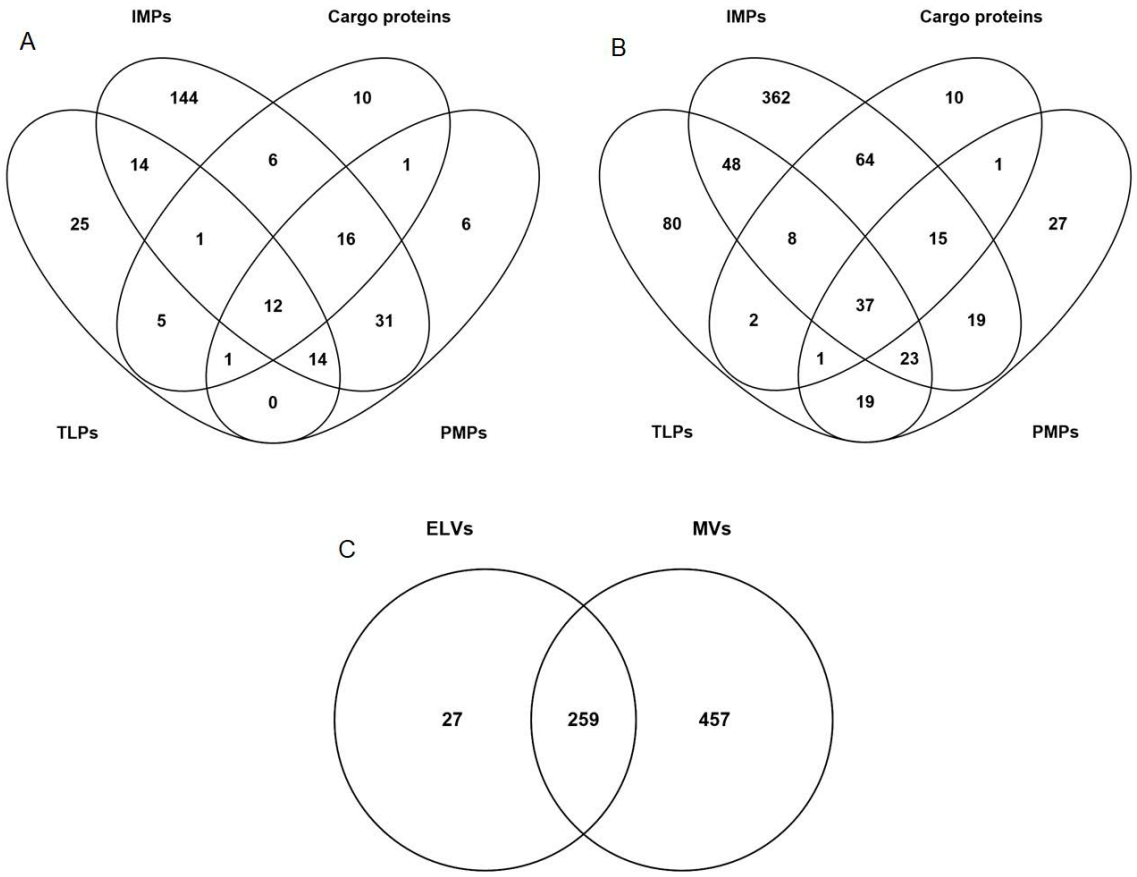


**Figure 2. 3. Shared and specific adult *S. mansoni* extracellular vesicles proteins.** Venn diagram representing the number of proteins identified from the four sub-vesicular components, enumerating specific and shared proteins of ELVs (A) and MVs (B) and between the two vesicle types (C).

**Table 2. 1. Functional annotation of proteins from *S. mansoni* exosome-like vesicles.**

| | Description | # Unique peptides | | | |
|---|---|---|---|---|---|
| **Accession number** | **Proteases/inhibitors** | **TLPs** | **Cargo** | **IMPs** | **PMPs** |
| Smp_032580.1 | subfamily T1A non-peptidase homologue (T01 family) | 2 | 4 | 0 | 0 |
| Smp_070930.1 | proteasome (prosome macropain) subunit alpha type 4 | 4 | 3 | 0 | 0 |
| Smp_034490.1 | Proteasome subunit beta type-6 | 0 | 2 | 0 | 0 |
| Smp_187140.1 | Cathepsin L-like proteinase precursor | 0 | 3 | 4 | 5 |
| Smp_301340.1 | proteasome (prosome, macropain) subunit, beta type,1 | 0 | 2 | 0 | 0 |
| Smp_214190.1 | Calpain | 4 | 4 | 11 | 3 |

| | | | | | |
|---|---|---|---|---|---|
| Smp_340060.1 | Mastin precursor | 0 | 6 | 9 | 8 |
| Smp_006390.1 | cysteine protease inhibitor | 0 | 0 | 3 | 0 |
| Smp_030000.1 | Putative aminopeptidase W07G4.4 | 10 | 0 | 7 | 0 |
| Smp_067060.1 | cathepsin B-like peptidase (C01 family) | 0 | 0 | 2 | 2 |
| Smp_103610.1 | cathepsin B-like peptidase (C01 family) | 0 | 0 | 4 | 2 |
| Smp_343260.1 | cathepsin L, a | 3 | 0 | 7 | 3 |
| Smp_083870.1 | Putative aminopeptidase W07G4.4 | 4 | 0 | 0 | 0 |
| Smp_029500.1 | Thimet oligopeptidase | 2 | 0 | 0 | 0 |
| Smp_212920.1 | 20S proteasome subunit alpha 6 | 2 | 0 | 0 | 0 |
| Smp_207080.1 | Proteasome subunit alpha type-6 | 2 | 0 | 0 | 0 |
| Smp_089670.1 | Alpha-2-macroglobulin-like protein 1 | 5 | 35 | 0 | 2 |
| Smp_090080.1 | Estrogen-regulated protein EP45 precursor | 0 | 5 | 0 | 0 |
| Smp_075800.1 | hemoglobinase (C13 family) | 0 | 0 | 2 | 0 |
| Smp_007550.1 | Uncharacterized | 2 | 0 | 0 | 0 |
| | **Biogenesis/vesicle trafficking** | | | | |
| Smp_035620.1 | Multivesicular body subunit 12B | 0 | 0 | 3 | 0 |
| Smp_048940.1 | Vacuolar protein sorting-associated protein 37B | 0 | 0 | 3 | 0 |
| Smp_055880.1 | chmp1 (chromatin modifying protein) (charged multivesicular body protein), putative | 0 | 0 | 8 | 0 |
| Smp_067540.1 | Vacuolar protein sorting-associated protein 28 homolog | 0 | 0 | 2 | 0 |
| Smp_034870.1 | AP-2 complex subunit beta | 0 | 0 | 4 | 0 |
| Smp_055870.1 | vesicle-associated membrane protein 7-like | 0 | 2 | 11 | 2 |
| Smp_068530.1 | putative syntenin | 0 | 2 | 8 | 3 |
| Smp_074140.1 | Annexin A13 (Annexin XIII) | 3 | 4 | 13 | 9 |
| Smp_013690.1 | BRO1 domain-containing protein BROX | 3 | 0 | 16 | 9 |
| Smp_071630.1 | Ras-related protein Rab-2A | 0 | 0 | 6 | 0 |
| Smp_077720.1 | putative annexin | 0 | 0 | 6 | 5 |
| Smp_062300.1 | Ras-related C3 botulinum toxin substrate 1 | 0 | 0 | 3 | 0 |
| Smp_045550.1 | putative annexin | 0 | 0 | 11 | 0 |
| Smp_045560.1 | putative annexin | 0 | 0 | 5 | 2 |
| Smp_067140.1 | Ras-related protein Rab-7a | 0 | 0 | 2 | 0 |
| Smp_104670.1 | ras-related protein Rab-8A isoform X1 | 0 | 0 | 3 | 0 |
| Smp_139340.1 | Ras-related protein Rab-27A | 0 | 0 | 4 | 0 |
| Smp_094820.1 | Vacuolar protein sorting-associated protein VTA1-like protein | 0 | 0 | 4 | 0 |
| Smp_094420.1 | Rab GDP dissociation inhibitor alpha | 0 | 0 | 4 | 4 |
| Smp_210430.1 | Rab-protein 8 | 0 | 0 | 2 | 0 |
| Smp_104310.1 | rab11, putative | 0 | 0 | 7 | 0 |
| Smp_312770.1 | Ras-related protein Ral-A | 0 | 0 | 3 | 0 |
| Smp_045710.1 | Charged multivesicular body protein 4b | 0 | 0 | 6 | 0 |
| | **Antioxidants** | | | | |
| Smp_309480.1 | Uncharacterized | 2 | 2 | 4 | 0 |
| Smp_004470.1 | Peroxiredoxin, Prx3 | 2 | 0 | 0 | 0 |
| Smp_158110.1 | Thioredoxin peroxidase | 2 | 0 | 0 | 0 |
| | **Membrane structure** | | | | |
| Smp_040970.1 | putative vacuolar proton atpases | 0 | 2 | 23 | 5 |

| | | | | | |
|---|---|---|---|---|---|
| Smp_041460.1 | tetraspanin, putative (*Sm*-TSP-D76) | 0 | 7 | 9 | 7 |
| Smp_017730.1 | 200-kDa GPI-anchored surface glycoprotein | 7 | 14 | 0 | 0 |
| Smp_017430.1 | CD63 antigen | 0 | 5 | 9 | 5 |
| Smp_055780.1 | Multidrug resistance protein 1 | 4 | 4 | 50 | 24 |
| Smp_140000.1 | putative tetraspanin-CD63 receptor (*Sm*-TSP-4) | 0 | 3 | 7 | 4 |
| Smp_155310.1 | tetraspanin, putative (*Sm*-TSP-1) | 0 | 2 | 6 | 0 |
| Smp_104270.1 | Bis(5'-adenosyl)-triphosphatase enpp4 | 0 | 14 | 28 | 19 |
| Smp_313560.1 | alkaline phosphatase | 2 | 4 | 19 | 4 |
| Smp_344440.1 | putative tetraspanin 18, isoform 1 | 0 | 4 | 11 | 6 |
| Smp_015020.1 | Sodium/potassium-transporting ATPase subunit alpha | 0 | 0 | 11 | 0 |
| Smp_004310.1 | ATPase, H+ transporting, lysosomal, V0 subunit c | 0 | 0 | 4 | 0 |
| Smp_005720.1 | Aquaporin-3 (AQP-3) | 0 | 0 | 2 | 0 |
| Smp_011560.1 | putative tetraspanin | 0 | 0 | 2 | 0 |
| Smp_042910.1 | osteopetrosis associated transmembrane protein | 0 | 0 | 2 | 0 |
| Smp_043990.1 | basigin related | 0 | 0 | 3 | 0 |
| Smp_037540.1 | putative alpha-amylase | 0 | 0 | 6 | 0 |
| Smp_032520.1 | putative lysosome-associated membrane glycoprotein | 0 | 0 | 3 | 0 |
| Smp_031880.1 | Immunoglobulin-like domain-containing protein | 0 | 0 | 3 | 0 |
| Smp_073400.1 | putative lysosome-associated membrane glycoprotein | 0 | 0 | 2 | 0 |
| Smp_162510.1 | SJCHGC07463 protein | 0 | 0 | 6 | 0 |
| Smp_128110.1 | transporter, major intrinsic protein family protein | 0 | 0 | 2 | 0 |
| Smp_201730.1 | SJCHGC09800 protein | 0 | 0 | 2 | 0 |
| Smp_173150.1 | CD63 antigen | 0 | 0 | 3 | 0 |
| Smp_091650.1 | putative phospholipid-transporting ATPase IIB | 0 | 0 | 18 | 0 |
| Smp_153390.1 | putative ectonucleotide pyrophosphatase/phosphodiesterase | 0 | 0 | 2 | 0 |
| Smp_123280.1 | Major facilitator superfamily domain-containing protein 1 | 0 | 0 | 10 | 4 |
| Smp_244680.1 | protein VAC14 homolog | 0 | 0 | 2 | 0 |
| Smp_174490.1 | expressed conserved protein | 0 | 0 | 7 | 0 |
| Smp_169610.1 | putative zinc finger protein | 0 | 0 | 2 | 0 |
| Smp_159070.1 | hypothetical protein MS3_09367 | 0 | 0 | 2 | 0 |
| Smp_128940.1 | putative metabotropic glutamate receptor | 0 | 0 | 5 | 0 |
| Smp_131840.1 | 25 kDa integral membrane protein | 0 | 0 | 2 | 0 |
| Smp_169870.1 | putative cystinosin | 0 | 0 | 3 | 0 |
| Smp_095630.1 | CD9-like protein Sm-TSP-1 | 0 | 0 | 2 | 0 |
| Smp_130300.1 | Sodium/potassium-transporting ATPase subunit alpha | 0 | 0 | 4 | 0 |
| Smp_123670.1 | Lysosomal acid phosphatase | 0 | 0 | 4 | 2 |
| Smp_091240.1 | Voltage-dependent anion-selective channel protein 2 | 0 | 0 | 4 | 2 |
| Smp_165170.1 | putative transient receptor potential cation channel,subfamily m, member | 0 | 0 | 2 | 0 |
| Smp_150500.1 | Protein lifeguard 3 | 0 | 0 | 2 | 0 |

| | | | | | |
|---|---|---|---|---|---|
| Smp_167240.1 | SJCHGC05348 protein | 0 | 0 | 5 | 0 |
| Smp_210250.1 | CDC50 family protein, LEM3 family | 0 | 0 | 6 | 0 |
| Smp_089700.1 | integrin beta 2 | 0 | 0 | 4 | 0 |
| Smp_129820.1 | multi drug resistance-associated protein | 0 | 0 | 4 | 0 |
| Smp_166340.1 | SJCHGC03061 protein | 0 | 0 | 2 | 0 |
| Smp_147070.1 | Putative sodium-coupled neutral amino acid transporter 9 | 0 | 0 | 4 | 0 |
| Smp_160160.1 | putative sialin (solute carrier family 17 member 5) (sodium/sialic acid cotransporter) (ast) (membrane glycoprotein hp59) | 0 | 0 | 5 | 0 |
| Smp_162770.1 | lysosome-associated membrane glycoprotein | 0 | 0 | 3 | 0 |
| Smp_099150.1 | Pleckstrin homology domain-containing family B member 2 | 0 | 0 | 5 | 0 |
| Smp_194920.1 | T-cell immunomodulatory protein | 0 | 0 | 10 | 7 |
| Smp_164210.1 | Synaptosomal-associated protein 25 | 0 | 0 | 16 | 0 |
| Smp_246270.1 | ATP-binding cassette sub-family B member 6, mitochondrial | 0 | 0 | 16 | 7 |
| Smp_344430.1 | SID1 transmembrane family member 1 | 0 | 0 | 4 | 0 |
| Smp_302090.1 | putative ctl2 | 0 | 0 | 4 | 3 |
| Smp_267000.1 | ATPase, H+ transporting, lysosomal accessory protein 1 | 0 | 0 | 7 | 3 |
| Smp_324850.1 | SJCHGC01860 protein | 0 | 0 | 3 | 0 |
| Smp_300190.1 | Aquaporin-9 (AQP-9) (Small solute channel 1) | 0 | 0 | 2 | 0 |
| Smp_340540.1 | lysosome membrane protein 2 | 0 | 0 | 5 | 2 |
| Smp_245370.1 | Equilibrative nucleoside transporter 3 | 0 | 0 | 3 | 0 |
| Smp_141010.1 | Dysferlin | 0 | 0 | 0 | 6 |
| Smp_335630.1 | tetraspanin 2 (*Sm*-TSP-2) | 0 | 5 | 6 | 6 |
| Smp_040080.1 | SJCHGC08990 protein | 0 | 0 | 7 | 5 |
| Smp_074140.1 | Annexin 13 | 0 | 0 | 4 | 0 |
| Smp_069120.1 | Synaptotagmin-2 | 0 | 0 | 2 | 0 |
| Smp_127820.1 | SJCHGC05417 protein | 0 | 0 | 2 | 0 |

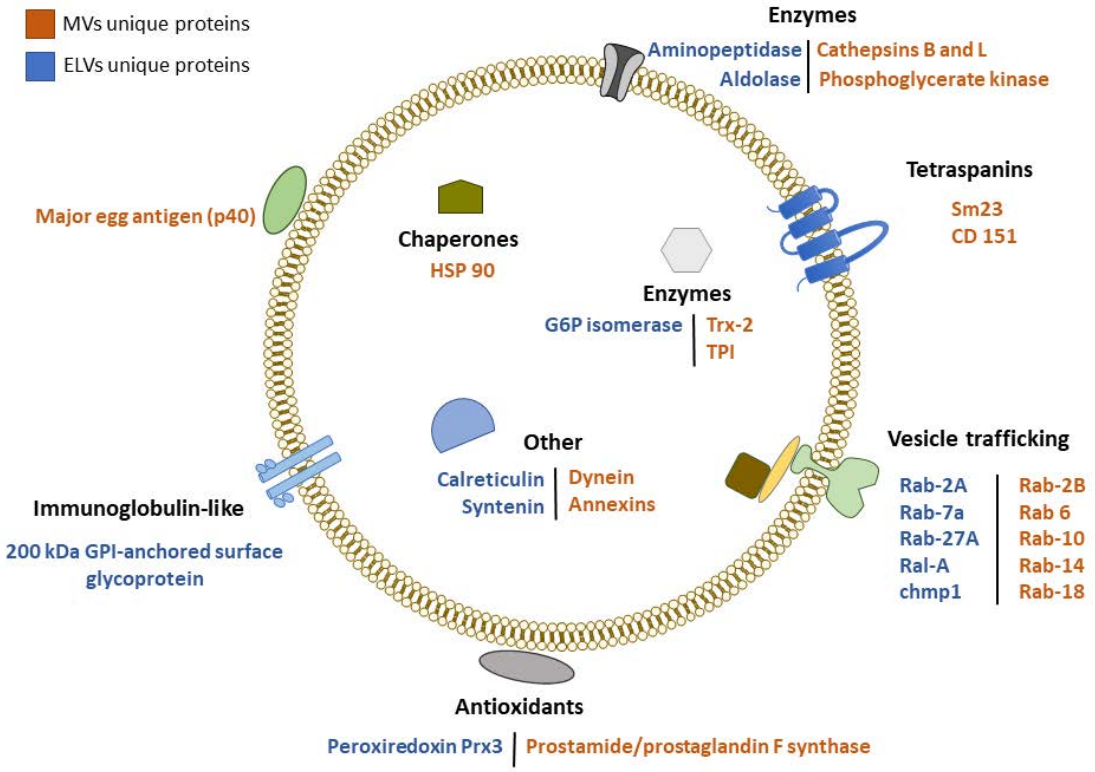


**Figure 2. 4. Schematic representation of most representative *S. mansoni* exosome-like vesicle and microvesicle-unique proteins.** Several unique membrane and cargo specific proteins were found in the different populations of extracellular vesicles isolated from the excretory/secretory products of *Schistosoma mansoni*.

A GO and protein family analysis of the identified proteins from both *S. mansoni*-derived ELVs and MVs was performed. The most abundant GO terms within the "biological process" ontology of ELVs (Figure 2.5A) were "primary metabolic process" followed by "cation transport", "carbohydrate metabolic process", "phosphorylation" and "ATP metabolic process"; whereas the most abundant biological process GO terms for MVs (Figure 2.5B) were "regulation of cellular process" followed by "positive regulation of biological process", "primary metabolic process", "cellular response to stimuli", and "positive regulation of cellular process".

The most prominent GO terms within the "molecular function" ontology of ELVs (Figure 2.6A) were "protein binding" followed by "transmembrane transporter activity", "transferase activity", and

"oxidoreductase activity"; whereas the most prominent molecular function GO terms for MVs (Figure 2.6B) were "heterocyclic compound binding" followed by "anion binding", "carbohydrate derivative binding" and "cytoskeletal protein binding".

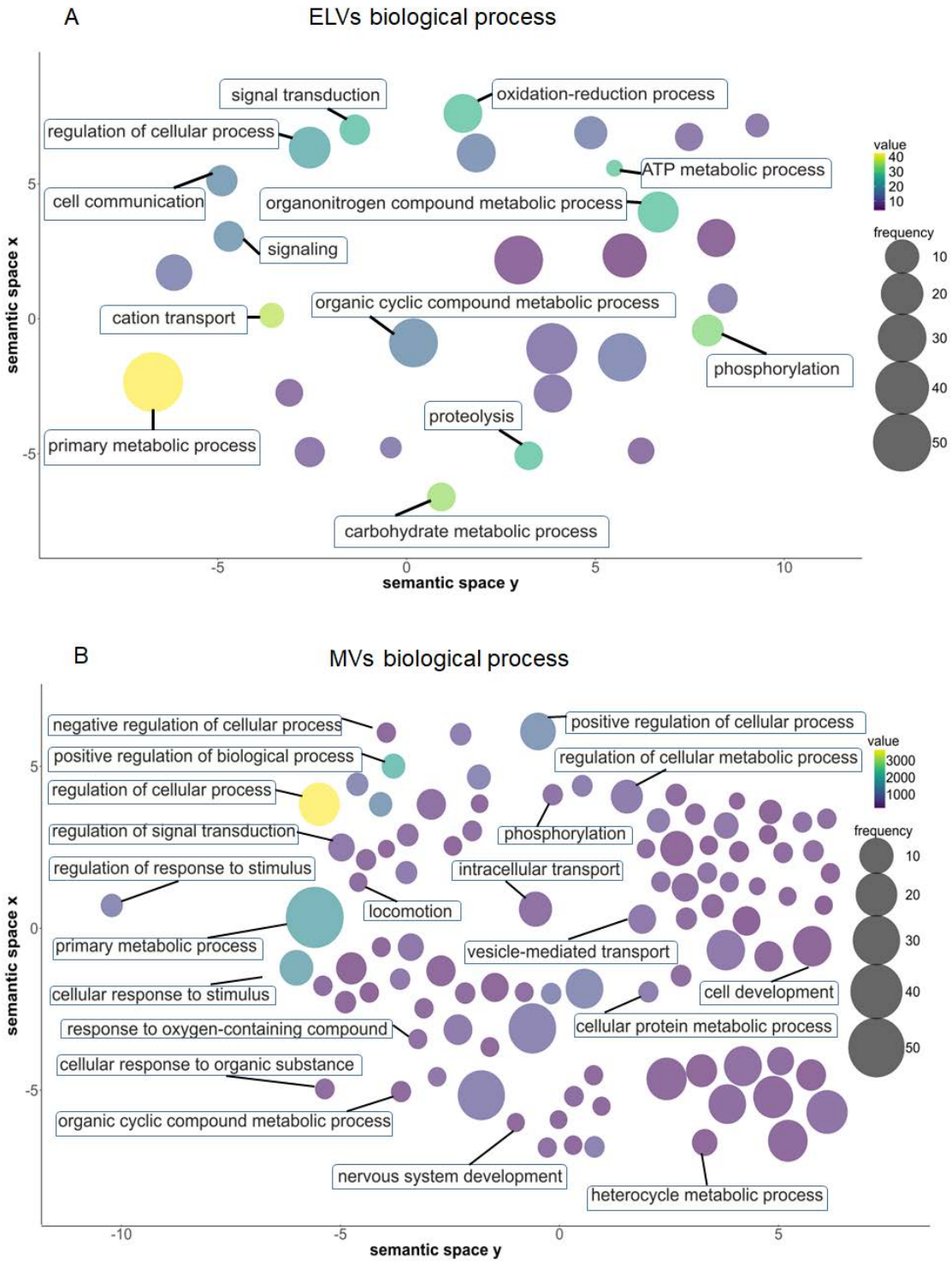


**Figure 2. 5. Bioinformatic analysis of gene ontology biological process terms in adult *S. mansoni* exosome-like vesicles and microvesicles.** REViGO plot showing the most abundantly represented

GO terms ranked by nodescore (Blast2GO). Increasing heatmap score signifies increasing nodescore from Blast2GO, while circle size denotes the frequency of the GO term from the underlying database.

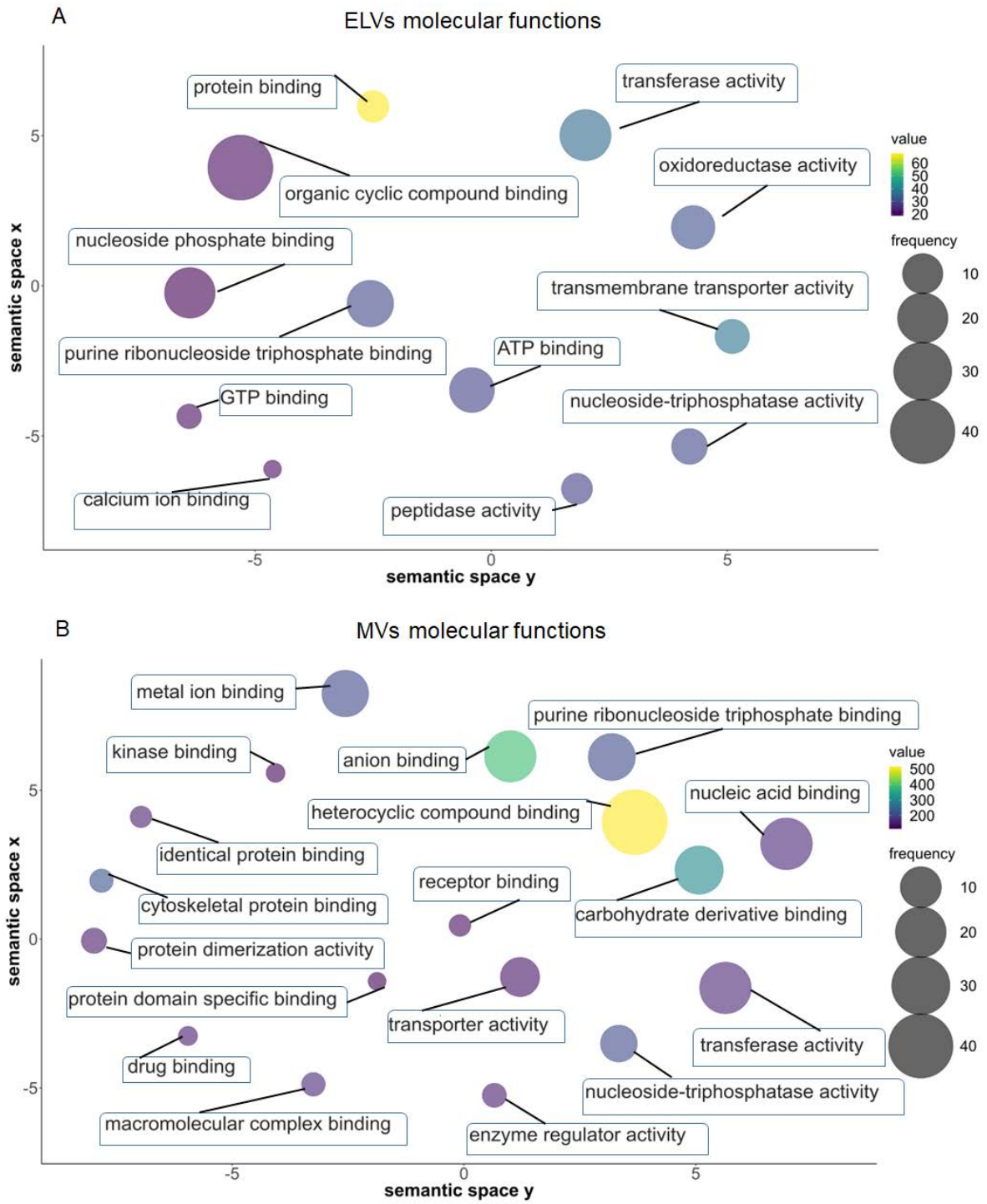


**Figure 2. 6. Bioinformatic analysis of gene ontology molecular function terms in adult *S. mansoni* exosome-like vesicles and microvesicles.** Bioinformatic analysis of gene ontology molecular function terms in adult S. mansoni ELVs and MVs. REViGO plot showing the most abundantly represented GO terms ranked by nodescore (Blast2GO). Increasing heatmap score signifies

increasing nodescore from Blast2GO, while circle size denotes the frequency of the GO term from the underlying database.

I have also reported the top 10 represented protein families in each vesicle type analysed (Figure 2.7). The eight most highly represented protein family domains (by amount of protein containing a particular domain) were common to both ELVs and MVs but presented different levels of abundance, including "EF-hand domain pair", "ADP-ribosylation factor family", "50s ribosome-binding GTPase" and "Ras" family proteins. In addition, proteins from the TSP family were abundant in the ELVs but less well represented in the MVs.

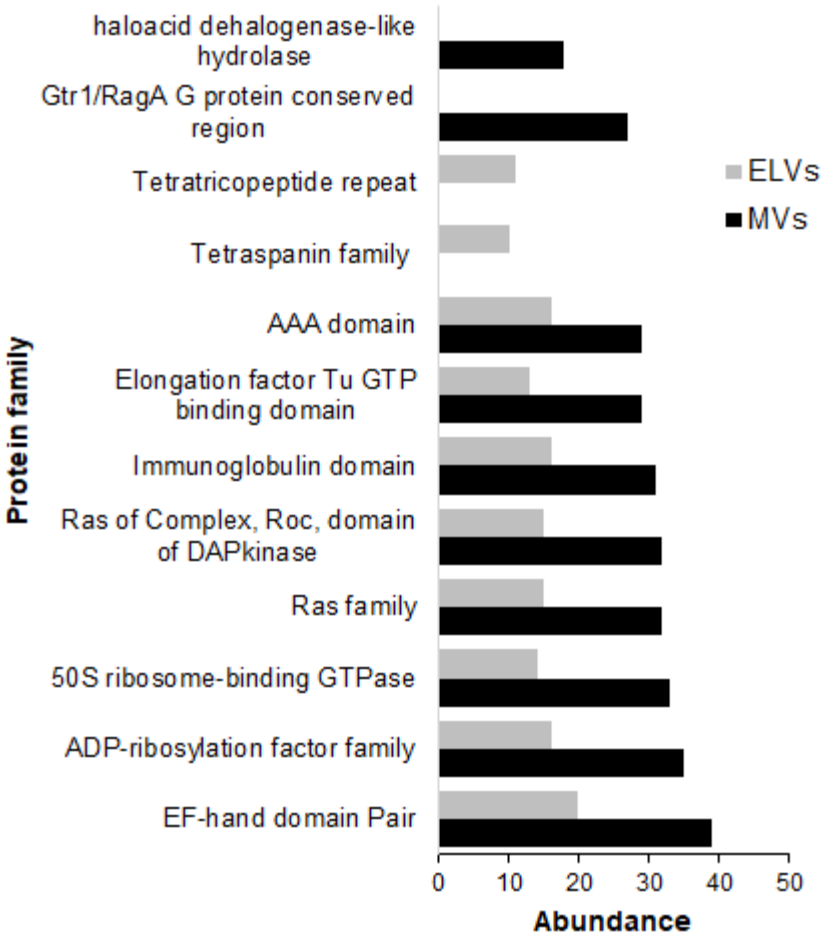


**Figure 2. 7. Pfam analysis of the proteins secreted by *S. mansoni* extracellular vesicles.** Bar graph showing the top 10 most represented protein families of ELVs and MVs of adult *S. mansoni*.

From a total of 286 proteins identified in ELVs 39 (13.6%) and 69 (24.1%) contained signal peptide and transmembrane domains, respectively (Supplementary Table 2.1-2.4 for the top 20 proteins ranked based on spectrum counting), whereas of the 716 proteins identified in MVs 64 (8.9 %) and 120 (16.8%) contained signal peptide and transmembrane domains, respectively (Supplementary Table 2.5-2.8 for the top 20 proteins ranked based on spectrum counting and (Kifle et al., 2020)).

Functional annotation revealed proteins of potential relevance for host-parasite communication in both types of EVs analysed, including proteases, protease inhibitors and antioxidants in all compartments of EVs and proteins associated with membrane structures from ELVs (Table 2.1) and MVs (Table 2.2). Moreover, previously described vaccine candidates, including, TSP-2, GST, Sm29, and calpain were identified in both vesicle types, while the TSP Sm23 was identified only in MVs. Moreover, proteases corresponding to cathepsin family proteins such as cathepsin B- and cathepsin L-like proteases were identified in both ELVs and MVs. Other proteases, including putative aminopeptidase W07G4.4, were released following trypsin shaving of both EV types. In addition, proteins from the annexin group, including annexin A3, annexin A7, annexin A8 and annexin A8-like protein 1, were identified only in MVs. Protease inhibitors such as serpin B9 and cystatin-B were also identified only in MVs, while cysteine protease inhibitors were identified only in ELVs. Further, proteins with antioxidant or defence roles such as thioredoxin peroxidase were identified in both EV types analysed, whereas, peroxiredoxin Prx3 was only found in ELVs, and prostamide/prostaglandin F, thioredoxin peroxidase-2 and thioredoxin-2 were anti-oxidant proteins found only in MVs (Table 2.1 and 2.2).

I identified proteins involved in vesicle biogenesis and trafficking exclusively in ELVs including chmp1 (chromatin modified protein), charged MVB proteins, vacuolar protein sorting-associated protein as well as Rab related proteins such as Rab-2A, Rab-7a, Rab-27A and Ral A. Moreover, other vesicle biogenesis proteins such as Ras related proteins (Rab-2B, Rab 6, Rab-10, Rab-14 and Rab-18) were

identified only in MVs. In addition, proteins with similar roles such as charged MVB protein 4b (SNF7 homolog associated with Alix 1), syntenin-1, annexin, Rab-8A and Rab-11A were identified from both vesicles types. Further, common exosome markers, such as heat shock protein (Hsp)-70, members of the TSP family (*Sm*TSP-1, *Sm*-TSP-2, *Sm*-TSP-4 and putative TSP-18), Rab protein families and enolase were identified in both ELVs and MVs, and hsp-90 was identified only in MVs (Tables 2.1 and 2.2 and (Kifle et al., 2020)).

Membrane transporters, channels, and other molecules involved in membrane structure were identified from different compartments of both EV types analysed including aquaporin, $Na^+/K^+$-transporting ATPase, $H^+$-transporting ATPase and phospholipid-transporting ATPase IIB. Moreover, other proteins with potential roles in membrane structure and signalling including, the TSPs noted above, as well as Sm13 and the 25 kDa integral membrane protein, were identified in both vesicle types, whereas other membrane proteins were unique to just one vesicle population, including the 200 kDa GPI-anchored surface glycoprotein, found in ELVs only, and Sm23, tegument antigen (I(H)A) and CD 151 homologue, found in MVs only (Tables 2.1 and 2.2 and (Kifle et al., 2020)).

**Table 2. 2. Functional annotations of proteins from *S. mansoni* microvesicles.**

| | **Description** | **# unique peptides** | | | |
|---|---|---|---|---|---|
| **Accession number** | **Proteases/inhibitors** | **TLPs** | **Cargo** | **IMPs** | **PMPs** |
| Smp_089670.1 | Alpha-2-macroglobulin-like protein 1 | 2 | 11 | 3 | 2 |
| Smp_089180.1 | Ubiquitin carboxyl-terminal hydrolase 7 | 2 | 0 | 3 | 0 |
| Smp_100090.1 | High mobility group protein DSP1 | 2 | 0 | 0 | 0 |
| Smp_103610.1 | cathepsin B-like peptidase (C01 family) | 2 | 0 | 6 | 2 |
| Smp_187140.1 | Cathepsin L-like proteinase precursor | 4 | 2 | 5 | 3 |
| Smp_207080.1 | Proteasome subunit alpha type-6 | 5 | 2 | 0 | 0 |
| Smp_214190.1 | Calpain | 6 | 12 | 41 | 4 |
| Smp_153960.1 | Presenilin homolog | 3 | 0 | 0 | 0 |
| Smp_155720.1 | Glycogen synthase kinase-3 alpha | 3 | 0 | 0 | 0 |
| Smp_141610.1 | Cathepsin B-like cysteine proteinase | 3 | 2 | 3 | 0 |
| Smp_212880.1 | Proteasome subunit beta type-5 | 5 | 0 | 0 | 0 |
| Smp_172590.1 | family S10 unassigned peptidase (S10 family) | 4 | 4 | 10 | 3 |
| Smp_247170.1 | Major egg antigen | 6 | 0 | 3 | 0 |

| | | | | | |
|---|---|---|---|---|---|
| Smp_340060.1 | Mastin precursor | 13 | 13 | 17 | 9 |
| Smp_343260.1 | cathepsin L, a | 23 | 0 | 12 | 12 |
| | | | | | |
| Smp_346350.1 | 26S proteasome non-ATPase regulatory subunit 1 | 38 | 0 | 2 | 0 |
| Smp_246110.1 | Kyphoscoliosis peptidase | 6 | 0 | 7 | 4 |
| Smp_307450.1 | U-actitoxin-Avd3s | 8 | 0 | 0 | 0 |
| Smp_303330.1 | Hemoglobinase | 7 | 0 | 0 | 0 |
| Smp_032580.1 | Proteasome subunit alpha type-5 | 0 | 3 | 2 | 0 |
| Smp_013040.1 | Lysosomal aspartic protease | 0 | 2 | 6 | 0 |
| Smp_074500.1 | Proteasome subunit beta type-2 | 0 | 2 | 0 | 0 |
| Smp_070930.1 | Proteasome subunit alpha type-4 | 0 | 3 | 3 | 0 |
| Smp_071610.1 | Dipeptidyl peptidase 2 | 0 | 2 | 4 | 0 |
| Smp_034490.1 | Proteasome subunit beta type-6 | 0 | 5 | 4 | 0 |
| Smp_082030.1 | Protein dj-1beta | 0 | 3 | 3 | 0 |
| Smp_092280.1 | 20S proteasome subunit alpha 7 | 0 | 3 | 2 | 2 |
| Smp_076230.1 | Proteasome subunit alpha-type 7-like | 0 | 2 | 0 | 0 |
| Smp_212920.1 | Proteasome subunit alpha type-1 | 0 | 4 | 0 | 0 |
| Smp_301340.1 | Proteasome subunit beta type-1-B | 0 | 4 | 0 | 0 |
| Smp_006390.1 | Cystatin-B | 0 | 0 | 6 | 0 |
| Smp_003980.1 | Calpain-B | 0 | 0 | 6 | 0 |
| Smp_008545.1 | 60 kDa heat shock protein, mitochondrial | 0 | 0 | 3 | 0 |
| Smp_027610.1 | 40S ribosomal protein S3 | 0 | 0 | 3 | 0 |
| Smp_022400.1 | Glucose-6-phosphate isomerase | 0 | 0 | 11 | 0 |
| Smp_030000.1 | Putative aminopeptidase W07G4.4 | 0 | 0 | 21 | 0 |
| Smp_028500.1 | Caspase-3 | 0 | 0 | 2 | 0 |
| Smp_018240.1 | Transitional endoplasmic reticulum ATPase | 0 | 0 | 19 | 0 |
| Smp_019010.1 | Dipeptidyl peptidase 3 | 0 | 0 | 9 | 0 |
| Smp_029500.1 | Thimet oligopeptidase | 0 | 0 | 4 | 0 |
| Smp_061920.1 | UV excision repair protein RAD23 homolog B | 0 | 0 | 5 | 0 |
| Smp_056970.2 | Glyceraldehyde-3-phosphate dehydrogenase | 0 | 0 | 27 | 0 |
| | | | | | |
| Smp_031730.1 | Signal peptidase complex catalytic subunit SEC11C | 0 | 0 | 2 | 0 |
| Smp_067490.1 | Sorcin | 0 | 0 | 6 | 0 |
| Smp_067480.1 | Sorcin | 0 | 0 | 6 | 0 |
| Smp_033710.1 | ATP-dependent RNA helicase DDX3Y | 0 | 0 | 3 | 0 |
| Smp_067060.1 | Cathepsin B-like cysteine proteinase | 0 | 0 | 5 | 0 |
| Smp_089460.1 | Calpain-B | 0 | 0 | 13 | 0 |
| Smp_083870.1 | Putative aminopeptidase W07G4.4 | 0 | 0 | 5 | 0 |
| Smp_099030.1 | Casein kinase II subunit alpha | 0 | 0 | 5 | 0 |
| Smp_136640.1 | Sorcin | 0 | 0 | 5 | 0 |
| Smp_085640.1 | COP9 signalosome complex subunit 4 | 0 | 0 | 2 | 0 |
| Smp_079770.1 | Probable protein disulfide-isomerase ER-60 | 0 | 0 | 2 | 0 |
| Smp_090800.1 | Xaa-Pro dipeptidase | 0 | 0 | 3 | 0 |
| Smp_102040.1 | Guanine nucleotide-binding protein subunit beta-2-like 1 | 0 | 0 | 3 | 0 |
| Smp_072140.1 | Rho-related GTP-binding protein RhoC | 0 | 0 | 5 | 0 |
| Smp_091470.1 | Puromycin-sensitive aminopeptidase | 0 | 0 | 4 | 0 |
| Smp_104110.1 | Ras-like GTP-binding protein RHO | 0 | 0 | 4 | 0 |
| Smp_089100.1 | Glutathione hydrolase 7 | 0 | 0 | 12 | 0 |

| | | | | | |
|---|---|---|---|---|---|
| Smp_075800.1 | Hemoglobinase | 0 | 0 | 7 | 0 |
| Smp_247080.1 | Aminopeptidase N | 0 | 0 | 3 | 4 |
| Smp_165490.1 | Serine/threonine-protein phosphatase 2A catalytic subunit alpha isoform | 0 | 0 | 3 | 0 |
| Smp_214180.1 | Calpain | 0 | 0 | 10 | 0 |
| Smp_155560.1 | Serpin B9 | 0 | 0 | 2 | 0 |
| Smp_213550.1 | 26S proteasome non-ATPase regulatory subunit 14 | 0 | 0 | 2 | 0 |
| Smp_213240.1 | Prolyl endopeptidase | 0 | 0 | 7 | 0 |
| Smp_243200.1 | Calpain-7 | 0 | 0 | 2 | 0 |
| | **Biogenesis/vesicle trafficking** | | | | |
| Smp_099310.1 | Protein transport protein Sec23A | 2 | 0 | 3 | 0 |
| Smp_118830.1 | F-actin-capping protein subunit alpha-2 | 2 | 0 | 3 | 0 |
| Smp_131870.2 | Syntaxin-binding protein 1 | 3 | 0 | 0 | 0 |
| Smp_157410.1 | Cytoplasmic dynein 1 heavy chain 1 | 3 | 0 | 0 | 0 |
| Smp_154420.1 | clathrin heavy chain | 3 | 0 | 14 | 3 |
| Smp_332400.1 | Coatomer subunit delta | 12 | 0 | 3 | 0 |
| Smp_333910.1 | F-actin-capping protein subunit beta | 12 | 0 | 5 | 0 |
| Smp_008660.2 | Severin | 0 | 0 | 7 | 0 |
| Smp_071630.1 | Ras-related protein Rab-2B | 0 | 0 | 11 | 0 |
| Smp_077720.2 | Annexin A5 | 0 | 0 | 4 | 0 |
| Smp_004910.1 | Ras-related protein Rab-14 | 0 | 0 | 4 | 0 |
| Smp_005670.1 | Ras-related protein Rab-11A | 0 | 0 | 2 | 0 |
| Smp_014020.1 | Cell cycle control protein 50A | 0 | 0 | 3 | 0 |
| Smp_010090.1 | Charged multivesicular body protein 5 | 0 | 0 | 3 | 0 |
| Smp_008230.1 | Ras-related protein Rab-18 | 0 | 0 | 4 | 0 |
| Smp_014660.1 | Ras-related protein Rab-10 | 0 | 0 | 4 | 0 |
| Smp_022810.1 | Ras-related protein Rab-2B | 0 | 0 | 6 | 0 |
| Smp_048940.1 | Vacuolar protein sorting-associated protein 37B | 0 | 0 | 2 | 0 |
| Smp_045710.1 | Charged multivesicular body protein 4b | 0 | 0 | 6 | 0 |
| Smp_055880.1 | Charged multivesicular body protein 1a | 0 | 0 | 8 | 0 |
| Smp_032150.1 | Charged multivesicular body protein 3 | 0 | 0 | 3 | 0 |
| Smp_047450.1 | Synaptobrevin homolog YKT6 | 0 | 0 | 3 | 0 |
| Smp_057320.1 | Vesicle-fusing ATPase 2 | 0 | 0 | 4 | 0 |
| Smp_035620.1 | Multivesicular body subunit 12B | 0 | 0 | 2 | 0 |
| Smp_045500.1 | Annexin A7 | 0 | 0 | 4 | 0 |
| Smp_034870.1 | AP-2 complex subunit beta | 0 | 0 | 5 | 0 |
| Smp_055870.1 | Vesicle-associated membrane protein 8 | 0 | 0 | 7 | 0 |
| Smp_104670.1 | Ras-related protein Rab-8A | 0 | 0 | 4 | 0 |
| Smp_146400.1 | Syntaxin-binding protein 1 | 0 | 0 | 3 | 0 |
| Smp_074020.1 | AP-2 complex subunit alpha | 0 | 0 | 6 | 0 |
| Smp_093230.1 | Actin-related protein 10 | 0 | 0 | 2 | 0 |
| Smp_068530.1 | Syntenin-1 | 0 | 0 | 10 | 0 |
| Smp_092770.1 | Coatomer subunit gamma-2 | 0 | 0 | 2 | 0 |
| Smp_079000.1 | Charged multivesicular body protein 1b | 0 | 0 | 3 | 0 |
| Smp_104310.1 | Ras-related protein Rab-11A | 0 | 0 | 5 | 0 |
| Smp_174580.1 | Vesicular integral-membrane protein VIP36 | 0 | 0 | 2 | 0 |
| Smp_169460.1 | GTP-binding protein YPTC1 | 0 | 0 | 7 | 0 |
| Smp_210250.1 | Cell cycle control protein 50A | 0 | 0 | 8 | 0 |

| | | | | | |
|---|---|---|---|---|---|
| Smp_340230.1 | Charged multivesicular body protein 2a | 0 | 0 | 4 | 0 |
| Smp_245450.1 | Coatomer subunit alpha | 0 | 0 | 3 | 0 |
| Smp_337410.1 | Tumor susceptibility gene 101 protein | 0 | 0 | 3 | 0 |
| Smp_163580.1 | Ras-related protein Rab6 | 0 | 0 | 2 | 0 |
| | **Antioxidants** | | | | |
| Smp_194940.1 | Prostamide/prostaglandin F synthase | 4 | 0 | 7 | 0 |
| Smp_158110.1 | Thioredoxin peroxidase | 3 | 3 | 7 | 3 |
| Smp_309480.1 | Thioredoxin peroxidase 2 | 8 | 6 | 9 | 5 |
| Smp_008070.1 | Thioredoxin-2 | 0 | 3 | 2 | 0 |
| | **Membrane structure** | | | | |
| Smp_121160.2 | Mitochondrial dicarboxylate carrier | 2 | 0 | 0 | 0 |
| Smp_103200.1 | V-type proton ATPase subunit D | 2 | 0 | 8 | 0 |
| Smp_099890.1 | Receptor expression-enhancing protein 5 | 2 | 2 | 5 | 2 |
| Smp_104270.1 | Bis(5'-adenosyl)-triphosphatase enpp4 | 2 | 0 | 20 | 2 |
| Smp_127820.1 | SJCHGC05417 protein | 2 | 0 | 0 | 2 |
| Smp_130300.1 | Sodium/potassium-transporting ATPase subunit alpha | 3 | 0 | 12 | 0 |
| Smp_130280.1 | cell polarity protein | 3 | 0 | 0 | 2 |
| Smp_141010.1 | Dysferlin | 3 | 0 | 0 | 2 |
| Smp_340630.1 | putative endoplasmin | 15 | 0 | 0 | 10 |
| Smp_313560.1 | alkaline phosphatase | 9 | 4 | 17 | 6 |
| Smp_315900.1 | Plasma membrane calcium-transporting ATPase 3 | 10 | 0 | 2 | 0 |
| Smp_005720.1 | Aquaporin-3 | 0 | 2 | 5 | 0 |
| Smp_020370.1 | Reticulon-4 | 0 | 2 | 7 | 0 |
| Smp_017430.1 | 23 kDa integral membrane protein | 0 | 4 | 16 | 0 |
| Smp_012440.1 | Solute carrier family 2, facilitated glucose transporter member 1 | 0 | 7 | 13 | 0 |
| Smp_041460.1 | tetraspanin D76 | 0 | 2 | 8 | 0 |
| Smp_153390.1 | putative ectonucleotide pyrophosphatase/phosphodiesterase | 0 | 7 | 5 | 3 |
| Smp_155310.1 | tetraspanin, putative (*Sm*-TSP-1) | 0 | 2 | 6 | 0 |
| Smp_140000.1 | putative tetraspanin-CD63 receptor (*Sm*-TSP-4) | 0 | 5 | 8 | 2 |
| Smp_162770.1 | lysosome-associated membrane glycoprotein | 0 | 2 | 0 | 3 |
| Smp_335630.1 | tetraspanin 2 (*Sm*-TSP-2) | 0 | 6 | 7 | 8 |
| Smp_300190.1 | Aquaporin-9 (AQP-9) (Small solute channel 1) | 0 | 3 | 6 | 4 |
| Smp_267000.1 | ATPase, H+ transporting, lysosomal accessory protein 1 | 0 | 2 | 7 | 4 |
| Smp_007260.1 | Sarcoplasmic/endoplasmic reticulum calcium ATPase 2 | 0 | 0 | 3 | 0 |
| Smp_011560.1 | CD151 antigen | 0 | 0 | 5 | 0 |
| Smp_029390.1 | V-type proton ATPase subunit B | 0 | 0 | 14 | 0 |
| Smp_015020.1 | Sodium/potassium-transporting ATPase subunit alpha | 0 | 0 | 22 | 0 |
| Smp_024820.1 | CD9 antigen | 0 | 0 | 3 | 0 |
| Smp_048230.1 | High affinity copper uptake protein 1 | 0 | 0 | 4 | 0 |
| Smp_039130.1 | NPC intracellular cholesterol transporter 1 | 0 | 0 | 16 | 0 |
| Smp_055780.1 | Multidrug resistance protein 1 | 0 | 0 | 54 | 0 |

| | | | | | |
|---|---|---|---|---|---|
| Smp_040080.1 | Glycosylated lysosomal membrane protein B | 0 | 0 | 7 | 0 |
| Smp_059530.1 | 25 kDa integral membrane protein | 0 | 0 | 3 | 0 |
| Smp_091650.1 | putative phospholipid-transporting ATPase IIB | 0 | 0 | 20 | 2 |
| Smp_136710.1 | putative calcium-transporting atpase sarcoplasmic/endoplasmic reticulum type (calcium pump) | 0 | 0 | 7 | 2 |
| Smp_105680.1 | Dolichyl-diphosphooligosaccharide--protein glycosyltransferase subunit 1 | 0 | 0 | 2 | 0 |
| Smp_105410.1 | Solute carrier family 2, facilitated glucose transporter member 3 | 0 | 0 | 4 | 0 |
| Smp_129820.1 | Canalicular multispecific organic anion transporter 2 | 0 | 0 | 9 | 0 |
| Smp_131890.1 | Sodium- and chloride-dependent glycine transporter 1 | 0 | 0 | 2 | 0 |
| Smp_127940.1 | Sodium-driven chloride bicarbonate exchanger | 0 | 0 | 2 | 0 |
| Smp_123280.1 | Major facilitator superfamily domain-containing protein 1 | 0 | 0 | 15 | 0 |
| Smp_130230.1 | Ras-related protein Rac1 | 0 | 0 | 2 | 0 |
| Smp_128940.1 | Metabotropic glutamate receptor 7 | 0 | 0 | 3 | 0 |
| Smp_136240.1 | Vesicle-associated membrane protein/synaptobrevin-binding protein | 0 | 0 | 3 | 0 |
| Smp_141680.1 | Fasciclin-1 | 0 | 0 | 2 | 0 |
| Smp_079220.1 | ADP,ATP carrier protein | 0 | 0 | 3 | 0 |
| Smp_082810.1 | Cell division control protein 42 homolog | 0 | 0 | 7 | 0 |
| Smp_069120.1 | Synaptotagmin-2 | 0 | 0 | 11 | 0 |
| Smp_075210.1 | Prohibitin-2 | 0 | 0 | 3 | 0 |
| Smp_127650.1 | Secretory carrier-associated membrane protein 1 | 0 | 0 | 2 | 0 |
| Smp_099150.1 | Pleckstrin homology domain-containing family B member 2 | 0 | 0 | 4 | 0 |
| Smp_162510.1 | Solute carrier family 46 member 3 | 0 | 0 | 5 | 0 |
| Smp_246400.1 | Glycosyltransferase 1 domain-containing protein 1 | 0 | 0 | 6 | 4 |
| Smp_173150.1 | CD63 antigen | 0 | 0 | 2 | 0 |
| Smp_194970.1 | 25 kDa integral membrane protein | 0 | 0 | 2 | 0 |
| Smp_167240.1 | Nicastrin | 0 | 0 | 3 | 0 |
| Smp_332300.1 | Glucose-6-phosphate exchanger SLC37A2 | 0 | 0 | 2 | 0 |
| Smp_194920.1 | T-cell immunomodulatory protein | 0 | 0 | 12 | 3 |
| Smp_246270.1 | ATP-binding cassette sub-family B member 6, mitochondrial | 0 | 0 | 16 | 4 |
| Smp_196110.1 | Ferric-chelate reductase 1 | 0 | 0 | 6 | 0 |
| Smp_176940.1 | High affinity cationic amino acid transporter 1 | 0 | 0 | 4 | 0 |
| Smp_333250.1 | Putative phospholipid-transporting ATPase C4F10.16c | 0 | 0 | 3 | 0 |
| Smp_171870.1 | Synaptic vesicle 2-related protein; Short=SV2-related protein | 0 | 0 | 3 | 0 |
| Smp_244710.1 | ATP-binding cassette sub-family A member 3 | 0 | 0 | 2 | 0 |
| Smp_344440.1 | putative tetraspanin 18, isoform 1 | 0 | 0 | 6 | 14 |

| | | | | | |
|---|---|---|---|---|---|
| Smp_343120.1 | Plasma membrane calcium-transporting ATPase 3 | 0 | 0 | 13 | 0 |
| Smp_160160.1 | Sialin | 0 | 0 | 2 | 0 |
| Smp_340540.1 | lysosome membrane protein 2 | 0 | 0 | 6 | 9 |
| Smp_245370.1 | Equilibrative nucleoside transporter 3 | 0 | 0 | 3 | 0 |
| Smp_346900.1 | 25 kDa integral membrane protein | 0 | 0 | 3 | 0 |
| Smp_190770.1 | LanC-like protein 2 | 0 | 0 | 0 | 3 |
| Smp_248070.1 | putative dock | 0 | 0 | 0 | 4 |
| Smp_315840.1 | Kinase D-interacting substrate of 220 kDa | 0 | 0 | 0 | 6 |
| Smp_336620.1 | Gamma-aminobutyric acid receptor subunit gamma-3 | 0 | 0 | 0 | 9 |
| Smp_323680.1 | SJCHGC06792 protein | 0 | 0 | 0 | 8 |
| Smp_095630.1 | CD81 antigen | 0 | 0 | 3 | 0 |

## 2.4. Discussion

Cells release different populations of EVs, which may either derive from the endosomal pathway, formed by inward budding of the MVB membrane and allowing capture of cytoplasmic cargo (ELVs, 30-150 nm in diameter), or bud directly from their plasma membrane (MVs, 100-1000 nm in diameter) (Kalra et al., 2016). Parasite-secreted EVs are released from different tissues of the parasite but are thought to be primarily from the tegument and gut (de la Torre-Escudero et al., 2016). In this work, a proteomic analysis of two subpopulations of EVs secreted from adult *S. mansoni* was performed to gain more comprehensive coverage of these EV proteomes. The ELVs that I isolated fit the characteristics and flotation properties on a iodixanol-density gradient for classification as exosomes (Théry et al., 2006). Moreover, the size distribution and concentration of both *S. mansoni*-derived ELVs and MVs were analysed by TRPS, allowing me to confirm the presence of these EV types. Importantly, well-standardised techniques (Tauro et al., 2013) were used to isolate these two EV types, giving me confidence in the purity of the vesicle samples.

The ELV sample purified in the present study had a higher purity (number of particles/µg of protein) than the MV sample. The purity ratio was primarily described for exosomes (Webber and Clayton, 2013), but since MVs are physically much larger than exosomes, it is expected that they contain

more proteins and hence the purity ratio should be lower. The particle diameter range for the two vesicle types appeared to be similar and overlapped (Raposo and Stoorvogel, 2013). Accordingly, the size range of ELVs had a wider range than that of MVs, however the median size obtained corresponded to that of exosomes (van Niel et al., 2018). MVs, however, had a relatively higher concentration (particles/ml) than ELVs for any given size (Figure 2A and 2B). Although apoptotic bodies differ clearly from exosomes by their larger size, other vesicle types are more difficult to separate since MVs with a similar size to exosomes can also bud at the plasma membrane (Booth et al., 2006). Moreover, the size overlap observed between the two vesicles analysed can be explained at least in part by the nanopore size used to measure the size distribution of these vesicles – NP150 was used to analyse ELVs (60 to 480 nm) whereas NP300 was used for MVs (115 to 1150 nm). Several studies have reported helminth EVs that correspond to exosomes in terms of vesicle size, including *S. mansoni* (Nowacki et al., 2015, Sotillo et al., 2016b, Samoil et al., 2018), other trematodes (Marcilla et al., 2012, Bernal et al., 2014, Cwiklinski et al., 2015, Chaiyadet et al., 2015a, Zhu et al., 2016a), nematodes (Bernal et al., 2014, Zamanian et al., 2015, Simbari et al., 2016, Tzelos et al., 2016, Eichenberger et al., 2018a, Eichenberger et al., 2018c, Shears et al., 2018), and cestodes (Siles-Lucas et al., 2017, Nicolao et al., 2019). To my knowledge, only one study was done prior to this one involving helminth-derived MVs, which reported a 15K pelleted fraction from *F. hepatica* (Cwiklinski et al., 2015) with size range of 50-200 nm and, furthermore, MVs analysed in this study were within the expected size range for mammalian MVs (van Niel et al., 2018). Using sequential extraction to attribute proteins to sub-vesicular compartments of EVs coupled with highly accurate tandem mass spectrometry, I identified more than twice as many ELV proteins than reported earlier (Sotillo et al., 2016b).

To determine the location of each protein within their respective vesicles, I performed a sequential extraction as described previously for *F. hepatica*- (Cwiklinski et al., 2015) and *Mycoplasma*

*hyopneumoniae*-derived ELVs (Robinson et al., 2013). Proteins identified with high abundance following trypsin shaving of both ELVs and MVs include a fatty acid binding protein with a role in biosynthesis of fatty acids and cholesterols in schistosomes (Tendler et al., 1996), the antioxidants thioredoxin peroxidase (Macalanda et al., 2018) and GST (Bourke et al., 2014, Boulanger et al., 1991), dynein light chain (Hoffmann and Strand, 1996) and membrane structure proteins, for example the Sm13 tegument antigen (Tebeje et al., 2016). Proteases and peptidases including calpain, cathepsins B, cathepsin L, cathepsin A, legumain, and a Pro-Xaa carboxypeptidase were also identified following trypsin shaving of both vesicle types analysed but with relatively less abundance. Similar peptidases were released following trypsin shaving of the *F. hepatica*-derived EV surface (Cwiklinski et al., 2015). Whether these proteases and peptidases, many of which do not contain transmembrane or other membrane-anchoring motifs, are found on the surface of EVs *in vivo* remains to be determined. Proteases and other enzymes have been reported on the surface of mammalian exosomes following invagination of the cell membrane whereby molecules on the cell surface become localized to the luminal side of the endosomal membrane. Some of these proteases then make their way to the exosome surface through small invaginations of the endosomal membrane where they remain once the multi-vesicular body forms and eventually fuses with the cell membrane to release the newly formed exosome into the extracellular space (Sanderson et al., 2019). Another possibility is that soluble proteases bind to the exosome surface within either the endosomal compartment or following secretion of the exosomes into the extracellular space. Once localized to the exosome surface, proteases are free to encounter substrates either at the cell surface or within the extracellular matrix, including ectodomain shedding (Shimoda and Khokha, 2017). Interestingly, most of the proteases associated with the mammalian cell surface are metalloproteases, particularly matrix metalloproteases (Shimoda and Khokha, 2017), whereas there was only a single MMP (nardilysin or ADAM17) identified on the MV surface and none were detected on ELVs despite the presence of a family of leishmanolysin-like clan M metallopeptidases in the *S.*

*mansoni* genome (Silva et al., 2011). Instead, cysteine proteases were abundantly represented on the surface of the schistosome vesicles, reflecting their genome-wide over-representation in many blood-feeding helminths (Caffrey et al., 2018), and suggestive of a role for EVs in feeding. Further, production of reactive oxygen species (oxygen radicals, superoxide, and hydrogen peroxide) by phagocytes is a primary pathway of immune attack against parasites including schistososmes (Hewitson et al., 2009). Correspondingly, EV cargo contains high levels of antioxidants, including catalases, glutathione and thioredoxin peroxidases, and peroxiredoxins (Sotillo et al., 2016b, Samoil et al., 2018, Cwiklinski et al., 2015, Coakley et al., 2017).

HSP-70 (Simpson et al., 2012, Mathivanan et al., 2010) and TSPs (Tauro et al., 2013, Crescitelli et al., 2013) are widely considered as biomarkers of EVs from mammalian cells; for example, HSP-70 has been reported from MVs (Kowal et al., 2016, Jeppesen et al., 2019, van Niel et al., 2018) and the TSPs CD9, CD63 and CD81 have been found in exosomes, MVs and apoptotic bodies (Booth et al., 2006, Lenassi et al., 2010, Fang et al., 2007). Similarly, our data support these findings in that HSP-70 was identified in both ELVs (identified in cargo and PMP compartments) and MVs (TLP and PMP compartments). Likewise, members of the TSP family including *Sm*-TSP-1, TSP-2, and TSP-4 were identified in cargo, PMP and IMP compartments of both ELVs and MVs. My data presented herein revealed that MVs and ELVs share many proteins, notably the surface membrane TSPs, so distinguishing EV types by their proteomic content requires caution. Now that a catalogue of shared and unique EV sub-type proteins has been produced, antibodies to select candidate proteins can be generated to aid in classifying the various cellular/tissue origins of helminth EVs and to monitor their trafficking and release.

Previously described schistosomiasis vaccine candidates were identified in both ELVs and MVs, including TSP-2 (Tran et al., 2006), GST (Bergquist et al., 2002, Capron et al., 2001), Sm29 (Cardoso

et al., 2006) and calpain (Jankovic et al., 1996, Le et al., 2014, Karmakar et al., 2014c), whereas Sm23 (Bergquist et al., 2002, Krautz-Peterson et al., 2017) was identified from cargo and IMP components of MVs only. Indeed, TSP-2, GST, and Sm29 were among the most abundant proteins identified in both EV types, further supporting the notion of EVs as a major reservoir of vaccine candidates against schistosomiasis and other helminth infections. My data also showed clear abundance of schistosome surface antigens such as TSP-1,TSP-2, TSP-4, as well as TSP-18 (relatively less abundant) and a variety of other tegumental antigens in both EV types analysed, some of which have been implicated in schistosome evasion of the host immune response (Han et al., 2009, Salzet et al., 2000). Although TSP-1 has been reported to have vaccine efficacy in a mouse model (Tran et al., 2006), TSP-4 and TSP-18 remain to be tested. EVs secreted by other related trematodes were also found to be abundant in TSPs (Chaiyadet et al., 2015b, Cwiklinski et al., 2015). Further, antibodies generated against an EV surface TSP were able to block the internalisation of *O. viverrini* EVs by human cholangiocytes (Chaiyadet et al., 2015a), and EVs and recombinant TSPs from *O. viverrini* and other helminth parasites have been shown to be efficacious as vaccines in animal models (Shears et al., 2018, Trelis et al., 2016, Chaiyadet et al., 2019).

One of the proteins identified from the integral membrane component of both ELVs and MVs was annexin, a protein involved in a wide range of cellular processes, and, notably has an anti-inflammatory role (D'Acquisto et al., 2008). Moreover, annexins function as plasminogen receptors and enhance fibrinolysis-prolonging blood clot formation (Madureira et al., 2011), roles that are likely to be important for an intra-vascular parasite. Together with the identification of other proteins with known and proposed roles in red cell lysis (saponin-like proteins) (Don et al., 2008), haem storage (ferritin isoforms) and blood feeding (endoproteases and aminopeptidases), a role is emerging for EVs in the nutrient acquisition process in haematophagous trematode parasites. Moreover, enolase, found only in MVs in this study, has been identified as a tissue plasminogen

activator which subsequently results in the generation of the potent fibrinolytic agent plasmin which could degrade blood clots forming around *S. mansoni* parasites *in vivo* (Figueiredo et al., 2015).

Proteins involved in vesicle biogenesis and trafficking were particularly abundant in the IMP compartment of both vesicle types. Among these were members of the endosomal sorting complex required for transport-I and -III pathways with known essential roles in vesicle biogenesis and secretion in mammalian cells (Kowal et al., 2014). Charged MVB proteins such as chromatin modified protein (chmp1) were identified only in ELVs. It was unexpected to identify proteins involved in exosome biogenesis also in MVs. While every effort was made to minimise the occurrence of contamination of MV sample by ELVs, I could not discount the possibility of isolation of ELVs (if at all) in MV sample preparation. Even though the generation of MVs and exosomes occurs at distinct sites within the cell, common intracellular mechanisms and sorting machineries are involved in the biogenesis of both entities (reviewed in (van Niel et al., 2018)). In many cases, these shared mechanisms hinder the possibility of distinguishing between the different vesicle sub-populations (Colombo et al., 2014). Further, Rab GTPases/Ras family proteins (identified in IMP and PMPs) such as Rab-2A, Rab-7a, Rab-27A and Ral-A identified only in ELVs and Rab-2B, Rab 6, Rab-10, Rab-14 and Rab-18 in MVs were identified, while Rab-8A as well as Rab-11A were identified from both vesicle types analysed. Ral-A is a small GTPase required for MVB biogenesis and EV release in *Caenorhabditis elegans* (Hyenne et al., 2018) and *F. hepatica* (de la Torre-Escudero et al., 2019). Contrary to my findings, Rab10 has been detected in *S. japonicum*- (Zhu et al., 2016a) and *F. hepatica*-derived ELVs (de la Torre-Escudero et al., 2019). It was unexpected to identify Rab proteins, usually involved in ELV biogenesis and trafficking (Zhao et al., 2019), also in MV samples, but this might be explained by the reasons mentioned earlier. Rab proteins are one of the main regulators of intracellular EV trafficking between subcellular compartments through processes including vesicle budding, mobility along the cytoskeleton, and membrane fusion (Stenmark, 2009).

Herein, I have isolated and characterised the proteomic composition of two sub-populations of *S. mansoni* secreted EVs (ELVs and MVs) using sequential extraction of proteins from the different sub-vesicular compartments to provide a comprehensive molecular snapshot. Future research should investigate whether *S. mansoni* ELVs and MVs interact with defined host cell types as it is unclear whether they are internalised by host cells. A more comprehensive understanding of schistosome EV biology will facilitate development of methods to interrupt vesicle-mediated communication between host and parasite, as well as inter-parasite interactions. Schistosome EVs are clearly a rich source of target antigens for the development of novel approaches for preventing, treating and diagnosing infections, and further research is essential to add to the schistosomiasis control toolbox.

# Chapter 3

## Uptake of *Schistosoma mansoni* EVs by host cells, impact on gene expression, and antibody-mediated interruption

### Preamble

Determining the role of *S. mansoni*-derived EVs in host-schistosome communication was one of the main aims of my thesis. For this purpose, *S. mansoni* ELVs and MVs were isolated and purified from adult worm ES products as described in Chapter 2. Moreover, MV concentration and particle size were determined using TRPS on a qNano instrument. Both EV types were labelled with PKH-67 fluorescent dye and incubated with human umbilical vein endothelia cells (HUVEC) as well as the THP-1 human monocyte cell line. The uptake of EVs by both cell lines was assessed and confirmed using confocal fluorescence microscopy. This study presents evidence demonstrating the internalisation of *S. mansoni*-derived ELVs and MVs into target cells, highlighting their roles in host-parasite cell-cell communication. Once I had confirmed the uptake of EVs by host cells, the next goal was to determine the impact of ELV internalisation on host cell gene regulation – there was insufficient material available to do the same analysis with MVs. For assessing the impact of *S. mansoni* ELVs on host cell gene expression, vesicles were incubated with HUVEC cells; there was insufficient EV material to conduct gene expression studies on THP-1 cells. RNA was extracted and sent for deep sequencing. Moreover, to identify key proteins on the surface of EVs that might be involved in their uptake by host cells, selected *S. mansoni* TSP proteins were expressed in recombinant form and antibodies were produced against them and used to disrupt EV uptake and therefore EV-mediated parasite-host communication.

## 3.1. Introduction

Cells often exchange information to maintain cellular homeostasis or to respond to pathogens. A universal method of communication is physical interaction by adhesion molecules, cell junctions, and soluble factors. However, increasing data are emerging that show EVs play significant roles in genetic cross-talk between cells by transferring proteins, nucleic acids, lipids, and other components, and in this way, cells can adjust the behaviour of other cells (Deolindo et al., 2013, Meldolesi, 2018).

EVs are membrane-surrounded vesicles that are continually secreted by different types of cells in disease and normal states (de la Torre-Escudero et al., 2016). Although once EVs were regarded to be "cellular garbage cans" with the only function of removing unnecessary cellular debris (Thebaud and Stewart, 2012), now they are known to have key roles in intercellular communication involving their mRNA, miRNA, lipids, and proteins including TSPs (Record et al., 2014).

Studies have demonstrated that parasite-derived EVs play a key role during the infection process (Eichenberger et al., 2018b, Marcilla et al., 2014). Since 2012, EVs have been described from a growing number of parasitic helminths including trematodes (Marcilla et al., 2012, Chaiyadet et al., 2015b, Zhu et al., 2016a, Zhu et al., 2016b, de la Torre-Escudero et al., 2019), nematodes (Zamanian et al., 2015, Coakley et al., 2017, Eichenberger et al., 2018a, Eichenberger et al., 2018c, Hansen et al., 2019) and cestodes (Nicolao et al., 2019, Ancarola et al., 2017, Siles-Lucas et al., 2017), and many of these studies demonstrated the uptake of EVs by target cells *in vitro* at least, indicating likely roles in host-parasite interactions.

Further, secreted EVs are increasingly recognized as mediators of cell communication (Fromm et al., 2017, Fromm et al., 2015), and they have been shown in parasitic nematodes to suppress inflammatory responses *in vitro* (Buck et al., 2014, Zamanian et al., 2015, Eichenberger et al., 2018a). On the other hand, EVs from other parasites such as the liver fluke *O. viverrini* are endocytosed by

human cholangiocytes *in vitro* and elicit a cascade of inflammatory and pre-tumorigenic changes within the cell, thereby providing a plausible mechanism by which the parasite causes bile duct cancer (Chaiyadet et al., 2015b). In addition, studies on *H. polygyrus*, *Leishmania* spp., *Cryptococcus* spp., and *Trypanosoma* spp. have shown that parasite EVs can carry and confer virulence factors to the host (Buck et al., 2014, Barteneva et al., 2013, Silverman et al., 2010a).

Current vaccine development endeavors target the prevention of schistosome infection and/or decrease egg output to reduce transmission. Major advances in schistosome molecular biology such as genomics, transcriptomics, proteomics and immunomics have aided new antigen discovery (Loukas et al., 2011, Gaze et al., 2012, Driguez et al., 2016b). Access to this information in conjunction with improved postgenomic technologies has the capacity to facilitate the discovery of many new vaccine candidates. Molecules exposed to host antibodies, notably ES products and proteins anchored to the outer tegument of the worm are the most important candidates (El Ridi and Tallima, 2013), and many of these ES and tegument proteins are also found in EVs (Sotillo et al., 2016b, Samoil et al., 2018, Kifle et al., 2020, Nowacki et al., 2015). EVs secreted by other related trematodes were found be enriched in TSPs (Chaiyadet et al., 2015b, Cwiklinski et al., 2015). The roles of TSPs in EV biogenesis and cargo selection have been reviewed by Andreu and Yanez-Mo (2014). The significance of specific proteins such as TSPs in EV uptake was shown with *O. viverrini*, where antibodies against *O. viverrini* (*Ov*)-TSP blocked EV internalisation and decreased IL-6 secretion by cholangiocytes (Chaiyadet et al., 2015b). Furthermore, the ability of antibodies against *Ov*-TSP-1 (Chaiyadet et al., 2017) as well as *Ov*-TSP-2 and *Ov*-TSP-3 (Chaiyadet et al., 2019) to block the uptake of EVs by host cells has been demonstrated. Pertaining to this study, TSPs have been found to be enriched in *S. mansoni*-derived EVs (Sotillo et al., 2016b, Samoil et al., 2018, Kifle et al., 2020) and are abundantly expressed on the outermost tegument of both adult worms (Tran et al.,

2006, Braschi and Wilson, 2006) and schistosomula (Sotillo et al., 2015), and I propose that antibodies against *S. mansoni* TSPs could be used to interrupt host-parasite communication.

In this chapter, I demonstrated that S*. mansoni*-derived ELVs and MVs are internalised by human endothelial and monocyte cell lines using confocal fluorescence microscopy. In addition, I have shown that uptake of ELVs by host cells results in differential expression of genes involved in pathways that are critical to parasitism. Moreover, recombinant forms of selected TSPs identified on the surface of EVs were produced and antibodies raised against these recombinant proteins were used to successfully block the uptake of both ELVs and MVs by both cell lines.

## 3.2. Material and methods

### 3.2.1. *S. mansoni* EV isolation and purification

*S. mansoni*-derived EVs used in this experiment were isolated and purified following the standard procedures as described in section 2.2.5 (of this thesis).

### 3.2.2. Cell culture

Primary HUVEC and THP-1 human monocytes cell lines used in in this experiment were cultured following standard protocols as described below:

#### 3.2.2.1. HUVEC culture

HUVEC (ATCC® PCS-100-010™) were purchased together with vascular cell basal medium (ATCC® PCS-100-030™) and endothelial cell growth kit-VEGF (ATCC PCS-100-041™) from the ATCC (Manassas, VA, USA), and cells were maintained following the manufacturer's protocol. In brief, HUVEC were grown using 25-$cm^2$ culture flasks ( CELLSTAR®) under 5% $CO_2$ at 37 °C in cell media supplemented with the following: recombinant human (rh) VEGF (5 ng/ml), rh EGF (5 ng/ml), rh

FGF basic (5 ng/ml), rh IGF-1 (15 ng/ml), ascorbic acid (50 µg/ml), L-glutamine (10 mM), heparin sulphate (0.75 U/ml), hydrocortisone hemisuccinate (1µg/ml) and 2% Foetal Bovine Serum containing 10 U/ml of penicillin, 10 µg/ml of streptomycin and 25 ng/ml Amphotericin B solution (ATCC PCS-999-002). Cells were maintained until they reached approximately 80% confluence before sub-culturing with $5 \times 10^3$ cells per 25 $cm^2$ culture flask, and finally aliquoted as approximately 5 $x10^5$ viable cells/cryotube, and stored in liquid nitrogen until further use.

#### 3.2.2.2. THP-1 cell culture

THP-1 human monocyte cells were donated by Prof Andreas Suhrbier from QIMR-Berghofer Medical Research Institute, Brisbane, Queensland, Australia. They were maintained under 5% $CO_2$ at 37°C in complete medium comprising RPMI 1640 supplemented with penicillin (10 U/ml), streptomycin (10 µg/ml) and gentamycin (10 µg/ml) (Invitrogen) and 10% low endotoxin foetal calf serum (Invitrogen) until they reached approximately 80% confluence before sub-culturing with $5 \times 10^3$ cells per $cm^2$, and finally aliquoted with approximately $5 \times 10^5$ viable cells/cryotube, and stored in liquid nitrogen until further use.

### 3.2.3. *S. mansoni* EV labelling and their uptake by host cells

Fluorescent labelling of EVs was performed with PKH-67 (Sigma-Aldrich), a green lipophilic fluorescent dye, following the manufacturer's procedure. Briefly, EVs were labelled with PKH-67 for 5 min at RT, and the staining reaction was stopped by adding an equal amount of 1% purified bovine serum albumin (BSA), and incubated at RT for 1 min. PKH-67 excess dye was removed by centrifugation using 100 kDa cut-off spin filters (Amicon, Merk Millipore) at 3000 *g* and 15°C for 2 min, and vesicles were washed using PBS. Cells were cultured in the presence of PBS as control. HUVEC and THP-1 cells were grown to 80% confluence as described elsewhere using slide chambers (SPL life sciences) in the presence of labelled EVs (1.25 µg of total EV proteins) for 30, 60 or 120 min

at 37°C with 5% $CO_2$. Cell-culture medium was removed, wells were washed 3 times with PBS, cells were fixed in 4% paraformaldehyde, and incubated for 30 min at RT. Glycine (100 mM) was added to cultured cells for 15 min at RT to quench autofluorescence caused by paraformaldehyde residue on the samples. Finally, Hoechst (Abcam) was used to stain nuclei, and images were visualized using a laser scanning confocal microscope (Zeiss, LSM800).

### 3.2.4. Confocal microscopy

After thorough washing with PBS, cells were mounted in fluoroshield mounting medium (Abcam), and pictures were taken using a Zeiss confocal microscope (LSM800). All images were captured using standard excitation (EX) and emission (EM) filters, DAPI (348 nm EX/455 nm EM) and PKH-67 (495 nm EX/519 nm EM). The 2D deconvolution images were controlled with Zen 2.1 software (Carl Zeiss). Fluorescence intensity of internalised PKH-67-stained EVs was quantified using ImageJ and expressed as a percentage of corrected total cell fluorescence (CTCF) adjusted by background fluorescence.

### 3.2.5. *Sm*-TSP gene cloning

The cDNAs encoding for the open reading frames of the *Sm*-TSPs Smp_155310 (TSP-1) and Smp_140000 (TSP-2) were obtained from www.parasite.wormbase.org. The regions of the cDNAs encoding the large extracellular loop (LEL) of *Sm*-TSP-1 (Smp_155310, amino acids 110 to 202) were identified using Tmpred (https://embnet.vital-it.ch/software/TMPRED_form.html), and amplified using oligonucleotide forward primer (FP) (5' -CGCCCATGGGTCGAGAGGAGATCATGAAATAC-3' and reverse primer (RP) (5' -CGCCTCGAGCAACTTATCTTTTAACATCAC-3'), and for *Sm*-TSP-4 (Smp_140000, amino acid 130 to 249): FP (5'-CGCCCATGGGTTCTCGTAAAGATGAGATTGGA-3'),

RP (5'-CGCCTCGAGGTCCATATATTTAAGGAAAAG-3') incorporating *Nco*I and *Xho*I restriction sites (underlined) by using plasmid DNA containing genes of interest (already available in our laboratory)

as templates. The PCR reactions were performed as follows: 0.5µl (12.5 ng) plasmid DNA, 3µl (10 µM) forward primer and reverse primer each, 10 µl MyTaq red reaction buffer (Bioline), 0.5µl MyTaq DNA polymerase (Bioline), and 33 µl water. Cycling conditions were: initial cycle of denaturation at 95°C for 5 min, 35 cycles of denaturation at 95°C for 15 sec, annealing at 50°C for 15 sec and extension at 72°C for 30 sec, and a final extension step at 72°C for 7 min. Each amplicon was then ligated into the *Nco*I and *Xho*I sites of the pET32ΔHis (Novagen) expression vector such that they were in-frame with the vector's N-terminal thioredoxin and C-terminal 6xHis tags, produces a recombinant thioredoxin (TRX) fusion protein. The vector pET-32aΔHis is an in-house modified version of pET-32a (Novagen) which has the N-terminal 6xHis-tag absent (but retains the C-terminal 6xHis tag) to facilitate efficient purification after cleavage of the thioredoxin tag. The construct was then transformed into chemically competent *E. coli* BL21 (DE3) (ThermoFischer) using the heat-shock method following the manufacturer's instructions. *E. coli* transformants harbouring the plasmids were screened on Luria Bertani (LB) agar (1% yeast extract, 1% tryptone, 0.5% NaCl and 1.5% agar in water) plates containing ampicillin (100 µg/ml) (Sigma), and incubated overnight at 37$^{o}$C. Recombinant colonies were confirmed by colony PCR. DNA sequencing was performed to confirm the presence and the correct orientation of the open reading frame. A third TSP was produced, *Sm*-TSP-2 (Smp_181530), using *E. coli* BL21 (DE3) transformed with pET41a vector to facilitate native N-terminal expression without the TRX fusion tag, but retaining the C-terminal 6xHis tag.

### 3.2.6. Expression and purification of recombinant *Sm*-TSPs

#### 3.2.6.1. Pilot recombinant protein expression and detection

The *Sm*-TSP recombinant proteins (r*Sm*-TSPs) were pilot-expressed by inoculating 5 ml of LB broth (1% yeast extract, 1% tryptone and 0.5% NaCl in water) supplemented with ampicillin (100 µg/ml) (Sigma) with a single recombinant *E. coli* BL21 (DE3) colony containing the recombinant plasmid and

grown overnight with shaking (225 rpm) at 37°C. Glycerol stocks were made from each overnight culture and stored at -80°C. Overnight cultures were diluted 1:100 in 5 ml 2YT broth (1% yeast extract, 2% tryptone and 0.5% NaCl in water) containing ampicillin and grown to log phase (OD600 0.5-1.0) for 2 h with shaking (225 rpm) at 37°C. To find the optimal condition for protein induction, each culture was divided in half, one culture was induced by adding 1 mM isopropyl-b-d-1-thiogalactopyranoside (IPTG) (Bioline), and the second culture did not receive IPTG and served as the non-induced control sample. Cultures were incubated for 4 h with shaking (225 rpm) at 37°C. From each culture 1 ml was taken and pelleted at 16,000 *g* for 1 min, the supernatants were removed, and pellet was kept at -20$^{o}$C, and the growing cultures were maintained overnight with shaking (225 rpm) at 37°C. The following morning, 1 ml of each culture was pelleted at 16,000 *g* for 1 min, and supernatant was removed, and pellet samples including those harvested from the 4 h culture were resuspended in 250 µl of resuspension buffer (50 mM $Na_2HPO_4/NaH_2PO_4$, pH=8, 300 mM NaCl, 40 mM imidazole), and lysed by three cycles of freeze/thawing (-80$^{o}$C/42$^{o}$C). Samples were sonicated three times for 10 sec each and kept on ice between cycles. Samples were centrifuged at 16,000 *g* at 4$^{o}$C for 5 min to separate pelleted insoluble fractions and soluble fractions. Samples of both the insoluble and soluble fractions were subjected to 15% SDS-PAGE and were visualised by Coomassie staining.

#### 3.2.6.2. Large-scale Sm-TSP recombinant protein expression and purification

The r*Sm*-TSPs were expressed and purified as soluble proteins. Expression cultures were grown from glycerol stocks. First, 10 ml of broth media (1% yeast extract, 1% tryptone and 0.5% NaCl in water) supplemented with 100 µg/ml ampicillin (Sigma) was inoculated with a single recombinant *E. coli* BL21-DE3 colony containing the recombinant plasmid and grown overnight at 37$^{o}$C with shaking (200 rpm). The entire overnight culture were then used to seed 1 litre of LB broth media supplemented with 100 µg/ml ampicillin, and after 4 h of incubation protein expression was induced

using 1 mM IPTG. After 18 h of induction bacteria were pelleted by centrifugation at 8,000 *g* at 4°C for 20 min, and resuspended in 50 ml of lysis buffer (50 mM $Na_2HPO_4$ buffer, pH=8, 300 mM NaCl and 40 mM imidazole). Subsequently, the cells were submitted to 10 cycles of sonication lasting 5 sec each, and centrifuged at 16,000 *g* at 4°C for 5 min. Recombinant proteins were collected from supernatant as soluble proteins and stored at -80°C until further use. Recombinant proteins were thawed, and diluted (1:4) using buffer A (1 × PBS, 300 mM NaCl, pH=8), the resultant recombinant proteins solution were filtered through a 0.22 µm filter (Millipore Express™ Plus), and purified under non-denaturing conditions via 1 ml Hi-Trap nickel-sulphate affinity chromatography column (GE Healthcare Life Sciences) using an AKTApurifier™ (UPC 10, Sweden) at a flow rate of 1 ml/min. Bound proteins were eluted with an increasing concentration gradient of imidazole in elution buffer (1× PBS, 300 mM NaCl, 500 mM imidazole, pH=8). Various fractions obtained from the purification process were visualized by 15% SDS-PAGE gel with Coomassie staining. The fractions containing a clear single protein band were pooled, buffer-exchanged in PBS using 10 kDa Amicon centrifugal concentration devices (Millipore). The recombinant proteins were quantified using Pierce BCA protein assay kit (ThermoScientific) using BSA as the standard. For r*Sm*-TSP-2 expression and purification in *E. coli*, all the above processes were adhered to. After purification by IMAC, proteins were buffer exchanged into PBS using 3kDa Amicon centrifugal concentration devices (Millipore).

### 3.2.7. SDS-PAGE and immunoblotting

Each recombinant protein was electrophoresed on a 15% SDS-PAGE gel (Laemmli, 1970) and electroblotted onto nitrocellulose membrane (Towbin et al., 1979) for 1 h at 200 mA. Membrane was then blocked with Western blocking buffer (5% non-fat dry milk in TBST (0.5 M NaCl, 0.02 M Tris (pH 7.5) with 0.05% Tween-20) for 1 h with shaking at RT. Membrane was washed with PBST (PBS/0.05% Tween) 3 times each for 5 min, and probed with anti-6×His antibodies (ThermoScientific) diluted 1:2,000 in PBST at 4°C overnight, followed by washing (3 ×5 min with

PBS/0.05% Tween), then probing with goat anti-mouse IgG horseradish peroxidase (HRP)-conjugated (Invitrogen) diluted 1:2,000 in PBST at 4$^{o}$C for 1 h. Membrane was washed again with PBST three times for 5 min each, and developed using Amersham ECL$^{TM}$Prime Western Blotting Detection (GE Healthcare) as per the manufacturer's instructions. Briefly, working reagent was prepared by mixing 1 ml of each of solution A and B and applied onto the nitrocellulose membrane for 5 min. Excess of working reagent was removed and bound antibody was detected using a Versa DOC$^{TM}$ imaging system (Bio-Rad Laboratories).

### 3.2.8. Production of rabit antisera

Antibodies to *Sm*-TSP-2 and *Sm*-TSP-4 were raised in New Zealand white rabbits housed at the Institute of Medical and Veterinary Sciences, South Australia, as described previously (Pearson et al., 2012). Briefly, 100 µg of *Sm*-TSP-2 or *Sm*-TSP-4 (1 mg/ml) adjuvanted with an equal volume of Freund's complete adjuvant was subcutaneously administred 2 and 4 weeks later into a single New Zealand White. The rabbit was bled 2 weeks later and the serum collected by centrifugation.

### 3.2.9. Interruption of *S. mansoni* EV uptake by host cells using *Sm*-TSP antibodies

PKH-67-labelled *S. mansoni* ELVs and MVs (1.25µg of each) were incubated with anti-r*Sm*-TSP-2 or anti-r*Sm*-TSP-4 rabbit sera or control sera (naive rabbit sera) at 1:2.5 dilution with end-to-end mixing using a 360$^{o}$ rotator for 1 h at RT. *S. mansoni* EV-antibody complexes were then washed with 1× PBS using a 100 kDa cut-off centrifugation column (Amicon, Merk Millipore) at 3000 *g,* 4$^{o}$ C for 10 min to a final volume of 200 µl and cultured with $8 \times 10^3$ cells cells of both HUVEC and THP-1 human monocyte cells for 2 h under 5% $CO_2$ and at 37$^{o}$C. Nuclei were stained with 2 µg/ml of Hoechst (Invitrogen) for 15 min. Images were captured using a Zeiss LSM800 confocal microscope at 200 × the original magnification. A total of thirty cells were analysed from each sample for fluorescence intensity analysis using ImageJ version 1.50i.

### 3.2.10. EV internalisation or blockage data analysis

Data are represented as mean ± SD using GraphPad Prism™ Software version 7.03 (www.graphpad.com). Fluorescence intensity data were evaluated by Student's t-test and $P<0.05$ was considered as statistically significant.

### 3.2.11. RNA extraction

Initially, HUVEC cells were seeded at $7.5 \times 10^4$ using 25 $cm^2$ culture flasks (CELLSTAR®) and cultured for 24 h. *S. mansoni* ELVs (5 µg) were filtered using 0.2 µm filters (Whatman™) and added to cells, and incubated for another 72 h at 5% $CO_2$ and 37°C. Both HUVEC cells as well as mouse fibroblast derived-MVs (isolated from supernatant solution collected from cultured mouse fibroblasts following the same procedure used to isolate *S. mansoni* MVs) incubated with HUVEC cells were used as control. After three days of incubation, the cells were washed with PBS 3 times, and then 1 ml Trizol (Sigma-Aldrich) was added to preserve RNA prior to storage at -80°C. Total RNA was extracted using standard procedures as described elsewhere (Eichenberger et al., 2018c). Briefly, 0.2 ml chloroform (Sigma-Aldrich) was added to thawed samples, shaken vigorously for 15 sec, incubated at RT for 5 min, and centrifuged at 12,000 *g* for 15 min at 4°C. The upper aqueous phase was transferred to a fresh tube, and 0.5 ml isopropyl alcohol (Sigma-Aldrich) and 3 µl glycoblue (Invitrogen) were added, and incubated for 10 min at RT. Samples were centrifuged at 12,000 *g* for 10 min at 4°C, supernatant was discarded, and the pellet washed with 1 ml of 75% ethanol in diethyl pyrocarbonate (DEPC) water (Invitrogen), mixed by vortexing and centrifuged at 7,500 *g* for 5 min at 4°C. The supernatant was then discarded, pellets air dried, and dissolved in 20 µl DEPC water, and stored at -80°C until further processed. Two biological replicates of each sample were prepared for RNA-Seq – the difficulty in obtaining sufficient quantities of *S. mansoni* ELVs prevented the use of a third biological replicate for RNA-Seq.

### 3.2.12. DNase digestion of RNA and RNA clean-up

To digest contaminating DNA in RNA solutions prior to RNA clean-up, 10 µl Buffer RDD (DNA Digest Buffer) (Qiagen), and 2.5 µl DNase I stock solution (Qiagen) were added to the RNA samples and mixed, and the final volume was brought up to 100 µl with RNase-free water (Qiagen), and samples were incubated for 10 min at RT. For RNA clean-up, 350 µl Buffer RLT (guanidine-thiocyanate–containing lysis buffer) (Qiagen) was added, mixed well, and 250 µl of 100% ethanol was added to the diluted RNA, and mixed well by pipetting. Samples were transferred immediately to an RNeasy Mini spin column (Qiagen) placed in a 2 ml collection tube, and centrifuged for 15 sec at 8,000 *g*, and flow-through was discarded. Buffer RPE 500 µl (Qiagen) was added to the sample in the RNeasy spin column, followed by centrifugation of the columns for 15 sec at 8,000 *g*. Column flow-through was discarded, and this procedure was repeated at the same speed but for 2 min. The sample collection tube was changed, and samples were centrifuged for 1 min at 16,000 *g*. Again, RNeasy spin column was placed in a new 1.5 ml collection tube, and 50 µl of RNase-free water was added directly to the spin column membrane, and centrifuged for 2 min at 8,000 *g* to elute the RNA. Finally, the concentration of RNA in the samples was measured using a nanodrop (LabGear). Extracted RNA from the different samples was sent to the Australian Genome Research Facility (AGRF) in Melbourne, Victoria, Australia for RNA deep sequencing.

### 3.2.13. RNA quality control, library preparation and sequencing

Sample quality control was performed using a Bioanlayzer RNA 6000 Nano kit. Library preparation and sequencing were performed at the AGRF. Total RNA was prepared for sequencing using an Illumina TruSeq stranded Total RNA-seq library preparation kit (Illumina). RNAseq was performed on a NovaSeq SP (S-Pime) 300 cycle kit (Illumina, paired-end 150-bp PE read, approximately 30M reads per sample).

### 3.2.14. RNAseq mapping

Gencode version 29, RNA annotations (in gtf format) for human were downloaded from ftp.ebi.ac.uk/pub/databases/gencode/Gencode_human/release_29/. "chr" was stripped from the transcript annotations, and chromosomes relabeled 1-22, X, Y, MT for compatibility with hg38/GRCb38, release 95 annotations. STAR version 2.7.0e (Dobin et al., 2013) was used for building genome indices and mapping. For genome indices, gtf (complete) and genome fasta files (as described above) were provided to STAR as parameters –sjdbGTFfile and –geneFastaFiles with --runMode genomeGenerate to generate indices. --sjdbOverhand was set to 149 for total RNA and 49 for miRNA (read length – 1). All other parameters remained default. Adapter trimming was performed using trimgalore version 0.5.0 (https://github.com/FelixKrueger/TrimGalore) (implemented in python version 3.6.5) and run in paired-end mode (using the-paired parameter) and adapters trimmed were "–illumina". Sequence end soft clipping was performed using the default phred score of 20 and paired reads less than 20 bp were discarded. All other parameters were default. For mapping of RNA, STAR was run in paired end mode with --runMode alignReads –sjdbGTFfile and –genomeDir using the pre-built STAR genome index and gtf generated as described, --readFilesIn with specified paired reads. Non-default parameters used were: --outFilterMultimapNmax 20; --outFilterMismatchNmax; --outFilterMismatchNoverReadLmax 0.04; --outFilterType BySJout; --alignIntronMin 20; --alignIntronMax 1000000; --alignMatesGapMax 1000000; --alignSJoverhangMin 8; --alignSJDBoverhangMin 1; --sjdbScore 1. All other parameters were default. Bam files were sorted by name (-n), with samtools version 1.7, and reads summarized using htseq-count version 0.11.1 (Anders et al., 2015) (implemented with python version 3.6.5) and stranded mode was selected (reverse - for TruSeq stranded library). All other parameters were default. FastQC version 0.11.7 (Simon, 2010), was used for the assessment of read quality before and after adapter trimming.

### 3.2.15. Differential gene expression analysis

consensusDE (Waardenberg and Field, 2019) (BioConductor development version 1.3.3) in R version 3.5.1 was used for subsequent differential expression (DE) analysis. A summarized table containing read counts of all RNAseq experiments was built using the buildSummarized function in consensusDE, with a sample table provided that described the experimental design, the path to the HTSEQ files generated above and the same gtf file described above, and low read counts filtered by selecting, filter = TRUE. multi_de_pairs was then called using the filtered summarized experiment object generated with buildSummarized and transcript annotations conducted with both org.Hs.eg.db (version 3.6.0) provided as input to ensembl_annotate, adjust method (being the method for multiple hypothesis correction) set to "bonferonni" and the beforementioned gtf provided to gtf_annotate. ruv_correct was set to TRUE (Risso et al., 2014) and all other parameters remained default. consensusDE then generated all pairwise comparisons possible and combined the results of voom (as implemented in limma version 3.36.5) (Ritchie et al., 2015), edgeR (version 3.22.5) (Robinson et al., 2010, McCarthy et al., 2012) and DESeq2 (1.20.0) (Love et al., 2014) algorithms.

### 3.2.16. Bioinformatics analysis

Gene ontology analysis was then conducted using GO analysis, KEGGgraph version 1.42.0 (Zhang and Wiemann, 2009), and STRINGdb version 9.1 (Franceschini et al., 2013) packages for R where differential expression was defined as a $P<0.01$ and a fold change greater than 1.5 or -1.5.

## 3.3. Results

### 3.3.1. *S. mansoni* EVs are internalised by both HUVEC and THP-1 human monocyte cells

To test the hypothesis that *S. mansoni*-derived EVs interact with host cells *in vitro*, HUVEC (Figure 3.1) and THP-1 monocytes (Figure 3.2) were incubated with PKH-67 labelled ELVs and MVs. Uptake of ELVs and MVs was observed with both HUVEC and THP-1 cells. Stained EVs are visible inside the cytoplasm of both cell lines, and the fluorescence intensity increased over time. There was a significant increase in uptake of both ELVs and MVs by HUVEC cells incubated for 30 min (68% ($P$<0.05) and 93% ($P$<0.0001)), 60 min (98% ($P$<0.0001) and 99 % ($P$<0.0001)), and 120 min (99.7 % ($P$<0.0001) and 100% ($P$<0.0001)), respectively, compared to PBS control (Figure 3.1D). Similarly, there was a significant increase in uptake of both ELVs and MVs by THP-1 cells incubated for 30 min (86% ($P$<0.0001) and 92% ($P$<0.0001)), 60 min 86% ($P$<0.0001) and 95% ($P$<0.0001)), and 120 min (99% ($P$<0.0001) and 100% ($P$<0.0001)), respectively, compared to PBS control (Figure 3.2D).

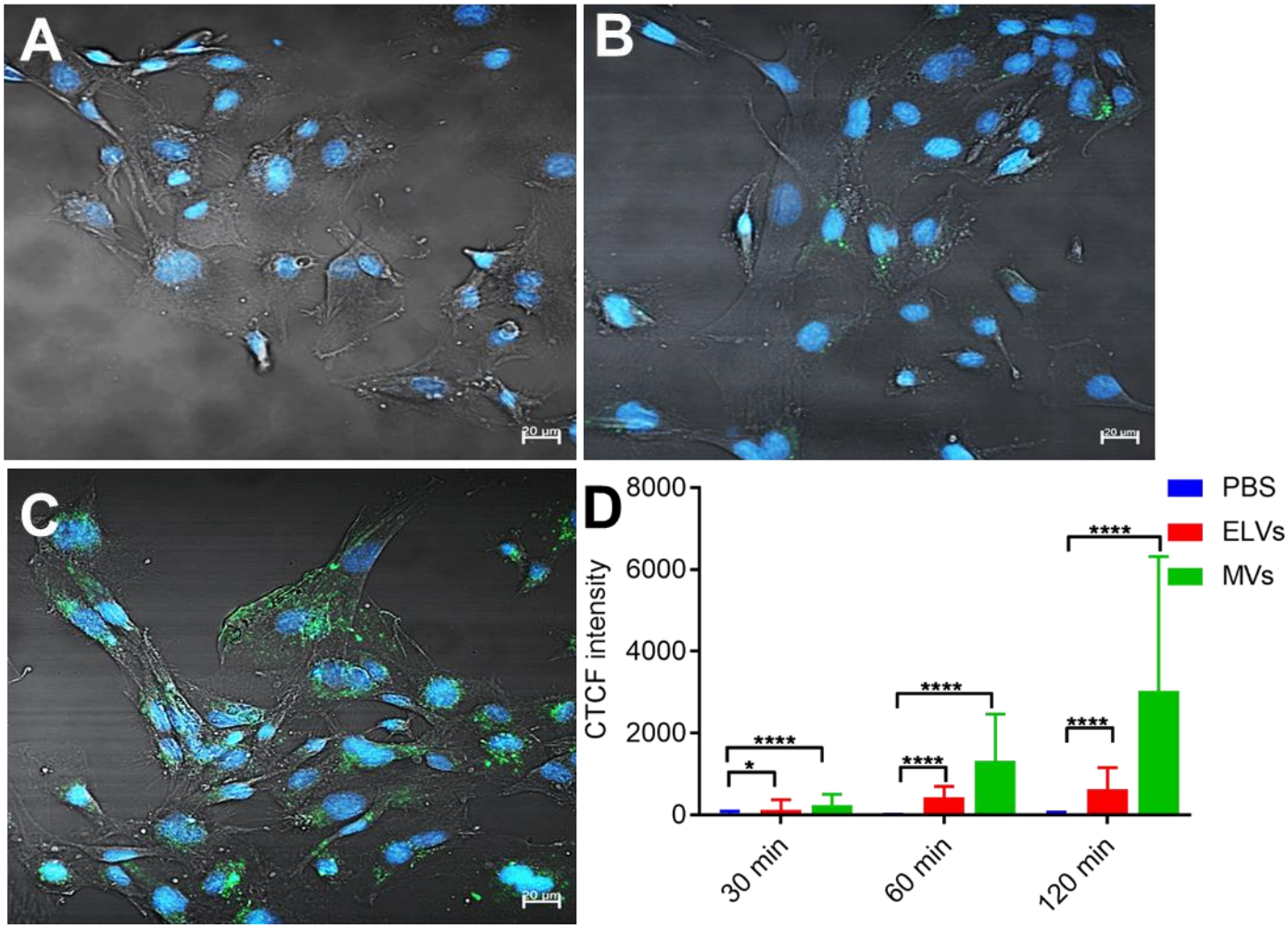


**Figure 3.1. Uptake of *S. mansoni* extracellular vesicles by epithelial HUVEC cells.** Panel A = PBS control, Panel B = PKH67-labelled *S. mansoni* ELVs, C= PKH67-labelled *S. mansoni* MVs after 120 min incubation and Panel D= shows fluorescence intensity at 490 nm (green channel) for *S. mansoni* both ELVs and MVs and PBS control incubated with HUVEC cells for 30, 60 and 120 min. The nuclei were stained by Hoechst (blue colour). Scale bars = 20µm. Data were presented as the mean ± SD of fluorescence quantification using ImageJ software. Asterisks indicate significant differences (Student's t-test, **P* < 0.05, *****P* <0.0001).

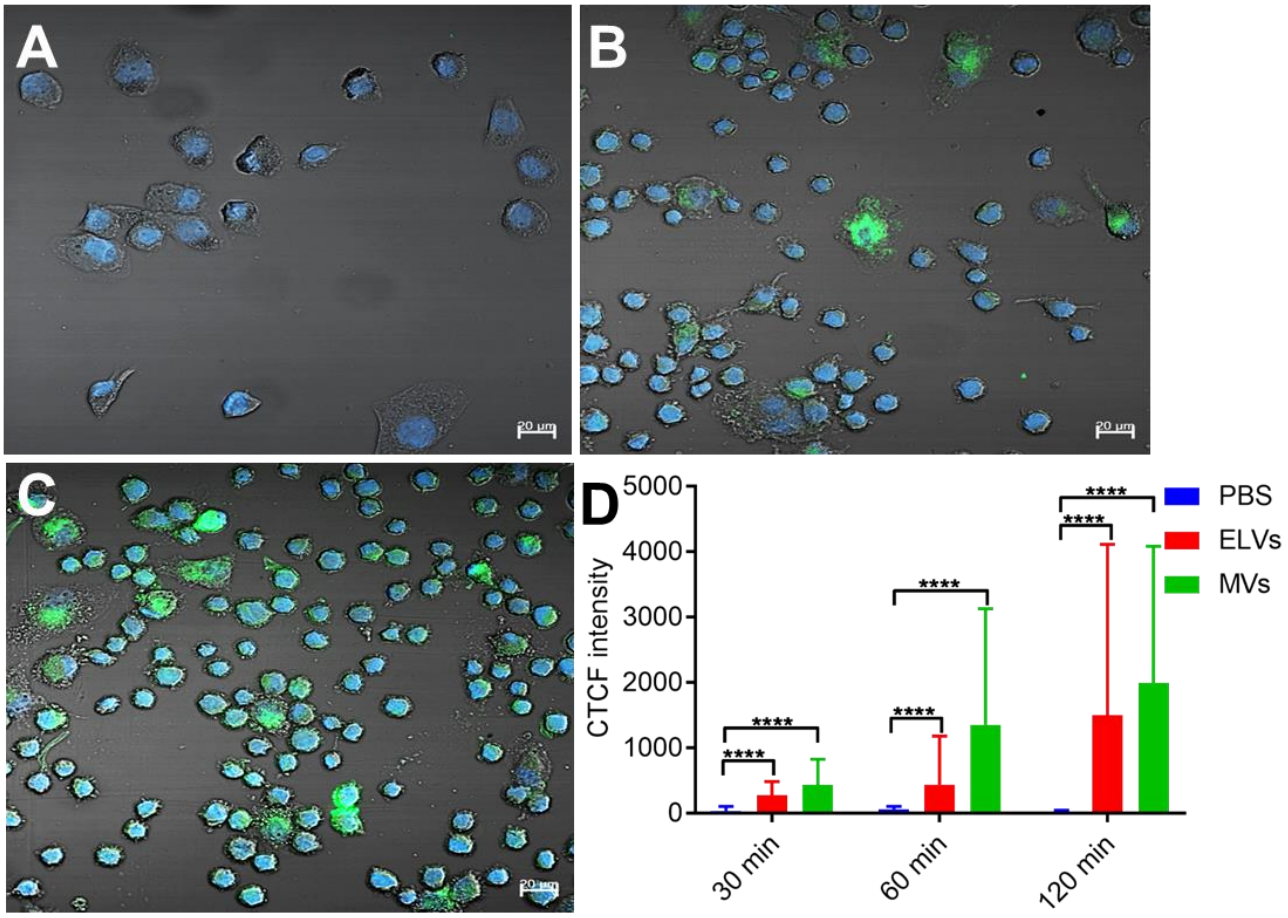


**Figure 3.2. Uptake of *S. mansoni* extracellular vesicles by THP-1 human monocyte cells.** Panel A = PBS control, Panel B = *S. mansoni* ELVs; Panel C = *S. mansoni* MVs after 120 min incubation; Panel D shows fluorescence intensity at 490 nm (green channel) for both *S. mansoni* ELVs and MVs and PBS control incubated with THP-1 human monocyte cells for 30, 60 and 120 min. The nuclei were stained by Hoechst (blue colour). Scale bars = 20 µm. Data are presented as the mean ± SD of fluorescence quantification using ImageJ software. Asterisks indicate significant differences (Student's t-test, ****$P$ <0.0001).

### 3.3.2. Recombinant protein production

TRX fused LEL of *Sm*-TSP-1 (corresponding to predicted molecular weights (mw) including 6 ×His tag = 32.3 kDa) and *Sm*-TSP-4, mw = 34.3 kDa, as well as *Sm*-TSP-2 without TRX, mw = 12.4 kDa, were expressed in *E. coli* BL21 (DE3) using IPTG-induction at 37°C overnight and purified by IMAC. The

size and purity of the recombinant TSPs (rTSPs) were assessed by SDS-PAGE and stained with Coomassie Brilliant Blue (Figure 3.3A) and Western blotting with anti-6xHis-HRP (Figure 3.3B).

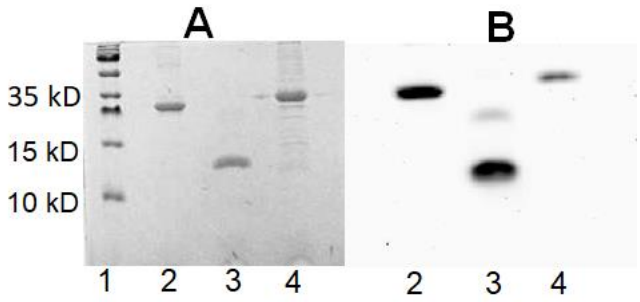


**Figure 3.3. SDS-PAGE and Western blot analysis of recombinant purified *Sm*-TSP proteins.** (A) Coomassie blue stained SDS-PAGE profile of the purified recombinant proteins and (B) identically loaded Western blot analysis of recombinant proteins probed with anti-6xHis-HRP. (1) protein ladder; (2) IMAC-purified *Sm*-TSP-1 fused to N-terminal thioredoxin and C-terminal 6xHis tags; (3) *Sm*-TSP-2 with C-terminal 6xHis tag; (4) *Sm*-TSP-4 fused to N-terminal thioredoxin and C-terminal 6xHis tags.

### 3.3.3. Anti-*S. mansoni* TSP antibodies block the uptake of *Sm*-derived EVs by both HUVEC and THP-1 human monocyte cells

PKH-67-labelled *S. mansoni* ELVs and MVs were incubated with rabbit antisera raised to *Sm*-TSP-2 or *Sm*-TSP-4 or pre-immunisation rabbit sera as control at a dilution of 1:2.5 before being cultured with HUVEC cells or THP-1 monocytes. Both anti-r*Sm*-TSP-2 and anti-r*Sm*-TSP-4 antibodies compared to naïve rabbit sera significantly reduced the internalisation of both *S. mansoni* ELVs (Figure 3.4) and *S. mansoni* MVs (Figure 3.5) by HUVEC cells. Moreover, anti-r*Sm*-TSP-2 and anti-r*Sm*-TSP-4 resulted in a significant reduction of 94% ($P$<0.0001) and 97% ($P$<0.0001)), and (93% ($P$<0.0001) and 96% ($P$<0.0001) in the uptake of *S. mansoni* ELVs (Figure 4B and 4C) and *S. mansoni* MVs (Figure 5B and 5C), respectively. CTCF analysis highlights the extent to which internalisation of *S. mansoni* ELVs (Figure 3.4D) and *S. mansoni* MVs (Figure 3.5D) into HUVEC cells was blocked.

Comparably, anti-r*Sm*-TSP-2 and anti-r*Sm*-TSP-4 also resulted in significant reductions of 99% (*P*<0.0001) and 99.5% (*P*<0.0001), respectively, in uptake of *S. mansoni* ELVs (Figure 3.6) by THP-1 human monocyte cells. Anti-r*Sm*-TSP-2 and anti-r*Sm*-TSP-4 also showed 80% (*P*<0.0001) and 53% (*P*<0.001) reductions, respectively, in the uptake of *S. mansoni* MVs (Figure 3.7) by THP-1 human monocyte cells.

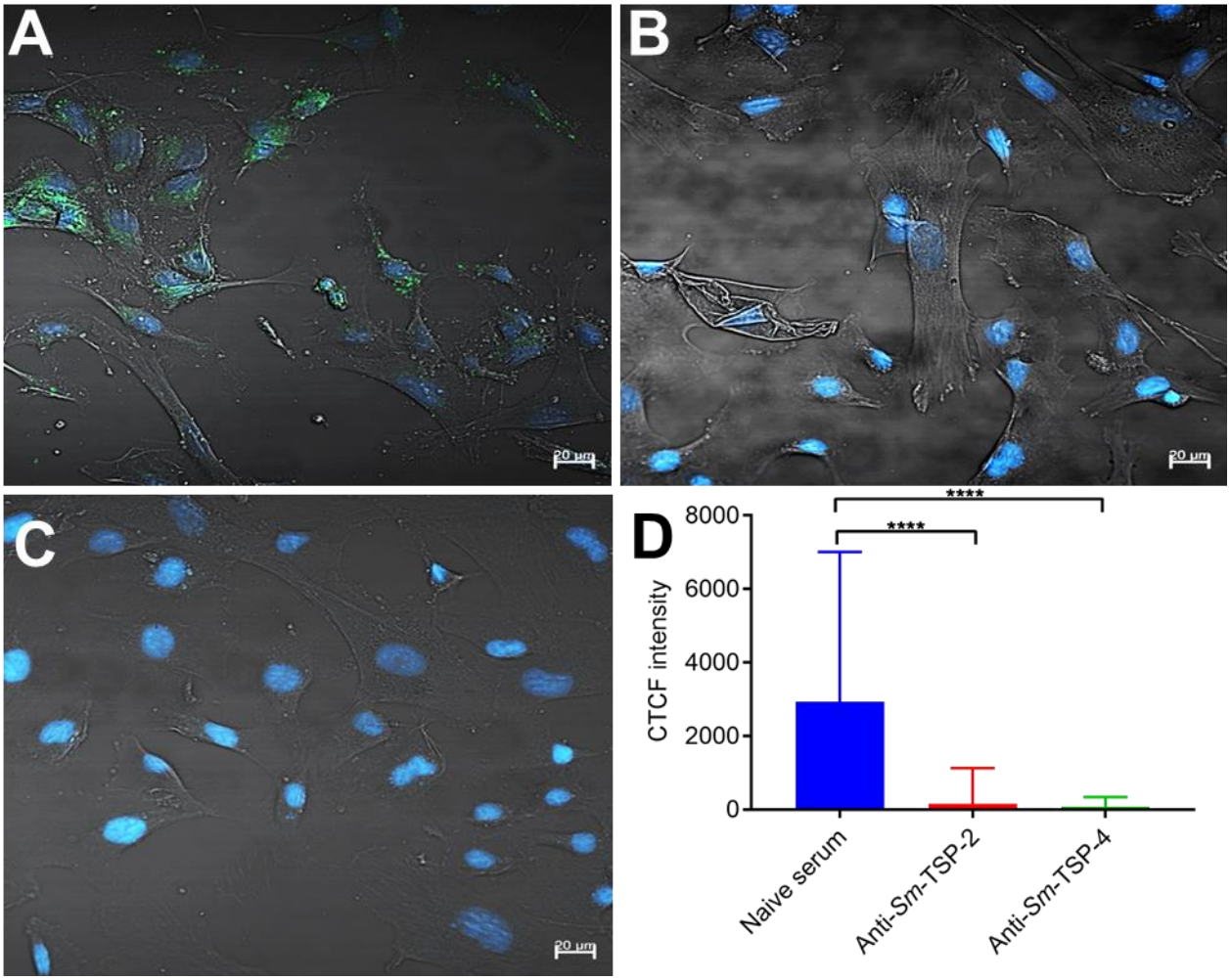


**Figure 3.4. *Sm*-TSP antisera blocks *S. mansoni* exosome-like vesicle uptake by HUVEC cells.** PKH67-labeled *S. mansoni* ELVs were incubated for 1 h with rabbit antisera to r*Sm*TSP-2 or r*Sm*-TSP-4 or pre-immunisation serum as control prior to co-culture with HUVEC cells for 2 h. Panel A = pre-immunisation serum diluted 1:2.5, panel B = antiserum to r*Sm*-TSP-2 diluted 1:2.5, panel C = rabbit antiserum to r*Sm*-TSP-4 diluted 1:2.5; panel D shows fluorescence intensity at 490 nm (green channel). The nuclei were stained by Hoechst (blue colour). Scale bars = 20µm. Data were presented

as the mean ± SD of fluorescence quantification using ImageJ software. Asterisks indicate significant differences (Student's t-test, ****$P < 0.0001$).

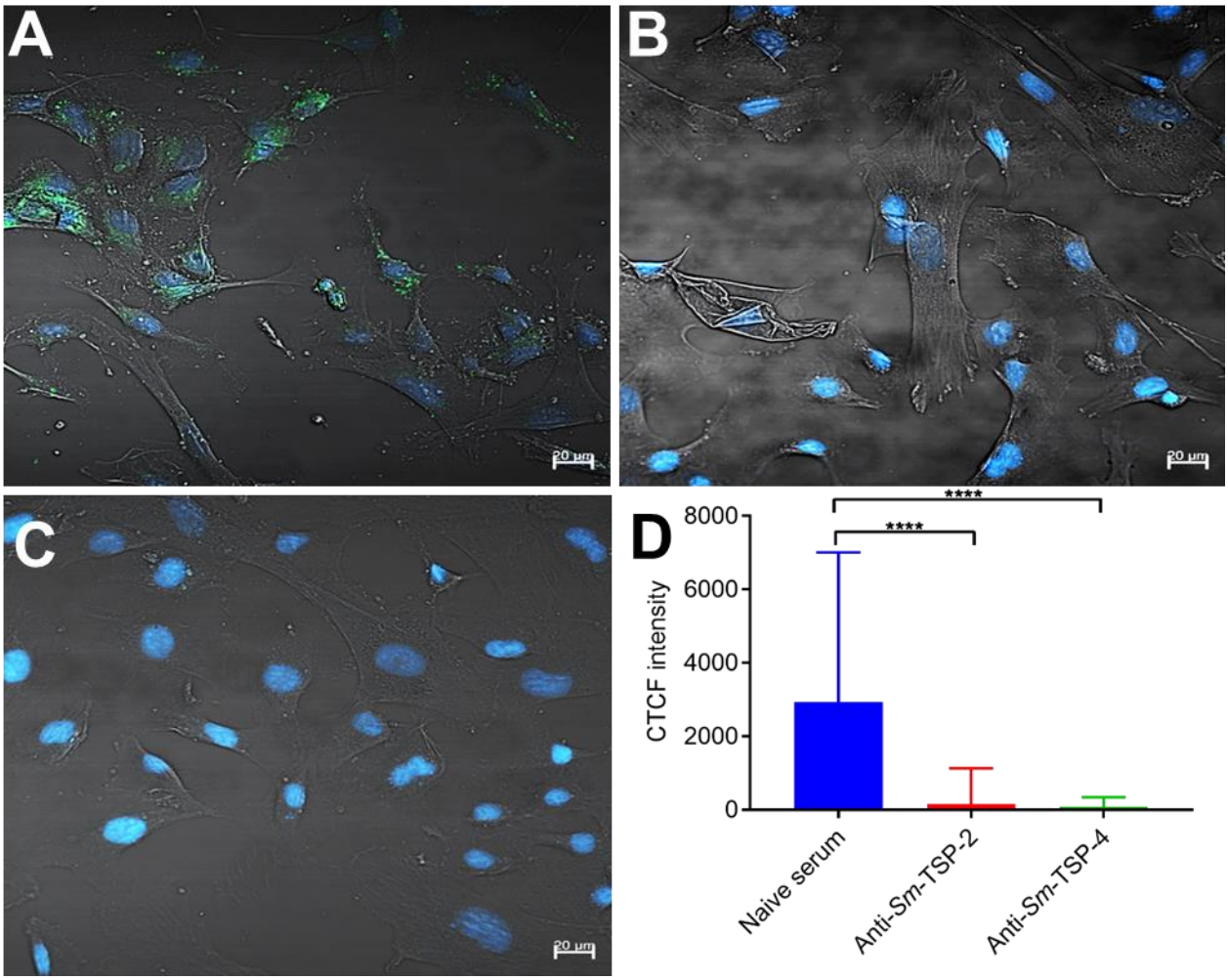


**Figure 3.5. *Sm*-TSP antisera blocks *S. mansoni* microvesicle internalisation by HUVEC cells.** PKH67-labeled *S. mansoni* MVs were incubated for 1 h with rabbit antisera to r*Sm*TSP-2 or r*Sm*-TSP-4 or pre-immunisation serum as control prior to co-culture with HUVEC cells for 2 h. Panel A = pre-immunisation serum diluted 1:2.5, panel B = antiserum to r*Sm*-TSP-2 diluted 1:2.5, panel C = rabbit antiserum to r*Sm*-TSP-4 diluted 1:2.5; panel D= shows fluorescence intensity at 490 nm (green channel). The nuclei were stained by Hoechst (blue colour). Scale bars =20µm. Data were presented as the mean ± SD of fluorescence quantification using ImageJ software. Asterisks indicate significant differences (Student's t-test, ****$P < 0.0001$).

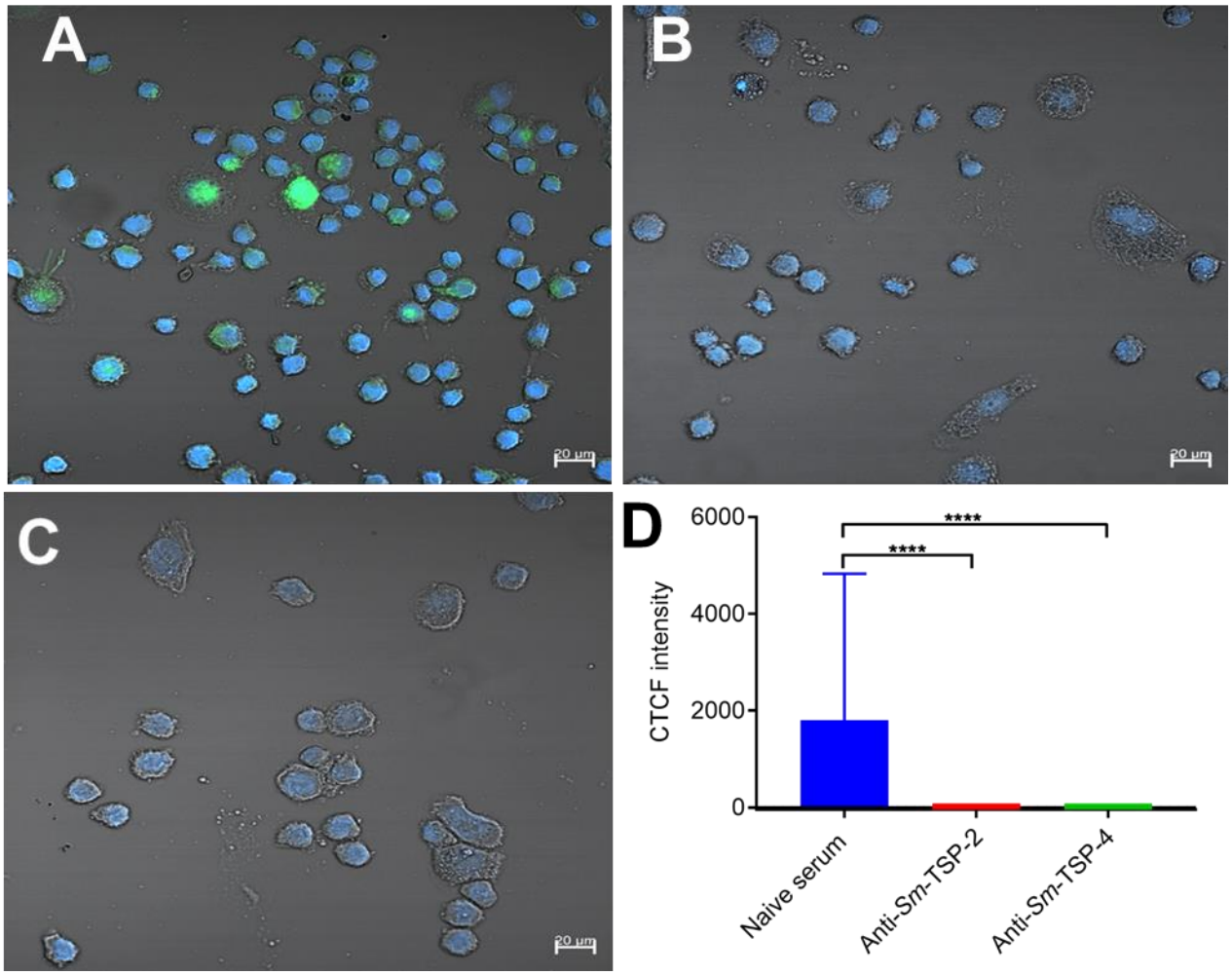


**Figure 3.6. *Sm*-TSP antisera blocks *S. mansoni* exosome-like vesicle internalisation by THP-1 human monocyte cells.** PKH67-labeled *S. mansoni* ELVs were incubated for 1 h with rabbit antisera to r*Sm*TSP-2 or r*Sm*-TSP-4 or pre-immunisation serum as control prior to co-culture with THP-1 human monocyte cells lines for 2 h. Panel A = pre-immunisation serum diluted 1:2.5, panel B = antiserum to r*Sm*-TSP-2 diluted 1:2.5, panel C = rabbit antiserum to r*Sm*-TSP-4 diluted 1:2.5; panel D shows fluorescence intensity at 490 nm (green channel) using confocal fluorescence microscopy. The nuclei were stained by Hoechst (blue colour). Scale bars =20µm. Data were presented as the mean ± SD of fluorescence quantification using ImageJ software. Asterisks indicate significant differences (Student's t-test, ****$P < 0.0001$).

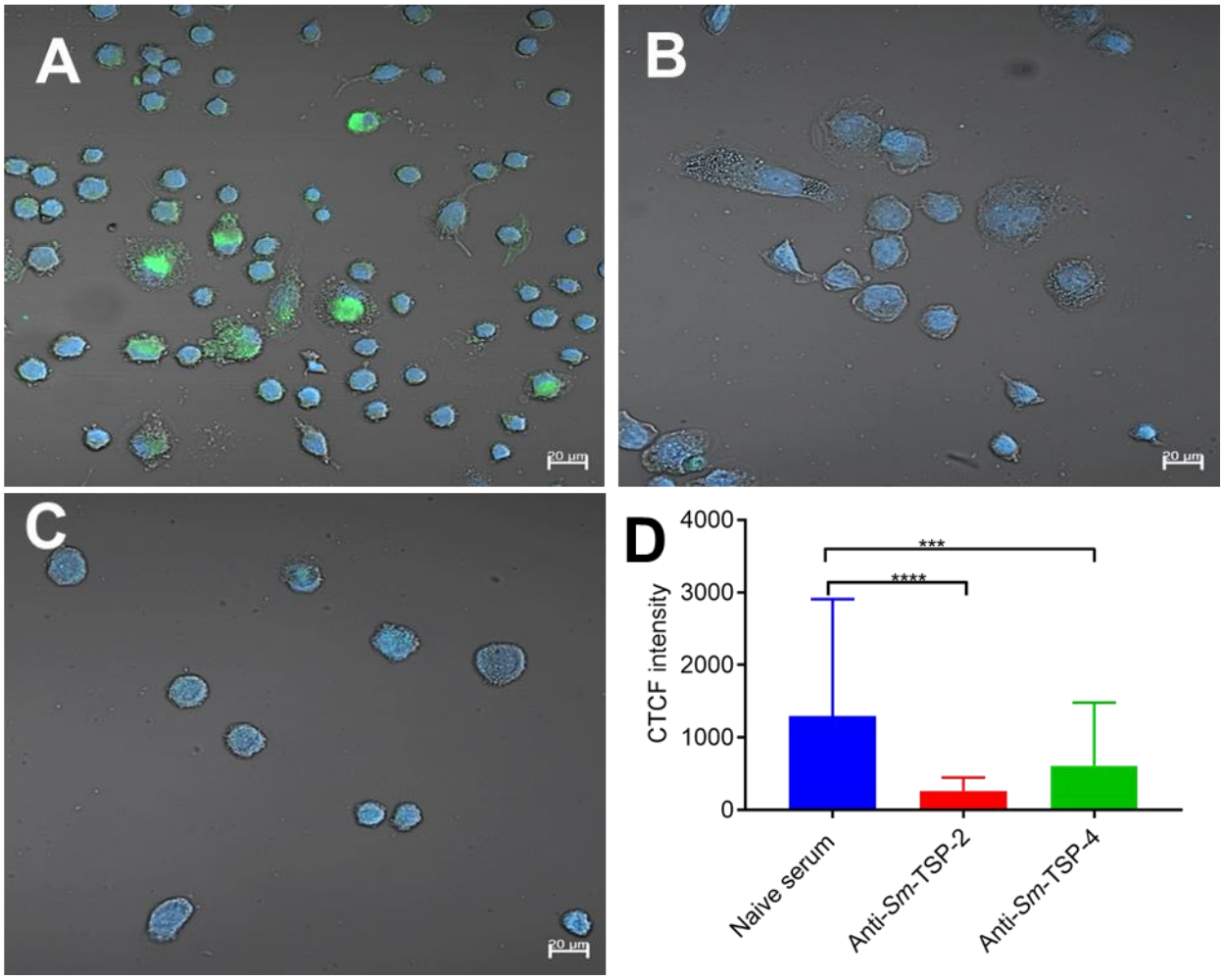


**Figure 3.7. *Sm*-TSP antisera blocks *S. mansoni* microvesicle internalisation by THP-1 human monocyte cells.** PKH67-labeled *S. mansoni* MVs were incubated for 1 h with rabbit antisera to r*Sm*TSP-2 or r*Sm*-TSP-4 or pre-immunisation serum as control prior to co-culture with THP-1 human monocyte cells lines for 2 h. Panel A = pre-immunisation serum diluted 1:2.5, panel B = antiserum to r*Sm*-TSP-2 diluted 1:2.5, panel C = rabbit antiserum to r*Sm*-TSP-4 diluted 1:2.5; panel D shows fluorescence intensity at 490 nm (green channel) using confocal fluorescence microscopy. The nuclei were stained by Hoechst (blue colour). Scale bars =20µm. Data were presented as the mean ± SD of fluorescence quantification using ImageJ software. Asterisks indicate significant differences (Student's t-test, ***$P$<0.001, ****$P$ < 0.0001).

### 3.3.4. Differential gene expression

RNAseq data analysis of HUVEC cells incubated with *S. mansoni* ELVs revealed 59 differentially expressed genes (DEGs) compared to HUVEC controls. Of these, 42 were upregulated and 17 were downregulated compared to control cells at *P*<0.01 and logFC of 1.5 (Table 3.1 and Figure 3.8).

**Table 3.1. Differential gene expression of HUVEC cells upon incubation with *S. mansoni* exosome-like vesicles** at log2-foldchange, FC > 50%, and adjusted *P*-value =FDR, P<0.01.

| Gene name | Gene Symbol | Foldchange | P-value |
|---|---|---|---|
| Arachidonate 15-lipoxygenase, type B | ALOX15B | -3.973312244 | 3.91E-08 |
| Solute carrier family 14 member 1 (Kidd blood group) | SLC14A1 | -3.75152481 | 8.85E-05 |
| Uncharacterized | AL445305.1 | -3.688949405 | 0.0095907 |
| Metallothionein 3 | MT3 | -3.27432529 | 3.15E-05 |
| Cytochrome P450 family 1 subfamily B member 1 | CYP1B1 | -2.862460755 | 0.0001033 |
| Annexin A10 | ANXA10 | -2.265138015 | 0.0022851 |
| L1 cell adhesion molecule | L1CAM | -2.083537678 | 0.0005084 |
| Coagulation factor III, tissue factor | F3 | -2.044594965 | 4.59E-06 |
| Uncharacterized | AC234772.2 | -1.901623016 | 0.0008176 |
| Myopalladin | MYPN | -1.888286159 | 9.86E-06 |
| lncRNA sorafenib resistance in renal cell carcinoma associated | LNCSRLR | -1.849184496 | 0.0039688 |
| ADAM metallopeptidase with thrombospondin type 1 motif 1 | ADAMTS1 | -1.837069559 | 8.27E-06 |
| Keratin associated protein 2-3 | KRTAP2-3 | -1.830788931 | 1.06E-06 |
| Sushi, von Willebrand factor type A, EGF and pentraxin domain containing 1 | SVEP1 | -1.697428425 | 1.10E-06 |
| Serpin family G member 1 | SERPING1 | -1.613517902 | 0.0002031 |
| G protein-coupled receptor class C group 5 member A | GPRC5A | -1.610223006 | 1.89E-10 |
| Homeobox A13 | HOXA13 | -1.521581888 | 0.0018089 |
| Spectrin beta, non-erythrocytic 5 | SPTBN5 | 1.501242743 | 0.0003031 |
| Interferon alpha inducible protein 27 | IFI27 | 1.503973236 | 7.44E-05 |
| Adhesion G protein-coupled receptor G1 | ADGRG1 | 1.511365191 | 0.0009681 |

| | | | |
|---|---|---|---|
| Solute carrier family 29 member 2 | SLC29A2 | 1.51172568 | 0.0052509 |
| Proline rich 15 | PRR15 | 1.529170415 | 0.0010466 |
| Receptor activity modifying protein 2 | RAMP2 | 1.565471238 | 0.0002012 |
| Desmoplakin | DSP | 1.594792001 | 0.0002465 |
| C-X-C motif chemokine ligand 2 | CXCL2 | 1.625825806 | 1.28E-06 |
| Neurotensin receptor 1 | NTSR1 | 1.629169423 | 0.0037779 |
| Interleukin 6 | IL6 | 1.683722285 | 0.0021358 |
| Mesenteric estrogen dependent adipogenesis | MEDAG | 1.684277397 | 0.0013488 |
| RAB3A interacting protein like 1 | RAB3IL1 | 1.687254515 | 0.0001589 |
| Bone marrow stromal cell antigen 2 | BST2 | 1.697082808 | 3.08E-07 |
| G protein-coupled receptor 4 | GPR4 | 1.698444579 | 0.0002736 |
| Lysosomal associated membrane protein 3 | LAMP3 | 1.713792795 | 3.51E-05 |
| Tribbles pseudokinase 3 | TRIB3 | 1.719404631 | 0.0006135 |
| Growth differentiation factor 15 | GDF15 | 1.767357785 | 0.0005193 |
| Integrin subunit beta 4 | ITGB4 | 1.778296215 | 0.0081078 |
| ChaC glutathione specific gamma-glutamylcyclotransferase 1 | CHAC1 | 1.834863558 | 0.008595 |
| Dishevelled binding antagonist of beta catenin 1 | DACT1 | 1.878293141 | 0.0009148 |
| Carboxypeptidase X, M14 family member 1 | CPXM1 | 1.897608027 | 2.99E-05 |
| Phospholipase A2 group III | PLA2G3 | 1.912424965 | 0.0033182 |
| DNA damage inducible transcript 3 | DDIT3 | 1.920769774 | 0.007029 |
| Prostaglandin I2 synthase | PTGIS | 1.935688955 | 0.000287 |
| CDC42 binding protein kinase gamma | CDC42BPG | 1.946425707 | 0.0098185 |
| Apolipoprotein E | APOE | 1.956098223 | 0.0064436 |
| Protein phosphatase 1 regulatory inhibitor subunit 14A | PPP1R14A | 2.024533301 | 7.20E-05 |
| KIAA1755 | KIAA1755 | 2.096818517 | 4.43E-05 |
| Homeobox B9 | HOXB9 | 2.183061954 | 0.0041297 |
| Forkhead box S1 | FOXS1 | 2.230204253 | 0.002425 |
| Proprotein convertase subtilisin/kexin type 9 | PCSK9 | 2.255661834 | 3.58E-07 |
| Interleukin 21 receptor | IL21R | 2.281196663 | 0.0014368 |
| C-type lectin domain family 4 member G pseudogene 1 | CLEC4GP1 | 2.325996829 | 6.95E-07 |
| GLI family zinc finger 1 | GLI1 | 2.565422205 | 0.0047162 |

| | | | |
|---|---|---|---|
| Aggrecan | ACAN | 2.727991377 | 4.26E-06 |
| Follistatin like 5 | FSTL5 | 2.775761257 | 3.13E-06 |
| Cadherin 8 | CDH8 | 2.787079061 | 0.0045313 |
| Musculin | MSC | 2.948933812 | 0.0016573 |
| Cadherin related family member 1 | CDHR1 | 3.049841871 | 1.87E-10 |
| NIPA like domain containing 4 | NIPAL4 | 3.264323401 | 2.58E-09 |
| Kelch domain containing 7B | KLHDC7B | 4.301916647 | 0.0003094 |
| Derlin 3 | DERL3 | 4.336143784 | 0.0002043 |

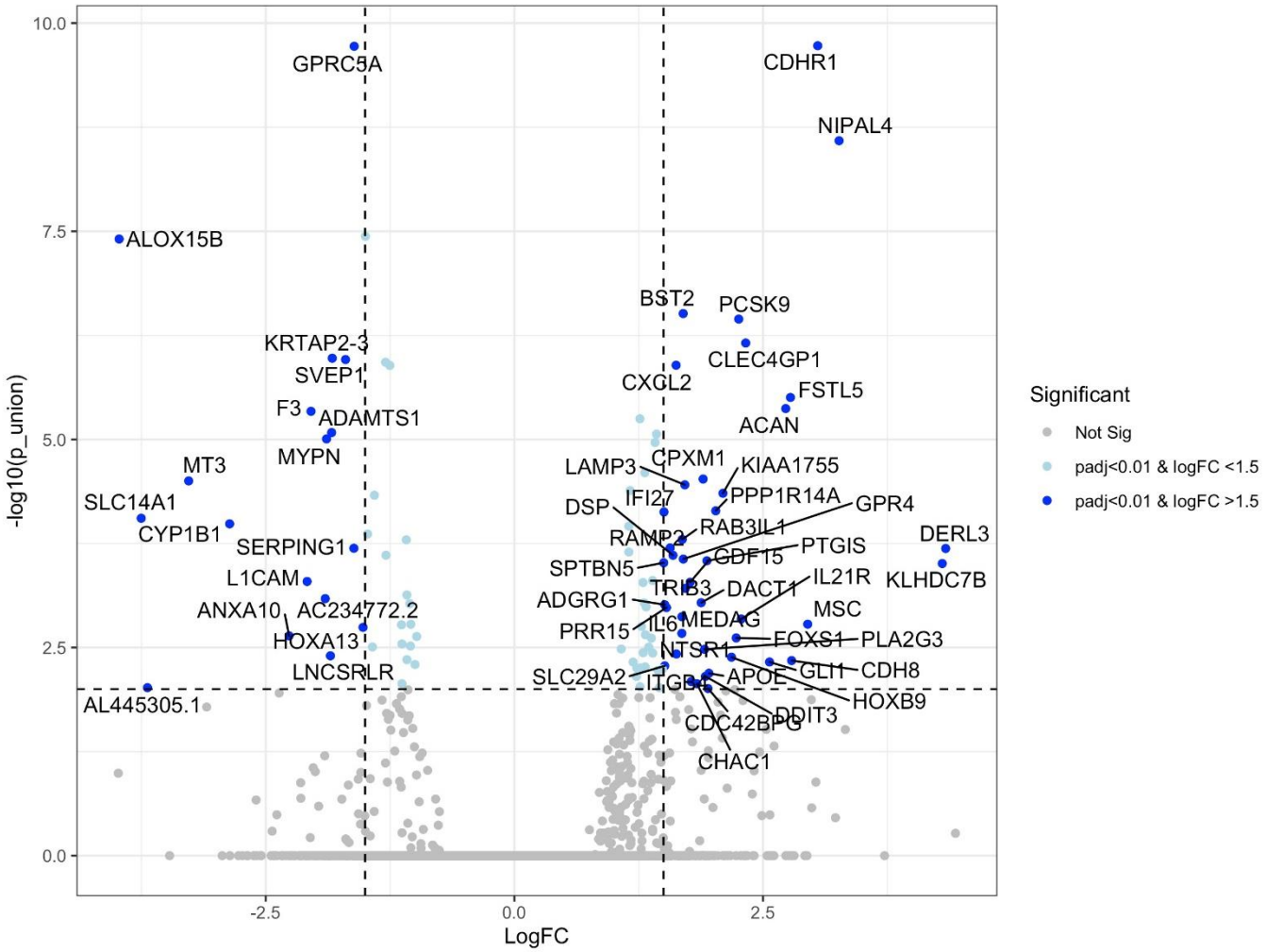


**Figure 3.8. Volcano plot of differential gene expression of HUVEC cells upon incubation with *S. mansoni* exosome-like vesicles.** Vertical axis represents log2-foldchange, FC > 50%, and horizontal

axis represents adjusted *P*-value = FDR, P<0.01. Genes with significant expression changes are represented in distinct shades of blue.

GO analysis revealed that DEGs have primary roles in cell communication, developmental processes, response to stress, signalling and regulation of metabolic process (Figure 3.9).

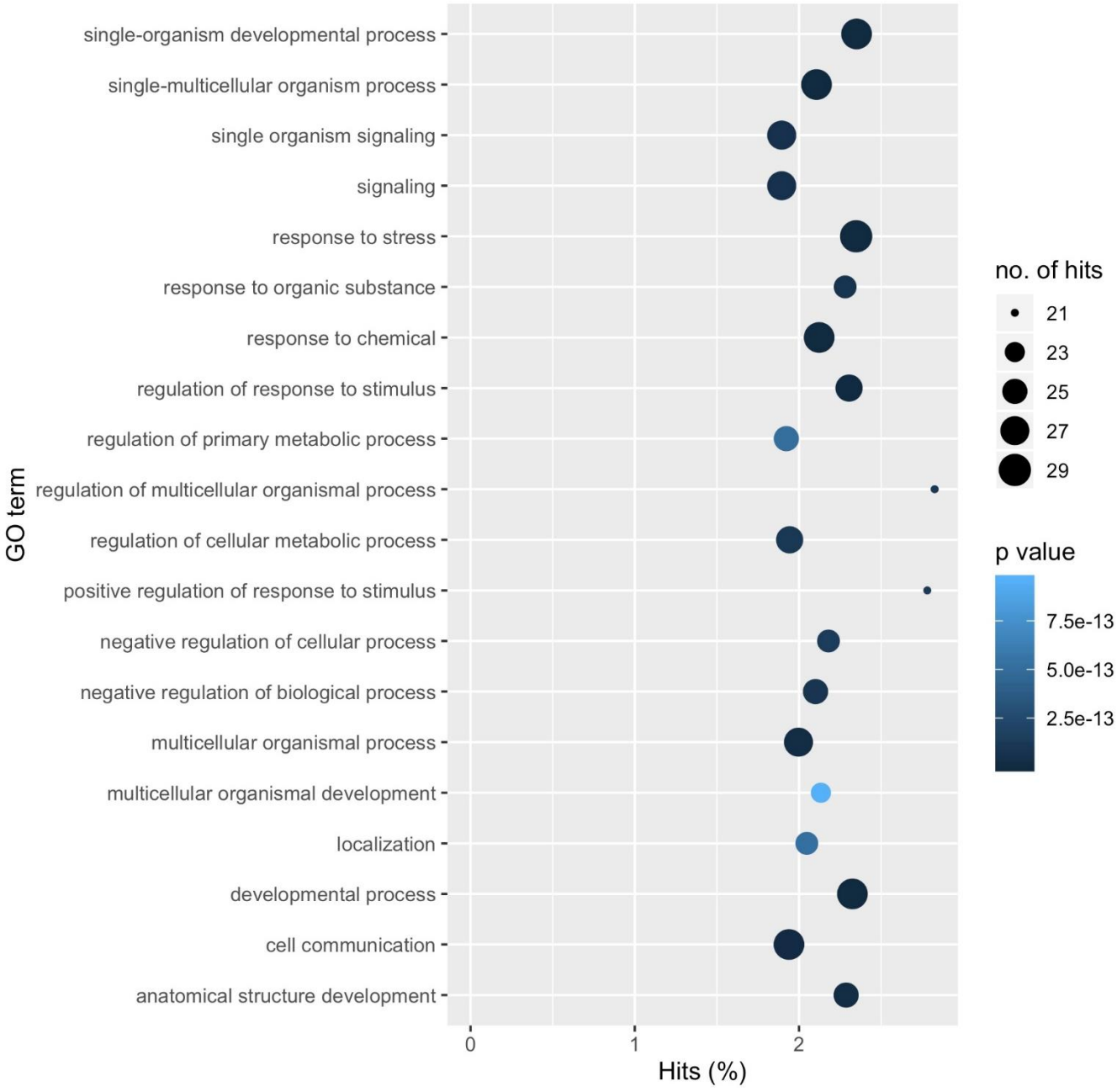


**Figure 3.9. Gene ontology biological process classification of proteins encoded by DEGs detected in HUVEC cells incubated with *S. mansoni* exosome-like vesicles.** Grammar of graphics (gg)plot2 showing GO terms ranked by number of hits, as defined by the GO consortium.

Additionally, KEGG pathway analysis of DGEs identified major intracellular pathways including metabolism (notably arachidonic acid metabolism), signalling (TNF, Jak-STAT, NF-kB and HIF-1), cytokine-cytokine receptor interaction, complement cascade, coagulation cascade and vascular smooth muscle contraction (Figure 3.10).

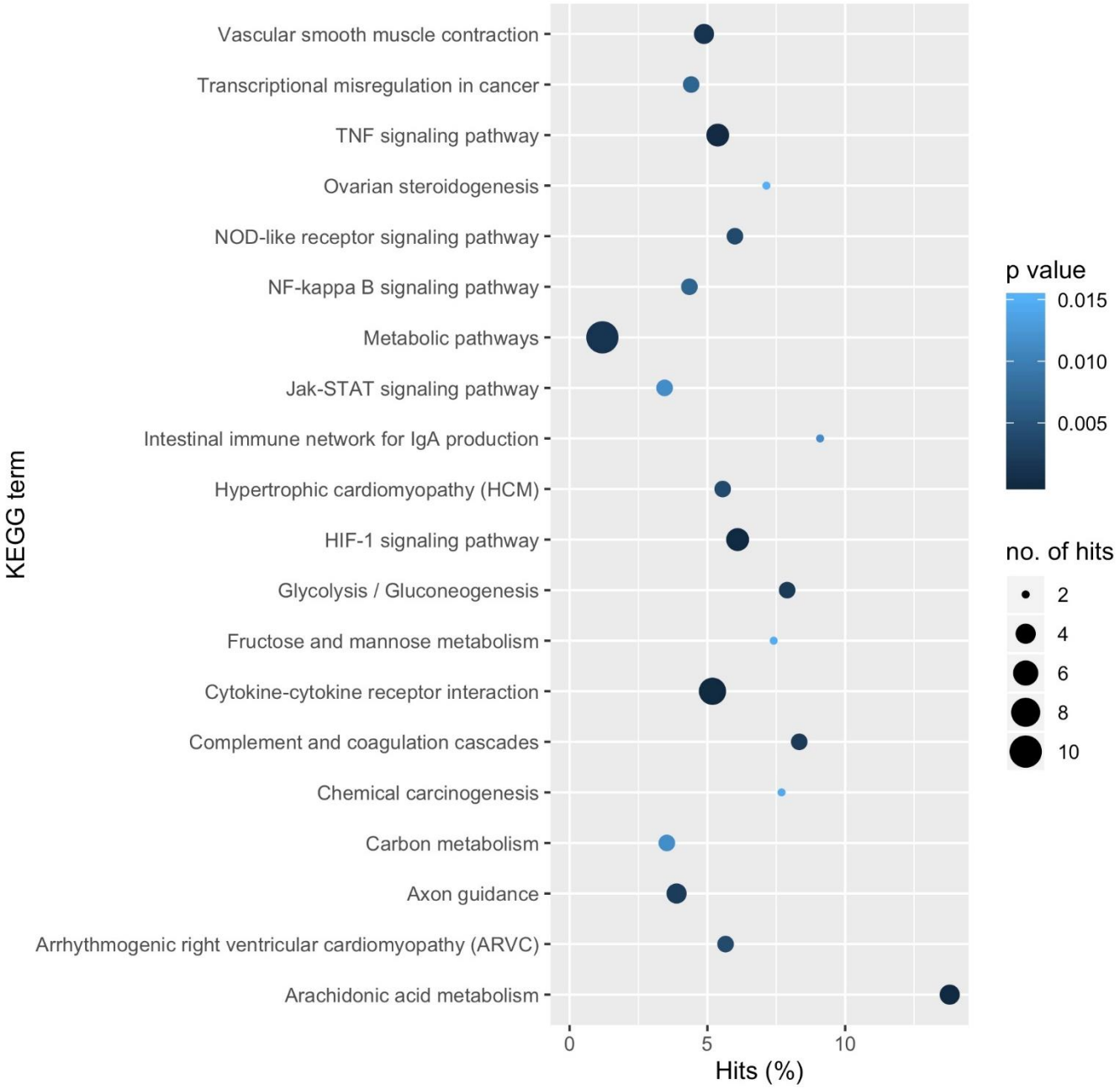


**Figure 3.10. KEGG pathway analysis for proteins encoded by DEGs detected in HUVEC cells incubated with *S. mansoni* exosome-like vesicles.** ggplot2 showing KEGG pathway ranked by number of hits, as categorized defined by PantherDB signaling pathway.

Of interest, downregulated DGEs in HUVEC cells treated with *S. mansoni* ELVs encoded proteins involved in blood clotting (F3), and vasoconstriction (EDN1). DGEs that were upregulated in HUVEC cells treated with *S. mansoni* ELVs encoded proteins involved in inhibition of platelet aggregation and vasodilation (PTGIS), inflammation and immune-regulation (IL-6 and CXCL2), cell proliferation, differentiation and signalling (IL21R), stress response following cell-injury (GDF15 and DDIT3), vascular smooth muscle contraction (PPP1R14A and NTSR1), and vesicle-mediated transport (RAB3IL1) (Figure 3.11).

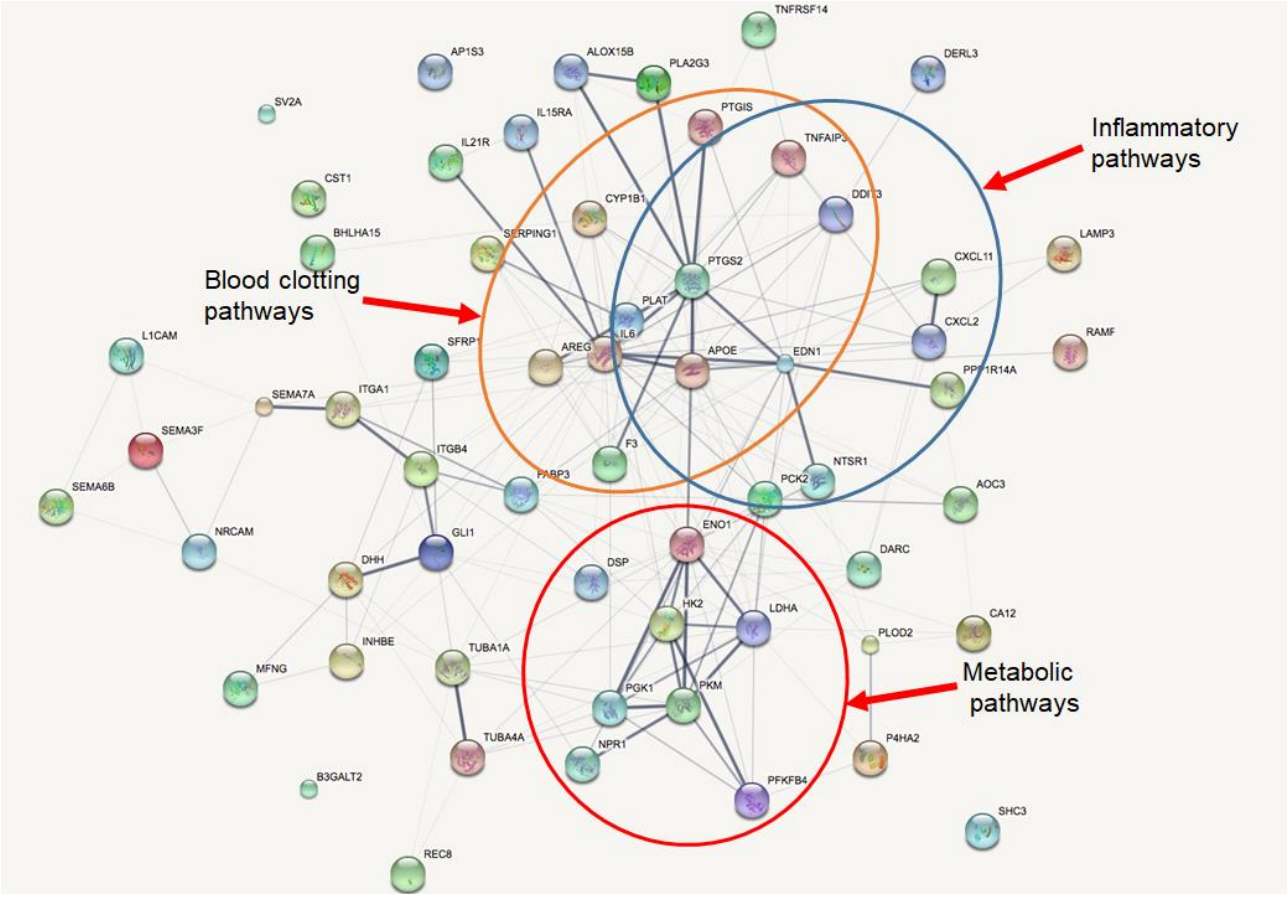


**Figure 3.11. String analysis for proteins encoded by DEGs detected in HUVEC cells incubated with *S. mansoni* exosome-like vesicles compared to HUVEC control.** The network edges refer to the interaction types between gene pairs and the node colours refer to the pathway in which the gene node participates.

## 3.4. Discussion

In mammals, cell-to-cell communication is mediated at least in part by EVs, which can deliver their cargo to recipient cells (Guay and Regazzi, 2017, Xu and Wang, 2017), and impart specific functions such as immune response activation and cell development (Robbins and Morelli, 2014, Xiao et al., 2016), but the specificity of the cell populations with which these EVs interact is largely unknown. The secretion of small EVs was demonstrated in various intracellular and extracellular parasites, but knowledge about target cells and specific cell surface receptors are still mostly lacking (Coakley et al., 2015).

Previous studies, including those by our group showed the internalisation of parasitic helminth EVs by biologically relevant target cells, indicating potential roles in host-parasite communication *in vivo* (Eichenberger et al., 2018a, Eichenberger et al., 2018c, Marcilla et al., 2012, Zhu et al., 2016a, Zhu et al., 2016b). Therefore, EVs derived from *S. mansoni* may potentially act as vehicles to package and deliver miRNAs to host cells and regulate host gene expression, which may facilitate parasitism. The primary mechanism for uptake of parasite EVs by recipient cells appears to be via endocytosis (Coakley et al., 2017). However, a recent study on *F. hepatica* EVs identified specific molecules involved in their internalisation to target cells (de la Torre-Escudero et al., 2019), and hence further study is needed to clarify the mechanisms at play. Several molecules have been identified on the surface of mammalian EVs and target cells with suspected roles in vesicle uptake; lectins/proteoglycans (Christianson et al., 2013), integrins (Morelli et al., 2004, Hoshino et al., 2015) T cell immunoglobulin- and mucin-domain-containing protein 4 (Miyanishi et al., 2007) have been speculated to play instrumental roles in EV internalisation and hence could also dictate target cell specificity. However, none has been identified as a unique EV receptor by demonstrating that it is necessary and sufficient for EV uptake by target cells. Many EV subtypes have common surface molecules and it is possible that one or more of them function as a common ligand or receptor that

assists vesicle uptake, similarly to the internalisation pathway of low-density lipoprotein (Brown and Goldstein, 1974). In this study, confocal microscopy revealed efficient internalisation of *S. mansoni* EVs by human host target cells, and they were observed diffusely throughout the cell cytoplasm. *S. mansoni* EV uptake steadily increased over 2 h of incubation with both HUVEC as well as THP-1 human monocyte cells, suggesting that EV internalisation is a time-dependent process (Marcilla et al., 2012, Chaiyadet et al., 2015b), which correlates with increased CTCF due to labelled vesicle uptake.

HUVEC cells were chosen for internalisation studies because adult flukes are in intimate contact with the vascular endothelium *in vivo*. On the other hand, monocytes were also used because these cells and their differentiated progeny (dendritic cells and macrophages) would encounter *S. mansoni* EVs in the blood and are critical mediators of immune regulation in schistosomiasis (Colley et al., 2014, Fairfax et al., 2012). Moreover, phagocytic cells including macrophages and dendritic cells can adsorb exosomes and thus modify T cell responses or internalise these vesicles by endocytosis, present antigens and modify their own functional conditioning of T cell responses (Montecalvo et al., 2008, Morelli et al., 2004). Wang et al. demonstrated that macrophages were preferentially differentiated into the M1 subtype while being treated with *S. japonicum* ELVs (Wang et al., 2015a).

EV surface proteins or other molecules that could serve as ligands for surface receptors on the host cell could be targeted to interrupt parasite-derived EV-host cell interactions. Herein, I have demonstrated that antibodies against the LEL of r*Sm*-TSP-2 and r*Sm*-TSP-4 have blocked EV uptake by host cells. An earlier study demonstrated that EV uptake by dendritic cells can be blocked using antibodies to TSPs (Morelli et al., 2004). Similarly, treatment of EVs derived from adult *O. viverrini*, with anti-TSP antibodies blocks their uptake by cholangiocytes *in vitro* (Chaiyadet et al., 2015b). More recently, Chaiyadet et al. showed that antibodies raised by vaccinating hamsters with *O.*

*viverrini* EV recombinant TSPs significantly blocked EV internalisation by cholangiocytes (Chaiyadet et al., 2019). In mammalian cells, TSPs on the surface of EVs are key molecules in cell-to-cell interaction and EV internalisation by target cells (Andreu and Yanez-Mo, 2014). Moreover, TSPs are thought to influence cell selectivity (Rana et al., 2012) and have a role in miRNA recruitment and regulation of protein assembly in mammalian exosomes (Perez-Hernandez et al., 2013, Villarroya-Beltri et al., 2013). In addition, TSPs are key in the development of the *S. mansoni* tegument (Tran et al., 2010) and are abundant on the surface membranes of parasitic helminths (Loukas et al., 2007). Indeed, my proteomic data (Kifle et al., 2020) has revealed that *S. mansoni* EV surface membranes are rich in TSPs, which is consistent with previous studies on whole (unfractionated) EVs from adult (Sotillo et al., 2016b) and larval (Nowacki et al., 2015) stages of *S. mansoni*. Of note, the proteomic data revealed not only ELVs but also MVs are enriched for TSPs. Moreover, TSPs are efficacious helminth vaccine antigens (Tran et al., 2006, Dang et al., 2012, Joseph and Ramaswamy, 2013). The use of TSPs as vaccines is marked in schistosomiasis where *Sm*-TSP-2 is one of the most promising vaccine antigens for human use (Tran et al., 2006) and has completed phase 1 clinical trials (Merrifield et al., 2016, Hotez et al., 2019). The data shown herein, highlight the potential of EVs as vaccine candidates, whereby immunisation with rTSPs might generate antibodies that block host-parasite communication *in vivo* (Chaiyadet et al., 2019) and disrupt vital pathways by which the parasite promotes its long-term survival. In addition, it has been previously shown that blocking of *O. viverrini* EV internalisation decreases the levels of IL-6 (fibrosis associated cytokine) and cell proliferation (Chaiyadet et al., 2015b) that ultimately drive tumour formation in this carcinogenic fluke infection. A recent vaccine trial in hamsters with *O. viverrini* adjuvanted EVs and recombinant TSPs from the surface of EVs resulted in significantly reduced worm burdens as well as stunted growth of those flukes that survived and matured in the bile ducts (Chaiyadet et al., 2019) compared to hamsters that received adjuvant alone, suggesting these antibodies might block the ability of the parasite to communicate with its host, thereby impairing the establishment and growth of the

parasite by interrupting its ability to suppress inflammation. Indeed, a vaccine based on TSPs or other EV surface proteins derived from *S. haematobium* might also have an anti-cancer effect and reduce the inflammatory processes that underpin development of squamous cell carcinoma in the bladder. Hence, it is intriguing to guide future research to enhance the evidence for the role of TSPs and their associated proteins in the formation of EVs, their shedding, and internalisation by the recipient cell, both *in vivo* and *ex vivo*.

In disagreement with the findings presented herein where antibodies to *S. mansoni* EV TSPs block their uptake by target cells, one report described enhanced uptake of *F. hepatica* EVs by macrophages in the presence of antibodies against a CD63-like TSP on the surface of these EVs (de la Torre-Escudero et al., 2019). It was speculated by the authors that this is likely due to opsonisation of EVs and FcR-mediated uptake by antigen presenting cells (de la Torre-Escudero et al., 2019, Coakley et al., 2017) as opposed to distinct EV uptake by non-phagocytic target cells such as cholangiocytes (Chaiyadet et al., 2019) and HUVEC cells as shown in this study. Moreover, de la Torre-Escudero et al. did not formulate their *F. hepatica* EVs with an adjuvant, so one might argue that their study was not a vaccine trial per se but rather a therapeutic administration of EVs that might have been expected to have an immunoregulatory impact as opposed to an immunogenic one.

Increased understanding of how schistosome EVs interact with host cells could provide insights into schistosome-host interactions and pave the way for the development of key intervention strategies. Schistosomula (Nowacki et al., 2015) and adult (Samoil et al., 2018, Sotillo et al., 2016b, Kifle et al., 2020) *S. mansoni* release EVs, but the molecular impact of their uptake by recipient host cells has not, until now been determined. Here, I have shown that *S. mansoni* ELV could potentially function as signal messengers that regulate host cell gene expression and thereby facilitate parasitism.

DGEs from HUVEC cells incubated with *S. mansoni* ELVs compared to untreated HUVEC cells revealed reduced expression of genes encoding for proteins involved in blood clotting such as coagulation factor III (F3) and the vasoconstrictor peptide EDN1. Moreover, over-expressed genes in *S. mansoni* ELV-treated HUVEC cells encoded for proteins with roles in inhibition of platelet aggregation and vasodilation such as PTGIS, vascular smooth muscle contraction such as PPP1R14A and NTSR1, as well as genes involved in stress response following cell injury including GDF15 and DDIT3. These findings support the emerging role for EVs as virulence factors used by parasitic helminths (Chaiyadet et al., 2015b, Zhu et al., 2016a), but also shed light on processes that are unique to intravascular helminths. For example, schistosomes employ a variety of mechanisms to hinder platelet aggregation and prevent formation of clots (Mebius et al., 2013, Wang et al., 2017). This is of relevance to *S. mansoni* because of the large size of the worm pair compared to the narrow blood vessels in which they reside. The DGE analysis provided herein suggests that schistosome ELVs might modulate host blood clotting pathways by reducing vasoconstriction and clot formation and promoting vasodilation, all of which would facilitate their long-term existence in the mesenteries. Interestingly, *S. mansoni* EVs (Nowacki et al., 2015, Sotillo et al., 2016b, Samoil et al., 2018, Kifle et al., 2020) contain proteins with anti-clotting activities including annexin, saponin-B domain containing protein, and aminopeptidases, further supporting a role for EV molecules and their impact on host cell gene expression in targeting defined pathways that are essential for schistosomes to thrive in the microvasculature.

Among the up-regulated DGEs in ELV-treated HUVEC cells were those involved in inflammation and immune-regulation including IL-6 and CXCL2, and cell proliferation, differentiation and signalling such as IL21R. An immunoregulatory role for helminth derived EVs (including *S. japonicum*) is well documented (Zamanian et al., 2015, Buck et al., 2014, Roig et al., 2018, Eichenberger et al., 2018a, Coakley et al., 2017, Chaiyadet et al., 2015b, Fromm et al., 2015, Wang et al., 2015a). IL-6, an acute

phase protein induced during inflammation (Hirano, 1998), inhibits the generation of Foxp3$^{+}$ $T_{reg}$ cells induced by TGF-β, and exerts an important influence on Th17-cell differentiation (Bettelli et al., 2006). Tissue injury initiates a cascade of inflammatory mediators including cytokines, chemokines and prostaglandins that leads to over-expression of genes regulating IL6 and chemokine receptor CXCL2 expression (Wang et al., 2009). IL21R, is a receptor which transduces the growth promoting signal of IL21, and is important for the proliferation and differentiation of T cells, NK cells and B cells (Bubier et al., 2009). *O. viverrini* ES (Chaiyadet et al., 2015a) and *O. viverrini* EVs (Chaiyadet et al., 2015b) elicit production of IL-6 from recipient human cholangiocytes, which is thought to contribute to chronic periductal fibrosis and bile duct cancer in *O. viverrini*-infected individuals (Sripa et al., 2011). Moreover, *O. viverrini* EVs also drive proliferation of cholangiocytes, a condition that has been reported in both the hamster infection model and infected human subjects (Sripa et al., 2012). Zhu et al. identified the transfer of schistosome-specific miRNAs, such as EV associated Bantam, into hepatic cells, indicating a common down-regulation of mRNAs involved in tumour suppression pathways in the livers of *S. japonicum* infected mice and in liver cells treated with *S. japonicum* EVs (Zhu et al., 2016a), as well as cell growth and suppression of cell death. Moreover, many *N. brasiliensis* EV miRNAs map to interleukin networks of mouse cells, including the IL-6 receptor and IL-6 signal transducers, IL-17 receptor and IL-21 (Eichenberger et al., 2018a). Another study showed that downregulation of IL-6 promoted susceptibility of mice to Th2-mediated killing of *H. polygyrus* (Smith and Maizels, 2014).

The findings herein, describe the uptake of *S. mansoni* secreted ELVs and MVs by human vascular endothelial and monocyte cell lines, highlighting their diverse potential roles in host-parasite communication. These findings indicate that *S. mansoni* EVs may play an important regulatory role in parasite-host interactions and could be involved in the pathogenesis of schistosomiasis. Their roles in driving gene expression changes in target host cells identifies a mechanism by which host-

parasite communication could be manipulated (Zamanian et al., 2015). Further, blocking this process using specific antibodies to EV-TSPs could be impairing critical parasite-host communication mechanisms which impact on parasite survival, and thereby offer hope for the eventual control of this debilitating neglected tropical disease. Further work is required to identify whether or not there is specificity or selectivity in host cells or tissues targeted by EVs and if so, what molecular mechanisms underscore this specificity. In addition, further work is required to characterise multiple pathways downstream of the process of host-parasite communication, as well as the individual fluke proteins and/or miRNAs involved and their cellular receptors. Moreover, it would be of interest to further explore the role of *S. mansoni* EV internalisation by THP-1 human monocyte cells. Exploration of the role of these vesicles as vaccine targets may help identify novel strategies which could be applied to identify potential vaccines/therapeutics to control schistosomiasis and other helminthiases.

# Chapter 4

## Assessment of *Schistosoma mansoni* extracellular vesicles as vaccines in a mouse model of schistosomiasis

### Preamble

Helminth-derived EVs have been demonstrated to have vaccine potential using different animal models. In this chapter, I assess *S. mansoni* MVs as a novel vaccine modality in a mouse model of schistosomiasis; there was insufficient material to do a vaccine trial with *S. mansoni* ELVs. For this purpose, *S. mansoni* MVs were isolated from ES products as described in Chapter 2 following a standard procedure. Before the start of the experiment, protein concentration was determined for the MV sample. Moreover, MV concentration and particle size were determined using TRPS on a qNano instrument. A total of 60 BALB/C mice were used in two independent vaccine trials. Three groups of mice, 10 animals per group, were immunised intraperitoneally with two doses, two weeks apart, of 1) *S. mansoni* MVs; 2) mouse fibroblast-derived MVs; and 3) PBS control, adjuvanted with alum/CpG. Vaccine efficacy was assessed by calculating the worm burden, liver and intestine egg loads and egg viability (hatching index) of mice immunised with *S. mansoni* MVs compared to the control group. Finally, sera from mice immunised with *S. mansoni* ELVs and MVs were utilized to identify antibody signatures using a protein microarray containing ~1,000 *S. mansoni* recombinant proteins.

## 4.1. Introduction

Despite substantial efforts to eradicate schistosomiasis through integrated control strategies, such as snail control, community education and mass drug admiration using PZQ, it continues to be a major public health concern and causes significant morbidity and disability in disease endemic countries (McManus et al., 2018). As a sustainable prevention and control strategy, a vaccine for schistosomiasis is therefore urgently needed. Recent advances in schistosome molecular biology including genomics, transcriptomics, proteomics and immunomics have assisted the discovery of new antigens (Loukas et al., 2011, Gaze et al., 2012, Driguez et al., 2016b), however only a few subunit vaccines have been taken into early stage clinical trials.

There is emerging evidence from mouse models that helminth-derived EVs have a role as vaccine antigens, (reviewed in (Kifle et al., 2017). In addition, several studies have reported that EVs released from helminths are capable of modulating host immune responses (Buck et al., 2014, Wang et al., 2015a, Coakley et al., 2017, Zamanian et al., 2015, Eichenberger et al., 2018a). In one study, immune reactivity towards *S. japonicum* EVs was identified using rabbit anti-sera raised against *S. japonicum* infection (Zhu et al., 2016a). Indeed, helminth-secreted EVs as vaccine antigens and therapeutic agents have shown promising results (Trelis et al., 2016, Coakley et al., 2017, Shears et al., 2018, Chaiyadet et al., 2019). Trelis and colleagues in a mouse model of fluke infection demonstrated that *E. caproni* EVs can induce an antibody response upon vaccination and reduce the severity of symptoms of infection (Trelis et al., 2016). Vaccination of mice with nematode EVs has also been shown to induce protective immunity. Vaccination of mice with *H. polygyrus*-derived EVs resulted in greatly diminished worm burdens (Coakley et al., 2017), and EVs secreted by *T. muris* when administered to mice without adjuvant and induced anti-EV antibodies and a significant reduction in worm burdens (Shears et al., 2018). Recently, Chaiyadet et al. reported that hamsters vaccinated with *O. viverrini* EVs showed a significant increase in serum IgG titres against *O. viverrini* ES, *O.*

*viverrini* EVs and recombinant EV TSP proteins compared with sera from hamsters that received adjuvant only (Chaiyadet et al., 2019). Moreover, vaccinated hamsters had significantly reduced adult worm loads and egg burdens compared to control animals after challenge with *O. viverrini* metacercariae. In addition, the body length of worms recovered from vaccinated hamsters was significantly shorter than those collected from control animals, implying that anti-TSP antibodies interfere with fluke maturation and cause stunting. Pertinent to this Chapter, previously described *S. mansoni* vaccine candidates (Tran et al., 2006, Cardoso et al., 2006, Rezende et al., 2011, Sotillo et al., 2016b, Samoil et al., 2018, Pearson et al., 2012) have also been identified in *S. mansoni* EVs (Sotillo et al., 2016b, Nowacki et al., 2015, Samoil et al., 2018), supporting the hypothesis that *S. mansoni* EVs may be an important source of protective antigens. Indeed, my experimental findings from earlier chapters confirm this.

Furthermore, there are reports that not only EVs from parasites but host cell-derived EVs induce protective immunity against parasitic infection. For instance, chickens immunised with dendritic cell-derived EVs pulsed with *Eimeria* parasites resulted in reduced mortality, intestinal inflammation and faecal oocyst shedding (del Cacho et al., 2012). Martin-Jaular and colleagues purified EVs from peripheral blood of mice infected with a non-lethal strain of *Plasmodium yoelii* (17X strain) and identified parasite proteins in the reticulocyte EVs. Vaccination of mice with adjuvanted EVs from 17X-infected reticulocytes induced IgG antibodies that attenuated parasitaemia and prolonged survival after challenge infection with a lethal strain of the parasite (Martin-Jaular et al., 2011). Similarly, Beauvillain et al. showed that vaccinating mice with EVs from splenic dendritic cells pulsed with *Toxoplasma gondii* antigens prior to pregnancy showed protective immunity in pups, and led to lower mortality and fewer brain cysts with eventual congenital exposure to infection (Beauvillain et al., 2009).

Key to the identification of new target vaccine molecules and high throughput antigen discovery are the published complete genomes of schistosomes (Zhou et al., 2009, Berriman et al., 2009, Young et al., 2012), and related post-genomic research on the schistosome proteome, transcriptome, glycome and immunome (Sotillo et al., 2019b). The proteome microarray approach to antigen discovery is ideal for high-throughput profiling of the repertoire of antigens that can elicit defined immune responses in schistosomiasis. Schistosome protein microarrays have been used to examine the antibody profiles for different clinical grades of schistosomiasis (Chen et al., 2014, Gaze et al., 2014, Pearson et al., 2015, de Assis et al., 2016, Driguez et al., 2015), and this approach is well suited to the current project. This chapter aimed to assess *S. mansoni* MVs as vaccines in a mouse model of schistosomiasis. I confirmed that these EVs induce partial protection in mice against infection as assessed using worm burdens, liver and intestine egg loads and egg hatching-index. Moreover, I have shown here that protein arrays provide an ideal means by which to explore humoral immunity and vaccine antigen discovery for schistosome infections. Sera from mice immunised with *S. mansoni* ELVs and MVs were used to probe arrays of *S. mansoni* antigens in an effort to identify reactive and potentially protective antigens.

## 4.2. Material and methods

### 4.2.1. Ethics statement

All experimental procedures were approved by JCU animal ethics, as described in section 2.2.1.

### 4.2.2. Study animals and *S. mansoni*

Study animals and S*. mansoni* parasite species used in the experiment are described in section 2.2.2.

### 4.2.3. Snails shedding and mice infection

Snails shedding and experimental mice infection with cercariae were performed following standard procedures, as described in section 2.2.3.

### 4.2.4. Adult worm perfusion

Adult worms after 6-8 weeks post-infection of mice were obtained as described in section 2.2.4.

### 4.2.5. Parasite culture and ES products collection

Adult parasites were cultured and ES products were collected as described in section 2.2.4.

### 4.2.6. *S. mansoni* EV isolation and purification

*S. mansoni* EVs were isolated and purified by Optiprep iodixalon gradient method as described in section 2.2.5.

### 4.2.7. EV analysis

Size and concentration determination of EVs were carried using TRPS as described in section 2.2.6.

### 4.2.8. Immunisation studies

Three groups of 10 male BALB/c mice, 6-8 weeks, were used for assessing vaccine efficacy of *S. mansoni* MVs. Prior to each vaccine trial, the amount of protein in each MV sample was measured using a Bradford assay kit (ThermoFischer) according to the manufacturer's instructions, and mice were immunised intraperitoneally on day-1 (10 µg /mouse) with either *S. mansoni* MVs, mouse-fibroblast MVs or PBS, each formulated with an equal volume of Imject alum adjuvant (ThermoFisher) and 5 µg of CpG ODN1826 (InvivoGen). Mice were given a booster dose 2 weeks later at day-14. All vaccinations were carried out using a 25 G needle (BD Microlance). At day 28, all mice were challenged with 120 *S. mansoni* cercariae using the tail technique (Harn et al., 1984). At day-26 blood samples were collected and sera isolated to assess antibody responses. Two independent vaccine trials were carried out for data reproducibility. There was insufficient material to do a vaccine trial with *S. mansoni* ELVs.

### 4.2.9. Mice necropsy and estimation of worm and tissue egg burdens

Seven weeks after parasite challenge, all mice were euthanized using an intraperitoneal injection of 0.2 ml pentobarbital/heparin solution followed by $CO_2$ gas administration and worms were perfused using perfusion solution (0.15 M sodium chloride with 0.03 M sodium citrate dehydrate in water) from the mesenteric veins to collect adult worms, as described elsewhere (Smithers and Terry, 1965). Worm as well as egg burden assessments were carried out as described previously (Pearson et al., 2012). Livers and intestines were removed and weighed then each sample was digested for 4 h at 37°C using 10 ml of 5% KOH. Samples were centrifuged for 10 min at 1000 *g* and pellets were resuspended using 1 ml of 4% paraformaldehyde. Counts were performed in triplicate with 5 µl volume from each sample under light microscopy at 200 × magnification. Eggs per gram (EPG) in liver and intestine homogenates were calculated as follows: (average number of eggs × total drops of tissue solution)/g of tissue. For each group, total adult worm burdens as well as liver and intestinal egg burdens were measured and reductions were calculated as a percentage of the parasite burdens in the control group by using the formula:

$$\% \text{ change} = \frac{(\text{mean number in infected controls} - \text{mean number in infected experimental mice})}{\text{mean number in infected controls}} \times 100$$

### 4.2.10. Egg viability test

Liver portions from each mouse were pooled within groups, homogenized in $H_2O$ in identical volumetric flasks (foil-covered with top 1 cm exposed) and placed under bright light to hatch eggs from the livers. After 1 h of exposure to light, the number of miracidia in 50 µl aliquots of $H_2O$ sampled 10 times from the very top of each flask were counted by adding 2 µl bioiodine to each aliquot. Egg viability (hatching-index) was calculated by multiplying the weight of pooled liver halves by the average EPG of that group (calculated once liver EPG from KOH digested livers had been determined) to get number of eggs per flask, and then expressing the number of hatched eggs

(miracidia) in each aliquot as a percentage of this. Hatching reduction was determined by expressing the hatching index of the vaccinated groups as a percentage of the control group.

#### 4.2.11. Probing of *S. mansoni* protein arrays with sera from mice immunised with *S. mansoni* EVs

Protein microarrays, each containing 992 *S. mansoni* recombinant proteins (de Assis et al., 2016) were probed with sera from: (a) mice immunised with ELVs (sera pooled from 5 mice), (b) mice immunised with MVs (2 pools of sera – each from 5 mice from 2 separate immunisation experiments), (c) mice infected with *S. mansoni* parasites (sera pooled from 10 mice at 7 weeks post-infection) and (d) naïve mice. Probing was performed in duplicate. Samples were pre-adsorbed for anti-*E. coli* antibodies by rocking for 30 min at RT with *E. coli* lysate—impregnated fliters before probing of arrays. Protein arrays were blocked in blocking solution (Maine Manufacturing) for 2 h at RT prior to probing with mouse sera (1:50 in TBS/0.05% Tween 20 (TTBS)) at 4°C overnight with gentle constant rocking. Arrays were washed 3 times for 5 min with TTBS, probed with goat anti-mouse IgG1-biotin (1:200 in TTBS) (Sigma) for 2 h at RT, washed again and then incubated for 2 h in streptavidin-Cy-5 (1:400 in TTBS). Following a final 3 washes with TTBS, 3 washes with TBS and 3 washes with MQ water, slides were air-dried and scanned on a Genepix 4200AL scanner (Molecular Devices) and signal intensities (SI) quantified using the ScanArray Express Microarray Analysis System Version 3.0 (Molecular Devices). Raw SI were corrected for spot-specific background using the Axon GenePix Pro 7 software and then further refined by determining the mean SI of the negative control (empty vector) spots (n=12) for each serum sample and subtracting that value from each spot. Finally, the refined SI for each spot from the array probed with naïve sera was subtracted from the corresponding spot on each of the other arrays to correct for background (naïve sera) reactivity.

### 4.2.12. Data analysis

For all vaccine trial data, unpaired Student's t-test was used to analyse any statistical differences between experimental and control groups. Power calculations were conducted to determine group sizes and the ability to detect at least 40% reduction in worm and egg burdens. Further, the mean and standard error of the mean (SEM) for each test group were compared with the control group for the variable of interest (worm recovery, tissue worm burdens as well as egg viability). GraphPad Prism™ version 7.03 was used for analysis. $P < 0.05$ was considered as statistically significant.

## 4.3. Results

### 4.3.1. Vaccination with *S. mansoni* MVs induces partial reduction in tissue egg burden

Mice immunised with *S. mansoni* MVs did not show a significant reduction in adult worm counts in both vaccine trial 1 (Figure 4.1A) and trial 2 (Figure 4.1B).

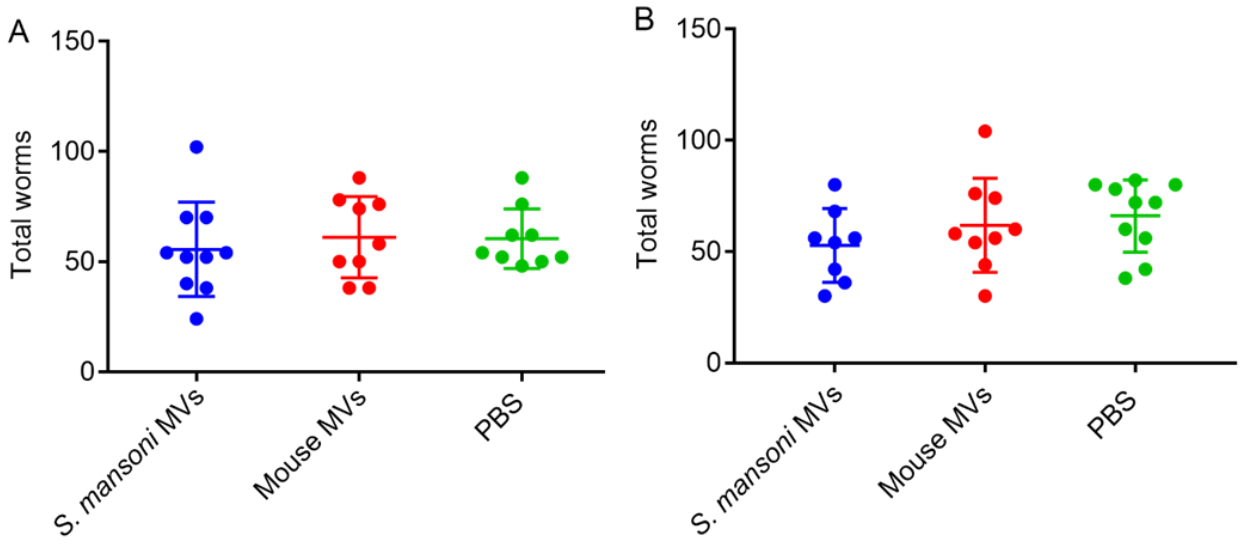


**Figure 4. 1. Worm counts for individual mice immunised with *S. mansoni* microvesicles formulated with alum/CPG for vaccine trial 1 (A) and vaccine trial 2 (B) compared to mice vaccinated with fibroblast-derived MVs or PBS control groups.** Worm burdens were determined seven weeks post cercarial challenge.

In vaccine trial 1, liver egg burdens (expressed as eggs per gram – EPG) (Figure 4.2A) compared to both control groups was unaffected. However, a significant reduction in liver egg burden (28%, *P* <0.01, Figure 4.2B) was obtained in vaccine trial 2 compared to mice that were treated with PBS but not with mice vaccinated with mouse MVs.

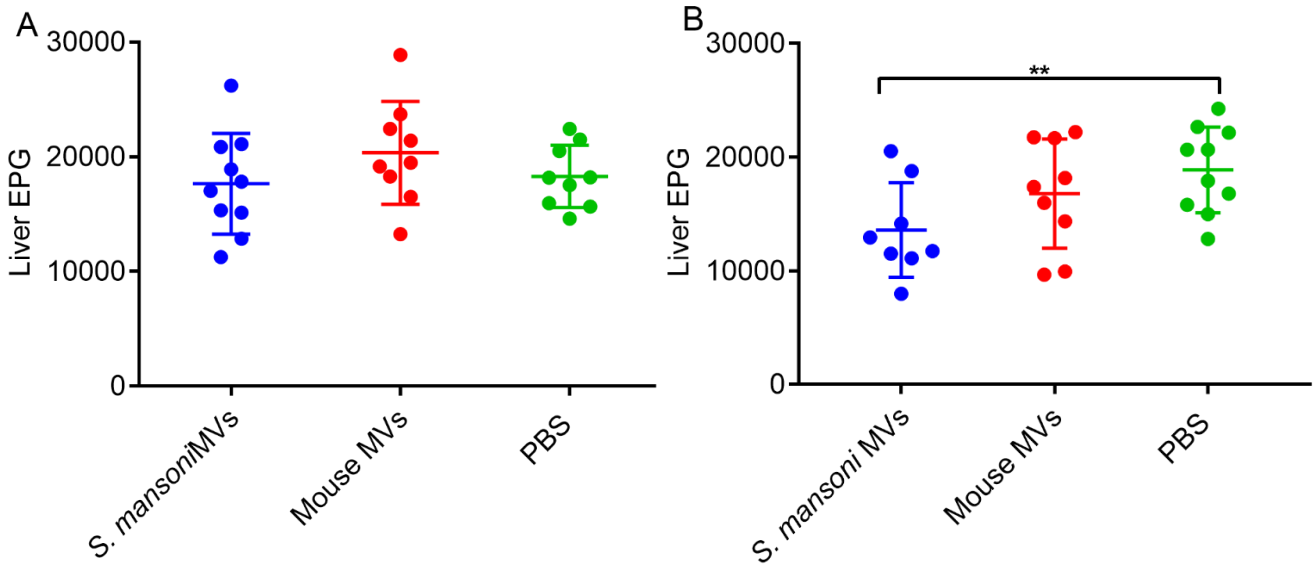


**Figure 4. 2. Egg burden per gram of liver for individual mice immunised with *S. mansoni* microvesicles formulated with alum/CPG for vaccine trial 1 (A) and vaccine trial 2 (B) compared to mice vaccinated with fibroblast-derived MVs or PBS control groups.** Liver egg burdens were determined seven weeks post cercarial challenge (** *P*<0.01).

Mice immunised with *S. mansoni* MVs compared to either of the control groups did not show protection (Figure 4.3A) measured by intestinal egg loads (expressed as EPG) in vaccine trial 1. In vaccine trial 2 however, intestinal egg burdens were significantly reduced (35%, *P*<0.01, Figure 4.3B) in mice vaccinated with *S. mansoni* MVs compare to mice that were immunised with PBS but not with fibroblast MVs.

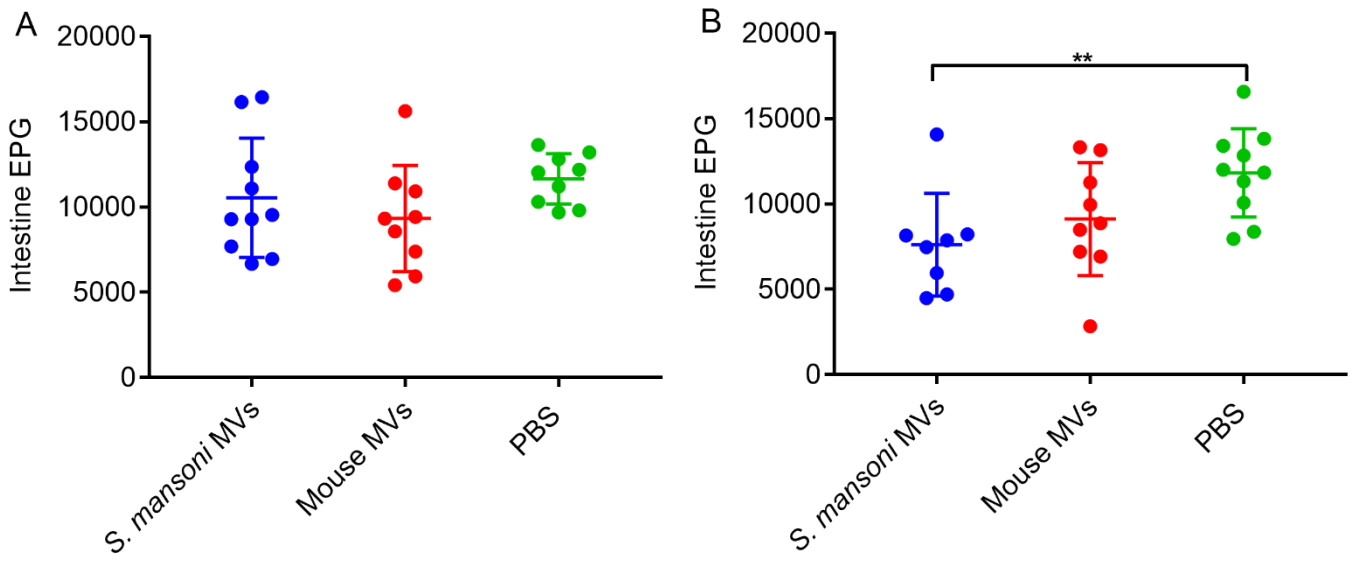


**Figure 4. 3. The egg burden per gram of intestine for individual mice immunised with *S. mansoni* microvesicles formulated with alum/CPG for vaccine trial 1 (A) and vaccine trial 2 (B) compared to mice immunised with fibroblast-derived MVs or PBS.** Intestine egg loads were determined seven weeks post cercarial challenge (** *P*<0.01).

No significant reduction in egg viability (hatching-index, as determined by egg hatching from liver homogenates) was reported in mice immunised with *S. mansoni* MVs compared to control groups both in vaccine trial 1 (Figure 4.4A) and vaccine trial 2 (Figure 4.4B).

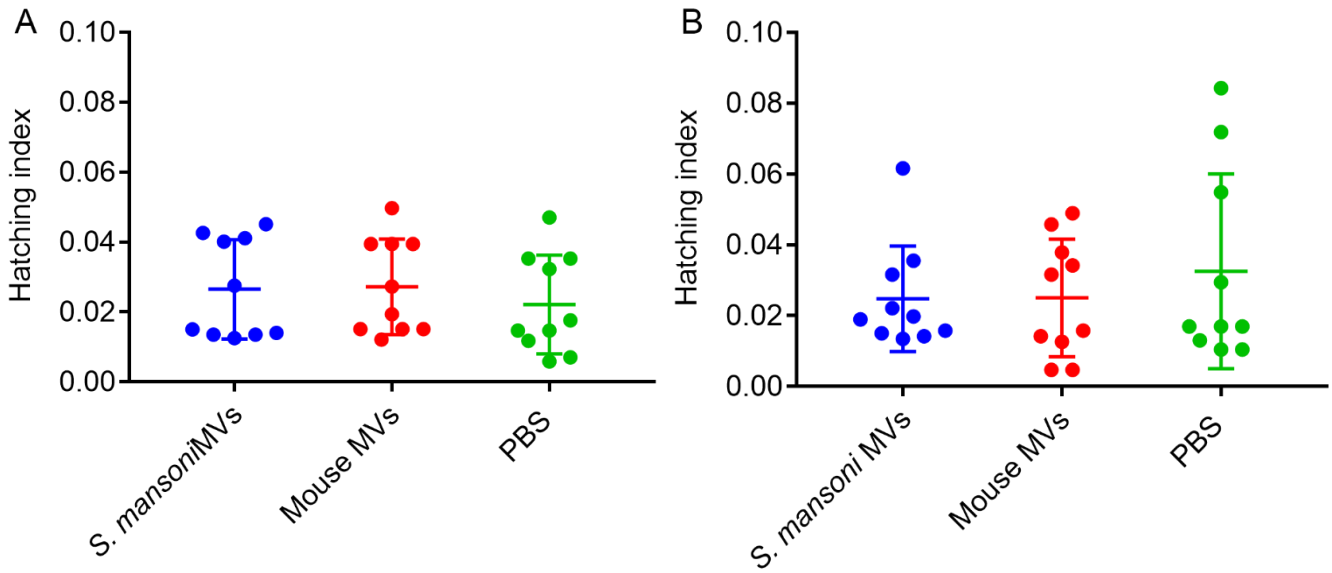

**Figure 4. 4. Egg viability assessment (hatching index) per individual mouse vaccinated with *S. mansoni* microvesicles formulated with alum/CPG for vaccine trial 1 (A) and vaccine trial 2 (B) compared to mice immunised with fibroblast microvesicles or PBS.** Egg hatching index of each group was calculated by expressing the hatched eggs (miracidia) as a percentage of the total liver eggs obtained after EPG was computed.

Parasitological data including adult worm counts, liver and intestinal egg loads as well as egg viability assays were summarized for vaccine trial 1 (Table 4.1) and vaccine trial 2 (Table 4.2).

**Table 4.1. Parasitological data for mice immunised with *S. mansoni* microvesicles formulated with alum/CPG for vaccine trial 1 compared to mice immunised with fibroblast microvesicles or PBS.**

| Group | Adult worms, range | Adult worms Mean ± SEM reduction (%) | Liver EPG Mean ± SEM, reduction (%) | Intestine EPG Mean ± SEM, reduction (%) | Hatching index Mean ± SEM, reduction (%) |
|---|---|---|---|---|---|
| Mouse MVs; n=9 | 38-84 | 61 ± 5.8 | 20350 ± 1218 | 9335 ± 983 (-) | 0.027 ± 0.004 |
| PBS; n=9 | 48-88 | 60.4 ± 4.2 | 18294 ± 858 | 11658 ± 721 | 0.022 ± 0.005 |
| *S. mansoni* MVs; n=10 | 26-102 | 55.6 ± 7.1 (9% compared to mouse MVs; 8% to PBS) | 17653 ± 1461(13% mouse MVs; 3.5% PBS) | 10549 ± 1166 (no reduction mouse MVs; 9.5% PBS) | 0.026 ± 0.004 (3% mouse MVs; no reduction PBS) |

**Table 4.2. Parasitological data for mice immunised with *S. mansoni* microvesicles formulated with alum/CPG for vaccine trial 2 compared to mice immunised with fibroblast microvesicles or PBS.**

| Group | Adult worms, range | Adult worms Mean ± SEM reduction (%) | Liver EPG Mean ± SEM, reduction (%) | Intestine EPG Mean ± SEM, reduction (%) | Hatching index Mean ± SEM, reduction (%) |
|---|---|---|---|---|---|
| Mouse MVs; n=9 | 30-104 | 62 ± 7.0 | 16802 ± 1601 | 9119 ± 1102 | 0.025 ± 0.005 |
| PBS; n=10 | 38-82 | 66 ± 5.1 | 18880 ± 1188 | 11825 ± 818 | 0.03 ± 0.008 |
| *S. mansoni* MVs; n=8 | 30-80 | 53 ± 5.2 (15% compared to mouse MVs; 20% to PBS) | 13601 ± 1315 (19% mouse MVs; 28% **$P$<0.01 PBS) | 7620 ± 952 (16% mouse MVs; 35% **$P$<0.01 PBS) | 0.025 ± 0.004 (no reduction mouse MVs; 24% PBS) |

### 4.3.2. Antibody signatures of mice immunised with *S. mansoni* EVs to arrayed antigens

Probing of *S. mansoni* protein arrays with pooled sera from BALB/c mice immunised with *S. mansoni* ELVs and *S. mansoni* MVs demonstrated specific recognition of *S. mansoni* EV antigens by IgG1 antibodies. Numerous antigens on the protein arrays were recognised by sera from immunised mice, including hypothetical, tegumental and metabolic proteins. The top 20 proteins recognised by sera from mice immunised with either *S. mansoni*-derived ELVs (Figure 4.5) or MVs (Figure 4.6) are presented. The three most strongly recognised antigens in mice immunised with *S. mansoni* ELVs were hypothetical protein (Smp_187080.1), the integral membrane protein Sm23 (Smp_017430.1) and the tegmental antigen Sm13 (Smp_195190.1). Likewise, the three top recognized antigens by sera from mice immunised with *S. mansoni* MVs were NADH dehydrogenase subunit 1 (mitochondrial) (Smp_900110.1), thioredoxin glutathione reductase (Smp_048430.1) and Sm13 (Smp_195190.1). Of the 20 top reactive arrayed antigens that were targets of significantly elevated

IgG1 responses in mice immunised with *S. mansoni* ELVs or *S. mansoni* MVs, six of them were common targets of antibody responses to both: Sm13 (Smp_195190.1), NADH dehydrogenase subunit 1 (Smp_900110.1), putative glutaredoxin, grx (Smp_006550.1), and the three hypothetical proteins: Smp_187080.1, Smp_176400.1 and Smp_118020.1. Moreover, antigens which were among the top 20 immunoreactive proteins include known and potential schistosome vaccine candidates: Sm23 (Smp_017430.1), Sm13 (Smp_195190.1), cathepsin B-like peptidase (Smp_158420.1), annexin (Smp_045500.1) and thioredoxin glutathione reductase (Smp_048430.1).

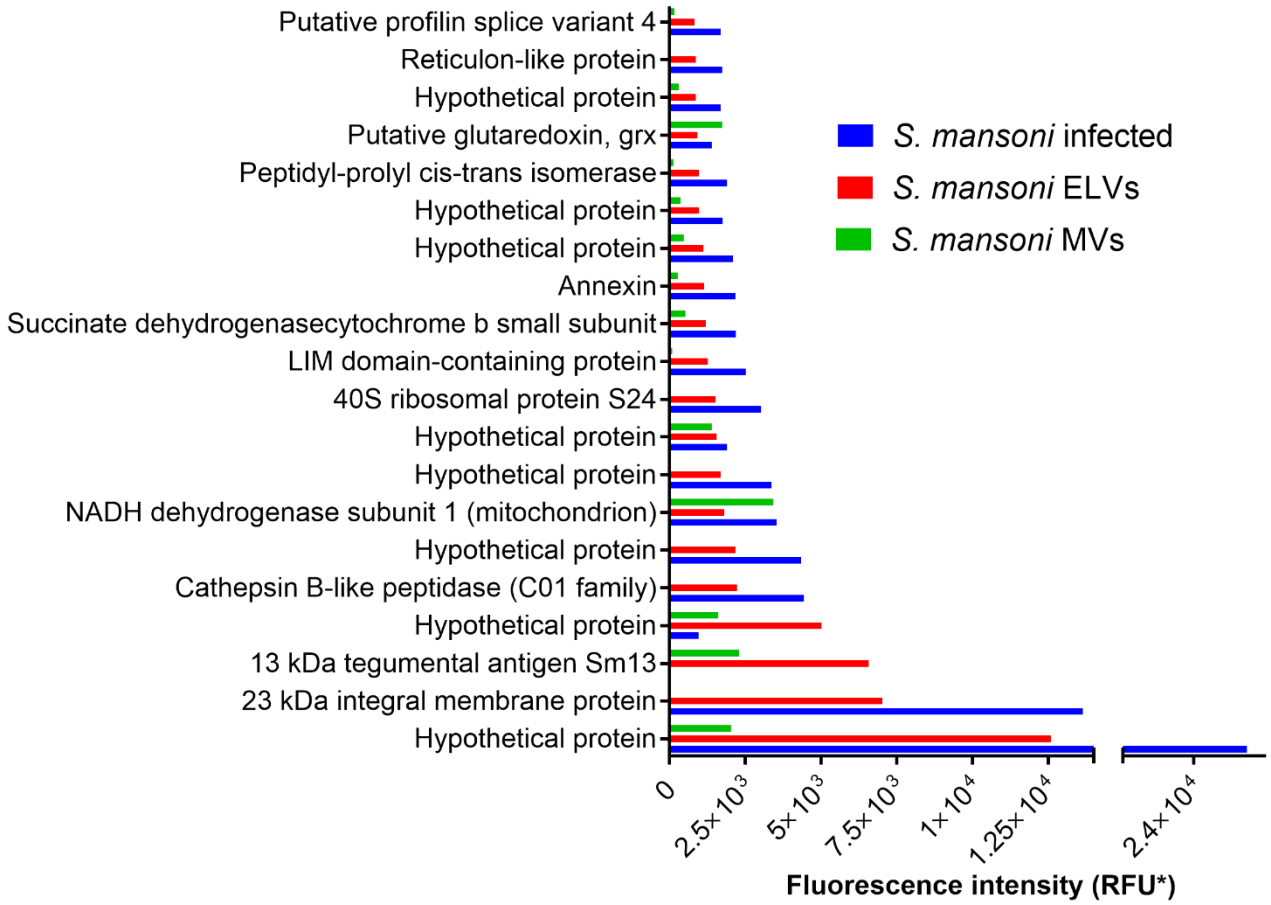


**Figure 4. 5. IgG1 reactivity profiles of sera from mice immunised with *S. mansoni* exosome-like vesicles to *S. mansoni* proteins printed on a proteome microarray.** The graph shows the average fluorescence intensity of the top 20 most immunoreactive proteins. *RFU: relative fluorescence unit.

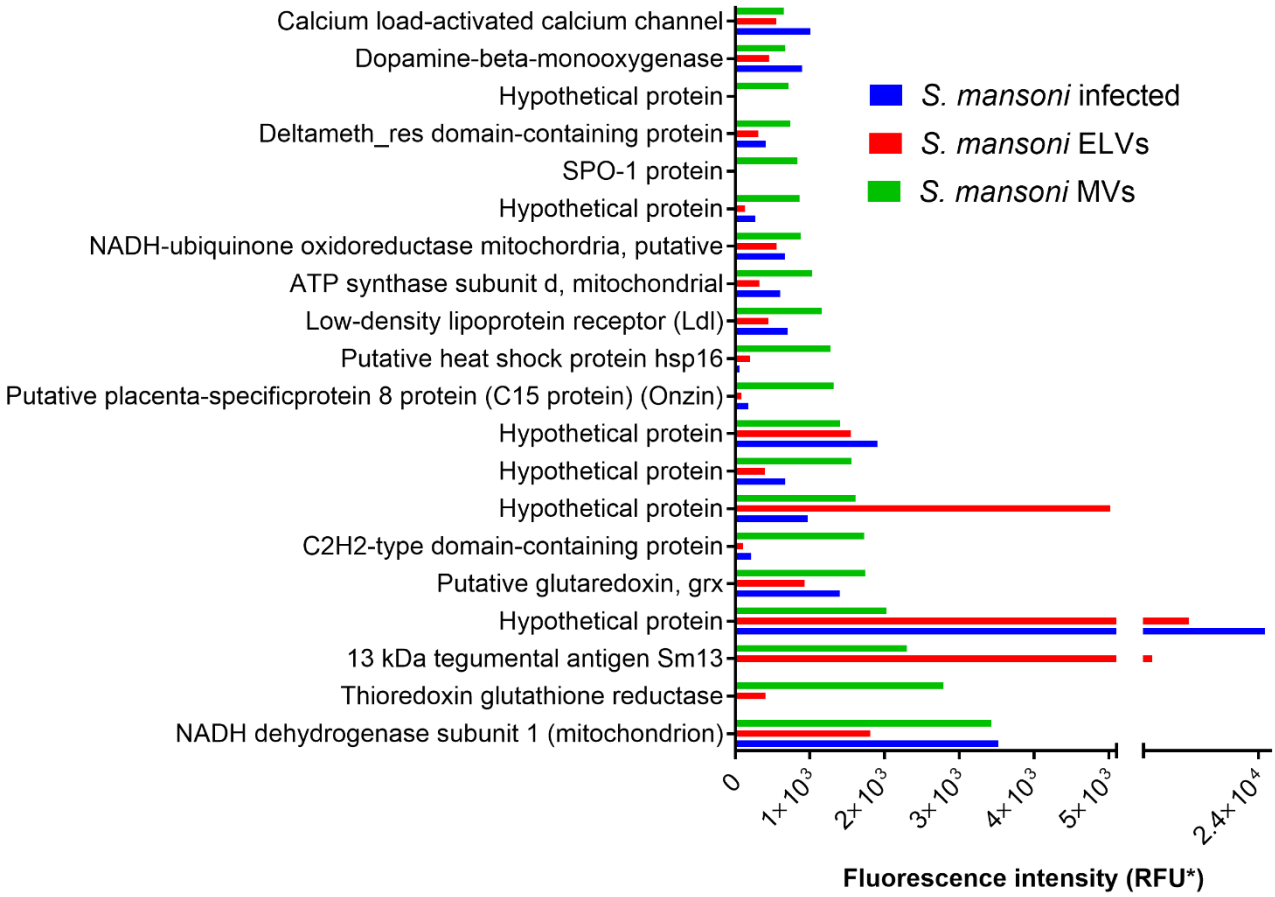


**Figure 4. 6. IgG1 reactivity profiles of sera from mice immunised with *S. mansoni* microvesicles to *S. mansoni* proteins printed on a proteome microarray.** The graph shows the average fluorescence intensity of the top 20 most immunoreactive proteins. *RFU: relative fluorescence unit.

## 4.4. Discussion

EVs have diverse roles in host-pathogen interactions from participating in pathogen dissemination to provoking and even suppressing distinct arms of the host immune system (Lambertz et al., 2015, Regev-Rudzki et al., 2013, Silverman et al., 2008). The ability of helminths, such as *S. mansoni*, to secrete EVs highlights a newly identified strategy by which the parasite hijacks the host to promote its longevity (Sotillo et al., 2016b). EVs can have immunomodulatory roles that is largely based on their cargo, which is characteristic of both their cellular origin and physiological or pathological

conditions that trigger their secretion (Buck et al., 2014). Helminth derived EVs have shown promising results as potential vaccine targets (Zhu et al., 2016a, Shears et al., 2018, Coakley et al., 2017, Trelis et al., 2016). Moreover, previously described *S. mansoni* vaccine candidates (Tran et al., 2006, Cardoso et al., 2006, Rezende et al., 2011, Sotillo et al., 2016b, Samoil et al., 2018, Chaiyadet et al., 2019) have also been identified in the EV proteome.

The degree of protection induced by vaccination with *S. mansoni* MVs was relatively low, and inconsistent between trials. Significant reduction in egg counts was only observed in trial 2. These variabilities in protection levels over two vaccine trials could be due to the modest levels of protection reported (28-35%) being drowned out by the expected degree of variation observed in mouse models. The differences in adult worm burdens and liver and intestinal egg burdens in mice immunised with *S. mansoni* MVs compared to mice that received fibroblast MVs was not statistically significant. Future studies might test higher concentrations of EVs and vaccinate with three doses instead of two. Moreover, more work involving a third vaccine trial is needed to allow robust statistical comparisons between trials which could address data inconsistency observed herein.

Egg production rate is one of the parameters that is proposed as a measure of the reproductive success of *S. mansoni* in a particular host species (Bergquist and Colley, 1998), and is one of the criteria used to prioritise vaccine candidates for schistosomiasis. Vaccination with *S. mansoni* MVs resulted in a significantly lower number of tissue eggs in trial 2, suggesting a possible effect on worm fecundity as a consequence of the host immune response against these EVs. There was no significant difference in egg viability as calculated by hatching-index between both test and control groups, and these results were consistent for both trials.

Vaccines formulated as microparticles and liposomes may provide clues as to why EVs make efficient antigenic targets (Guy, 2007). For instance, encapsulating vaccine antigens using lipid spheres prevents their degradation and ensures slow release over time (Guy, 2007, Chadwick et al., 2010, Gregoriadis, 1994). Moreover, nanoparticles in the range of 40-50 nm are selectively taken up by murine dendritic cells compared to particles of up to 2 μm (Fifis et al., 2004). Therefore, it could be argued that the nature of helminth-derived EVs makes them better suited to internalisation by antigen presenting cells such as dendritic cells and macrophages, thus enhancing their antigenicity. This, however, should be investigated further as encapsulating recombinant or purified native schistosome EV antigens may improve efficacy.

The low level of protection observed in this study was probably because the mice didn't receive sufficient immunogen, and an extra boost was warranted to enhance IgG production. In Chapter 3 however, I demonstrated that there are some efficacious antigens present on the surface of the EVs, as antibodies to TSP-2 and TSP-4 blocked the uptake of the vesicles *in vitro.* It is tempting to suggest the protection observed in mice with recombinant *Sm*-TSP-2 is due to antibodies blocking the ability of schistosome parasites to communicate with host cells.

Protein microarrays allow rapid screening of a large repertoire of antigens by serological interrogation. My findings demonstrate that screening of a schistosome protein array rapidly revealed targets of the anti-ELV and anti-MV immune responses in mice. IgG1 is an important component of the protective humoral immune response to schistosomes (Mitchell et al., 2012, Wilson et al., 2014), and tegumental antigens like *Sm*-TSP-2, Sm29 and Smp80 (calpain) are the targets of IgG1 responses in schistosome-resistant individuals (Cardoso et al., 2006, Tran et al., 2006, Ahmad et al., 2011, Gaze et al., 2014). Antigens for which the strongest IgG1 responses were detected in this study included proteins that were predicted and/or proven to be located on the

tegument membrane, intracellular proteins, and metabolic enzymes that have key roles in parasitism. These findings support the notion that EVs are rich in antigens which could elicit specific immune responses against proteins with important roles in parasitism. Moreover, many of the strongly recognized antigens from the protein array were identified in the *S. mansoni* EV sub-proteomes described in Chapter 2.

Among the top 20 most immunoreactive antigens were proteins recognized by sera from mice immunised with both *S. mansoni* ELVs and *S. mansoni* MVs, including the tegmental antigen Sm-13 and NADH dehydrogenase subunit 1. They are both reactive because the protein is probably found in both vesicle types. Sm13 is one of the most strongly recognised proteins by antibodies from mice immunised with adult worm tegumental membranes (Abath et al., 2000), and has been localized to the adult worm tegument. NADH dehydrogenase and Sm13 were found also to be reactive antigens in *S. mansoni* infected individuals using the same protein microarray as used herein (de Asssi et al., 2016). A *S. japonicum* homologue of Sm13, Sj13, allowed detection of low intensity infections with high specificity and sensitivity when a panel of *S. japonicum* recombinant proteins were probed with sera, and to assess pre- and post-drug treatment follow up (Xu et al., 2014).

In this study, a number of proteins that were differentially recognized by sera from mice immunised with *S. mansoni* ELVs or *S. mansoni* MVs compared with controls are noteworthy. Indeed, some of these antigens, for example the TSP Sm23 (Smp_017430.1) was one of the most reactive targets of IgG1 responses in mice immunised with ELVs and has previously been shown to be protective in recombinant form in a mouse model of schistosomiasis (Bergquist et al., 2002, Krautz-Peterson et al., 2017). Further, *S. mansoni* infection of rats, mice and humans produces a strong antibody response to Sm23 (Krautz-Peterson et al., 2017). Moreover, its *S. japonicum* homologue Sj23 (Zhu et al., 2003, Shi et al., 2001) was shown to be protective in animal challenge models of schistosomiasis.

Cathepsin B-like peptidase (C01 family) (Smp_158420.1) was amongst the top 20 IgG1-reactive proteins recognized by antibodies from mice immunised with *S. mansoni* ELVs. Peptidases are essential for development of *S. mansoni,* and a number of gut-associated peptidases digest host blood proteins in the schistosome gastrodermis to facilitate nutrition (Sajid et al., 2003). Recombinant *S. mansoni*-cathepsin B formulated with Montanide elicited high levels of specific antibodies and provided protection against challenge infection by significantly reducing adult worm and egg burdens in mice and inducing high levels of Th1 and Th2 cytokine production by splenocytes (Ricciardi et al., 2016).

One of the most strongly recognised targets of IgG1 antibodies in mice immunised with *S. mansoni* ELVs was annexin (Smp_045500.1). Annexin is thought to be of integral importance for the stability of apical cell membranes in schistosomes and is proposed to play diverse roles in distinct cellular processes, notably suppression of inflammatory (D'Acquisto et al., 2008) and fibrinolysis (Madureira et al., 2011, de la Torre-Escudero et al., 2011). Annexin was recognized by sera from mice infected with *S. mansoni* (Leow et al., 2019), and is localized in the teguments of both schistosomula and adult worms (Leow et al., 2019, Tararam et al., 2010).

A possible anti-schistosome drug target is the seleno-protein thioredoxin-glutathione reductase (TGR) (Smp_048430.1). TGR was among the top 20 immunoreactive antigens in mice immunised with *S. mansoni* MVs, and is a key enzyme in detoxification of reactive oxygen species in schistosome parasites (Cioli et al., 2008). TGR from *S. japonicum* was assessed as a vaccine antigen in a mouse model of schistosomiasis and vaccination induced a significant decrease in adult worm and egg burdens (Han et al., 2012). TGR was also shown to be essential for schistosome survival using RNA interference *in vitro*, and was concluded to be a key drug target (Kuntz et al., 2007). Indeed, TGR has been flagged as a potential drug target against most neglected tropical diseases (Prast-Nielsen et al., 2011).

Importantly, probing of the protein arrays with anti-EV sera revealed several *S. mansoni* antigens which were not detected in EVs using proteomic approaches (Chapter 2), and for which there is supporting literature on their vaccine and/or diagnostic potential for schistosomiasis. Only four of the top 20 most immunoreactive *S. mansoni* proteins identified using sera from mice immunised with *S. mansoni* ELVs were also found from proteomic analysis on *S. mansoni* ELVs: Sm13 (Smp_195190.1), cathepsin B (C01 family) (Smp_158420.1), annexin (Smp_045500.1) and peptidyl-prolyl cis-trans isomerase (Smp_040790.1). Strikingly, only two of the top 20 recognised proteins from mice immunised with *S. mansoni* MVs were also identified from *S. mansoni* MVs by proteomic: Sm13 and putative GRX (Smp_006550.1). These findings can be interpreted in different ways: (1) proteomics is only revealing a small subset of the total EV proteome, and proteins that are less abundant and less readily digested into easily identified tryptic peptides by LC-MS/MS are detected; (2) substantial immunologic cross-reactivity between EV and non-EV proteins exists. Targeted MS approaches such as multiple reaction monitoring can be conducted on EV proteomes to specifically search for tryptic peptides from antigens identified serologically to confirm their presence.

Since there is an increasing body of evidence that helminth ELVs are efficacious vaccines in murine models (Trelis et al., 2016, Coakley et al., 2017, Shears et al., 2018, Chaiyadet et al., 2019), and *S. mansini* ELVs have been identified as a source of immunomodulatory effector molecules that can manipulate the host environment (Sotillo et al., 2016b, Samoil et al., 2018, Kifle et al., 2020), there is now compelling reasons to direct future research to assess *S. mansoni* ELVs for their vaccine efficacy.

Nonetheless, studies involving helminth-derived EVs as vaccines are still in their infancy, and future studies should be tailored towards evaluating different routes of vaccine administration and animal models used based on their suitability for vaccine trials and translatability to the human setting. For

instance, vaccination studies involving helminth-derived ELVs used different routes of antigen administration and/or mouse strains (Trelis et al., 2016, Coakley et al., 2017, Shears et al., 2018).

In conclusion, the data shown herein demonstrates the ability of *S. mansoni* MVs to provide modest levels of protective immunity in a mouse model of schistosomiasis as observed by reduction in both liver and intestinal egg burdens, but noting this outcome was only achieved in one of two trials conducted. Antibodies against EVs are hypothesized to target key physiological processes that can be potentially interrupted via subunit vaccines. Moreover, mice immunised with *S. mansoni* ELVs and MVs generated IgG1 antibodies that recognise defined antigens on these EVs. The potential of helminth-derived EVs to modulate the immune system offers a new strategy of targeting EVs as vaccine and therapeutic targets. Future work should investigate recombinant forms of EV surface proteins as protective antigens. Such insights will have paramount importance in determining how we can exploit the information gained to prevent and cure infectious diseases.

# Chapter 5

## Assessment of recombinant *Schistosoma mansoni* EV tetraspanins as vaccines in a mouse model of schistosomiasis

### Preamble

TSPs from helminths have been demonstrated to have vaccine potential using different animal models. In this Chapter, the three TSP proteins identified on the surface of *S. mansoni*-EVs (Chapter 2) were selected for assessment as recombinant subunit vaccines. rTSP proteins were expressed in *E. coli* (Chapter 3) and their vaccine efficacy assessed in a mouse model of schistosomiasis. Two trials with different vaccine regimens were carried out in BALB/c male mice. In each vaccine trial, five groups, 10 mice per group, were immunised intraperitoneally with the LEL of 1) r*Sm*-TSP-1; 2) r*Sm*-TSP-2; 3) r*Sm*-TSP-4; 4) cocktail of r*Sm*-TSP-1 + r*Sm*-TSP-2 + r*Sm*-TSP-4; or 5) rTRX, with all antigen preparations formulated with Alum/CpG adjuvant. Parasitological data including worm burdens, liver and intestine egg loads and egg viability assessment were performed to evaluate the level of protection for each vaccinated group compared to TRX control. Moreover, IgG serum antibody responses to each antigen were assessed using indirect-enzyme linked immunosorbent assay (ELISA). Immunohistochemistry was used to anatomically localize the TSP proteins within adult *S. mansoni*.

## 5.1. Introduction

Although strident efforts have been put in place for the prevention and control of schistosomiasis through integrated approaches such as MDA of PZQ, targeting the snail intermediate host, and improved sanitation, most importantly the development of a vaccine is needed to eliminate schistosomiasis (Rollinson et al., 2013). Molecules on the apical membrane of the schistosome tegument are accessible targets by host antibodies for immunological attack because of their close association with the host immune system (Braschi and Wilson, 2006).

Rigorous efforts are required to progress early stage discoveries towards a clinically validated and approved vaccine. Herein, I have assessed vaccine efficacy of the selected *S. mansoni* rTSP LELs in a mouse model of schistosomiasis. TSPs are efficacious helminth vaccine antigens (Tran et al., 2006, Dang et al., 2012, Joseph and Ramaswamy, 2013, Pearson et al., 2012). The vaccine potential of the LEL of r*Sm*-TSP-1(Tran et al., 2006) and r*Sm*-TSP-2 (Tran et al., 2006, Pearson et al., 2012) has been described. The LEL of r*Sm*-TSP-1 and r*Sm*-TSP-2 formulated with Freund adjuvants (Tran et al., 2006) or r*Sm*-TSP-2 adjuvanted with alum/CpG (Pearson et al., 2012) have proven to be an effective anti-schistosomiasis vaccine in a murine model, with significant reductions in both adult worm loads and egg burdens compared to controls. Other schistosome rTSPs have also shown protection in mouse vaccination models of schistosomiasis (Braschi and Wilson, 2006), including *Sm*23 (Da'Dara et al., 2008, Da'dara et al., 2001) and *S. japonicum*-TSP-2 (Yuan et al., 2010). Moreover, *Sm*-TSP-2 was strongly recognised by IgG from putatively resistant human subjects (Tran et al., 2006, Pearson et al., 2012), further highlighting the potential of some TSPs as subunit vaccines against human schistosomiasis. Moreover, TSPs have also been identified from *S. mansoni* EVs (Sotillo et al., 2016b, Samoil et al., 2018, Nowacki et al., 2015), and numerous TSPs (including those mentioned above) were identified herein following proteomic analysis of *S. mansoni*-derived EV fractions (Chapter 2). Furthermore, my findings from Chapter 3 show that antisera raised to TSPs successfully blocked *S.*

*mansoni* EV uptake by human host cell lines and hence have putative roles in host-parasite communication.

This chapter aimed to assess the efficacy of selected r*Sm*-TSPs identified on *S. mansoni*-derived EVs as vaccines. The findings from my study confirmed that select r*Sm*-TSPs conferred protection against infection as assessed by reduced worm burdens and liver and intestine egg loads, as well as ability of eggs to hatch and release viable miracidia.

## 5.2. Material and methods

### 5.2.1. Ethics statement

The study secured ethical clearance from the Animal Ethics Committee at JCU as described in section 2.2.1.

### 5.2.2. Mice and *S. mansoni*

Information on mice and *S. mansoni* used in the vaccine trial are described in section 2.2.2.

### 5.2.3. Cloning, expression and purification of r*Sm*-TSPs

Information on *Sm*-TSP gene cloning, expression and protein purification are outlined in sections 3.2.5 and 3.2.6.

### 5.2.4. Mouse immunisation and infection

Groups of ten male BALB/c mice 6 to 8 weeks of age were used for vaccination studies. Sample size was calculated by comparing two independent samples inference for means formula (Rosner, 2011). A sample size of n = 10 was selected on the assumption of a vaccine trial resulting in a 40% reduction in worm burdens in the test group, i.e. mean of 42 worms per mouse for μ1 (TRX control) and 25 worms per mouse for μ2 (test group), σ = 13, two-sided test, with α = 0.05 and power of 0.80. A

total of 50 mice were divided into five groups (10 mice/group) and each group was vaccinated with 50 µg of each of the following recombinant proteins as antigens: r*Sm*-LEL-TSP-1; r*Sm*-LEL-TSP-2; r*Sm*-LEL-TSP-4; a cocktail of r*Sm*-LEL-TSP-1 + r*Sm*-LEL-TSP-2 + r*Sm*-LEL-TSP-4 with 16.67 µg each; TRX control. TRX, was used as control because the recombinant proteins were cloned so as to produce TRX fusion proteins, and hence, protections conferred in vaccine trials were only be attributed to recombinant proteins assessed. All rTSPs and rTRX were constituted with an equal volume of Imjust alum adjuvant (Imject® Alum/Thermo Scientific) and 5 µg/dose of CpG oligodeoxynucleotides 1826 (InvivoGen). Immunisation of experimental mice were conducted as previously reported (Pearson et al., 2012) using the intraperitoneal route. Mice in vaccine trial 1 received three doses at 2-week intervals. Antibody titres in trial 1, however, were lower than we had observed in previous trials, therefore, the decision was made in trial 2 to give a fourth immunisation. Mice were challenged with 120 *S. mansoni* cercariae two weeks after the final vaccination using the tail technique (Harn et al., 1984). Serum samples were collected at day-2 (pre-immunisation), prior to each protein boost and pre-challenge to monitor immune responses. Mice were euthanized seven weeks after cercarial challenge as described in section 4.2.4, and necropsy was undertaken to obtain parasitological data including the number of adult worms, liver as well as intestinal egg burdens, and egg hatching index. Two independent vaccine trials were conducted on different dates using different batches of cercariae.

### 5.2.5. Egg viability test

Egg viability test was assesses as described in section 4.2.10.

### 5.2.6. Enzyme-linked immunosorbent assay

Specific IgG antibody responses in sera collected from mice vaccinated with r*Sm*-TSP-1, r*Sm*-TSP-2, r*Sm*-TSP-4, r*Sm*-TSP-1 + r*Sm*-TSP-2 + r*Sm*-TSP-4 and TRX were measured by ELISA as described previously. Ninety-six-well flat-bottom microtiter plates (NUNC-F96, FisherScientific) were coated

with 2 µg/ml of each antigen in triplicate in 100 mM carbonate-bicarbonate buffer (pH=9.6), and incubated with 5% skim milk for 1 h at 37°C before addition of 100 µl of serially diluted test sera (1:1,000 to 1: 2,560,000) as primary antibodies at 37°C for 1 h. Plates were then washed 3 times with PBS/0.05% Tween-20 (PBST) between incubations. After addition of IgG HRP-conjugated goat anti-mouse secondary antibody (Invitrogen) at a dilution of 1: 6,000 in PBST, peroxidase activity was detected with tetramethyl benzidine chromogenic substrate (ThermoFisher), and the reaction was stopped by adding 50 µl of 3 M HCl. The colorimetric reaction was read at 450 nm using a microplate spectrophotometer (Bio-Rad Laboratories). Positive results were expressed as endpoint titres with 3 standard deviations above background wells containing baseline sera.

### 5.2.7. Immunolocalisation

Immunohistochemistry was performed to determine the anatomic sites of *S. mansoni* TSP expression in sectioned adult worms. Fixed adult worm sections were deparaffinised using the following procedures: first washed with 100% xylene two times for 3 min each, and slides were transferred to coplin jars containing 50% xylene and 50% ethanol and kept for 3 min. Slides were rehydrated with two washes of 100% ethanol, then consecutively with 95%, 70% and 50% ethanol each for 3 min before rinsing in cold water two times for 5 min each. Antigen retrieval was performed by boiling the slides in citrate buffer (10 mM sodium citrate, pH 6) for 40 min followed by Tris buffer (10 mM Tris, 1 mM EDTA, 0.05% Tween, pH 9.0) for 20 min. Sections were washed using TBS/0.05% Tween-20 (TBST) and blocked with 10% goat serum for 1 h at RT. After washing with TBST three times each for 5 min, sections were incubated with sera from vaccinated mice diluted 1:50 in 1% BSA/TBST overnight at 4°C. Samples were washed using TBST three times each for 5 min. The sections were then probed with goat anti-mouse IgG-Alexa Fluor 647 (Sigma-Aldrich) diluted 1:200 in TBST/1% BSA for 1 h at RT, and samples were kept in the dark. Slides were washed

three times with TBST, mounted with Entellan mounting medium (Millipore), covered with cover slips, and examined with an AxioImager M1 fluorescence microscope (Zeiss) using Nuance software.

### 5.2.8. Mice necropsy and estimation of worm and tissue egg burdens

Mice were necropsied and worm as well as egg burden assessments were carried out as described in section 4.2.9.

### 5.2.9. Data analysis

For all vaccine trial data, unpaired Student's t-test was used to analyse any statistical differences between experimental and control groups as described in section 4.2.12.

## 5.3. Results

### 5.3.1. Antibodies against *S. mansoni*-TSPs recognize adult worm surface antigens

Antibodies to both r*Sm*-TSP-2 and TSP-4 bound to the tegument of sectioned adult flukes. Antibodies to TSP-2 bound more strongly to the tegument compared to the less pronounced binding of antibodies to TSP-4 (Figure 5.1). The distribution pattern of TSP-2 was reasonably uniform across the tegument, which is in agreement with earlier studies (Tran et al., 2006), but TSP-4 has not previously been localized and revelaed a punctate distribution pattern across the tegument. It is possible that TSP-4 is expressed in distinct tegumental regions, possibly tegumentay cytons, and future work using transmission electron microscopy could shed light on the specific sub-cellular distribution of this protein. Naïve mouse sera did not show any binding to schistosome tissues.

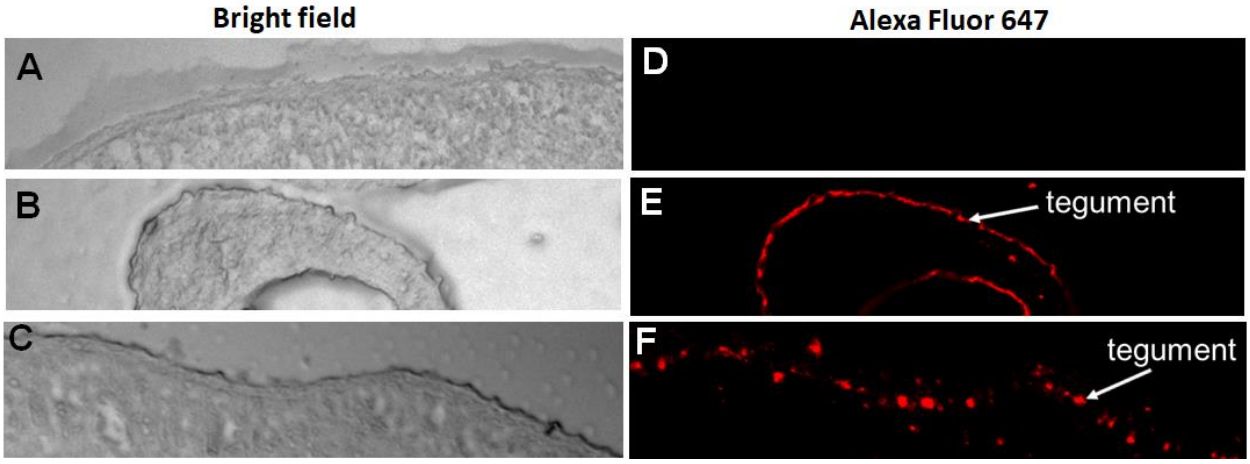


**Figure 5. 1. Anti-rTSP antibodies recognise proteins in the tegument of adult worms.** Immunofluorescence micrographs showing adult *S. mansoni* sections probed with either 1) naive mouse serum (panels A and D), mouse anti-r*Sm*-TSP-2 serum (panels B and E) and mouse anti-r*Sm*-TSP-4 serum (panels C and F) followed by goat anti-mouse IgG-Alexa Fluor-647. Red fluorescence denotes regions where antibody has bound. Note fluorescence of only the tegument with antibodies to r*Sm*-TSP-2 and r*Sm*-TSP-4 but not naïve serum. All images are shown at 400× original magnification.

### 5.3.2. *S. mansoni* rTSPs showed a moderate efficacy in protecting infections

Mice in vaccine trial 1 showed no significant reduction in adult worm burdens compared to mice immunised with TRX control (Figure 5.2A). In vaccine trial 2, however, mice vaccinated with r*Sm*-TSP-2 36% ($P<0.01$) and TSP cocktail 30% ($P<0.01$) showed significant reduction in worm burdens (Figure 5.2B).

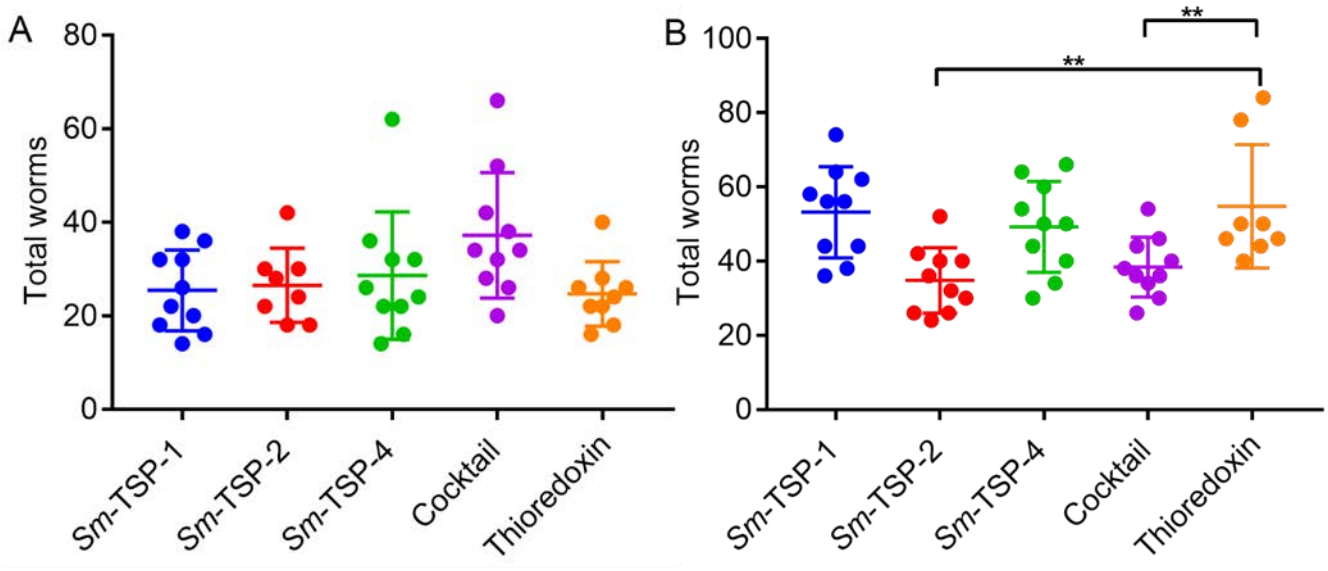


**Figure 5. 2. Worm counts for individual mice in vaccine trial 1 (A) and vaccine trial 2 (B) immunised with either r*Sm*-TSP-1, r*Sm*-TSP-2, r*Sm*-TSP4 or TSP cocktail compared to TRX control group formulated with alum/CpG.** Worm burdens were determined seven weeks post-cercarial challenge. ** *P*< 0.01.

Moreover, mice vaccinated with r*Sm*-TSP-1, r*Sm*-TSP-2, r*Sm*-TSP-4 or TSP cocktail in vaccine trial 1 resulted in no significant reduction in mean liver egg burdens (Figure 5.3A). On the contrary, a significant reduction in mean liver egg burdens of 36% (r*Sm*-TSP-2; *P*<0.01) and 26% (TSP cocktail; *P*<0.05) were observed (Figure 5.3B) in vaccine trial 2 compared to TRX control.

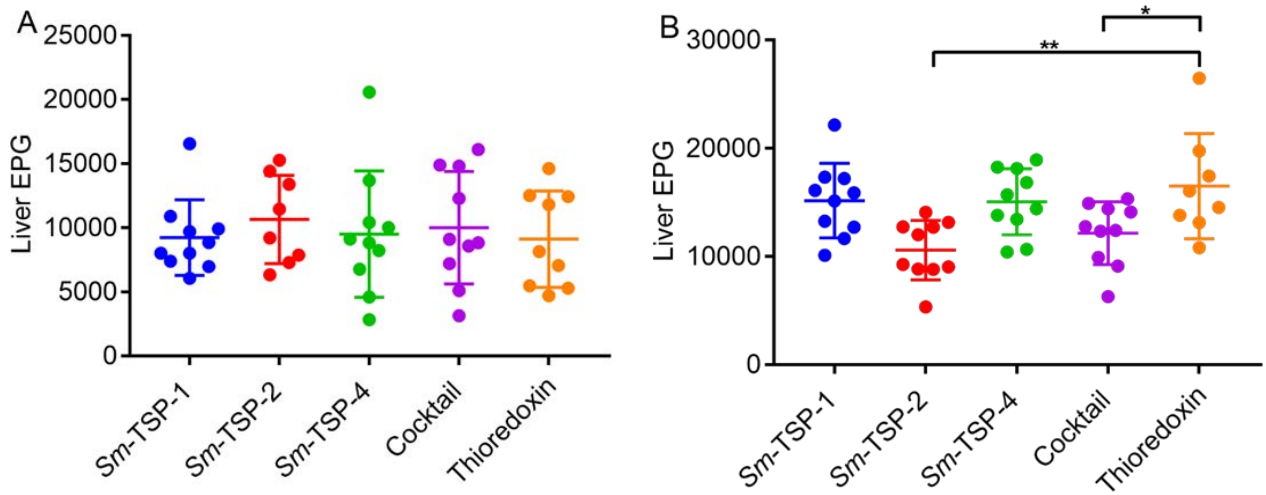

**Figure 5. 3. The egg loads per gram of liver tissue for individual mice in vaccine trial 1 (A) and vaccine trial 2 (B) immunised with either r*Sm*-TSP-1, r*Sm*-TSP-2, r*Sm*-TSP4 or TSP cocktail compared to TRX control formulated with alum/CpG.** Liver egg loads were determined seven weeks post-cercarial challenge. * *P*<0.05, ** *P*< 0.01.

To evaluate the effect of the vaccines on reducing transmission, intestinal eggs were counted; intestines from any of the groups in vaccine trial 1 had no significant reduction in intestinal egg loads (Figure 5.4A); however, mice vaccinated with TSP cocktail had a 31% (*P*<0.05) reduction in mean egg burdens than those in the control group (Figure 5.4B) in vaccine trial 2.

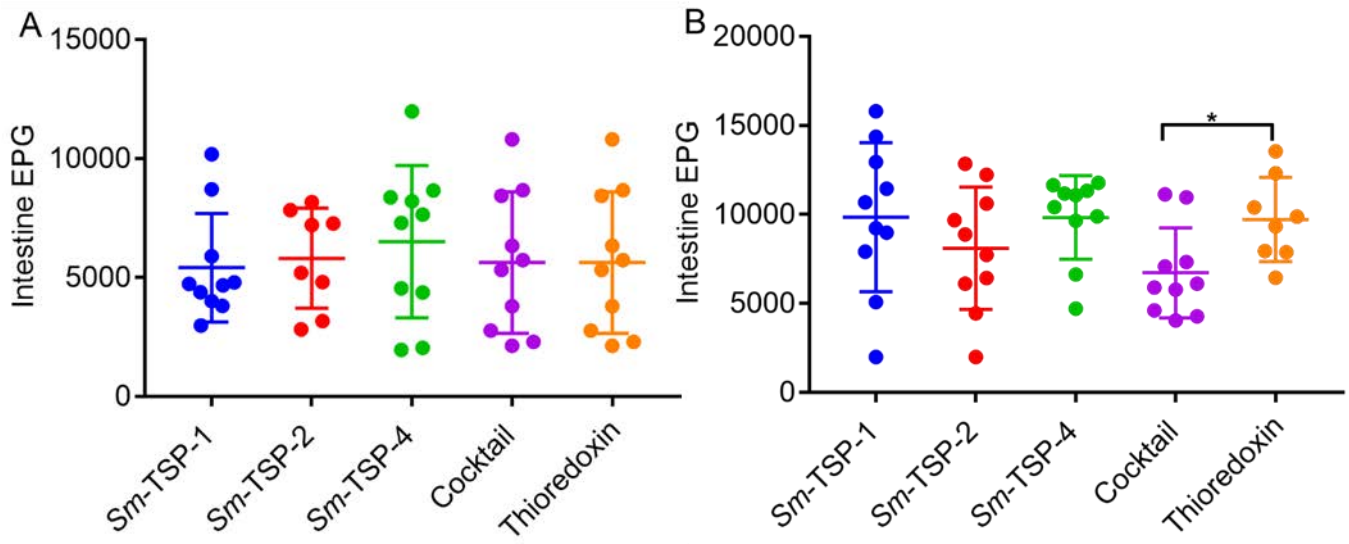


**Figure 5. 4. The egg load per gram of intestine tissue for individual mice in vaccine trial 1 (A) and vaccine trial 2 (B) immunised with either r*Sm*-TSP-1, r*Sm*-TSP-2, r*Sm*-TSP4 or TSP cocktail compared to TRX control group formulated with alum/CpG.** Intestine egg loads were determined seven weeks post-cercarial challenge. * *P*<0.05.

A significant reduction in egg hatching index (Figure 5.5A) was obtained in mice immunised with r*Sm*-TSP-2 (*P*<0.05) and TSP cocktail (*P*<0.001) in vaccine trial 1. In vaccine trial 2, however, mice vaccinated with only r*Sm*-TSP-4 had a lower egg hatching index compared to TRX control (Figure 5.5B), but this difference was not statistically significant.

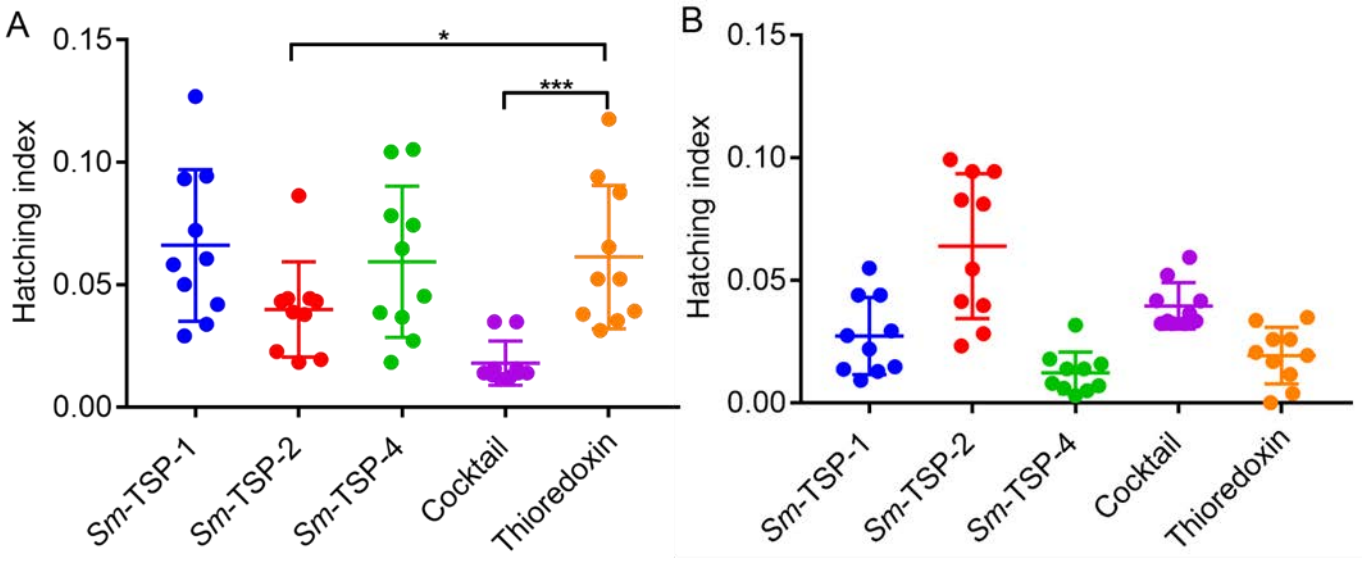


**Figure 5. 5. Egg hatching index per individual mouse in vaccine trial 1 (A) and vaccine trial 2 (B) immunised with either r*Sm*-TSP-1, r*Sm*-TSP-2, r*Sm*-TSP4 or TSP cocktail compared to TRX control group formulated with alum/CpG.** Egg hatching index was determined seven weeks post cercarial challenge. * *P*<0.05, *** *P*< 0.001.

### 5.3.3. Mice vaccinated with rTSPs mounted IgG antibody responses

Antibody responses to rTSPs and rTRX were measured by IgG endpoint titres on pre-challenge pooled sera collected from mice in vaccine trial 1 and vaccine trial 2. Mice generated antibody titres in excess of 1:320,000 in vaccine trial 1 against r*Sm*-TSP-1 and in excess of 1:160,000 against r*Sm*-TSP2, r*Sm*-TSP-4, TSP cocktail or TRX control (Table 5.1).

**Table 5. 1. Pre-challenge IgG endpoint titres and parasitological data for mice in vaccine trial 1 immunised with either r*Sm*-TSP-1, r*Sm*-TSP-2, r*Sm*-TSP4 or TSP cocktail compared to TRX control formulated with alum/CPG.**

| Group | IgG endpoint titres/pre-challenge | Adult worms, range | Adult worms Mean ± SE | Liver EPG Mean ± SE | Intestine EPG Mean ± SE | Hatching index Mean ± SE (% reduction) |
|---|---|---|---|---|---|---|
| Control (thioredoxin); n=9 | 1:160,000 | 16-40 | 24.7 ± 2.3 | 9107 ± 1257 | 5351 ± 627 | 0.061 ± 0.01 |
| *Sm*-TSP-1; n=10 | 1:320,000 | 14-38 | 25.4 ± 2.7 | 9227 ± 935 | 5415 ± 721 | 0.066 ± 0.01 |
| *Sm*-TSP-2; n=8 | 1:160,000 | 18-42 | 26.5± 2.8 | 10642 ± 1220 | 5907 ± 745 | 0.04 ± 0.01 (35%, **P*<0.05) |
| *Sm*-TSP-4; n=10 | 1:160,000 | 14-62 | 28.6 ± 4.3 | 9499 ± 1560 | 6506 ± 1010 | 0.59 ± 0.01 (3%) |
| Cocktail; n=10 | 1:160,000 | 20-66 | 37. 2 ± 4.2 | 9998 ± 1384 | 5628 ± 939 | 0.02 ± 0.01 (71%, ****P*<0.001) |

Endpoint titres measured on pre-challenge sera collected from mice in vaccine trial 2 were much higher than trial 1. Titres of 1:2,560,000 were recorded for r*Sm*-TSP-1 and 1:1,280,000 for either *Sm*-TSP2, r*Sm*-TSP-4, TSP cocktail or TRX control (Table 5.2).

**Table 5. 2. Pre-challenge IgG endpoint titres and parasitological data for mice in vaccine trial 2 immunised with r*Sm*-TSP-1, r*Sm*-TSP-2, r*Sm*-TSP4, TSP cocktail compared to thioredoxin control formulated with alum/CPG.**

| Group | IgG endpoint titres/pre-challenge | Adult worms, range | Adult worms Mean ± SE (% reduction) | Liver EPG Mean ± SE (%reduction) | Intestine EPG Mean ± SE (% reduction) | Hatching index Mean ± SE (% reduction) |
|---|---|---|---|---|---|---|
| Control (thioredoxin); n=8 | 1: 600,000 | 40-84 | 54.7 ± 5.2 | 16503 ± 1539 | 9713 ± 748 | 0.02 ± 0.004 |
| *Sm*-TSP-1; n=10 | 1: 2,560,000 | 36-74 | 53.2 ± 4.1 (3%) | 15159 ± 1217 (8%) | 9838 ± 1480 (0) | 0.03 ± 0.005 (0) |
| *Sm*-TSP-2; n=10 | 1: 1, 280,000 | 26-52 | 34.8± 2.9 (36%, ***P*<0.01) | 10598 ± 916 (36%, ***P*<0.01) | 8090 ± 1145 (17%) | 0.06 ± 0.01 (0) |
| *Sm*-TSP-4; n=10 | 1: 1, 280,000 | 34-66 | 49.2 ± 3.9 (10%) | 15060 ± 965 (9%) | 9827 ± 742 (0) | 0.01 ± 0.003 (37%) |
| Cocktail; n=10 | 1: 1, 280,000 | 26-54 | 38.4 ± 2.6 (30%, ***P*<0.01) | 12159 ± 918 (26%, **P*<0.05) | 6719 ± 798 (31%, **P*<0.05) | 0.04 ± 0.003 (0) |

## 5.4. Discussion

Molecules exposed to host antibodies, notably proteins anchored to the outer tegument of the worm are the most important vaccine candidates (El Ridi and Tallima, 2013). Tegument proteins are key candidates as schistosome vaccine antigens because of their location at the parasite-host interface (Loukas et al., 2007, Pinheiro et al., 2011). Many tegumental proteins have been characterised as vaccine candidates, including the TSPs *Sm*-TSP-1, *Sm*-TSP-2 and Sm23 (Tebeje et

al., 2016). Helminth secreted EVs have shown promising results as vaccines in mice infected with *E. caproni* (Trelis et al., 2016), *H. polygyrus* (Coakley et al., 2017) and *T. muris* (Shears et al., 2018), and in hamsters infected with *O. viverrini* (Chaiyadet et al., 2019), but we know little about the specific antigens targeted by protective antibodies. Since at least some of these protective molecules likely make contact with ligands on the target cell plasma membrane, they present as potential targets for vaccines that prevent EV-host cell communication. Applying intact helminth EVs as vaccines, however, is not feasible because of the difficulty in the collection and isolation of sufficient EVs. Instead, assessing vaccine efficacy of recombinant forms of select EV surface antigens with known roles in host cell communication is technically feasible.

The aim of this Chapter was to assess selected r*Sm*-TSP proteins identified on the surface of *S. mansoni* EVs as vaccines in a mouse model of schistosomiasis. To this end, the LEL of *Sm*-TSP-1, *Sm*-TSP-2 and *Sm*-TSP-4 recombinant proteins and a cocktail of all three antigens adjuvanted with alum/CpG were tested for their vaccine efficacy compared to TRX control in a mouse model of schistosomiasis. In this study, the protection level obtained for some of the antigens in vaccine trial 2 was higher compared to the same antigen used in vaccine trial 1 and was inconsistent across the two experiments conduced. r*Sm*-TSP-2 and TSP cocktail vaccine formulations were capable of eliciting a significant reduction in both adult worm and liver egg burdens in vaccine trial 2; moreover vaccination with the TSP cocktail induced significant reductions in intestinal egg burdens in vaccine trial 2. Antibody titres in trial 1 were lower than we had observed in previous (published) trials with TSP-2 and TSP-4 and, therefore, the decision was made in trial 2 to give a fourth immunisation, and that is the likely reason why antibody titres and protection were higher in trial 2. Previous studies done by our group to assess the vaccine efficacy of the LEL of r*Sm*-TSP-2 formulated with Freunds (Tran et al., 2006) or alum/CpG (Pearson et al., 2012) adjuvants in a murine model of schistosomiasis achieved 57% and 64% vs 25-27% and 20-27% reductions in mean adult worm and liver egg burdens,

respectively, over two independent vaccine trials. The discrepancies observed in protection levels among the different studies could be attributed to the differences in experimental conditions such as adjuvants, route of cercarial challenge, and/or fitness of different cercarial batches. Moreover, r*Sm*-TSP-2 showed even higher immunogenicity and protection when used as a chimeric vaccine with a protective hookworm vaccine antigen (*Na*-APR-1), resulting in 54-58% and 48-56% reductions in mean worm and liver egg burdens, respectively, compared to mice immunised with r*Sm*-TSP-2 alone over two independent trials (Pearson et al., 2012). Similarly, a multivalent chimeric antigen with r*Sm*TSP-2/rSm29 formulated with alum/CpG showed reductions of 28 to 34% in adult worm counts and up to 48% reductions in liver pathology compared to 20% and 38% reductions in adult worm and liver pathology, respectively, compared to mice that received rSm29 alone (Pinheiro et al., 2014). In the current study, vaccination of BALB/c mice with r*Sm*-TSP-1 or r*Sm*-TSP-4 did not produce significant reductions in adult worm burdens or liver egg loads compared to mice in the TRX control group. In contrary to my findings, previous studies done by our group (Tran et al., 2006) demonstrated that CBA/CaH mice immunised with the LEL of r*Sm*-TSP-1 formulated with Freunds adjuvants displayed 34% and 52% reductions in mean adult worm burdens and liver egg loads, respectively. The discrepancy between the two studies might be due to the different experimental conditions such as different adjuvants and mouse strains used. Indeed, the different experimental conditions used by different research groups, including different routes of administration, adjuvants, vaccination regimen, antigen doses, and even mouse strains could attribute to the apparent discrepancy seen in the literature for select vaccine antigens for schistosomiasis. This makes it difficult to compare and contrast published data, and consistency in protocols used to assess putative vaccine antigens would be a welcome approach for the field. In a simulated field condition of human schistosomiasis, Siddiqui and collegues showed a moderate reduction in worm burden but significant reduction in tissue egg burdens in baboons immunised with recombinant Sm-p80 + CpG-ODN compared with adjuvant-treated control baboons (Siddiqui et al., 2018). Further,

rSm-p80 formulated with GLA-Alum provided 33–53% and 38% reduction in worm burdens in mice and baboons, respectively, compared to those immunised with adjuvant only (Zhang et al., 2018b). In a similar study, Zhang et al. reported a significant reduction (90%) in the tissue egg load in baboons immunised with rSm-p80 adjuvanted with glucopyranosyl lipid A/GLA-SE compared to baboons that received GLA-SE only (Zhang et al., 2018c).

Because most of the morbidity of schistosomiasis is linked to eggs trapped in the tissues rather than the adult worms, reducing tissue egg burdens and granuloma formation would be desirable criteria of any effective schistosomiasis vaccine antigen. In the present study, TSP cocktail with alum/CpG was capable of achieving significant reductions in worm burdens and liver and intestinal egg loads compared to mice immunised with TRX control. Indeed, vaccination with the cocktail resulted in greater reductions in intestinal egg burdens compared to vaccination with r*Sm*TSP-2 alone, highlighting the need for further research on multivalent vaccine antigen discovery and development for schistosomiasis. A vaccine that reduces intestinal egg burden will have an impact on transmission. Recombinant *O. viverrini* EV surface proteins, combination of r*Ov*-TSP-2 + r*Ov*-TSP-3 when adjuvanted with alum/CpG showed a significant reduction in worm loads compared to mice vaccinated with r*Ov*-TSP-2 or r*Ov*-TSP-3 alone in a hamster model of opisthorchiasis (Chaiyadet et al., 2019). The reduced number of tissue eggs from my study herein and others in the literature may reflect either an immediate anti-fecundity effect of the vaccine or a delayed inception of egg laying (Cheever et al., 2002). To this end, further research assessing generation of developmental oograms and examination of egg laying at different experimental intervals should be performed (Cheever et al., 2002, Mati and Melo, 2013). Moreover, Chaiyadet et al. showed that the average length of worms obtained from hamsters vaccinated with r*Ov*-TSP-2 or r*Ov*-TSP-3 was significantly shorter compared to those collected from control hamsters, revelaing a stunting effect on worm development (Chaiyadet et al., 2019). In this study, eggs recovered from mice immunised with r*Sm*-

TSP-2 and TSP cocktail had showed a reduction trend in hatching-index, possibly as a result of attenuated development of the parasites caused by binding of antibodies to the tegument having an effect on parasite fitness. However, additional studies are necessary to support the association between protection levels measured by hatching-index. Eggs recovered from baboons immunised with rSm-p80 + CpG-ODN had significantly reduced viability and hatching rates compared to eggs from baboons that received adjuvant only (Siddiqui et al., 2018). Moreover, an 81% reduction in hatching of eggs was reported in baboons immunised with rSm-p80 adjuvanted with GLA-SE compared to baboons immunised with GLA-SE only (Zhang et al., 2018c).

Investigational vaccines against *S. mansoni* are more likely to succeed if they can elicit robust immune responses against multiple antigenic targets in the schistosome. In this study, pre-challenge sera collected from mice vaccinated with rTSPs showed IgG antibody titres that were higher for all groups of mice in vaccine trial 2 compared to mice in vaccine trial 1, and this might be due to an extra (fourth) dose of antigen administered to mice in vaccine trial 2. In trial 1, mice were challenged with parasites before antibody titres were assessed. In trial 2, antibody titres were assessed after the third vaccination and were found to be lower than that obtained in earlier studies from our laboratory. A fourth vaccination was therefore conducted in trial 2, resulting in substantially higher IgG titres. Studies done in humans showed that r*Sm*-TSP-2 is strongly recognised by IgG1 and IgG3 (Tran et al., 2006) from naturally resistant individuals but is not recognised as strongly by IgG from chronically infected individuals. In my study, there was no association between antibody titres and parasite burdens in mice immunised with r*Sm*-TSP-1. Despite producing the highest IgG titres of all the antigens in both vaccine trials, vaccination with r*Sm*-TSP-1 did not result in significant reductions in adult worm or tissue egg burdens. Similarly, high levels of antigen-specific IgG1 antibodies were measured in mice immunised with the tegument surface protein Sm14 adjuvanted with alum hydroxide, but no reduction in adult worm burden was observed (Fonseca et al., 2004), suggesting

that high antibody titres against any surface antigen is not sufficient for protection, and only certain surface antigens can generate meaningful protective humoral responses.

In this study, I have demonstrated immunolocalization of *Sm*-TSP-2 and *Sm*-TSP-4 to the outer tegument of *S. mansoni*. While the surface localisation of TSP-2 has been previously reported (Tran et al., 2006), this is the first report of surface localisation for TSP-4. Strong localization seen to *Sm*-TSP-2 on the tegument compared to *Sm*-TSP-4 could be best explained by a higher level of abundance/expression of TSP-2 in the tegument compared to TSP-4, or its accessibility to the host immune system due to its anatomical location within the tegument. While not addressed herein for TSP-4, *Sm*-TSP-2 is also expressed on the surface of live schistosomula (Tran et al., 2010), the developmental stage that is widely thought to be the most vulnerable stage for immune-mediated attack (Tebeje et al., 2016). The role of *Sm*-TSP-2 in maintaining tegument membrane integrity has been demonstrated *in vitro* using RNAi (Tran et al., 2010). Moreover, it was recently demonstrated that the tegument relies on a stem cell (neoblasts) population that replace tegumental cells lost to turnover that are enriched in TSP-2, prompting the authors to speculate that stem cell-driven renewal of this tegumental lineage represents an important strategy for parasite survival, and hence revealed new therapeutic targets (Wendt et al., 2018, Collins et al., 2016). Furthermore, *S. mansoni*-infected rats show a higher titer for schistosome apical tegumental antigens (primarily *Sm*-TSP-2 and Sm29) compared with non-apical membrane antigens, and these antibodies were also bound to the surface of living lung-stage worms and to formaldehyde-fixed adult worms (Sepulveda et al., 2010). *S. mansoni* infection in experimentally infected mice and rats, as well as naturally infected humans, elicits high levels of antibodies that recognise five major tegumental membrane proteins, including *Sm*-TSP-2, Sm23 and Sm29 (Krautz-Peterson et al., 2017).

Mode of vaccine delivery and selection of mouse strain used in any given vaccine model are an important aspect to consider in the experimental design and for critical interpretation of results.

Several studies reported that antigens irrespective of their routes of administration resulted in similar levels of protection and immune responses in a *S. mansoni* challenge model. For instance, the levels of protection against *S. mansoni* infection obtained by the intranasal route with 9B peptide-1 (Ben-Yedidia et al., 1999) was comparable to that obtained by intraperitoneal with this same peptide, and both modes of delivery yielded comparable humoral responses (Tarrab-Hazdai et al., 1998). Moreover, single-dose mucosal immunisation with biodegradable microparticles containing a *S. mansoni* antigen administered using nasal or oral routes induced a long-lasting specific humoral response (Baras et al., 1999). Further, oral immunisation of mice with recombinant *S. japonicum* proteins induced antigen-specific antibodies and damage to adult worms after a challenge infection (Yang et al., 1997). Similarly, mucosal immunization of mice with a recombinant fusion protein vaccine against schistosomiasis conferred protection against infection and immunopathology (Lebens et al., 2003). An additional factor that might affect antigen/adjuvant responses is the mouse strain used. For instance, BL/6 and BALB/c mice are regarded as high responders to the irradiated *S. mansoni* cercariae vaccine with fewer worms obtained after challenge infection compared to CBA mice which are considered moderate responders (Stephenson et al., 2014). On the other hand, infected CBA mice show stronger splenic T cell proliferation with a reduced suppressor T cell response once a schistosome infection becomes patent compared to that of BL/6 and BALB/c mice (Lewis and Wilson, 1981).

In summary, my findings herein demonstrated that immunisation of mice with r*Sm*-TSP-2 or TSP cocktail formulated with alum/CpG resulted in protection against schistosomiasis infection compared to TRX control group as observed by a trend towards reduction of adult worms, liver egg burdens and hatching index, and reduction in intestinal egg loads in mice that received TSP cocktail in one of the vaccine trials. Repeated multiple trials with the same vaccine regimen is recommended for the future to address data inconcistancy between trials. Moreover, r*Sm*-TSP specific IgG

antibodies were elicited and these antibodies recognise TSPs on the worm surface. My findings along with previous studies by our group (Tran et al., 2006, Pearson et al., 2012) implicate the relevance of testing different experimental conditions in order to get the most protective and immunologically favourable formulation. Finally, EV recombinant proteins might be best delivered in the form of synthetic vesicles so that they are embedded on/in the surface and adopt the proper conformation and are correctly presented to the immune system.

# Chapter 6

# General discussion and future directions

## 6.1. General discussion

Schistosomiasis is a debilitating neglected disease that mainly occurs in tropical and subtropical regions. Treatment depends solely on PZQ, which is effective in killing adult schistosome parasites, but has poor activity against immature worms, and does not prevent reinfection. Further, the development of drug resistance by the parasite is also a concern that has to be considered (Gryseels et al., 2006, Doenhoff and Pica-Mattoccia, 2006, McManus et al., 2010). Currently, there are no anti-schistosomiasis vaccines that have received regulatory approval and made it into the clinic. In terms of vaccine targets, there has been much recent interest in assessing helminth EVs.

As defined in the introduction of this thesis, EVs are heterogeneous vesicles of membranous origin released by different types of cells. EVs comprise a complex mixture of genetic information, proteins, lipids, and glycans. Pertinent to this thesis was addressing the roles of *S. mansoni* EVs in host-parasite interactions: What are the proteome profiles of the different compartments of these EVs? Do EVs secreted from *S. mansoni* bind to and get internalised by host cells? Do the internalised EVs have a role in host cell gene regulation? Do antibodies against surface TSPs disrupt EV-mediated parasite-host communication? Will vaccines against EVs and recombinant versions of their surface proteins display efficacy in a mouse model of schistosomiasis? Research conducted within this thesis has begun to address these questions.

In Chapter 2 of this thesis, I presented the first comprehensive proteomic analysis of two populations of adult *S. mansoni*-derived EVs – ELVs and MVs, and have provided valuable information on the protein composition of these two EV types. I identified 286 and 716 proteins in

ELVs and MVs, respectively. Among the proteins identified were potential vaccine candidates and proteins relevant to host-parasite communication, which are unique and common to both EV types. MS-based proteomic analysis has undoubtedly advanced our understanding of schistosome EV protein content; however, coupled with other approaches such as metabolomics and transcriptomics, interrogation of the schistosome proteome (particularly the surface molecules) provided a mechanism by which to identify important clinically-relevant proteins, notably those with potential as new vaccine targets. Therefore, these vesicular proteomes provide diverse information on the nature of EVs secreted by schistosomes, and help us to translate the molecular mechanisms that are involved in vesicular cargo sorting and biogenesis, as well as the diverse physiological and pathological functions of EVs (Bandu et al., 2019, Rontogianni et al., 2019). Further, high-throughput mass spectrometry based proteomic studies on EVs facilitate biomarker discovery based on the protein signatures of the originating cells.

Perhaps the most intriguing aspect of the interactions between EVs and target cells is the active internalisation of these EVs by target cells, and their potential roles in host cell gene regulation. Based upon the increasing realisation that EVs facilitate intercellular communication in eukaryotes (Guay and Regazzi, 2017, Xu and Wang, 2017, Alcayaga-Miranda et al., 2016), it was hypothesised that *S. mansoni*-secreted EVs contribute to maintenance of long-term host-parasite interactions during schistosomiasis. It is clear from my work in Chapter 3, that both *S. mansoni* ELVs and MVs are internalised by both endothelial and monocyte cell lines (at least *in vitro*), and have a role in regulation of host gene expression. This is the second documentation of a role for *S. mansoni* EVs in host-parasite communication, and reveals novel insights into the mechanisms of host-schistosome interactions. The first report of internalisation and subsequent functional consequences of *S. mansoni* EVs was recently described by Meningher et al. (2020) who showed that internalisation of adult worm EVs modulated host T helper cell differentiation. The mechanism underlying *S. mansoni*

EV internalisation and cargo deliver into target cells is key area for future research. EVs recognize and attach to their target cells through surface molecules and are internalised by endocytosis/phagocytosis (Mulcahy et al., 2014) or with direct fusion of EVs with the plasma membrane of target cells (Feng et al., 2010). Many EV subtypes have common surface molecules and it is possible that one or more of these serve as a common ligand or receptor.

After determining that *S. mansoni* EVs were internalised by host target cells, I wanted to determine whether they could have a role in host target cell gene regulation. The findings from Chapter 3 on differential gene expression using HUVEC cells revealed that *S. mansoni* ELVs are indeed involved in regulating host cell gene expression, with notable effects on genes involved in coagulation, nutrient acquisition and immune regulation. Moreover, differential gene expression analysis revealed that *S. mansoni* EVs might assist the parasite's migration through host tissue and help it to evade attack by host immune cells. Transfer of EV molecules, such as proteins and miRNAs can influence the physiology of the target cell and exert an effect on both normal physiological as well as pathological processes (Robbins and Morelli, 2014). Therefore, EVs derived from *S. mansoni* parasites potentially act as vehicles to package and deliver signalling molecules to host cells and regulate host gene expression, which may facilitate survival of the schistosome. These findings need due consideration as further investigation in this area may facilitate the discovery of new vaccines and therapeutic targets.

Recombinant forms of selected *S. mansoni* EV surface proteins - *Sm*-TSP-1 (Smp_155310), *Sm*-TSP-2 (Smp_181530), *Sm*-TSP-4 (Smp_140000) and their cocktail r*Sm*-TSP-1 + r*Sm*-TSP-2 + r*Sm*-TSP-4 - were expressed to assess their vaccine efficacy over two independent trials. None of the antigens (either individually or in combination) were found to be protective in vaccine trial 1. However, in vaccine trial 2, reduction in the burden of adult worms, liver and intestinal eggs was detected in mice vaccinated with r*Sm*-TSP-2 and a cocktail of TSPs, compared with mice vaccinated with TRX

control. Anti-TSP IgG antibodies bound and hence recognised *S. mansoni* TSP proteins present on the tegument of sectioned adult worms. This suggests that TSP-2 at least is accessible on the surface of live parasites and renders them susceptible to immune mediated killing. *Sm*-TSP-2 is abundant in the *S. mansoni* EV membrane (Sotillo et al., 2016b, Kifle et al., 2020), and is currently in clinical development as a vaccine for *S. mansoni* infection (Merrifield et al., 2016, Hotez et al., 2019). *Sm*-TSP-1 and TSP-4 which were assessed herein did not confer protection in either trial and are likely not good candidate antigens. Identifying an effective single antigen with a high level of protection against schistosomiasis would be ideal for a vaccine candidate; however, the complexity of the schistosome genome and its immunomodulatory sophistication makes single-target vulnerability improbable (Mei and LoVerde, 1997, Gouveia et al., 2019), so combining multiple subunit antigens is most likely required based on the lessons learned from the attenuated cercariae vaccine (Mastin et al., 2009) and the use of rhesus macaques (Li et al., 2015, Wilson et al., 2008). Selection of the best vaccine antigens will only be achieved after thorough characterisation of the proteins that are crucial for the parasite's survival. For this purpose, combining proteomics, immunomics, and transcriptomics will provide invaluable information. Finally, tegumental proteins, ES products, and gut proteins play key roles in host-parasite cross-talk, and comprehensive characterization of their content is a priority for vaccine discovery against schistosomiasis and other helminthiases.

Altogther, this thesis has provided a comprehensive characterisation of the proteomic composition of two populations of *S. mansoni*-secreted EVs. It has also demonstrated that *S. mansoni* EVs have a role in host-parasite communication by influencing expression of genes in pathways are essential for parasitism. Finally, I have demonstrated (in one trial at least) the vaccine efficacy of *S. mansoni* EVs and identified the antigen targets of anti-EV mouse sera using an immunomics approach. Lastly, although our knowledge on the roles of EVs in the context of diseases caused by schistosomes is still inadequate, my experiments presented in this body of work have generated compelling

information, and important findings of value in advancing schistosome EV research. In addition, my work may have broader implications in understanding the biology of other multicellular parasites. Fundamental understanding of aspects of schistosome cell biology is key in order to advance our knowledge of the strategies by which the parasite's survive for many years and do not generally succumb to protective immune reponses. Finally, the past decade has seen much progress in understanding the basic biology of helminth-derived EVs, but further investigations are required to fully characterize the functional capabilities of these vesicles. A growing body of evidence indicates that helminth-derived EVs as novel carriers of immunomodulatory molecules, exceptionally well-suited to manipulate the unfavourable environments encountered by parasites within their hosts. To this end, targeting pathways in the biogenesis and uptake of helminth EVs will provide key insights into strategies for the control of helminth infections. In addition, comprehensive knowledge of helminth EVs on the infective process is needed to understand physiological and pathological functions and may pave the way for utilizing EVs in therapeutic and vaccination approaches. Also, from a diagnostic point of view, EVs released by helminths may offer opportunities for developing new diagnostic tests that can detect early and low intensity helminth infections. Finally, new perspectives in the area should enhance the interrogation by focusing on the roles of EVs and on their translation from the bench to the bedside.

## 6.2. Future directions

In Chapter 2 I presented a comprehensive proteomic analysis on *S. mansoni* ELVs and MVs. This work provides a molecular snapshot of *S. mansoni* EVs, and lays the foundation for further studies on vesicular protein-protein interaction networks involved in vesicle cargo sorting, biogenesis and uptake by target cells (Choi et al., 2012, Choi et al., 2013). Deciphering the molecular mechanisms underpinning packaging and targeted delivery of EV cargo will be required to utilize EVs as key

mediators of intracellular signaling entities via the delivery of effector molecules. While this study identified unique proteins in both *S. mansoni* ELVs and MVs, confirmation of the specificity of these markers to each vesicle population, by western blotting or immunogold electron microscopy, will be an important focus of future studies. In the future, schistosome EV proteome data could be combined with other approaches used in systems biology to shed light on the roles of helminth EVs.

In Chapter 3 I demonstrated the uptake of *S. mansoni* EVs by host cells, their impact on gene expression using biologically relevant cell lines that schistosomes encounter *in vivo*, and antibody mediated interruption of their uptake by target cells. It would be of interest to further explore the specific impact of S*. mansoni* EV uptake by host immune cells, particularly antigen-presenting cells (e.g. macrophages and dendritic cells). In addition to investigation of helminth EV cell targeting and routes of uptake, future research into the routes of intracellular trafficking in target cells is required to optimally utilize these EVs for therapeutic purposes. Further work is now required to characterise multiple pathways downstream of the process of parasite EV internalisation, as well as the individual EV proteins and miRNAs involved and their cellular receptors. This will allow a more strategic and rational approach to future vaccine or anthelmintic development programs. Moreover, it would be interesting to direct future research to address silencing of some of the genes involved in host-schistosome communication using RNA interference (RNAi) or gene knockout techniques such as clustered regularly interspaced short palindromic repeats (CRISPR) (Waaijers et al., 2013). While the importance of *Sm*-TSP-2 in impacting tegument development, maturation and stability has been demonstrated using RNAi (Tran et al., 2010), determining the specific role of TSP-2 knock-out or knock-down in terms of its impact on EVs needs further investigation. Given that antibodies against *Sm*-TSPs successfully blocked EV internalisation by host cells (Chapter 3), it is tempting to speculate that human sera from a *Sm*-TSP-2 vaccine trial will have the ability to block EV uptake, and as

protection conferred in resistant subjects could be, at least in part, due to interception of EV internalisation by host cells.

*S. mansoni* MVs showed modest protection against schistosomiasis when administered as a vaccine in a single trial (Chapter 4). *S. mansoni* ELVs could also be assessed for vaccine efficacy but insufficient quantities were available herein. Indeed, there is a growing body of evidence that helminth-derived ELVs are efficacious as vaccines in animal models (Trelis et al., 2016, Coakley et al., 2017, Shears et al., 2018, Chaiyadet et al., 2019), and offers an exciting new therapeutic strategy. Further, I have demonstrated that probing a *S. mansoni* protein microarray with antibodies from *S. mansoni* EV-immunised mice (Chapter 4) identified potential vaccine antigens. Future research identifying ways to improve efficacy of MVs and ELVs as vaccines are warranted; this might involve testing higher doses (if not limited by availability), different routes of administration and different adjuvants.

In this thesis, recombinant *Sm*-TSP-2 when administered as a vaccine was shown to provide modest protection in a mouse model of schistosomiasis (Chapter 5). Moreover, I have demonstrated that TSPs are located on the surface of the parasite by probing adult worm sections with anti-*Sm*-TSP IgG antibodies. Moreover, future work towards assessing multivalent vaccines against schistosomiasis is warranted. Much of our current understanding of immune mechanisms in play in schistosomiasis are from studies conducted on mice, but over-reliance on the use of mice as an experimental animal model for human schistosomiasis vaccine discovery and development is undesirable, and can results in certain antigens being prematurely advanced into human clinical trials. Future work on schistosome EVs will likely lead to a new cohort of protective vaccine and diagnostic antigens for schistosomiasis. While the field is still very much in its infancy, new and exciting data is constantly being published, and this evolving field will surely prove to be a fruitful avenue of academic endeavour.

# References

ABATH, F., XAVIER, E., ALLEN, R., GOMES, Y., LUCENA-SILVA, N., BALIZA, M. & SIMPSON, A. 2000. Characterization of Sm13, a tegumental antigen of *Schistosoma mansoni*. *Parasitol Res,* 86**,** 745-752.

AGNEW, A. M., MURARE, H. M. & DOENHOFF, M. J. 1989. Specific cross-protection between *Schistosoma bovis* and *S. haematobium* induced by highly irradiated infections in mice. *Parasite Immunol,* 11**,** 341-349.

AHMAD, G., ZHANG, W., TORBEN, W., AHROROV, A., DAMIAN, R. T., WOLF, R. F., WHITE, G. L., CAREY, D. W., MWINZI, P. N., GANLEY-LEAL, L., KENNEDY, R. C. & SIDDIQUI, A. A. 2011. Preclinical prophylactic efficacy testing of Sm-p80-based vaccine in a nonhuman primate model of *Schistosoma mansoni* infection and immunoglobulin G and E responses to Sm-p80 in human serum samples from an area where schistosomiasis is endemic. *J Infect Dis,* 204**,** 1437-49.

AHMAD, G., ZHANG, W., TORBEN, W., DAMIAN, R. T., WOLF, R. F., WHITE, G. L., CHAVEZ-SUAREZ, M., KENNEDY, R. C. & SIDDIQUI, A. A. 2009a. Protective and antifecundity effects of Sm-p80-based DNA vaccine formulation against *Schistosoma mansoni* in a nonhuman primate model. *Vaccine,* 27**,** 2830-7.

AHMAD, G., ZHANG, W., TORBEN, W., HASKINS, C., DIGGS, S., NOOR, Z., LE, L. & SIDDIQUI, A. A. 2009b. Prime-boost and recombinant protein vaccination strategies using Sm-p80 protects against *Schistosoma mansoni* infection in the mouse model to levels previously attainable only by the irradiated cercarial vaccine. *Parasitol Res,* 105**,** 1767-77.

AHN, S. Y., PARK, W. S., KIM, Y. E., SUNG, D. K., SUNG, S. I., AHN, J. Y. & CHANG, Y. S. 2018. Vascular endothelial growth factor mediates the therapeutic efficacy of mesenchymal stem cell-derived extracellular vesicles against neonatal hyperoxic lung injury. *Exp Mol Med,* 50**,** 26.

AL-NEDAWI, K., MEEHAN, B., MICALLEF, J., LHOTAK, V., MAY, L., GUHA, A. & RAK, J. 2008. Intercellular transfer of the oncogenic receptor EGFRvIII by microvesicles derived from tumour cells. *Nat Cell Biol,* 10**,** 619-24.

ALCAYAGA-MIRANDA, F., VARAS-GODOY, M. & KHOURY, M. 2016. Harnessing the angiogenic potential of stem cell-derived exosomes for vascular regeneration. *Stem Cells Int,* 2016**,** 3409169.

ALVAREZ-ERVITI, L., SEOW, Y., YIN, H., BETTS, C., LAKHAL, S. & WOOD, M. J. 2011. Delivery of siRNA to the mouse brain by systemic injection of targeted exosomes. *Nat Biotechnol,* 29**,** 341-5.

ALVES, C. C., ARAUJO, N., CASSALI, G. D. & FONSECA, C. T. 2016. Parasitological, pathological, and immunological parameters associated with *Schistosoma mansoni* infection and reinfection in BALB/c and C57BL/6 mice. *J Parasitol,* 102**,** 336-341.

ANCAROLA, M. E., MARCILLA, A., HERZ, M., MACCHIAROLI, N., PEREZ, M., ASURMENDI, S., BREHM, K., PONCINI, C., ROSENZVIT, M. & CUCHER, M. 2017. Cestode parasites release extracellular vesicles with microRNAs and immunodiagnostic protein cargo. *Int J Parasitol,* 47**,** 675-686.

ANDERS, S., PYL, P. T. & HUBER, W. 2015. HTSeq--a Python framework to work with high-throughput sequencing data. *Bioinformatics (Oxford, England),* 31**,** 166-169.

ANDERSON, S., SHIRES, V. L., WILSON, R. A. & MOUNTFORD, A. P. 1998. In the absence of IL-12, the induction of Th1-mediated protective immunity by the attenuated schistosome vaccine is impaired, revealing an alternative pathway with Th2-type characteristics. *Eur J Immunol,* 28**,** 2827-38.

ANDRESEN, K., SIMONSEN, P. E., ANDERSEN, B. J. & BIRCH-ANDERSEN, A. 1989. *Echinostoma caproni* in mice: shedding of antigens from the surface of an intestinal trematode. *Int J Parasitol,* 19**,** 111-8.

ANDREU, Z. & YANEZ-MO, M. 2014. Tetraspanins in extracellular vesicle formation and function. *Front Immunol,* 5**,** 442.

ASAI, H., IKEZU, S., TSUNODA, S., MEDALLA, M., LUEBKE, J., HAYDAR, T., WOLOZIN, B., BUTOVSKY, O., KUGLER, S. & IKEZU, T. 2015. Depletion of microglia and inhibition of exosome synthesis halt tau propagation. *Nat Neurosci,* 18**,** 1584-93.

BAIETTI, M. F., ZHANG, Z., MORTIER, E., MELCHIOR, A., DEGEEST, G., GEERAERTS, A., IVARSSON, Y., DEPOORTERE, F., COOMANS, C., VERMEIREN, E., ZIMMERMANN, P. & DAVID, G. 2012. Syndecan-syntenin-ALIX regulates the biogenesis of exosomes. *Nat Cell Biol,* 14**,** 677-85.

BANDU, R., OH, J. W. & KIM, K. P. 2019. Mass spectrometry-based proteome profiling of extracellular vesicles and their roles in cancer biology. *Exp Mol Med,* 51**,** 1-10.

BANERJEE, S., XIE, N., CUI, H., TAN, Z., YANG, S., ICYUZ, M., ABRAHAM, E. & LIU, G. 2013. MicroRNA let-7c regulates macrophage polarization. *J Immunol,* 190**,** 6542-9.

BARAS, B., BENOIT, M.-A., DUPRÉ, L., POULAIN-GODEFROY, O., SCHACHT, A.-M., CAPRON, A., GILLARD, J. & RIVEAU, G. 1999. Single-dose mucosal immunization with biodegradable microparticles containing a *Schistosoma mansoni* antigen. *Infect Immun,* 67**,** 2643-2648.

BARTENEVA, N. S., MALTSEV, N. & VOROBJEV, I. A. 2013. Microvesicles and intercellular communication in the context of parasitism. *Front Cell Infect Microbiol,* 3**,** 49.

BASCH, P. F. 1981. Establishment of cultures from cercariae and development until pairing. *J. Parasitol. ,* 67**,** 179–185.

BATAGOV, A. O., KUZNETSOV, V. A. & KUROCHKIN, I. V. 2011. Identification of nucleotide patterns enriched in secreted RNAs as putative cis-acting elements targeting them to exosome nano-vesicles. *BMC Genomics,* 12 Suppl 3**,** S18.

BEAUVILLAIN, C., JUSTE, M. O., DION, S., PIERRE, J. & DIMIER-POISSON, I. 2009. Exosomes are an effective vaccine against congenital toxoplasmosis in mice. *Vaccine,* 27**,** 1750-7.

BELLINGHAM, S. A., COLEMAN, B. M. & HILL, A. F. 2012. Small RNA deep sequencing reveals a distinct miRNA signature released in exosomes from prion-infected neuronal cells. *Nucleic Acids Res,* 40**,** 10937-49.

BEN-YEDIDIA, T., TARRAB-HAZDAI, R., SCHECHTMAN, D. & ARNON, R. 1999. Intranasal administration of synthetic recombinant peptide-based vaccine protects mice from infection by *Schistosoma mansoni*. *Infect Immun,* 67**,** 4360-4366.

BERGQUIST, N. R. & COLLEY, D. G. 1998. Schistosomiasis Vaccine:Research to Development. *Parasitol Today,* 14**,** 99-104.

BERGQUIST, N. R., LEONARDO, L. R. & MITCHELL, G. F. 2005. Vaccine-linked chemotherapy: can schistosomiasis control benefit from an integrated approach? *Trends Parasitol,* 21**,** 112-7.

BERGQUIST, R., AL-SHERBINY, M., BARAKAT, R. & OLDS, R. 2002. Blueprint for schistosomiasis vaccine development. *Acta Tropica,* 82**,** 183-192.

BERGQUIST, R., UTZINGER, J. & KEISER, J. 2017. Controlling schistosomiasis with praziquantel: How much longer without a viable alternative? *Infect Dis Poverty,* 6**,** 74.

BERGSMEDH, A., SZELES, A., HENRIKSSON, M., BRATT, A., FOLKMAN, M. J., SPETZ, A. L. & HOLMGREN, L. 2001. Horizontal transfer of oncogenes by uptake of apoptotic bodies. *Proc Natl Acad Sci U S A,* 98**,** 6407-11.

BERNAL, D., TRELIS, M., MONTANER, S., CANTALAPIEDRA, F., GALIANO, A., HACKENBERG, M. & MARCILLA, A. 2014. Surface analysis of *Dicrocoelium dendriticum*. The molecular characterization of exosomes reveals the presence of miRNAs. *J Proteomics,* 105**,** 232-41.

BERNIMOULIN, M., WATERS, E. K., FOY, M., STEELE, B. M., SULLIVAN, M., FALET, H., WALSH, M. T., BARTENEVA, N., GENG, J. G., HARTWIG, J. H., MAGUIRE, P. B. & WAGNER, D. D. 2009. Differential stimulation of monocytic cells results in distinct populations of microparticles. *J Thromb Haemost,* 7**,** 1019-28.

BERRIMAN, M., HAAS, B. J., LOVERDE, P. T., WILSON, R. A., DILLON, G. P., CERQUEIRA, G. C., MASHIYAMA, S. T., AL-LAZIKANI, B., ANDRADE, L. F., ASHTON, P. D., ASLETT, M. A., BARTHOLOMEU, D. C., BLANDIN, G., CAFFREY, C. R., COGHLAN, A., COULSON, R., DAY, T. A., DELCHER, A., DEMARCO, R., DJIKENG, A., EYRE, T., GAMBLE, J. A., GHEDIN, E., GU, Y., HERTZ-

FOWLER, C., HIRAI, H., HIRAI, Y., HOUSTON, R., IVENS, A., JOHNSTON, D. A., LACERDA, D., MACEDO, C. D., MCVEIGH, P., NING, Z., OLIVEIRA, G., OVERINGTON, J. P., PARKHILL, J., PERTEA, M., PIERCE, R. J., PROTASIO, A. V., QUAIL, M. A., RAJANDREAM, M. A., ROGERS, J., SAJID, M., SALZBERG, S. L., STANKE, M., TIVEY, A. R., WHITE, O., WILLIAMS, D. L., WORTMAN, J., WU, W., ZAMANIAN, M., ZERLOTINI, A., FRASER-LIGGETT, C. M., BARRELL, B. G. & EL-SAYED, N. M. 2009. The genome of the blood fluke *Schistosoma mansoni*. *Nature,* 460**,** 352-8.

BETTELLI, E., CARRIER, Y., GAO, W., KORN, T., STROM, T. B., OUKKA, M., WEINER, H. L. & KUCHROO, V. K. 2006. Reciprocal developmental pathways for the generation of pathogenic effector TH17 and regulatory T cells. *Nature,* 441**,** 235-238.

BICKLE, Q. D. 2009. Radiation-attenuated schistosome vaccination – a brief historical perspective. *Parasitology,* 136**,** 1621-1632.

BISSIG, C. & GRUENBERG, J. 2014. ALIX and the multivesicular endosome: ALIX in Wonderland. *Trends Cell Biol,* 24**,** 19-25.

BOOTH, A. M., FANG, Y., FALLON, J. K., YANG, J.-M., HILDRETH, J. E. K. & GOULD, S. J. 2006. Exosomes and HIV Gag bud from endosome-like domains of the T cell plasma membrane. *J Cell Biol,* 172**,** 923-935.

BOULANGER, D., REID, G. D., STURROCK, R. F., WOLOWCZUK, I., BALLOUL, J. M., GREZEL, D., PIERCE, R. J., OTIENO, M. F., GUERRET, S., GRIMAUD, J. A. & ET AL. 1991. Immunization of mice and baboons with the recombinant Sm28GST affects both worm viability and fecundity after experimental infection with *Schistosoma mansoni*. *Parasite Immunol,* 13**,** 473-90.

BOURKE, C. D., NAUSCH, N., RUJENI, N., APPLEBY, L. J., TROTTEIN, F., MIDZI, N., MDULUZA, T. & MUTAPI, F. 2014. Cytokine responses to the anti-schistosome vaccine candidate antigen glutathione-S-transferase vary with host age and are boosted by praziquantel treatment. *PLoS Negl Trop Dis,* 8**,** e2846.

BRÄNNSTRÖM, K., SELLIN, M. E., HOLMFELDT, P., BRATTSAND, M. & GULLBERG, M. 2009. The Schistosoma mansoni protein Sm16/SmSLP/SmSPO-1 assembles into a nine-subunit oligomer with potential To inhibit Toll-like receptor signaling. *Infect immun,* 77**,** 1144-1154.

BRASCHI, S. & WILSON, R. A. 2006. Proteins exposed at the adult schistosome surface revealed by biotinylation. *Mol Cell Proteomics,* 5**,** 347-56.

BRINDLEY, P. J. & LOUKAS, A. 2017. Helminth infection–induced malignancy. *PLoS Pathogens,* 13.

BROWN, M. S. & GOLDSTEIN, J. L. 1974. Familial hypercholesterolemia: Defective binding of lipoproteins to cultured fibroblasts associated with impaired regulation of 3-hydroxy-3-methylglutaryl coenzyme a reductase activity. *Proc Natl Acad Sci USA* 71**,** 788-792.

BRUNO, S., GRANGE, C., DEREGIBUS, M. C., CALOGERO, R. A., SAVIOZZI, S., COLLINO, F., MORANDO, L., BUSCA, A., FALDA, M., BUSSOLATI, B., TETTA, C. & CAMUSSI, G. 2009. Mesenchymal stem cell-derived microvesicles protect against acute tubular injury. *J Am Soc Nephrol,* 20**,** 1053-67.

BUBIER, J. A., SPROULE, T. J., FOREMAN, O., SPOLSKI, R., SHAFFER, D. J., MORSE, H. C., LEONARD, W. J. & ROOPENIAN, D. C. 2009. A critical role for IL-21 receptor signaling in the pathogenesis of systemic lupus erythematosus in mice. *P NATL ACAD SCI,* 106**,** 1518-1523.

BUCK, A. H., COAKLEY, G., SIMBARI, F., MCSORLEY, H. J., QUINTANA, J. F., LE BIHAN, T., KUMAR, S., ABREU-GOODGER, C., LEAR, M., HARCUS, Y., CERONI, A., BABAYAN, S. A., BLAXTER, M., IVENS, A. & MAIZELS, R. M. 2014. Exosomes secreted by nematode parasites transfer small RNAs to mammalian cells and modulate innate immunity. *Nat Commun,* 5**,** 5488.

BURKE, M. L., JONES, M. K., GOBERT, G. N., LI, Y. S., ELLIS, M. K. & MCMANUS, D. P. 2009. Immunopathogenesis of human schistosomiasis. *Parasite Immunol,* 31**,** 163-76.

BUSCHOW, S. I., NOLTE-'T HOEN, E. N., VAN NIEL, G., POLS, M. S., TEN BROEKE, T., LAUWEN, M., OSSENDORP, F., MELIEF, C. J., RAPOSO, G., WUBBOLTS, R., WAUBEN, M. H. & STOORVOGEL,

W. 2009. MHC II in dendritic cells is targeted to lysosomes or T cell-induced exosomes via distinct multivesicular body pathways. *Traffic,* 10**,** 1528-42.

BUTTERWORTH, A. E. 1984. Cell-mediated damage to helminths. *Adv Parasitol,* 23**,** 143-235.

BUTTERWORTH, A. E., STURROCK, R. F., HOUBA, V. & REES, P. H. 1974. Antibody-dependent cell-mediated damage to schistosomula *in vitro*. *Nature* 252**,** 503-505.

CAFFREY, C. R., GOUPIL, L., REBELLO, K. M., DALTON, J. P. & SMITH, D. 2018. Cysteine proteases as digestive enzymes in parasitic helminths. *PLoS Negl Trop Dis,* 12**,** e0005840.

CAI, P., GOBERT, G. N., YOU, H. & MCMANUS, D. P. 2016. The Tao survivorship of schistosomes: implications for schistosomiasis control. *Int J Parasitol,* 46**,** 453-63.

CAI, Y.-C., XU, J.-F., STEINMANN, P., CHEN, S.-H., CHU, Y.-H., TIAN, L.-G., CHEN, M.-X., LI, H., LU, Y., ZHANG, L.-L., ZHOU, Y. & CHEN, J.-X. 2014. Field comparison of circulating antibody assays versus circulating antigen assays for the detection of schistosomiasis japonica in endemic areas of China. *Parasite Vector,* 7**,** 138.

CAO, J., LIU, W. J., XU, X. Y. & ZOU, X. P. 2010. Endoscopic findings and clinicopathologic characteristics of colonic schistosomiasis: a report of 46 cases. *World J Gastroenterol,* 16**,** 723-7.

CAPRON, A., CAPRON, M., DOMBROWICZ, D. & RIVEAU, G. 2001. Vaccine strategies against schistosomiasis: from concepts to clinical trials. *Int Arch Allergy Immunol,* 124**,** 9-15.

CAPRON, A., CAPRON, M. & RIVEAU, G. 2002. Vaccine development against schistosomiasis from concepts to clinical trials. *Br Med Bull,* 62**,** 139-148.

CAPRON, A., RIVEAU, G., CAPRON, M. & TROTTEIN, F. 2005. Schistosomes: the road from host-parasite interactions to vaccines in clinical trials. *Trends Parasitol,* 21**,** 143-9.

CARDOSO, F. C., PACIFICO, R. N., MORTARA, R. A. & OLIVEIRA, S. C. 2006. Human antibody responses of patients living in endemic areas for schistosomiasis to the tegumental protein Sm29 identified through genomic studies. *Clin Exp Immunol,* 144**,** 382-91.

CASS, C. L., JOHNSON, J. R., CALIFF, L. L., XU, T., HERNANDEZ, H. J., STADECKER, M. J., YATES, J. R., 3RD & WILLIAMS, D. L. 2007. Proteomic analysis of *Schistosoma mansoni* egg secretions. *Mol Biochem Parasitol,* 155**,** 84-93.

CHADWICK, S., KRIEGEL, C. & AMIJI, M. 2010. Nanotechnology solutions for mucosal immunization. *Adv Drug Deliv Rev,* 62**,** 394-407.

CHAIYADET, S., SMOUT, M., JOHNSON, M., WHITCHURCH, C., TURNBULL, L., KAEWKES, S., SOTILLO, J., LOUKAS, A. & SRIPA, B. 2015a. Excretory/secretory products of the carcinogenic liver fluke are endocytosed by human cholangiocytes and drive cell proliferation and IL6 production. *Int J Parasitol,* 45**,** 773-781.

CHAIYADET, S., SMOUT, M., LAHA, T., SRIPA, B., LOUKAS, A. & SOTILLO, J. 2017. Proteomic characterization of the internalization of *Opisthorchis viverrini* excretory/secretory products in human cells. *Parasitol Int,* 66**,** 494-502.

CHAIYADET, S., SOTILLO, J., KRUEAJAMPA, W., THONGSEN, S., BRINDLEY, P. J., SRIPA, B., LOUKAS, A. & LAHA, T. 2019. Vaccination of hamsters with *Opisthorchis viverrini* extracellular vesicles and vesicle-derived recombinant tetraspanins induces antibodies that block vesicle uptake by cholangiocytes and reduce parasite burden after challenge infection. *PLoS Negl Trop Dis,* 13**,** e0007450.

CHAIYADET, S., SOTILLO, J., SMOUT, M., CANTACESSI, C., JONES, M. K., JOHNSON, M. S., TURNBULL, L., WHITCHURCH, C. B., POTRIQUET, J., LAOHAVIROJ, M., MULVENNA, J., BRINDLEY, P. J., BETHONY, J. M., LAHA, T., SRIPA, B. & LOUKAS, A. 2015b. Carcinogenic liver fluke secretes extracellular vesicles that promote cholangiocytes to adopt a tumorigenic phenotype. *J Infect Dis,* 212**,** 1636-45.

CHEEVER, A. W., LENZI, J. A., LENZI, H. L. & ANDRADE, Z. A. 2002. Experimental models of *Schistosoma mansoni* infection. *Mem Inst Oswaldo Cruz,* 97**,** 917-40.

CHEN, D., LUO, X., XIE, H., GAO, Z., FANG, H. & HUANG, J. 2013a. Characteristics of IL-17 induction by *Schistosoma japonicum* infection in C57BL/6 mouse liver. *Immunology,* 139**,** 523-532.

CHEN, J.-H., ZHANG, T., JU, C., XU, B., LU, Y., MO, X.-J., CHEN, S.-B., FAN, Y.-T., HU, W. & ZHOU, X.-N. 2014. An integrated immunoproteomics and bioinformatics approach for the analysis of *Schistosoma japonicum* tegument proteins. *J Proteom,* 98**,** 289-299.

CHEN, J. J., SHEN, C. M. & KO, Y. W. 2013b. Analytical study of a microfludic DNA amplification chip using water cooling effect. *Biomedical Microdevices,* 15**,** 261-278.

CHENG, G., LUO, R., HU, C., CAO, J. & JIN, Y. 2013. Deep sequencing-based identification of pathogen-specific microRNAs in the plasma of rabbits infected with *Schistosoma japonicum*. *Parasitology,* 140**,** 1751-61.

CHO, Y.-E., MEZEY, E., HARDWICK, J. P., SALEM JR., N., CLEMENS, D. L. & SONG, B.-J. 2017. Increased ethanol-inducible cytochrome P450-2E1 and cytochrome P450 isoforms in exosomes of alcohol-exposed rodents and patients with alcoholism through oxidative and endoplasmic reticulum stress. *Hepatol Commun,* 1**,** 675-690.

CHOI, D. S., KIM, D. K., KIM, Y. K. & GHO, Y. S. 2013. Proteomics, transcriptomics and lipidomics of exosomes and ectosomes. *Proteomics,* 13**,** 1554-71.

CHOI, D. S., YANG, J. S., CHOI, E. J., JANG, S. C., PARK, S., KIM, O. Y., HWANG, D., KIM, K. P., KIM, Y. K., KIM, S. & GHO, Y. S. 2012. The protein interaction network of extracellular vesicles derived from human colorectal cancer cells. *J Proteome Res,* 11**,** 1144-51.

CHRISTIANSON, H. C., SVENSSON, K. J., VAN KUPPEVELT, T. H., LI, J.-P. & BELTING, M. 2013. Cancer cell exosomes depend on cell-surface heparan sulfate proteoglycans for their internalization and functional activity. *Proc Natl Acad Sci USA* 110**,** 17380-17385.

CIOLI, D., VALLE, C., ANGELUCCI, F. & MIELE, A. E. 2008. Will new antischistosomal drugs finally emerge? *Trends Parasitol,* 24**,** 379-82.

CNOPS, L., TANNICH, E., POLMAN, K., CLERINX, J. & VAN ESBROECK, M. 2012. Schistosoma real-time PCR as diagnostic tool for international travellers and migrants. *Trop Med Int Health,* 17**,** 1208-16.

COAKLEY, G., BUCK, A. H. & MAIZELS, R. M. 2016. Host parasite communications-Messages from helminths for the immune system: Parasite communication and cell-cell interactions. *Mol Biochem Parasitol,* 208**,** 33-40.

COAKLEY, G., MAIZELS, R. M. & BUCK, A. H. 2015. Exosomes and Other Extracellular Vesicles: The New Communicators in Parasite Infections. *Trends Parasitol,* 31**,** 477-89.

COAKLEY, G., MCCASKILL, J. L., BORGER, J. G., SIMBARI, F., ROBERTSON, E., MILLAR, M., HARCUS, Y., MCSORLEY, H. J., MAIZELS, R. M. & BUCK, A. H. 2017. Extracellular vesicles from a helminth parasite suppress macrophage activation and constitute an effective vaccine for protective immunity. *Cell Rep,* 19**,** 1545-1557.

COLLEY, D. G., BUSTINDUY, A. L., SECOR, W. E. & KING, C. H. 2014. Human schistosomiasis. *Lancet,* 383**,** 2253-2264.

COLLEY, D. G., GARCIA, A. A., LAMBERTUCCI, J. R., PARRA, J. C., KATZ, N., ROCHA, R. S. & GAZZINELLI, G. 1986. Immune responses during human schistosomiasis. XII. Differential responsiveness in patients with hepatosplenic disease. *Am J Trop Med Hyg,* 35**,** 793-802.

COLLEY, D. G. & SECOR, W. E. 2014. Immunology of human schistosomiasis. *Parasite Immunol,* 36**,** 347-357.

COLLINS, J. J., 3RD, KING, R. S., COGSWELL, A., WILLIAMS, D. L. & NEWMARK, P. A. 2011. An atlas for *Schistosoma mansoni* organs and life-cycle stages using cell type-specific markers and confocal microscopy. *PLoS Negl Trop Dis,* 5**,** e1009.

COLLINS, J. J., 3RD, WENDT, G. R., IYER, H. & NEWMARK, P. A. 2016. Stem cell progeny contribute to the schistosome host-parasite interface. *Elife,* 5**,** e12473.

COLLINS, J. J., WANG, B., LAMBRUS, B. G., THARP, M. E., IYER, H. & NEWMARK, P. A. 2013. Adult somatic stem cells in the human parasite *Schistosoma mansoni*. *Nature,* 494**,** 476-479.

COLOMBO, M., RAPOSO, G. & THERY, C. 2014. Biogenesis, secretion, and intercellular interactions of exosomes and other extracellular vesicles. *Annu Rev Cell Dev Biol,* 30**,** 255-89.

COLONNA, M., PULENDRAN, B. & IWASAKI, A. 2006. Dendritic cells at the host-pathogen interface. *Nat Immunol,* 7**,** 117-120.

CONESA, A., GOTZ, S., GARCIA-GOMEZ, J. M., TEROL, J., TALON, M. & ROBLES, M. 2005. Blast2GO: a universal tool for annotation, visualization and analysis in functional genomics research. *Bioinformatics,* 21**,** 3674-6.

CONIGLIO, S. J., ZAVARELLA, S. & SYMONS, M. H. 2008. Pak1 and Pak2 mediate tumor cell invasion through distinct signaling mechanisms. *Mol Cell Biol,* 28**,** 4162-72.

COSENZA, S., RUIZ, M., TOUPET, K., JORGENSEN, C. & NOEL, D. 2017. Mesenchymal stem cells derived exosomes and microparticles protect cartilage and bone from degradation in osteoarthritis. *Sci Rep,* 7**,** 16214.

COSENZA, S., TOUPET, K., MAUMUS, M., LUZ-CRAWFORD, P., BLANC-BRUDE, O., JORGENSEN, C. & NOEL, D. 2018. Mesenchymal stem cells-derived exosomes are more immunosuppressive than microparticles in inflammatory arthritis. *Theranostics,* 8**,** 1399-1410.

COSTAIN, A. H., MACDONALD, A. S. & SMITS, H. H. 2018. Schistosome egg migration: mechanisms, pathogenesis and host immune responses. *Front Immunol,* 9.

COULSON, P. S. & WILSON, R. A. 1997. Recruitment of lymphocytes to the lung through vaccination enhances the immunity of mice exposed to irradiated schistosomes. *Infect Immun,* 65**,** 42-48.

CRESCITELLI, R., LASSER, C., SZABO, T. G., KITTEL, A., ELDH, M., DIANZANI, I., BUZAS, E. I. & LOTVALL, J. 2013. Distinct RNA profiles in subpopulations of extracellular vesicles: apoptotic bodies, microvesicles and exosomes. *J Extracell Vesicles,* 2**,** 20677.

CURTI, E., KWITYN, C., ZHAN, B., GILLESPIE, P., BRELSFORD, J., DEUMIC, V., PLIESKATT, J., REZENDE, W. C., TSAO, E., KALAMPANAYIL, B., HOTEZ, P. J. & BOTTAZZI, M. E. 2013. Expression at a 20L scale and purification of the extracellular domain of the *Schistosoma mansoni* TSP-2 recombinant protein: a vaccine candidate for human intestinal schistosomiasis. *Hum Vaccin Immunother,* 9**,** 2342-50.

CURWEN, R. S., ASHTON, P. D., JOHNSTON, D. A. & WILSON, R. A. 2004. The *Schistosoma mansoni* soluble proteome: a comparison across four life-cycle stages. *Mol Biochem Parasitol,* 138**,** 57-66.

CURWEN, R. S., ASHTON, P. D., SUNDARALINGAM, S. & WILSON, R. A. 2006. Identification of novel proteases and immunomodulators in the secretions of schistosome cercariae that facilitate host entry. *Mol Cell Proteomics,* 5**,** 835-44.

CWIKLINSKI, K., DE LA TORRE-ESCUDERO, E., TRELIS, M., BERNAL, D., DUFRESNE, P. J., BRENNAN, G. P., O'NEILL, S., TORT, J., PATERSON, S., MARCILLA, A., DALTON, J. P. & ROBINSON, M. P. 2015. The extracellular vesicles of the helminth pathogen, *Fasciola hepatica*: biogenesis pathways and cargo molecules involved in parasite pathogenesis. *Mol Cell Proteomics,* 14**,** 3258-3273.

D'ACQUISTO, F., PERRETTI, M. & FLOWER, R. J. 2008. Annexin-A1: a pivotal regulator of the innate and adaptive immune systems. *Br J Pharmacol,* 155**,** 152-69.

DA'DARA, A. A., LI, Y. S., XIONG, T., ZHOU, J., WILLIAMS, G. M., MCMANUS, D. P., FENG, Z., YU, X. L., GRAY, D. J. & HARN, D. A. 2008. DNA-based vaccines protect against zoonotic schistosomiasis in water buffalo. *Vaccine,* 26**,** 3617-25.

DA'DARA, A. A., SKELLY, P. J., WANG, M. & HARN, D. A. 2001. Immunization with plasmid DNA encoding the integral membrane protein, Sm23, elicits a protective immune response against schistosome infection in mice. *Vaccine,* 20**,** 359-369.

DALTON, J. P., ROBINSON, M. W., MULCAHY, G., O'NEILL, S. M. & DONNELLY, S. 2013. Immunomodulatory molecules of *Fasciola hepatica*: candidates for both vaccine and immunotherapeutic development. *Vet Parasitol,* 195**,** 272-85.

DANG, Z., YAGI, K., OKU, Y., KOUGUCHI, H., KAJINO, K., MATSUMOTO, J., NAKAO, R., WAKAGURI, H., TOYODA, A., YIN, H. & SUGIMOTO, C. 2012. A pilot study on developing mucosal vaccine against alveolar echinococcosis (AE) using recombinant tetraspanin 3: Vaccine efficacy and immunology. *PLoS Negl Trop Dis,* 6**,** e1570.

DE ASSIS, R. R., LUDOLF, F., NAKAJIMA, R., JASINSKAS, A., OLIVEIRA, G. C., FELGNER, P. L., GAZE, S. T., LOUKAS, A., LOVERDE, P. T., BETHONY, J. M., CORREA-OLIVEIRA, R. & CALZAVARA-SILVA, C. E. 2016. A next-generation proteome array for *Schistosoma mansoni*. *Int J Parasitol,* 46**,** 411-415.

DE LA TORRE-ESCUDERO, E., BENNETT, A. P., CLARKE, A., BRENNAN, G. P. & ROBINSON, M. W. 2016. Extracellular vesicle biogenesis in helminths: More than one route to the surface? *Trends Parasitol,* 32**,** 921-929.

DE LA TORRE-ESCUDERO, E., GERLACH, J. Q., BENNETT, A. P. S., CWIKLINSKI, K., JEWHURST, H. L., HUSON, K. M., JOSHI, L., KILCOYNE, M., O'NEILL, S., DALTON, J. P. & ROBINSON, M. W. 2019. Surface molecules of extracellular vesicles secreted by the helminth pathogen *Fasciola hepatica* direct their internalisation by host cells. *PLoS Negl Trop Dis,* 13**,** e0007087.

DE LA TORRE-ESCUDERO, E., MANZANO-ROMAN, R., SILES, M., PÉREZ-SÁNCHEZ, R., MOYANO, J., MELLADO, I. & OLEAGA, A. 2011. Molecular and functional characterization of a *Schistosoma bovis* annexin: Fibrinolytic and anticoagulant activity. *Vet Parasitol,* 184**,** 25-36.

DEAN, D. A., MANGOLD, B. L., HARRISON, R. A. & RICCIARDONE, M. D. 1996. Homologous and heterologous protective immunity to Egyptian strains of *Schistosoma mansoni* and S. haematobium induced by ultraviolet-irradiated cercariae. *Parasite Immunol,* 18**,** 403-10.

DEL CACHO, E., GALLEGO, M., LEE, S. H., LILLEHOJ, H. S., QUILEZ, J., LILLEHOJ, E. P. & SANCHEZ-ACEDO, C. 2012. Induction of protective immunity against *Eimeria tenella*, *Eimeria maxima*, and *Eimeria acervulina* infections using dendritic cell-derived exosomes. *Infect Immun,* 80**,** 1909-16.

DENG, M., XIAO, H., ZHANG, H., PENG, H., YUAN, H., XU, Y., ZHANG, G. & HU, Z. 2017. Mesenchymal stem cell-derived extracellular vesicles ameliorates hippocampal synaptic impairment after transient global ischemia. *Front Cell Neurosci,* 11**,** 205.

DEOLINDO, P., EVANS-OSSES, I. & RAMIREZ, M. I. 2013. Microvesicles and exosomes as vehicles between protozoan and host cell communication. *Biochem Soc Trans,* 41**,** 252-7.

DOBIN, A., DAVIS, C. A., SCHLESINGER, F., DRENKOW, J., ZALESKI, C., JHA, S., BATUT, P., CHAISSON, M. & GINGERAS, T. R. 2013. STAR: ultrafast universal RNA-seq aligner. *Bioinformatics,* 29**,** 15-21.

DOEHRING-SCHWERDTFEGER, E., ABDEL-RAHIM, I. M., MOHAMED-ALI, Q., ELSHEIKH, M., SCHLAKE, J., KARDORFF, R., FRANKE, D., KAISER, C. & EHRICH, J. H. 1990. Ultrasonographical investigation of periportal fibrosis in children with *Schistosoma mansoni* infection: evaluation of morbidity. *Am J Trop Med Hyg,* 42**,** 581-6.

DOENHOFF, M. J., CHIODINI, P. L. & HAMILTON, J. V. 2004. Specific and sensitive diagnosis of schistosome infection: can it be done with antibodies? *Trends Parasitol,* 20**,** 35-9.

DOENHOFF, M. J. & PICA-MATTOCCIA, L. 2006. Praziquantel for the treatment of schistosomiasis: its use for control in areas with endemic disease and prospects for drug resistance. *Expert Rev Anti Infect Ther,* 4**,** 199-210.

DON, T. A., BETHONY, J. M. & LOUKAS, A. 2008. Saposin-like proteins are expressed in the gastrodermis of *Schistosoma mansoni* and are immunogenic in natural infections. *International Journal of Infectious Diseases,* 12**,** e39-e47.

DRIGUEZ, P., LI, Y., GAZE, S., PEARSON, M. S., NAKAJIMA, R., TRIEU, A., DOOLAN, D. L., FELGNER, P. L., HOU, X., CARDOSO, F. C., JASINSKAS, A., GOBERT, G. N., LOUKAS, A. & MCMANUS, D. P. 2015. Antibody signatures reflect different disease pathologies in patients with schistosomiasis due to *Schistosoma japonicum*. *J Infect Dis,* 213**,** 122-130.

DRIGUEZ, P., MCMANUS, D. P. & GOBERT, G. N. 2016a. Clinical implications of recent findings in schistosome proteomics. *Expert Rev Proteomics,* 13**,** 19-33.

DRIGUEZ, P., MCWILLIAM, H. E., GAZE, S., PIEDRAFITA, D., PEARSON, M. S., NAKAJIMA, R., DUKE, M., TRIEU, A., DOOLAN, D. L., CARDOSO, F. C., JASINSKAS, A., GOBERT, G. N., FELGNER, P. L., LOUKAS, A., MEEUSEN, E. & MCMANUS, D. P. 2016b. Specific humoral response of hosts with variable schistosomiasis susceptibility. *Immunol Cell Biol,* 94**,** 52-65.

DUNNE, D. W., JONES, F. M. & DOENHOFF, M. J. 1991. The purification, characterization, serological activity and hepatotoxic properties of two cationic glycoproteins (alpha 1 and omega 1) from Schistosoma mansoni eggs. *Parasitology,* 103 Pt 2**,** 225-36.

EBERL, M., LANGERMANS, J. A. M., FROST, P. A., VERVENNE, R. A., VAN DAM, G. J., DEELDER, A. M., THOMAS, A. W., COULSON, P. S. & WILSON, R. A. 2001. Cellular and humoral immune responses and protection against Schistosomes induced by a radiation-attenuated vaccine in chimpanzees. *Infect Immun,* 69**,** 5352-5362.

EGER, A., KIRCH, A., MANFRAS, B., KERN, P., SCHULZ-KEY, H. & SOBOSLAY, P. T. 2003. Pro-inflammatory (IL-1beta, IL-18) cytokines and IL-8 chemokine release by PBMC in response to *Echinococcus multilocularis* metacestode vesicles. *Parasite Immunol,* 25**,** 103-5.

EGESA, M., HOFFMANN, K. F., HOKKE, C. H., YAZDANBAKHSH, M. & COSE, S. 2017. Rethinking schistosomiasis vaccine development: synthetic vesicles. *Trends Parasitol,* 33**,** 918-921.

EICHENBERGER, R. M., RYAN, S., JONES, L., BUITRAGO, G., POLSTER, R., MONTES DE OCA, M., ZUVELEK, J., GIACOMIN, P. R., DENT, L. A., ENGWERDA, C. R., FIELD, M. A., SOTILLO, J. &

LOUKAS, A. 2018a. Hookworm secreted extracellular vesicles interact with host cells and prevent inducible colitis in mice. *Front Immunol,* 9.

EICHENBERGER, R. M., SOTILLO, J. & LOUKAS, A. 2018b. Immunobiology of parasitic worm extracellular vesicles. *Immunol Cell Biol,* 96**,** 704-713.

EICHENBERGER, R. M., TALUKDER, M. H., FIELD, M. A., WANGCHUK, P., GIACOMIN, P., LOUKAS, A. & SOTILLO, J. 2018c. Characterization of *Trichuris muris* secreted proteins and extracellular vesicles provides new insights into host-parasite communication. *J Extracell Vesicles,* 7**,** 1428004.

EIRIN, A., ZHU, X. Y., PURANIK, A. S., TANG, H., MCGURREN, K. A., VAN WIJNEN, A. J., LERMAN, A. & LERMAN, L. O. 2017. Mesenchymal stem cell-derived extracellular vesicles attenuate kidney inflammation. *Kidney Int,* 92**,** 114-124.

EL-SHABASY, E. A., REDA, E. S., ABDEEN, S. H., SAID, A. E. & OUHTIT, A. 2015. Transmission electron microscopic observations on ultrastructural alterations in *Schistosoma mansoni* adult worms recovered from C57BL/6 mice treated with radiation-attenuated vaccine and/or praziquantel in addition to passive immunization with normal and vaccinated rabbit sera against infection. *Parasitol Res,* 114**,** 1563-80.

EL RIDI, R., OTHMAN, A. A. & MCMANUS, D. P. 2015. Editorial: The schistosomiasis vaccine - It is time to stand up. *Front Immunol,* 6**,** 390.

EL RIDI, R. & TALLIMA, H. 2009. *Schistosoma mansoni* ex vivo lung-stage larvae excretory-secretory antigens as vaccine candidates against schistosomiasis. *Vaccine,* 27**,** 666-73.

EL RIDI, R. A. F. & TALLIMA, H. A. M. 2013. Novel therapeutic and prevention approaches for schistosomiasis: Review. *J Adv Res,* 4**,** 467-78.

ELDH, M., LOTVALL, J., MALMHALL, C. & EKSTROM, K. 2012. Importance of RNA isolation methods for analysis of exosomal RNA: evaluation of different methods. *Mol Immunol,* 50**,** 278-86.

EMANUELSSON, O., BRUNAK, S., VON HEIJNE, G. & NIELSEN, H. 2007. Locating proteins in the cell using TargetP, SignalP and related tools. *Nat Protoc,* 2**,** 953-71.

ESCOLA, J. M., KLEIJMEER, M. J., STOORVOGEL, W., GRIFFITH, J. M., YOSHIE, O. & GEUZE, H. J. 1998. Selective enrichment of tetraspan proteins on the internal vesicles of multivesicular endosomes and on exosomes secreted by human B-lymphocytes. *J Biol Chem,* 273**,** 20121-7.

FAIRFAX, K., NASCIMENTO, M., HUANG, S. C.-C., EVERTS, B. & PEARCE, E. J. 2012. Th2 responses in schistosomiasis. *Sem Immunopathol,* 34**,** 863-871.

FANG, Y., WU, N., GAN, X., YAN, W., MORRELL, J. C. & GOULD, S. J. 2007. Higher-order oligomerization targets plasma membrane proteins and HIV gag to exosomes. *PLoS biology,* 5**,** e158.

FARKAS, A. E., CAPALDO, C. T. & NUSRAT, A. 2012. Regulation of epithelial proliferation by tight junction proteins. *Ann N Y Acad Sci,* 1258**,** 115-24.

FATIMA, F., EKSTROM, K., NAZARENKO, I., MAUGERI, M., VALADI, H., HILL, A. F., CAMUSSI, G. & NAWAZ, M. 2017. Non-coding RNAs in mesenchymal stem cell-derived extracellular vesicles: Deciphering regulatory roles in stem cell potency, inflammatory resolve, and tissue regeneration. *Frontiers in Genetics,* 8.

FENG, D., ZHAO, W. L., YE, Y. Y., BAI, X. C., LIU, R. Q., CHANG, L. F., ZHOU, Q. & SUI, S. F. 2010. Cellular internalization of exosomes occurs through phagocytosis. *Traffic,* 11**,** 675-87.

FIFIS, T., GAMVRELLIS, A., CRIMEEN-IRWIN, B., PIETERSZ, G. A., LI, J., MOTTRAM, P. L., MCKENZIE, I. F. & PLEBANSKI, M. 2004. Size-dependent immunogenicity: therapeutic and protective properties of nano-vaccines against tumors. *J Immunol,* 173**,** 3148-54.

FIGUEIREDO, B. C., DA'DARA, A. A., OLIVEIRA, S. C. & SKELLY, P. J. 2015. Schistosomes enhance plasminogen activation: The role of tegumental enolase. *PLoS Pathog,* 11**,** e1005335.

FONSECA, C. T., BRITO, C. F. A., ALVES, J. B. & OLIVEIRA, S. C. 2004. IL-12 enhances protective immunity in mice engendered by immunization with recombinant 14 kDa *Schistosoma mansoni* fatty acid-binding protein through an IFN-γ and TNF-α dependent pathway. *Vaccine,* 22**,** 503-510.

FONSECA, C. T., OLIVEIRA, S. C. & ALVES, C. C. 2015. Eliminating schistosomes through vaccination: What are the best immune weapons? *Front Immunol,* 6**,** 95.

FRANCESCHINI, A., SZKLARCZYK, D., FRANKILD, S., KUHN, M., SIMONOVIC, M., ROTH, A., LIN, J., MINGUEZ, P., BORK, P., VON MERING, C. & JENSEN, L. J. 2013. STRING v9.1: protein-protein interaction networks, with increased coverage and integration. *Nucleic Acids Res,* 41**,** D808-D815.

FRANKLAND-SEARBY, S. & BHAUMIK, S. R. 2012. The 26S proteasome complex: an attractive target for cancer therapy. *Biochim Biophys Acta,* 1825**,** 64-76.

FROMM, B., OVCHINNIKOV, V., HØYE, E., BERNAL, D., HACKENBERG, M. & MARCILLA, A. 2017. On the presence and immunoregulatory functions of extracellular microRNAs in the trematode *Fasciola hepatica*. *Parasite Immunol,* 39**,** e12399.

FROMM, B., TRELIS, M., HACKENBERG, M., CANTALAPIEDRA, F., BERNAL, D. & MARCILLA, A. 2015. The revised microRNA complement of *Fasciola hepatica* reveals a plethora of overlooked microRNAs and evidence for enrichment of immuno-regulatory microRNAs in extracellular vesicles. *Int J Parasitol,* 45**,** 697-702.

FURUTA, T., MIYAKI, S., ISHITOBI, H., OGURA, T., KATO, Y., KAMEI, N., MIYADO, K., HIGASHI, Y. & OCHI, M. 2016. Mesenchymal stem cell-derived exosomes promote fracture healing in a mouse model. *Stem Cells Transl Med,* 5**,** 1620-1630.

GAZE, S., DRIGUEZ, P., PEARSON, M. S., MENDES, T., DOOLAN, D. L., TRIEU, A., MCMANUS, D. P., GOBERT, G. N., PERIAGO, M. V., CORREA OLIVEIRA, R., CARDOSO, F. C., OLIVEIRA, G., NAKAJIMA, R., JASINSKAS, A., HUNG, C., LIANG, L., PABLO, J., BETHONY, J. M., FELGNER, P. L.

& LOUKAS, A. 2014. An immunomics approach to schistosome antigen discovery: antibody signatures of naturally resistant and chronically infected individuals from endemic areas. *PLoS Pathog,* 10**,** e1004033.

GAZE, S., MCSORLEY, H. J., DAVESON, J., JONES, D., BETHONY, J. M., OLIVEIRA, L. M., SPEARE, R., MCCARTHY, J. S., ENGWERDA, C. R., CROESE, J. & LOUKAS, A. 2012. Characterising the mucosal and systemic immune responses to experimental human hookworm infection. *PLoS Pathog,* 8**,** e1002520.

GBD 2016 DALYS AND HALE COLLABORATORS 2017. Global, regional, and national disability-adjusted life-years (DALYs) for 333 diseases and injuries and healthy life expectancy (HALE) for 195 countries and territories, 1990-2016: a systematic analysis for the Global Burden of Disease Study 2016. *Lancet,* 390**,** 1260-1344.

GOUVEIA, M. J., BRINDLEY, P., RINALDI, G., GÄRTNER, F., CORREIA DA COSTA, J. M. & VALE, N. 2019. Combination anthelmintic/antioxidant activity against *Schistosoma mansoni*. *Biomolecules,* 9**,** 54.

GREGORIADIS, G. 1994. Liposomes as immunoadjuvants and vaccine carriers: Antigen entrapment. *ImmunoMethods,* 4**,** 210-216.

GRENFELL, R. F. Q., TABOADA, D., COUTINHO, L. A., PEDROSA, M. L. C., ASSIS, J. V., OLIVEIRA, M. S. P., CRUZ, R. R., ALMEIDA, A., SILVA-MORAES, V., KATZ, N. & COELHO, P. M. Z. 2018. Innovative methodology for point-of-care circulating cathodic antigen with rapid urine concentration for use in the field for detecting low *Schistosoma mansoni* infection and for control of cure with high accuracy. *Trans R Soc Trop Med Hyg,* 112**,** 1-7.

GRIMES, J. E. T., CROLL, D., HARRISON, W. E., UTZINGER, J., FREEMAN, M. C. & TEMPLETON, M. R. 2015. The roles of water, sanitation and hygiene in reducing schistosomiasis: a review. *Parasite Vector,* 8**,** 156.

GRYSEELS, B. 1992. Morbidity due to infection with *Schistosoma mansoni*: an update. *Trop Geogr Med,* 44**,** 189-200.

GRYSEELS, B., MBAYE, A., DE VLAS, S. J., STELMA, F. F., GUISSE, F., VAN LIESHOUT, L., FAYE, D., DIOP, M., LY, A., TCHUEM-TCHUENTE, L. A., ENGELS, D. & POLMAN, K. 2001. Are poor responses to praziquantel for the treatment of *Schistosoma mansoni* infections in Senegal due to resistance? An overview of the evidence. *Trop Med Int Health,* 6**,** 864-873.

GRYSEELS, B., POLMAN, K., CLERINX, J. & KESTENS, L. 2006. Human schistosomiasis. *Lancet,* 368**,** 1106-1118.

GU, H. Y., MARKS, N. D., WINTER, A. D., WEIR, W., TZELOS, T., MCNEILLY, T. N., BRITTON, C. & DEVANEY, E. 2017. Conservation of a microRNA cluster in parasitic nematodes and profiling of miRNAs in excretory-secretory products and microvesicles of *Haemonchus contortus*. *PLoS Negl Trop Dis,* 11**,** e0006056.

GUAY, C. & REGAZZI, R. 2017. Exosomes as new players in metabolic organ cross-talk. *Diabetes Obes Metab,* 19 Suppl 1**,** 137-146.

GUY, B. 2007. The perfect mix: recent progress in adjuvant research. *Nat Rev Microbiol,* 5**,** 505-17.

HAGA, H., YAN, I. K., TAKAHASHI, K., MATSUDA, A. & PATEL, T. 2017. Extracellular vesicles from bone marrow-derived mesenchymal stem cells improve survival from lethal hepatic failure in mice. *Stem Cells Transl Med,* 6**,** 1262-1272.

HAN, Y., ZHANG, M., HONG, Y., ZHU, Z., LI, D., LI, X., FU, Z. & LIN, J. 2012. Characterization of thioredoxin glutathione reductase in *Schiotosoma japonicum*. *Parasitol Int,* 61**,** 475-480.

HAN, Z.-G., BRINDLEY, P. J., WANG, S.-Y. & CHEN, Z. 2009. Schistosoma genomics: new perspectives on schistosome biology and host-parasite interaction. *Ann Rev Genomics Hum Genet,* 10**,** 211-240.

HANSELL, E., BRASCHI, S., MEDZIHRADSZKY, K. F., SAJID, M., DEBNATH, M., INGRAM, J., LIM, K. C. & MCKERROW, J. H. 2008. Proteomic analysis of skin invasion by blood fluke larvae. *PLoS Negl Trop Dis,* 2**,** e262-e262.

HANSEN, E. P., FROMM, B., ANDERSEN, S. D., MARCILLA, A., ANDERSEN, K. L., BORUP, A., WILLIAMS, A. R., JEX, A. R., GASSER, R. B., YOUNG, N. D., HALL, R. S., STENSBALLE, A., OVCHINNIKOV, V., YAN, Y., FREDHOLM, M., THAMSBORG, S. M. & NEJSUM, P. 2019. Exploration of extracellular vesicles from *Ascaris suum* provides evidence of parasite-host cross talk. *J Extracell Vesicles,* 8**,** 1578116.

HANSEN, E. P., KRINGEL, H., WILLIAMS, A. R. & NEJSUM, P. 2015. Secretion of RNA-containing extracellular vesicles by the porcine whipworm, *Trichuris suis*. *J Parasitol,* 101**,** 336-40.

HARGETT, L. A. & BAUER, N. N. 2013. On the origin of microparticles: From "platelet dust" to mediators of intercellular communication. *Pulm Circ,* 3**,** 329-40.

HARISCHANDRA, H., YUAN, W., LOGHRY, H. J., ZAMANIAN, M. & KIMBER, M. J. 2018. Profiling extracellular vesicle release by the filarial nematode Brugia malayi reveals sex-specific differences in cargo and a sensitivity to ivermectin. *PLoS Negl Trop Dis,* 12**,** e0006438.

HARN, D. A., M, M. & JR, D. 1984. *Schistosoma mansoni*. Anti-egg monoclonal antibodies protect against cercarial challenge in vivo. *J Exp Med,* 159**,** 1371-1387.

HARRISON, R. A., BICKLE, Q. D., KIARE, S., JAMES, E. R., ANDREWS, B. J., STURROCK, R. F., TAYLOR, M. G. & WEBBE, G. 1990. Immunization of baboons with attenuated schistosomula of *Schistosoma haematobium*: levels of protection induced by immunization with larvae irradiated with 20 and 60 krad. *Trans R Soc Trop Med Hyg,* 84**,** 89-99.

HEIJNEN, H. F., DEBILI, N., VAINCHENCKER, W., BRETON-GORIUS, J., GEUZE, H. J. & SIXMA, J. J. 1998. Multivesicular bodies are an intermediate stage in the formation of platelet alpha-granules. *Blood,* 91**,** 2313-25.

HEMLER, M. E. 2003. Tetraspanin proteins mediate cellular penetration, invasion, and fusion events and define a novel type of membrane microdomain. *Annu Rev Cell Dev Biol,* 19**,** 397-422.

HESSVIK, N. P. & LLORENTE, A. 2018. Current knowledge on exosome biogenesis and release. *Cell Mol Life Sci,* 75**,** 193-208.

HEWITSON, J. P., GRAINGER, J. R. & MAIZELS, R. M. 2009. Helminth immunoregulation: The role of parasite secreted proteins in modulating host immunity. *Mol Biochem Parasitol,* 167**,** 1-11.

HEWITSON, J. P., HAMBLIN, P. A. & MOUNTFORD, A. P. 2005. Immunity induced by the radiation-attenuated schistosome vaccine. *Parasite Immunol,* 27**,** 271-80.

HIRANO, T. 1998. Interleukin 6 and its receptor: ten years later. *Int Rev Immunol,* 16**,** 249-84.

HOFFMANN, K. F. & STRAND, M. 1996. Molecular identification of a *Schistosoma mansoni* tegumental protein with similarity to cytoplasmic dynein light chains. *J Biol Chem,* 271**,** 26117-26123.

HOSHINO, A., COSTA-SILVA, B., SHEN, T.-L., RODRIGUES, G., HASHIMOTO, A., TESIC MARK, M., MOLINA, H., KOHSAKA, S., DI GIANNATALE, A., CEDER, S., SINGH, S., WILLIAMS, C., SOPLOP, N., URYU, K., PHARMER, L., KING, T., BOJMAR, L., DAVIES, A. E., ARARSO, Y., ZHANG, T., ZHANG, H., HERNANDEZ, J., WEISS, J. M., DUMONT-COLE, V. D., KRAMER, K., WEXLER, L. H., NARENDRAN, A., SCHWARTZ, G. K., HEALEY, J. H., SANDSTROM, P., JØRGEN LABORI, K., KURE, E. H., GRANDGENETT, P. M., HOLLINGSWORTH, M. A., DE SOUSA, M., KAUR, S., JAIN, M., MALLYA, K., BATRA, S. K., JARNAGIN, W. R., BRADY, M. S., FODSTAD, O., MULLER, V., PANTEL, K., MINN, A. J., BISSELL, M. J., GARCIA, B. A., KANG, Y., RAJASEKHAR, V. K., GHAJAR, C. M., MATEI, I., PEINADO, H., BROMBERG, J. & LYDEN, D. 2015. Tumour exosome integrins determine organotropic metastasis. *Nature,* 527**,** 329.

HOTEZ, P. J., BETHONY, J. M., DIEMERT, D. J., PEARSON, M. & LOUKAS, A. 2010. Developing vaccines to combat hookworm infection and intestinal schistosomiasis. *Nat Rev Microbiol,* 8**,** 814-26.

HOTEZ, P. J., BOTTAZZI, M. E., BETHONY, J. & DIEMERT, D. D. 2019. Advancing the development of a human schistosomiasis vaccine. *Trends Parasitol,* 35**,** 104-108.

HSU, C., MOROHASHI, Y., YOSHIMURA, S., MANRIQUE-HOYOS, N., JUNG, S., LAUTERBACH, M. A., BAKHTI, M., GRONBORG, M., MOBIUS, W., RHEE, J., BARR, F. A. & SIMONS, M. 2010. Regulation of exosome secretion by Rab35 and its GTPase-activating proteins TBC1D10A-C. *J Cell Biol,* 189**,** 223-32.

HUBNER, M. P., MANFRAS, B. J., MARGOS, M. C., EIFFLER, D., HOFFMANN, W. H., SCHULZ-KEY, H., KERN, P. & SOBOSLAY, P. T. 2006. *Echinococcus multilocularis* metacestodes modulate cellular cytokine and chemokine release by peripheral blood mononuclear cells in alveolar echinococcosis patients. *Clin Exp Immunol,* 145**,** 243-51.

HUTVAGNER, G. & SIMARD, M. J. 2008. Argonaute proteins: key players in RNA silencing. *Nat Rev Mol Cell Biol,* 9**,** 22-32.

HYENNE, V., LABOUESSE, M. & GOETZ, J. G. 2018. The Small GTPase Ral orchestrates MVB biogenesis and exosome secretion. *Small GTPases,* 9**,** 445-451.

JANKOVIC, D., ASLUND, L., OSWALD, I. P., CASPAR, P., CHAMPION, C., PEARCE, E., COLIGAN, J. E., STRAND, M., SHER, A. & JAMES, S. L. 1996. Calpain is the target antigen of a Th1 clone that transfers protective immunity against *Schistosoma mansoni*. *J Immunol,* 157**,** 806-814.

JENKINS, S. J. & MOUNTFORD, A. P. 2005. Dendritic cells activated with products released by schistosome larvae drive Th2-type immune responses, which can be inhibited by manipulation of CD40 costimulation. *Infect immun,* 73**,** 395-402.

JEPPESEN, D. K., FENIX, A. M., FRANKLIN, J. L., HIGGINBOTHAM, J. N., ZHANG, Q., ZIMMERMAN, L. J., LIEBLER, D. C., PING, J., LIU, Q., EVANS, R., FISSELL, W. H., PATTON, J. G., ROME, L. H., BURNETTE, D. T. & COFFEY, R. J. 2019. Reassessment of exosome composition. *Cell,* 177**,** 428-445.e18.

JOSEPH, S. K. & RAMASWAMY, K. 2013. Single multivalent vaccination boosted by trickle larval infection confers protection against experimental lymphatic filariasis. *Vaccine,* 31**,** 3320-6.

KALINDA, C., CHIMBARI, M. & MUKARATIRWA, S. 2017. Implications of changing temperatures on the growth, fecundity and survival of intermediate host snails of schistosomiasis: A systematic review. *Int J Environ Res Public Health,* 14.

KALRA, H., DRUMMEN, G. P. & MATHIVANAN, S. 2016. Focus on extracellular vesicles: Introducing the next small big thing. *Int J Mol Sci,* 17**,** 170.

KALRA, H., SIMPSON, R. J., JI, H., AIKAWA, E., ALTEVOGT, P., ASKENASE, P., BOND, V. C., BORRAS, F. E., BREAKEFIELD, X., BUDNIK, V., BUZAS, E., CAMUSSI, G., CLAYTON, A., COCUCCI, E., FALCON-PEREZ, J. M., GABRIELSSON, S., GHO, Y. S., GUPTA, D., HARSHA, H. C., HENDRIX, A., HILL, A. F., INAL, J. M., JENSTER, G., KRAMER-ALBERS, E. M., LIM, S. K., LLORENTE, A., LOTVALL, J., MARCILLA, A., MINCHEVA-NILSSON, L., NAZARENKO, I., NIEUWLAND, R., NOLTE-'T HOEN, E. N., PANDEY, A., PATEL, T., PIPER, M. G., PLUCHINO, S., PRASAD, T. S., RAJENDRAN, L., RAPOSO, G., RECORD, M., REID, G. E., SANCHEZ-MADRID, F., SCHIFFELERS, R. M., SILJANDER, P., STENSBALLE, A., STOORVOGEL, W., TAYLOR, D., THERY, C., VALADI, H., VAN BALKOM, B. W., VAZQUEZ, J., VIDAL, M., WAUBEN, M. H., YANEZ-MO, M., ZOELLER, M. & MATHIVANAN, S. 2012. Vesiclepedia: a compendium for extracellular vesicles with continuous community annotation. *PLoS Biol,* 10**,** e1001450.

KARIUKI, T. M., FARAH, I. O., YOLE, D. S., MWENDA, J. M., VAN DAM, G. J., DEELDER, A. M., WILSON, R. A. & COULSON, P. S. 2004. Parameters of the attenuated schistosome vaccine evaluated in the olive baboon. *Infect Immun,* 72**,** 5526-9.

KARMAKAR, S., ZHANG, W., AHMAD, G., TORBEN, W., ALAM, M. U., LE, L., DAMIAN, R. T., WOLF, R. F., WHITE, G. L., CAREY, D. W., CARTER, D., REED, S. G. & SIDDIQUI, A. A. 2014a. Cross-species protection: *Schistosoma mansoni* Sm-p80 vaccine confers protection against *Schistosoma haematobium* in hamsters and baboons. *Vaccine,* 32**,** 1296-303.

KARMAKAR, S., ZHANG, W., AHMAD, G., TORBEN, W., ALAM, M. U., LE, L., DAMIAN, R. T., WOLF, R. F., WHITE, G. L., CAREY, D. W., CARTER, D., REED, S. G. & SIDDIQUI, A. A. 2014b. Use of an Sm-p80-based therapeutic vaccine to kill established adult schistosome parasites in chronically infected baboons. *J Infect Dis,* 209**,** 1929-1940.

KARMAKAR, S., ZHANG, W., AHMAD, G., TORBEN, W., ALAM, M. U., LE, L., DAMIAN, R. T., WOLF, R. F., WHITE, G. L., CAREY, D. W., CARTER, D., REED, S. G. & SIDDIQUI, A. A. 2014c. Use of an Sm-p80-based therapeutic vaccine to kill established adult schistosome parasites in chronically infected baboons. *J Infect Dis,* 209**,** 1929-40.

KEERTHIKUMAR, S., CHISANGA, D., ARIYARATNE, D., AL SAFFAR, H., ANAND, S., ZHAO, K., SAMUEL, M., PATHAN, M., JOIS, M., CHILAMKURTI, N., GANGODA, L. & MATHIVANAN, S. 2016. ExoCarta: A web-based compendium of exosomal cargo. *J Mol Biol,* 428**,** 688-692.

KEERTHIKUMAR, S., GANGODA, L., LIEM, M., FONSEKA, P., ATUKORALA, I., OZCITTI, C., MECHLER, A., ADDA, C. G., ANG, C. S. & MATHIVANAN, S. 2015. Proteogenomic analysis reveals exosomes are more oncogenic than ectosomes. *Oncotarget,* 6**,** 15375-96.

KHATRI, M., RICHARDSON, L. A. & MEULIA, T. 2018. Mesenchymal stem cell-derived extracellular vesicles attenuate influenza virus-induced acute lung injury in a pig model. *Stem Cell Res Ther,* 9**,** 17.

KIFLE, D. W., PEARSON, M. S., BECKER, L., PICKERING, D., LOUKAS, A. & SOTILLO, J. 2020. Proteomic analysis of two populations of *Schistosoma mansoni*-derived extracellular vesicles: 15k pellet and 120k pellet vesicles. *Mol Biochem Parasitol,* 236**,** 111264.

KIFLE, D. W., SOTILLO, J., PEARSON, M. S. & LOUKAS, A. 2017. Extracellular vesicles as a target for the development of anti-helminth vaccines. *Emerg Topics Life Sci,* 1**,** 659-665.

KIM, D. K., NISHIDA, H., AN, S. Y., SHETTY, A. K., BARTOSH, T. J. & PROCKOP, D. J. 2016. Chromatographically isolated CD63+CD81+ extracellular vesicles from mesenchymal stromal cells rescue cognitive impairments after TBI. *Proc Natl Acad Sci U S A,* 113**,** 170-5.

KING, C. H. 2015. It's time to dispel the myth of "asymptomatic" schistosomiasis. *PLoS Negl Trop Dis,* 9**,** e0003504.

KNUDSEN, G. M., MEDZIHRADSZKY, K. F., LIM, K.-C., HANSELL, E. & MCKERROW, J. H. 2005. Proteomic analysis of *Schistosoma mansoni* cercarial secretions. *Mol Cell Proteomics,* 4**,** 1862-1875.

KOWAL, J., ARRAS, G., COLOMBO, M., JOUVE, M., MORATH, J. P., PRIMDAL-BENGTSON, B., DINGLI, F., LOEW, D., TKACH, M. & THERY, C. 2016. Proteomic comparison defines novel markers to characterize heterogeneous populations of extracellular vesicle subtypes. *Proc Natl Acad Sci U S A,* 113**,** E968-77.

KOWAL, J., TKACH, M. & THERY, C. 2014. Biogenesis and secretion of exosomes. *Curr Opin Cell Biol,* 29**,** 116-25.

KRAUTZ-PETERSON, G., DEBATIS, M., TREMBLAY, J. M., OLIVEIRA, S. C., DA'DARA, A. A., SKELLY, P. J. & SHOEMAKER, C. B. 2017. *Schistosoma mansoni* infection of mice, rats and humans elicits a strong antibody response to a limited number of reduction-sensitive epitopes on five major tegumental membrane proteins. *PLoS Negl Trop Dis,* 11**,** e0005306.

KROGH, A., LARSSON, B., VON HEIJNE, G. & SONNHAMMER, E. L. 2001. Predicting transmembrane protein topology with a hidden Markov model: application to complete genomes. *J Mol Biol,* 305**,** 567-80.

KUNTZ, A. N., DAVIOUD-CHARVET, E., SAYED, A. A., CALIFF, L. L., DESSOLIN, J., ARNÉR, E. S. J. & WILLIAMS, D. L. 2007. Thioredoxin glutathione reductase from *Schistosoma mansoni*: an essential parasite enzyme and a key drug target. *PLoS Med,* 4**,** e206-e206.

LACHENAL, G., PERNET-GALLAY, K., CHIVET, M., HEMMING, F. J., BELLY, A., BODON, G., BLOT, B., HAASE, G., GOLDBERG, Y. & SADOUL, R. 2011. Release of exosomes from differentiated neurons and its regulation by synaptic glutamatergic activity. *Mol Cell Neurosci,* 46**,** 409-18.

LAEMMLI, U. K. 1970. Cleavage of structural proteins during the assembly of the head of bacteriophage T4. *Nature,* 227**,** 680-5.

LAI, R. C., ARSLAN, F., LEE, M. M., SZE, N. S., CHOO, A., CHEN, T. S., SALTO-TELLEZ, M., TIMMERS, L., LEE, C. N., EL OAKLEY, R. M., PASTERKAMP, G., DE KLEIJN, D. P. & LIM, S. K. 2010. Exosome secreted by MSC reduces myocardial ischemia/reperfusion injury. *Stem Cell Res,* 4**,** 214-22.

LAI, R. C., YEO, R. W., TAN, K. H. & LIM, S. K. 2013. Exosomes for drug delivery - a novel application for the mesenchymal stem cell. *Biotechnol Adv,* 31**,** 543-51.

LAMBERTUCCI, J. R., SERUFO, J. C., GERSPACHER-LARA, R., RAYES, A. A., TEIXEIRA, R., NOBRE, V. & ANTUNES, C. M. 2000. *Schistosoma mansoni*: assessment of morbidity before and after control. *Acta Trop,* 77**,** 101-9.

LAMBERTZ, U., OVIEDO OVANDO, M. E., VASCONCELOS, E. J., UNRAU, P. J., MYLER, P. J. & REINER, N. E. 2015. Small RNAs derived from tRNAs and rRNAs are highly enriched in exosomes from both old and new world Leishmania providing evidence for conserved exosomal RNA Packaging. *BMC Genomics,* 16**,** 151.

LARKIN, B. M., SMITH, P. M., PONICHTERA, H. E., SHAINHEIT, M. G., RUTITZKY, L. I. & STADECKER, M. J. 2012. Induction and regulation of pathogenic Th17 cell responses in schistosomiasis. *Semin Immunopathol,* 34**,** 873-888.

LATIFKAR, A., HUR, Y. H., SANCHEZ, J. C., CERIONE, R. A. & ANTONYAK, M. A. 2019. New insights into extracellular vesicle biogenesis and function. *J Cell Sci,* 132**,** jcs222406.

LAWSON, J. R. & WILSON, R. A. 1980. The survival of the cercariae of *Schistosoma mansoni* in relation to water temperature and glycogen utilization. *Parasitology,* 81**,** 337-48.

LE, L., ALAM, M. U., ZHANG, W., KARMAKAR, S., SIDDIQUI, A. A., AHMAD, G., TORBEN, W., DAMIAN, R. T., CAREY, D. W., WHITE, G. L., WOLF, R. F., REED, S. G. & CARTER, D. 2014. Use of an Sm-p80–based therapeutic vaccine to kill established dault schistosome parasites in chronically infected baboons. *J. Infect. Dis.,* 209**,** 1929-1940.

LEBENS, M., SUN, J.-B., SADEGHI, H., BÄCKSTRÖM, M., OLSSON, I., MIELCAREK, N., LI, B.-L., CAPRON, A., CZERKINSKY, C. & HOLMGREN, J. 2003. A mucosally administered recombinant fusion protein vaccine against schistosomiasis protecting against immunopathology and infection. *Vaccine,* 21**,** 514-520.

LEE, C., MITSIALIS, S. A., ASLAM, M., VITALI, S. H., VERGADI, E., KONSTANTINOU, G., SDRIMAS, K., FERNANDEZ-GONZALEZ, A. & KOUREMBANAS, S. 2012. Exosomes mediate the cytoprotective action of mesenchymal stromal cells on hypoxia-induced pulmonary hypertension. *Circulation,* 126**,** 2601-11.

LENASSI, M., CAGNEY, G., LIAO, M., VAUPOTIČ, T., BARTHOLOMEEUSEN, K., CHENG, Y., KROGAN, N. J., PLEMENITAŠ, A. & PETERLIN, B. M. 2010. HIV Nef is secreted in exosomes and triggers apoptosis in bystander CD4+ T cells. *Traffic,* 11**,** 110-122.

LEOW, C. Y., WILLIS, C., LEOW, C. H., HOFMANN, A. & JONES, M. 2019. Molecular characterization of *Schistosoma mansoni* tegument annexins and comparative analysis of antibody responses following parasite infection. *Mol Biochem Parasit,* 234**,** 111231.

LEWIS, F. A., STIREWALT, M. A., SOUZA, C. P. & GAZZINELLI, G. 1986. Large-scale laboratory maintenance of *Schistosoma mansoni*, with observations on three schistosome/snail host combinations. *J Parasitol,* 72**,** 813-29.

LEWIS, F. A. & WILSON, E. M. 1981. Strain differences in lymphocyte responses and in vitro suppressor cell induction between *Schistosoma mansoni*-infected C57BL/6 and CBA mice. *Infect Immun,* 32**,** 260-267.

LI, C. J., LIU, Y., CHEN, Y., YU, D., WILLIAMS, K. J. & LIU, M. L. 2013a. Novel proteolytic microvesicles released from human macrophages after exposure to tobacco smoke. *Am J Pathol,* 182**,** 1552-62.

LI, T., YAN, Y., WANG, B., QIAN, H., ZHANG, X., SHEN, L., WANG, M., ZHOU, Y., ZHU, W., LI, W. & XU, W. 2013b. Exosomes derived from human umbilical cord mesenchymal stem cells alleviate liver fibrosis. *Stem Cells Dev,* 22**,** 845-54.

LI, X. H., XU, Y. X., VANCE, G., WANG, Y., LV, L. B., VAN DAM, G. J., CAO, J. P. & WILSON, R. A. 2015. Evidence that rhesus macaques self-cure from a *Schistosoma japonicum* infection by disrupting worm esophageal function: A new route to an effective vaccine? *PLoS Negl Trop Dis,* 9**,** e0003925.

LIU, F., CUI, S. J., HU, W., FENG, Z., WANG, Z. Q. & HAN, Z. G. 2009. Excretory/secretory proteome of the adult developmental stage of human blood fluke, *Schistosoma japonicum*. *Mol Cell Proteomics,* 8**,** 1236-51.

LIU, L., JIN, X., HU, C. F., LI, R., ZHOU, Z. & SHEN, C. X. 2017. Exosomes derived from mesenchymal stem cells rescue myocardial ischaemia/reperfusion injury by inducing cardiomyocyte autophagy via AMPK and Akt pathways. *Cell Physiol Biochem,* 43**,** 52-68.

LOTVALL, J., HILL, A. F., HOCHBERG, F., BUZAS, E. I., DI VIZIO, D., GARDINER, C., GHO, Y. S., KUROCHKIN, I. V., MATHIVANAN, S., QUESENBERRY, P., SAHOO, S., TAHARA, H., WAUBEN, M. H., WITWER, K. W. & THERY, C. 2014. Minimal experimental requirements for definition of extracellular vesicles and their functions: a position statement from the International Society for Extracellular Vesicles. *J Extracell Vesicles,* 3**,** 26913.

LOUKAS, A., GAZE, S., MULVENNA, J. P., GASSER, R. B., BRINDLEY, P. J., DOOLAN, D. L., BETHONY, J. M., JONES, M. K., GOBERT, G. N., DRIGUEZ, P., MCMANUS, D. P. & HOTEZ, P. J. 2011. Vaccinomics for the major blood feeding helminths of humans. *Omics,* 15**,** 567-77.

LOUKAS, A., TRAN, M. & PEARSON, M. S. 2007. Schistosome membrane proteins as vaccines. *Int J Parasitol,* 37**,** 257-63.

LOVE, M. I., HUBER, W. & ANDERS, S. 2014. Moderated estimation of fold change and dispersion for RNA-seq data with DESeq2. *Genome Biol,* 15**,** 550.

LYDIC, T. A., TOWNSEND, S., ADDA, C. G., COLLINS, C., MATHIVANAN, S. & REID, G. E. 2015. Rapid and comprehensive 'shotgun' lipidome profiling of colorectal cancer cell derived exosomes. *Methods,* 87**,** 83-95.

MACALANDA, A. M. C., ANGELES, J. M. M., MOENDEG, K. J., DANG, A. T., HIGUCHI, L., INOUE, N., XUAN, X., KIRINOKI, M., CHIGUSA, Y., LEONARDO, L. R., VILLACORTE, E. A., RIVERA, P. T., GOTO, Y. & KAWAZU, S. I. 2018. Evaluation of *Schistosoma japonicum* thioredoxin peroxidase-1 as a potential circulating antigen target for the diagnosis of Asian schistosomiasis. *J Vet Med Sci,* 80**,** 156-163.

MADUREIRA, P. A., SURETTE, A. P., PHIPPS, K. D., TABOSKI, M. A. S., MILLER, V. A. & WAISMAN, D. M. 2011. The role of the annexin A2 heterotetramer in vascular fibrinolysis. *Blood,* 118**,** 4789-4797.

MAIZELS, R. M., HEWITSON, J. P., MURRAY, J., HARCUS, Y. M., DAYER, B., FILBEY, K. J., GRAINGER, J. R., MCSORLEY, H. J., REYNOLDS, L. A. & SMITH, K. A. 2012. Immune modulation and modulators in *Heligmosomoides polygyrus* infection. *Exp Parasitol,* 132**,** 76-89.

MARCILLA, A., MARTIN-JAULAR, L., TRELIS, M., DE MENEZES-NETO, A., OSUNA, A., BERNAL, D., FERNANDEZ-BECERRA, C., ALMEIDA, I. C. & DEL PORTILLO, H. A. 2014. Extracellular vesicles in parasitic diseases. *J Extracell Vesicles,* 3**,** 25040.

MARCILLA, A., TRELIS, M., CORTES, A., SOTILLO, J., CANTALAPIEDRA, F., MINGUEZ, M. T., VALERO, M. L., SANCHEZ DEL PINO, M. M., MUNOZ-ANTOLI, C., TOLEDO, R. & BERNAL, D. 2012. Extracellular vesicles from parasitic helminths contain specific excretory/secretory proteins and are internalized in intestinal host cells. *PLoS One,* 7**,** e45974.

MARTIN-JAULAR, L., NAKAYASU, E. S., FERRER, M., ALMEIDA, I. C. & DEL PORTILLO, H. A. 2011. Exosomes from *Plasmodium yoelii*-infected reticulocytes protect mice from lethal infections. *PLoS One,* 6**,** e26588.

MARTINEZ-IBEAS, A. M., PERTEGUER, M. J., GONZALEZ-LANZA, C., GARATE, T. & MANGA-GONZALEZ, M. Y. 2013. Analysis of an expressed sequence tag library from *Dicrocoelium dentriticum*. *Exp Parasitol,* 135**,** 287-96.

MASTIN, A. J., BICKLE, Q. D. & WILSON, R. A. 2009. *Schistosoma mansoni*: migration and attrition of irradiated and challenge schistosomula in the mouse. *Parasitology,* 87**,** 87-102.

MATHIESON, W., CASTRO-BORGES, W. & WILSON, R. A. 2011. The proteasome-ubiquitin pathway in the *Schistosoma mansoni* egg has development- and morphology-specific characteristics. *Mol Biochem Parasitol,* 175**,** 118-25.

MATHIESON, W. & WILSON, R. A. 2010. A comparative proteomic study of the undeveloped and developed *Schistosoma mansoni* egg and its contents: the miracidium, hatch fluid and secretions. *Int J Parasitol,* 40**,** 617-28.

MATHIEU, M., MARTIN-JAULAR, L., LAVIEU, G. & THÉRY, C. 2019. Specificities of secretion and uptake of exosomes and other extracellular vesicles for cell-to-cell communication. *Nat Cell Biol,* 21**,** 9-17.

MATHIVANAN, S., JI, H. & SIMPSON, R. J. 2010. Exosomes: extracellular organelles important in intercellular communication. *J Proteomics,* 73**,** 1907-20.

MATI, V. L. & MELO, A. L. 2013. Current applications of oogram methodology in experimental schistosomiasis; fecundity of female *Schistosoma mansoni* and egg release in the intestine of AKR/J mice following immunomodulatory treatment with pentoxifylline. *J Helminthol,* 87**,** 115-24.

MAYER, D. A. & FRIED, B. 2007. The role of helminth infections in carcinogenesis. *Adv Parasitol,* 65**,** 239-96.

MCCARTHY, D. J., CHEN, Y. & SMYTH, G. K. 2012. Differential expression analysis of multifactor RNA-Seq experiments with respect to biological variation. *Nucleic Acids Res,* 40**,** 4288-4297.

MCKENZIE, A. J., HOSHINO, D., HONG, N. H., CHA, D. J., FRANKLIN, J. L., COFFEY, R. J., PATTON, J. G. & WEAVER, A. M. 2016. KRAS-MEK Signaling Controls Ago2 Sorting into Exosomes. *Cell Reports,* 15**,** 978-987.

MCKERROW, J. H., CAFFREY, C., KELLY, B., LOKE, P. & SAJID, M. 2006. Proteases in parasitic diseases. *Annu Rev Pathol,* 1**,** 497-536.

MCMANUS, D. P., DUNNE, D. W., SACKO, M., UTZINGER, J., VENNERVALD, B. J. & ZHOU, X.-N. 2018. Schistosomiasis. *Nat Rev Dis Primers* 4**,** 13.

MCMANUS, D. P., GRAY, D. J., LI, Y., FENG, Z., WILLIAMS, G. M., STEWART, D., REY-LADINO, J. & ROSS, A. G. 2010. Schistosomiasis in the People's Republic of China: the era of the Three Gorges Dam. *Clin Microbiol Rev,* 23**,** 442-66.

MCMANUS, D. P. & LOUKAS, A. 2008. Current status of vaccines for schistosomiasis. *Clin Microbiol Rev,* 21**,** 225-42.

MEBIUS, M. M., VAN GENDEREN, P. J. J., URBANUS, R. T., TIELENS, A. G. M., DE GROOT, P. G. & VAN HELLEMOND, J. J. 2013. Interference with the host haemostatic system by schistosomes. *PLoS Pathog,* 9**,** e1003781.

MEHLHORN, H., BECKER, B., ANDREWS, P., THOMAS, H. & FRENKEL, J. K. 1981. In vivo and in vitro experiments on the effects of praziquantel on *Schistosoma mansoni*. A light and electron microscopic study. *Arzneimittelforschung,* 31**,** 544-54.

MEI, H. & LOVERDE, P. T. 1997. *Schistosoma mansoni*:The developmental regulation and immunolocalization of antioxidant enzymes. *Exp Parasitol,* 86**,** 69-78.

MELDOLESI, J. 2018. Exosomes and ectosomes in intercellular communication. *Curr Biol,* 28**,** R435-r444.

MENINGHER, T., BARSHESHET, Y., OFIR-BIRIN, Y., GOLD, D., BRANT, B., DEKEL, E., SIDI, Y., SCHWARTZ, E., REGEV-RUDZKI, N., AVNI, O. & AVNI, D. 2020. Schistosomal extracellular vesicle-enclosed miRNAs modulate host T helper cell differentiation. *EMBO Rep,* 21**,** e47882.

MENINGHER, T., LERMAN, G., REGEV-RUDZKI, N., GOLD, D., BEN-DOV, I. Z., SIDI, Y., AVNI, D. & SCHWARTZ, E. 2017. Schistosomal microRNAs isolated from extracellular vesicles in sera of infected patients: A new tool for diagnosis and follow-up of human schistosomiasis. *J Infect Dis,* 215**,** 378-386.

MERRIFIELD, M., HOTEZ, P. J., BEAUMIER, C. M., GILLESPIE, P., STRYCH, U., HAYWARD, T. & BOTTAZZI, M. E. 2016. Advancing a vaccine to prevent human schistosomiasis. *Vaccine,* 34**,** 2988-91.

MEURS, L., BRIENEN, E., MBOW, M., OCHOLA, E. A., MBOUP, S., KARANJA, D. M. S., SECOR, W. E., POLMAN, K. & VAN LIESHOUT, L. 2015. Is PCR the next reference standard for the diagnosis of *Schistosoma* in stool? A comparison with microscopy in Senegal and Kenya. *PLoS Negl Trop Dis,* 9**,** e0003959.

MEZOUAR, S., DARBOUSSET, R., DIGNAT-GEORGE, F., PANICOT-DUBOIS, L. & DUBOIS, C. 2015. Inhibition of platelet activation prevents the P-selectin and integrin-dependent accumulation of cancer cell microparticles and reduces tumor growth and metastasis in vivo. *Int J Cancer,* 136**,** 462-75.

MILAC, T. I., RANDOLPH, T. W. & WANG, P. 2012. Analyzing LC-MS/MS data by spectral count and ion abundance: two case studies. *Stat Interface,* 5**,** 75-87.

MINARD, P., DEAN, D. A., JACOBSON, R. H., VANNIER, W. E. & MURRELL, K. D. 1978. Immunization of Mice with Cobalt-60 Irradiated *Schistosoma Mansoni* Cercariae*. *Am J Trop Med Hyg,* 27**,** 76-86.

MINCIACCHI, V. R., YOU, S., SPINELLI, C., MORLEY, S., ZANDIAN, M., ASPURIA, P. J., CAVALLINI, L., CIARDIELLO, C., REIS SOBREIRO, M., MORELLO, M., KHARMATE, G., JANG, S. C., KIM, D. K., HOSSEINI-BEHESHTI, E., TOMLINSON GUNS, E., GLEAVE, M., GHO, Y. S., MATHIVANAN, S., YANG, W., FREEMAN, M. R. & DI VIZIO, D. 2015. Large oncosomes contain distinct protein

cargo and represent a separate functional class of tumor-derived extracellular vesicles. *Oncotarget,* 6**,** 11327-41.

MITCHELL, K., MUTAPI, F., SAVILL, N. & WOOLHOUSE, M. 2012. Protective immunity to *Schistosoma haematobium* infection is primarily an anti-fecundity response stimulated by the death of adult worms. *Proc Natl Acad Sci USA,* 109**,** 13347-52.

MIYANISHI, M., TADA, K., KOIKE, M., UCHIYAMA, Y., KITAMURA, T. & NAGATA, S. 2007. Identification of Tim4 as a phosphatidylserine receptor. *Nature,* 450**,** 435.

MO, A. X., AGOSTI, J. M., WALSON, J. L., HALL, B. F. & GORDON, L. 2014. Schistosomiasis elimination strategies and potential role of a vaccine in achieving global health goals. *Am J Trop Med Hyg,* 90**,** 54-60.

MOHAMED AR, AL KARAWI M & MI., Y. 1990. Schistosomal colonic disease. *Gut,* 31**,** 439-42.

MOLEHIN, A. J., ROJO, J. U., SIDDIQUI, S. Z., GRAY, S. A., CARTER, D. & SIDDIQUI, A. A. 2016. Development of a schistosomiasis vaccine. *Expert Rev Vaccines,* 15**,** 619-27.

MONTANER, S., GALIANO, A., TRELIS, M., MARTIN-JAULAR, L., DEL PORTILLO, H. A., BERNAL, D. & MARCILLA, A. 2014. The role of extracellular vesicles in modulating the host immune response during parasitic infections. *Front Immunol,* 5**,** 433.

MONTECALVO, A., LARREGINA, A. T., SHUFESKY, W. J., STOLZ, D. B., SULLIVAN, M. L., KARLSSON, J. M., BATY, C. J., GIBSON, G. A., ERDOS, G., WANG, Z., MILOSEVIC, J., TKACHEVA, O. A., DIVITO, S. J., JORDAN, R., LYONS-WEILER, J., WATKINS, S. C. & MORELLI, A. E. 2012. Mechanism of transfer of functional microRNAs between mouse dendritic cells via exosomes. *Blood,* 119**,** 756-66.

MONTECALVO, A., SHUFESKY, W. J., STOLZ, D. B., SULLIVAN, M. G., WANG, Z., DIVITO, S. J., PAPWORTH, G. D., WATKINS, S. C., ROBBINS, P. D., LARREGINA, A. T. & MORELLI, A. E. 2008. Exosomes as a short-range mechanism to spread alloantigen between dendritic cells during T cell allorecognition. *J Immunol,* 180**,** 3081-90.

MORELLI, A. E., LARREGINA, A. T., SHUFESKY, W. J., SULLIVAN, M. L., STOLZ, D. B., PAPWORTH, G. D., ZAHORCHAK, A. F., LOGAR, A. J., WANG, Z., WATKINS, S. C., FALO, L. D., JR. & THOMSON, A. W. 2004. Endocytosis, intracellular sorting, and processing of exosomes by dendritic cells. *Blood,* 104**,** 3257-66.

MOUNTFORD, A. P., ANDERSON, S. & WILSON, R. A. 1996. Induction of Th1 cell-mediated protective immunity to *Schistosoma mansoni* by co-administration of larval antigens and IL-12 as an adjuvant. *J Immunol* 156**,** 4739-4745.

MULCAHY, L. A., PINK, R. C. & CARTER, D. R. F. 2014. Routes and mechanisms of extracellular vesicle uptake. *J Extracell Vesicles* 3**,** 10.3402/jev.v3.24641.

MUTAPI, F., BILLINGSLEY, P. F. & SECOR, W. E. 2013. Infection and treatment immunizations for successful parasite vaccines. *Trends parasitol,* 29**,** 135-141.

MUTAPI, F., WINBORN, G., MIDZI, N., TAYLOR, M., MDULUZA, T. & MAIZELS, R. M. 2007. Cytokine responses to *Schistosoma haematobium* in a Zimbabwean population: contrasting profiles for IFN-gamma, IL-4, IL-5 and IL-10 with age. *BMC Infect Dis,* 7**,** 139-139.

NAUSCH, N., DAWSON, E. M., MIDZI, N., MDULUZA, T., MUTAPI, F. & DOENHOFF, M. J. 2014. Field evaluation of a new antibody-based diagnostic for *Schistosoma haematobium* and *S. mansoni* at the point-of-care in northeast Zimbabwe. *BMC infect dis,* 14**,** 165-165.

NDLOVU, H. & BROMBACHER, F. 2014. Role of IL-4Ralpha during acute schistosomiasis in mice. *Parasite Immunol,* 36**,** 421-7.

NICOLAO, M. C., RODRIGUEZ RODRIGUES, C. & CUMINO, A. C. 2019. Extracellular vesicles from *Echinococcus granulosus* larval stage: Isolation, characterization and uptake by dendritic cells. *PLoS Negl Trop Dis,* 13**,** e0007032.

NOLO, R., MORRISON, C. M., TAO, C., ZHANG, X. & HALDER, G. 2006. The bantam microRNA is a target of the hippo tumor-suppressor pathway. *Curr Biol,* 16**,** 1895-904.

NOLTE-'T HOEN, E. N., BUERMANS, H. P., WAASDORP, M., STOORVOGEL, W., WAUBEN, M. H. & T HOEN, P. A. 2012. Deep sequencing of RNA from immune cell-derived vesicles uncovers the selective incorporation of small non-coding RNA biotypes with potential regulatory functions. *Nucleic Acids Res,* 40**,** 9272-85.

NOWACKI, F. C., SWAIN, M. T., KLYCHNIKOV, O. I., NIAZI, U., IVENS, A., QUINTANA, J. F., HENSBERGEN, P. J., HOKKE, C. H., BUCK, A. H. & HOFFMANN, K. F. 2015. Protein and small non-coding RNA-enriched extracellular vesicles are released by the pathogenic blood fluke *Schistosoma mansoni*. *J Extracell Vesicles,* 4**,** 28665.

OBREGON, C., ROTHEN-RUTISHAUSER, B., GITAHI, S. K., GEHR, P. & NICOD, L. P. 2006. Exovesicles from human activated dendritic cells fuse with resting dendritic cells, allowing them to present alloantigens. *Am J Pathol,* 169**,** 2127-36.

OCHODO, E. A., GOPALAKRISHNA, G., SPEK, B., REITSMA, J. B., VAN LIESHOUT, L., POLMAN, K., LAMBERTON, P., BOSSUYT, P. M. & LEEFLANG, M. M. 2015. Circulating antigen tests and urine reagent strips for diagnosis of active schistosomiasis in endemic areas. *Cochrane Database Syst Rev***,** Cd009579.

OLIVEIRA, R. R., FIGUEIREDO, J. P., CARDOSO, L. S., JABAR, R. L., SOUZA, R. P., WELLS, M. T., CARVALHO, E. M., FITZGERALD, D. W., BARNES, K. C., ARAÚJO, M. I. & GLESBY, M. J. 2012. Factors associated with resistance to *Schistosoma mansoni* infection in an endemic area of Bahia, Brazil. *Am J Trop Med Hyg,* 86**,** 296-305.

OSTROWSKI, M., CARMO, N. B., KRUMEICH, S., FANGET, I., RAPOSO, G., SAVINA, A., MOITA, C. F., SCHAUER, K., HUME, A. N., FREITAS, R. P., GOUD, B., BENAROCH, P., HACOHEN, N., FUKUDA, M., DESNOS, C., SEABRA, M. C., DARCHEN, F., AMIGORENA, S., MOITA, L. F. & THERY, C. 2010. Rab27a and Rab27b control different steps of the exosome secretion pathway. *Nat Cell Biol,* 12**,** 19-30; sup pp 1-13.

PEARCE, E. J. 2002. The immunobiology of schistosomiasis. *Nature Rev Immunol,* 2**,** 499-511.

PEARSON, M. S., BECKER, L., DRIGUEZ, P., YOUNG, N. D., GAZE, S., MENDES, T., LI, X. H., DOOLAN, D. L., MIDZI, N., MDULUZA, T., MCMANUS, D. P., WILSON, R. A., BETHONY, J. M., NAUSCH, N., MUTAPI, F., FELGNER, P. L. & LOUKAS, A. 2015. Of monkeys and men: immunomic profiling of sera from humans and non-human primates resistant to schistosomiasis reveals novel potential vaccine candidates. *Front Immunol,* 6**,** 213.

PEARSON, M. S., PICKERING, D. A., MCSORLEY, H. J., BETHONY, J. M., TRIBOLET, L., DOUGALL, A. M., HOTEZ, P. J. & LOUKAS, A. 2012. Enhanced protective efficacy of a chimeric form of the schistosomiasis vaccine antigen Sm-TSP-2. *PLoS Negl Trop Dis,* 6**,** e1564.

PEREZ-HERNANDEZ, D., GUTIERREZ-VAZQUEZ, C., JORGE, I., LOPEZ-MARTIN, S., URSA, A., SANCHEZ-MADRID, F., VAZQUEZ, J. & YANEZ-MO, M. 2013. The intracellular interactome of tetraspanin-enriched microdomains reveals their function as sorting machineries toward exosomes. *J Biol Chem,* 288**,** 11649-61.

PEREZ-SANCHEZ, R., RAMAJO-HERNANDEZ, A., RAMAJO-MARTIN, V. & OLEAGA, A. 2006. Proteomic analysis of the tegument and excretory-secretory products of adult *Schistosoma bovis* worms. *Proteomics,* 6 Suppl 1**,** S226-36.

PEREZ DEL VILLAR, L., BURGUILLO, F. J., LOPEZ-ABAN, J. & MURO, A. 2012. Systematic review and meta-analysis of artemisinin based therapies for the treatment and prevention of schistosomiasis. *PLoS One,* 7**,** e45867.

PINHEIRO, C. S., MARTINS, V. P., ASSIS, N. R. G., FIGUEIREDO, B. C. P., MORAIS, S. B., AZEVEDO, V. & OLIVEIRA, S. C. 2011. Computational vaccinology: an important strategy to discover new potential *S. mansoni* vaccine candidates. *J Biomed Biotechnol,* 2011**,** 503068-503068.

PINHEIRO, C. S., RIBEIRO, A. P., CARDOSO, F. C., MARTINS, V. P., FIGUEIREDO, B. C., ASSIS, N. R., MORAIS, S. B., CALIARI, M. V., LOUKAS, A. & OLIVEIRA, S. C. 2014. A multivalent chimeric vaccine composed of *Schistosoma mansoni* SmTSP-2 and Sm29 was able to induce protection against infection in mice. *Parasite Immunol,* 36**,** 303-12.

PLEASS, R. J., KUSEL, J. R. & WOOF, J. M. 2000. Cleavage of human IgE mediated by *Schistosoma mansoni*. *Int Arch Allergy Immunol,* 121**,** 194-204.

POPE, S. M. & LASSER, C. 2013. *Toxoplasma gondii* infection of fibroblasts causes the production of exosome-like vesicles containing a unique array of mRNA and miRNA transcripts compared to serum starvation. *J Extracell Vesicles,* 2.

PRAST-NIELSEN, S., HUANG, H.-H. & WILLIAMS, D. L. 2011. Thioredoxin glutathione reductase: its role in redox biology and potential as a target for drugs against neglected diseases. *Biochim Biophys Acta,* 1810**,** 1262-1271.

QI, X., ZHANG, J., YUAN, H., XU, Z., LI, Q., NIU, X., HU, B., WANG, Y. & LI, X. 2016. Exosomes secreted by human-induced pluripotent stem cell-derived mesenchymal stem cells repair critical-sized bone defects through enhanced angiogenesis and osteogenesis in osteoporotic rats. *Int J Biol Sci,* 12**,** 836-49.

RAMAKRISHNAIAH, V., THUMANN, C., FOFANA, I., HABERSETZER, F., PAN, Q., DE RUITER, P. E., WILLEMSEN, R., DEMMERS, J. A., STALIN RAJ, V., JENSTER, G., KWEKKEBOOM, J., TILANUS, H. W., HAAGMANS, B. L., BAUMERT, T. F. & VAN DER LAAN, L. J. 2013. Exosome-mediated transmission of hepatitis C virus between human hepatoma Huh7.5 cells. *Proc Natl Acad Sci U S A,* 110**,** 13109-13.

RAMALHO-PINTO, F. J., GAZZINELLI, G., HOWELLS, R. E., MOTA-SANTOS, T. A., FIGUEIREDO, E. A. & PELLEGRINO, J. 1974. *Schistosoma mansoni*: defined system for stepwise transformation of cercaria to schistosomule in vitro. *Exp Parasitol,* 36**,** 360-72.

RANA, S., YUE, S., STADEL, D. & ZOLLER, M. 2012. Toward tailored exosomes: the exosomal tetraspanin web contributes to target cell selection. *Int J Biochem Cell Biol,* 44**,** 1574-84.

RAPOSO, G., MARKS, M. S. & CUTLER, D. F. 2007. Lysosome-related organelles: driving post-Golgi compartments into specialisation. *Curr Opin Cell Biol,* 19**,** 394-401.

RAPOSO, G. & STOORVOGEL, W. 2013. Extracellular vesicles: exosomes, microvesicles, and friends. *J Cell Biol,* 200**,** 373-83.

RAPOSO, G., TENZA, D., MECHERI, S., PERONET, R., BONNEROT, C. & DESAYMARD, C. 1997. Accumulation of major histocompatibility complex class II molecules in mast cell secretory granules and their release upon degranulation. *Mol Biol Cell,* 8**,** 2631-45.

RASTOGI, N. & MISHRA, D. P. 2012. Therapeutic targeting of cancer cell cycle using proteasome inhibitors. *Cell Div,* 7**,** 26.

RECORD, M., CARAYON, K., POIROT, M. & SILVENTE-POIROT, S. 2014. Exosomes as new vesicular lipid transporters involved in cell-cell communication and various pathophysiologies. *Biochim Biophys Acta,* 1841**,** 108-20.

RECORD, M., SILVENTE-POIROT, S., POIROT, M. & WAKELAM, M. J. O. 2018. Extracellular vesicles: lipids as key components of their biogenesis and functions. *J Lipid Res,* 59**,** 1316-1324.

REDA, E. S., OUHTIT, A., ABDEEN, S. H. & EL-SHABASY, E. A. 2012. Structural changes of *Schistosoma mansoni* adult worms recovered from C57BL/6 mice treated with radiation-attenuated vaccine and/or praziquantel against infection. *Parasitol Res,* 110**,** 979-92.

REGEV-RUDZKI, N., WILSON, D. W., CARVALHO, T. G., SISQUELLA, X., COLEMAN, B. M., RUG, M., BURSAC, D., ANGRISANO, F., GEE, M., HILL, A. F., BAUM, J. & COWMAN, A. F. 2013. Cell-cell communication between malaria-infected red blood cells via exosome-like vesicles. *Cell,* 153**,** 1120-33.

REINER, A. T., WITWER, K. W., VAN BALKOM, B. W. M., DE BEER, J., BRODIE, C., CORTELING, R. L., GABRIELSSON, S., GIMONA, M., IBRAHIM, A. G., DE KLEIJN, D., LAI, C. P., LOTVALL, J., DEL PORTILLO, H. A., REISCHL, I. G., RIAZIFAR, M., SALOMON, C., TAHARA, H., TOH, W. S., WAUBEN, M. H. M., YANG, V. K., YANG, Y. J., YEO, R. W. Y., YIN, H., GIEBEL, B., ROHDE, E. & LIM, S. K. 2017. Concise review: Developing best-practice models for the therapeutic use of extracellular vesicles. *Stem Cell Transl Med,* 6**,** 1730-1739.

REZENDE, C. M., SILVA, M. R., SANTOS, I. G., SILVA, G. A., GOMES, D. A. & GOES, A. M. 2011. Immunization with rP22 induces protective immunity against *Schistosoma mansoni*: effects on granuloma down-modulation and cytokine production. *Immunol Lett,* 141**,** 123-33.

RICCIARDI, A. & NDAO, M. 2015. Still hope for schistosomiasis vaccine. *Hum Vaccin Immunother,* 11**,** 2504-2508.

RICCIARDI, A., VISITSUNTHORN, K., DALTON, J. P. & NDAO, M. 2016. A vaccine consisting of *Schistosoma mansoni* cathepsin B formulated in Montanide ISA 720 VG induces high level protection against murine schistosomiasis. *BMC Infect Dis,* 16**,** 112-112.

RICHTER, J. 2003. The impact of chemotherapy on morbidity due to schistosomiasis. *Acta Trop,* 86**,** 161-83.

RICHTER, J., CORREIA DACAL, A. R., VERGETTI SIQUEIRA, J. G., POGGENSEE, G., MANNSMANN, U., DEELDER, A. & FELDMEIER, H. 1998. Sonographic prediction of variceal bleeding in patients with liver fibrosis due to *Schistosoma mansoni*. *Trop Med Int Health,* 3**,** 728-35.

RISSO, D., NGAI, J., SPEED, T. P. & DUDOIT, S. 2014. Normalization of RNA-seq data using factor analysis of control genes or samples. *Nat Biotechnol,* 32**,** 896.

RITCHIE, M. E., PHIPSON, B., WU, D., HU, Y., LAW, C. W., SHI, W. & SMYTH, G. K. 2015. limma powers differential expression analyses for RNA-sequencing and microarray studies. *Nucleic Acids Res,* 43**,** e47.

RIVEAU, G., DEPLANQUE, D., REMOUÉ, F., SCHACHT, A.-M., VODOUGNON, H., CAPRON, M., THIRY, M., MARTIAL, J., LIBERSA, C. & CAPRON, A. 2012. Safety and immunogenicity of rSh28GST antigen in humans: Phase 1 randomized clinical study of a vaccine candidate against urinary schistosomiasis. *PLoS Negl Trop Dis,* 6**,** e1704.

RIVEAU, G., SCHACHT, A. M., DOMPNIER, J. P., DEPLANQUE, D., SECK, M., WAUCQUIER, N., SENGHOR, S., DELCROIX-GENETE, D., HERMANN, E., IDRIS-KHODJA, N., LEVY-MARCHAL, C., CAPRON, M. & CAPRON, A. 2018. Safety and efficacy of the rSh28GST urinary schistosomiasis

vaccine: A phase 3 randomized, controlled trial in Senegalese children. *PLoS Negl Trop Dis,* 12**,** e0006968.

ROBBINS, P. D. & MORELLI, A. E. 2014. Regulation of immune responses by extracellular vesicles. *Nat Rev Immunol,* 14**,** 195-208.

ROBINSON, M. D., MCCARTHY, D. J. & SMYTH, G. K. 2010. edgeR: a Bioconductor package for differential expression analysis of digital gene expression data. *Bioinformatics,* 26**,** 139-40.

ROBINSON, M. W., BUCHTMANN, K. A., JENKINS, C., TACCHI, J. L., RAYMOND, B. B., TO, J., ROY CHOWDHURY, P., WOOLLEY, L. K., LABBATE, M., TURNBULL, L., WHITCHURCH, C. B., PADULA, M. P. & DJORDJEVIC, S. P. 2013. MHJ_0125 is an M42 glutamyl aminopeptidase that moonlights as a multifunctional adhesin on the surface of *Mycoplasma hyopneumoniae*. *Open Biol,* 3**,** 130017.

ROIG, J., L. SAIZ, M., GALIANO, A., TRELIS, M., GARCÍA, F., MONTEAGUDO, C., GINER, E., GINER, R., RECIO, M., BERNAL, D., SÁNCHEZ-MADRID, F. & MARCILLA, A. 2018. Extracellular vesicles from the helminth *Fasciola hepatica* prevent DSS-induced acute ulcerative colitis in a T-lymphocyte independent mode. *Front Microbiol,* 9.

ROLLINSON, D., KNOPP, S., LEVITZ, S., STOTHARD, J. R., TCHUEM TCHUENTE, L. A., GARBA, A., MOHAMMED, K. A., SCHUR, N., PERSON, B., COLLEY, D. G. & UTZINGER, J. 2013. Time to set the agenda for schistosomiasis elimination. *Acta Trop,* 128**,** 423-40.

RONTOGIANNI, S., SYNADAKI, E., LI, B., LIEFAARD, M. C., LIPS, E. H., WESSELING, J., WU, W. & ALTELAAR, M. 2019. Proteomic profiling of extracellular vesicles allows for human breast cancer subtyping. *Commun Biol,* 2**,** 325.

ROSNER, B. 2011. *Fundamentals of biostatistics,* Boston, Brooks/Cole, Cengage Learning.

ROSS, A. G., BARTLEY, P. B., SLEIGH, A. C., OLDS, G. R., LI, Y., WILLIAMS, G. M. & MCMANUS, D. P. 2002. Schistosomiasis. *N Engl J Med,* 346**,** 1212-20.

ROSS, A. G., CHAU, T. N., INOBAYA, M. T., OLVEDA, R. M., LI, Y. & HARN, D. A. 2017. A new global strategy for the elimination of schistosomiasis. *Int J Infect Dis,* 54**,** 130-137.

RUPPEL, A., SHI, Y. E. & MOLONEY, N. A. 1990. *Schistosoma mansoni* and *S. japonicum*: comparison of levels of ultraviolet irradiation for vaccination of mice with cercariae. *Parasitology,* 101 Pt 1**,** 23-6.

RUPPERT, K. A., NGUYEN, T. T., PRABHAKARA, K. S., TOLEDANO FURMAN, N. E., SRIVASTAVA, A. K., HARTING, M. T., COX, C. S., JR. & OLSON, S. D. 2018. Human mesenchymal stromal cell-derived extracellular vesicles modify microglial response and improve clinical outcomes in experimental spinal cord injury. *Sci Rep,* 8**,** 480.

SADUN, E. H. & LIN, S. S. 1959. Studies on the host parasite relationships to *Schistosoma japonicum*. IV. Resistance acquired by infection, by vaccination and by the injection of immune serum, in monkeys, rabbits and mice. *J Parasitol,* 45**,** 543-8.

SAJID, M., MCKERROW, J. H., HANSELL, E., MATHIEU, M. A., LUCAS, K. D., HSIEH, I., GREENBAUM, D., BOGYO, M., SALTER, J. P., LIM, K. C., FRANKLIN, C., KIM, J.-H. & CAFFREY, C. R. 2003. Functional expression and characterization of *Schistosoma mansoni* cathepsin B and its trans-activation by an endogenous asparaginyl endopeptidase. *Mol Biochem Parasit,* 131**,** 65-75.

SALEM, N., BALKMAN, J. D., WANG, J., WILSON, D. L., LEE, Z., KING, C. L. & BASILION, J. P. 2010. *In vivo* imaging of schistosomes to assess disease burden using positron emission tomography (PET). *PLoS Negl Trop Dis,* 4**,** e827.

SALZET, M., CAPRON, A. & STEFANO, G. B. 2000. Molecular crosstalk in host-parasite relationships: schistosome- and leech-host interactions. *Parasitol Today,* 16**,** 536-40.

SAMOIL, V., DAGENAIS, M., GANAPATHY, V., ALDRIDGE, J., GLEBOV, A., JARDIM, A. & RIBEIRO, P. 2018. Vesicle-based secretion in schistosomes: Analysis of protein and microRNA (miRNA) content of exosome-like vesicles derived from *Schistosoma mansoni*. *Sci Rep,* 8**,** 3286.

SANDERSON, R. D., BANDARI, S. K. & VLODAVSKY, I. 2019. Proteases and glycosidases on the surface of exosomes: Newly discovered mechanisms for extracellular remodeling. *Matrix Biol,* 75-76**,** 160-169.

SANTINI-OLIVEIRA, M., COLER, R. N., PARRA, J., VELOSO, V., JAYASHANKAR, L., PINTO, P. M., CIOL, M. A., BERGQUIST, R., REED, S. G. & TENDLER, M. 2016. Schistosomiasis vaccine candidate Sm14/GLA-SE: Phase 1 safety and immunogenicity clinical trial in healthy, male adults. *Vaccine,* 34**,** 586-94.

SAVINA, A., FADER, C. M., DAMIANI, M. T. & COLOMBO, M. I. 2005. Rab11 promotes docking and fusion of multivesicular bodies in a calcium-dependent manner. *Traffic,* 6**,** 131-43.

SAVINA, A., VIDAL, M. & COLOMBO, M. I. 2002. The exosome pathway in K562 cells is regulated by Rab11. *J Cell Sci,* 115**,** 2505-15.

SCHAFER, M. & WERNER, S. 2008. Cancer as an overhealing wound: an old hypothesis revisited. *Nat Rev Mol Cell Biol,* 9**,** 628-38.

SCHOREY, J. S., CHENG, Y., SINGH, P. P. & SMITH, V. L. 2015. Exosomes and other extracellular vesicles in host-pathogen interactions. *EMBO Rep,* 16**,** 24-43.

SCHWAB, A., MEYERING, S. S., LEPENE, B., IORDANSKIY, S., VAN HOEK, M. L., HAKAMI, R. M. & KASHANCHI, F. 2015. Extracellular vesicles from infected cells: potential for direct pathogenesis. *Front microbio,* 6**,** 1132-1132.

SCHWARTZ, C. & FALLON, P. G. 2018. Schistosoma “eggs-Iting” the host: Granuloma formation and egg excretion. *Front Immunol,* 9**,** 2492.

SEPULVEDA, J., TREMBLAY, J. M., DEGNORE, J. P., SKELLY, P. J. & SHOEMAKER, C. B. 2010. Schistosoma mansoni host-exposed surface antigens characterized by sera and recombinant antibodies from schistosomiasis-resistant rats. *Int J Parasitol,* 40**,** 1407-1417.

SHALABY, H. A. 2013. Anthelmintics resistance; How to overcome it? *Iran J Parasitol,* 8**,** 18-32.

SHEARS, R. K., BANCROFT, A. J., HUGHES, G. W., GRENCIS, R. K. & THORNTON, D. J. 2018. Extracellular vesicles induce protective immunity against *Trichuris muris*. *Parasite Immunol,* 40**,** e12536.

SHI, F., ZHANG, Y., YE, P., LIN, J., CAI, Y., SHEN, W., BICKLE, Q. D. & TAYLOR, M. G. 2001. Laboratory and field evaluation of *Schistosoma japonicum* DNA vaccines in sheep and water buffalo in China. *Vaccine,* 20**,** 462-7.

SHIFRIN, D. A., BECKLER, M. D., COFFEY, R. J. & TYSKA, M. J. 2013. Extracellular vesicles: communication, coercion, and conditioning. *Mol Biol Cell,* 24**,** 1253-9.

SHIMODA, M. & KHOKHA, R. 2017. Metalloproteinases in extracellular vesicles. *Biochim Biophys Acta Mol Cell Res,* 1864**,** 1989-2000.

SIDDIQUI, A. A., SIDDIQUI, B. A. & GANLEY-LEAL, L. 2011. Schistosomiasis vaccines. *Human Vaccines,* 7**,** 1192-1197.

SIDDIQUI, A. A. & SIDDIQUI, S. Z. 2017. Sm-p80-based schistosomiasis vaccine: Preparation for human clinical trials. *Trends Parasitol,* 33**,** 194-201.

SIDDIQUI, A. J., MOLEHIN, A. J., ZHANG, W., GANAPATHY, P. K., KIM, E., ROJO, J. U., REDMAN, W. K., SENNOUNE, S. R., SUDDUTH, J., FREEBORN, J., HUNTER, D., KOTTAPALLI, K. R., KOTTAPALLI, P., WETTASHINGHE, R., VAN DAM, G. J., CORSTJENS, P. L. A. M., PAPIN, J. F., CAREY, D., TORBEN, W., AHMAD, G. & SIDDIQUI, A. A. 2018. Sm-p80-based vaccine trial in baboons: efficacy when mimicking natural conditions of chronic disease, praziquantel therapy, immunization, and *Schistosoma mansoni* re-encounter. *Ann N Y Acad Sci,* 1425**,** 19-37.

SILES-LUCAS, M., SANCHEZ-OVEJERO, C., GONZALEZ-SANCHEZ, M., GONZALEZ, E., FALCON-PEREZ, J. M., BOUFANA, B., FRATINI, F., CASULLI, A. & MANZANO-ROMAN, R. 2017. Isolation and characterization of exosomes derived from fertile sheep hydatid cysts. *Vet Parasitol,* 236**,** 22-33.

SILVA, J., GARCIA, V., RODRIGUEZ, M., COMPTE, M., CISNEROS, E., VEGUILLAS, P., GARCIA, J. M., DOMINGUEZ, G., CAMPOS-MARTIN, Y., CUEVAS, J., PENA, C., HERRERA, M., DIAZ, R., MOHAMMED, N. & BONILLA, F. 2012. Analysis of exosome release and its prognostic value in human colorectal cancer. *Gene Chromosome Canc,* 51**,** 409-18.

SILVA, L. L., MARCET-HOUBEN, M., ZERLOTINI, A., GABALDON, T., OLIVEIRA, G. & NAHUM, L. A. 2011. Evolutionary histories of expanded peptidase families in *Schistosoma mansoni*. *Mem Inst Oswaldo Cruz,* 106**,** 864-77.

SILVERMAN, J. M., CHAN, S. K., ROBINSON, D. P., DWYER, D. M., NANDAN, D., FOSTER, L. J. & REINER, N. E. 2008. Proteomic analysis of the secretome of *Leishmania donovani*. *Genome Biol,* 9**,** R35.

SILVERMAN, J. M., CLOS, J., DE'OLIVEIRA, C. C., SHIRVANI, O., FANG, Y., WANG, C., FOSTER, L. J. & REINER, N. E. 2010a. An exosome-based secretion pathway is responsible for protein export from *Leishmania* and communication with macrophages. *J Cell Sci,* 123**,** 842-52.

SILVERMAN, J. M., CLOS, J., HORAKOVA, E., WANG, A. Y., WIESGIGL, M., KELLY, I., LYNN, M. A., MCMASTER, W. R., FOSTER, L. J., LEVINGS, M. K. & REINER, N. E. 2010b. *Leishmania* exosomes modulate innate and adaptive immune responses through effects on monocytes and dendritic cells. *J Immunol,* 185**,** 5011-22.

SIMBARI, F., MCCASKILL, J., COAKLEY, G., MILLAR, M., MAIZELS, R. M., FABRIÁS, G., CASAS, J. & BUCK, A. H. 2016. Plasmalogen enrichment in exosomes secreted by a nematode parasite versus those derived from its mouse host: implications for exosome stability and biology. *J Extracell Vesicles,* 5**,** 30741-30741.

SIMON, A. 2010. *FastQC: A quality control tool for high throughput sequence data* [Online]. Available: https://www.bioinformatics.babraham.ac.uk/projects/fastqc/ [Accessed 2019, October 21].

SIMPSON, R. J., KALRA, H. & MATHIVANAN, S. 2012. ExoCarta as a resource for exosomal research. *J Extracell Vesicles,* 1.

SKOTLAND, T., HESSVIK, N., SANDVIG, K. & LLORENTE, A. 2018. Exosomal lipid composition and the role of ether lipids and phosphoinositides in exosome biology. *J Lipid Res,* 60**,** jlr.R084343.

SMITH, K. A. & MAIZELS, R. M. 2014. IL-6 controls susceptibility to helminth infection by impeding Th2 responsiveness and altering the Treg phenotype in vivo. *Eur J Immunol,* 44**,** 150-161.

SMITHERS, S. & TERRY, R. 1969. Immunity in schistosomiasis *Ann NY Acad Sci,* 160**,** 826-840.

SMITHERS, S. R. & TERRY, R. J. 1965. The infection of laboratory hosts with cercariae of *Schistosoma mansoni* and the recovery of the adult worms. *Parasitology,* 55**,** 695-700.

SMOUT, M. J., LAHA, T., MULVENNA, J., SRIPA, B., SUTTIPRAPA, S., JONES, A., BRINDLEY, P. J. & LOUKAS, A. 2009. A granulin-like growth factor secreted by the carcinogenic liver fluke, *Opisthorchis viverrini*, promotes proliferation of host cells. *PLoS Pathog,* 5**,** e1000611.

SMOUT, M. J., SRIPA, B., LAHA, T., MULVENNA, J., GASSER, R. B., YOUNG, N. D., BETHONY, J. M., BRINDLEY, P. J. & LOUKAS, A. 2011. Infection with the carcinogenic human liver fluke, *Opisthorchis viverrini*. *Mol Biosyst,* 7**,** 1367-75.

SOISSON, L. A., REID, G. D., FARAH, I. O., NYINDO, M. & STRAND, M. 1993. Protective immunity in baboons vaccinated with a recombinant antigen or radiation-attenuated cercariae of *Schistosoma mansoni* is antibody-dependent. *J Immunol,* 151**,** 4782–4789.

SOTILLO, J., DOOLAN, D. & LOUKAS, A. 2016a. Recent advances in proteomic applications for schistosomiasis research: potential clinical impact. *Expert Rev Proteomics***,** 1-13.

SOTILLO, J., PEARSON, M., BECKER, L., MULVENNA, J. & LOUKAS, A. 2015. A quantitative proteomic analysis of the tegumental proteins from *Schistosoma mansoni* schistosomula reveals novel potential therapeutic targets. *Int J Parasitol,* 45**,** 505-16.

SOTILLO, J., PEARSON, M., POTRIQUET, J., BECKER, L., PICKERING, D., MULVENNA, J. & LOUKAS, A. 2016b. Extracellular vesicles secreted by *Schistosoma mansoni* contain protein vaccine candidates. *Int J Parasitol,* 46**,** 1-5.

SOTILLO, J., PEARSON, M. S., BECKER, L., MEKONNEN, G. G., AMOAH, A. S., VAN DAM, G., CORSTJENS, P. L. A. M., MURRAY, J., MDULUZA, T., MUTAPI, F. & LOUKAS, A. 2019a. In-depth proteomic characterization of *Schistosoma haematobium*: Towards the development of new tools for elimination. *PLoS Negl Trop Dis,* 13**,** e0007362.

SOTILLO, J., PEARSON, M. S. & LOUKAS, A. 2019b. Trematode genomics and proteomics. *Adv Exp Med Biol,* 1154**,** 411-436.

SOTILLO, J., SANCHEZ-FLORES, A., CANTACESSI, C., HARCUS, Y., PICKERING, D., BOUCHERY, T., CAMBERIS, M., TANG, S.-C., GIACOMIN, P., MULVENNA, J., MITREVA, M., BERRIMAN, M., LEGROS, G., MAIZELS, R. M. & LOUKAS, A. 2014. Secreted proteomes of different developmental stages of the gastrointestinal nematode *Nippostrongylus brasiliensis*. *Mol. cell proteomics,* 13**,** 2736-2751.

SOUSA-FIGUEIREDO, J. C., BETSON, M., ATUHAIRE, A., ARINAITWE, M., NAVARATNAM, A. M., KABATEREINE, N. B., BICKLE, Q. & STOTHARD, J. R. 2012. Performance and safety of praziquantel for treatment of intestinal schistosomiasis in infants and preschool children. *PLoS Negl Trop Dis,* 6**,** e1864.

SRIPA, B., BETHONY, J. M., SITHITHAWORN, P., KAEWKES, S., MAIRIANG, E., LOUKAS, A., MULVENNA, J., LAHA, T., HOTEZ, P. J. & BRINDLEY, P. J. 2011. Opisthorchiasis and *Opisthorchis*-associated cholangiocarcinoma in Thailand and Laos. *Acta Trop,* 120**,** S158-68.

SRIPA, B., BRINDLEY, P. J., MULVENNA, J., LAHA, T., SMOUT, M. J., MAIRIANG, E., BETHONY, J. M. & LOUKAS, A. 2012. The tumorigenic liver fluke *Opisthorchis viverrini*--multiple pathways to cancer. *Trends Parasitol,* 28**,** 395-407.

SRIPA, B., KAEWKES, S., SITHITHAWORN, P., MAIRIANG, E., LAHA, T., SMOUT, M., PAIROJKUL, C., BHUDHISAWASDI, V., TESANA, S., THINKAMROP, B., BETHONY, J. M., LOUKAS, A. & BRINDLEY, P. J. 2007. Liver fluke induces cholangiocarcinoma. *PLoS Med,* 4**,** e201.

STENMARK, H. 2009. Rab GTPases as coordinators of vesicle traffic. *Nat Rev Mol Cell Biol,* 10**,** 513-25.

STEPHENSON, R., YOU, H., MCMANUS, D. P. & TOTH, I. 2014. Schistosome vaccine adjuvants in preclinical and clinical research. *Vaccines,* 2**,** 654-685.

STIPP, C. S., KOLESNIKOVA, T. V. & HEMLER, M. E. 2003. Functional domains in tetraspanin proteins. *Trends Biochem Sci,* 28**,** 106-12.

STOTHARD, J. R., SOUSA-FIGUEIREDO, J. C., BETSON, M., GREEN, H. K., SETO, E. Y., GARBA, A., SACKO, M., MUTAPI, F., VAZ NERY, S., AMIN, M. A., MUTUMBA-NAKALEMBE, M., NAVARATNAM, A., FENWICK, A., KABATEREINE, N. B., GABRIELLI, A. F. & MONTRESOR, A. 2011. Closing the praziquantel treatment gap: new steps in epidemiological monitoring and control of schistosomiasis in African infants and preschool-aged children. *Parasitology,* 138**,** 1593-606.

STREMERSCH, S., DE SMEDT, S. C. & RAEMDONCK, K. 2016. Therapeutic and diagnostic applications of extracellular vesicles. *J Control Release,* 244**,** 167-183.

SUPEK, F., BOŠNJAK, M., ŠKUNCA, N. & ŠMUC, T. 2011. REVIGO summarizes and visualizes long lists of gene ontology terms. *PLoS One,* 6**,** e21800.

TARARAM, C. A., FARIAS, L. P., WILSON, R. A. & LEITE, L. C. D. C. 2010. *Schistosoma mansoni* Annexin 2: Molecular characterization and immunolocalization. *Exp Parasitol,* 126**,** 146-155.

TARRAB-HAZDAI, R., SCHECHTMAN, D. & ARNON, R. 1998. Synthesis and characterization of a protective peptide-based vaccine against *Schistosoma mansoni*. *Infect Immun,* 66**,** 4526-4530.

TAURO, B. J., GREENING, D. W., MATHIAS, R. A., MATHIVANAN, S., JI, H. & SIMPSON, R. J. 2013. Two distinct populations of exosomes are released from LIM1863 colon carcinoma cell-derived organoids. *Mol Cell Proteomics,* 12**,** 587-98.

TAYLOR, J. & BEBAWY, M. 2019. Proteins Regulating Microvesicle Biogenesis and Multidrug Resistance in Cancer. *Proteomics,* 19**,** 1800165.

TAYLOR, R. C., CULLEN, S. P. & MARTIN, S. J. 2008. Apoptosis: controlled demolition at the cellular level. *Nat Rev Mol Cell Biol,* 9**,** 231-41.

TEBEJE, B. M., HARVIE, M., YOU, H., LOUKAS, A. & MCMANUS, D. P. 2016. Schistosomiasis vaccines: where do we stand? *Parasit Vectors,* 9**,** 528.

TENDLER, M., ALMEIDA, M. & SIMPSON, A. 2015. Development of the Brazilian anti Schistosomiasis vaccine based on the recombinant fatty acid binding protein Sm14 plus GLA-SE adjuvant. *Front. Immunol.,* 6**,** 218.

TENDLER, M., ALMEIDA, M. S., VILAR, M. M., PINTO, P. M. & LIMAVERDE-SOUSA, G. 2018. Current Status of the Sm14/GLA-SE Schistosomiasis Vaccine: Overcoming Barriers and Paradigms towards the First Anti-Parasitic Human(itarian) Vaccine. *Trop Med Infect Dis,* 3.

TENDLER, M., BRITO, C. A., VILAR, M. M., SERRA-FREIRE, N., DIOGO, C. M., ALMEIDA, M. S., DELBEM, A. C., DA SILVA, J. F., SAVINO, W., GARRATT, R. C., KATZ, N. & SIMPSON, A. S. 1996. A *Schistosoma mansoni* fatty acid-binding protein, Sm14, is the potential basis of a dual-purpose anti-helminth vaccine. *Proc Natl Acad Sci U S A,* 93**,** 269-73.

THEBAUD, B. & STEWART, D. J. 2012. Exosomes: cell garbage can, therapeutic carrier, or trojan horse? *Circulation,* 126**,** 2553-5.

THÉRY, C., AMIGORENA, S., RAPOSO, G. & CLAYTON, A. 2006. Isolation and characterization of exosomes from cell culture supernatants and biological fluids. *Curr Protoc Cell Biol,* 30**,** 3.22.1-3.22.29.

THERY, C., BOUSSAC, M., VERON, P., RICCIARDI-CASTAGNOLI, P., RAPOSO, G., GARIN, J. & AMIGORENA, S. 2001. Proteomic analysis of dendritic cell-derived exosomes: A secreted subcellular compartment distinct from apoptotic vesicles. *J. Immunol.,* 166**,** 7309-7318.

THERY, C., OSTROWSKI, M. & SEGURA, E. 2009. Membrane vesicles as conveyors of immune responses. *Nat Rev Immunol,* 9**,** 581-93.

TIAN, Y., LI, S., SONG, J., JI, T., ZHU, M., ANDERSON, G. J., WEI, J. & NIE, G. 2014. A doxorubicin delivery platform using engineered natural membrane vesicle exosomes for targeted tumor therapy. *Biomaterials,* 35**,** 2383-90.

TORBEN, W., AHMAD, G., ZHANG, W., NASH, S., LE, L., KARMAKAR, S. & SIDDIQUI, A. A. 2012. Role of antibody dependent cell mediated cytotoxicity (ADCC) in Sm-p80-mediated protection against *Schistosoma mansoni*. *Vaccine,* 30**,** 6753-6758.

TOWBIN, H., STAEHELIN, T. & GORDON, J. 1979. Electrophoretic transfer of proteins from polyacrylamide gels to nitrocellulose sheets: procedure and some applications. *Proc Natl Acad Sci U S A,* 76**,** 4350-4.

TRAJKOVIC, K., HSU, C., CHIANTIA, S., RAJENDRAN, L., WENZEL, D., WIELAND, F., SCHWILLE, P., BRÜGGER, B. & SIMONS, M. 2008. Ceramide triggers budding of exosome vesicles into multivesicular endosomes. *Science,* 319**,** 1244-1247.

TRAN, M. H., FREITAS, T. C., COOPER, L., GAZE, S., GATTON, M. L., JONES, M. K., LOVAS, E., PEARCE, E. J. & LOUKAS, A. 2010. Suppression of mRNAs encoding tegument tetraspanins from *Schistosoma mansoni* results in impaired tegument turnover. *PLoS Pathog,* 6**,** e1000840.

TRAN, M. H., PEARSON, M. S., BETHONY, J. M., SMYTH, D. J., JONES, M. K., DUKE, M., DON, T. A., MCMANUS, D. P., CORREA-OLIVEIRA, R. & LOUKAS, A. 2006. Tetraspanins on the surface of *Schistosoma mansoni* are protective antigens against schistosomiasis. *Nat Med,* 12**,** 835-40.

TRELIS, M., GALIANO, A., BOLADO, A., TOLEDO, R., MARCILLA, A. & BERNAL, D. 2016. Subcutaneous injection of exosomes reduces symptom severity and mortality induced by *Echinostoma caproni* infection in BALB/c mice. *Int J Parasitol,* 46**,** 799-808.

TUCKER, M. S., KARUNARATNE, L. B., LEWIS, F. A., FREITAS, T. C. & LIANG, Y. S. 2013. Schistosomiasis. *Curr Protoc Immunol,* 103**,** Unit 19 1.

TURNER, H. C., TRUSCOTT, J. E., BETTIS, A. A., FARRELL, S. H., DEOL, A. K., WHITTON, J. M., FLEMING, F. M. & ANDERSON, R. M. 2017. Evaluating the variation in the projected benefit of community-wide mass treatment for schistosomiasis: Implications for future economic evaluations. *Parasit Vectors,* 10**,** 213.

TWU, O., DE MIGUEL, N., LUSTIG, G., STEVENS, G. C., VASHISHT, A. A., WOHLSCHLEGEL, J. A. & JOHNSON, P. J. 2013. *Trichomonas vaginalis* exosomes deliver cargo to host cells and mediate hostratioparasite interactions. *PLoS Pathog,* 9**,** e1003482.

TZELOS, T., MATTHEWS, J. B., BUCK, A. H., SIMBARI, F., FREW, D., INGLIS, N. F., MCLEAN, K., NISBET, A. J., WHITELAW, C. B. A., KNOX, D. P. & MCNEILLY, T. N. 2016. A preliminary proteomic characterisation of extracellular vesicles released by the ovine parasitic nematode, *Teladorsagia circumcincta*. *Vet Parasitol,* 221**,** 84-92.

UTZINGER, J., N'GORAN, E. K., N'DRI, A., LENGELER, C. & TANNER, M. 2000. Efficacy of praziquantel against *Schistosoma mansoni* with particular consideration for intensity of infection. *Trop Med Int Health,* 5**,** 771-8.

UTZINGER, J., RASO, G., BROOKER, S., DE SAVIGNY, D., TANNER, M., ØRNBJERG, N., SINGER, B. & N'GORAN, E. 2009. Schistosomiasis and neglected tropical diseases: towards integrated and sustainable control and a word of caution. *Parasitology,* 136**,** 1859-1874.

VALADI, H., EKSTRÖM, K., BOSSIOS, A., SJÖSTRAND, M., LEE, J. J. & LÖTVALL, J. O. 2007. Exosome-mediated transfer of mRNAs and microRNAs is a novel mechanism of genetic exchange between cells. *Nature Cell Biol,* 9**,** 654-659.

VALENTIM, C. L., CIOLI, D., CHEVALIER, F. D., CAO, X., TAYLOR, A. B., HOLLOWAY, S. P., PICA-MATTOCCIA, L., GUIDI, A., BASSO, A., TSAI, I. J., BERRIMAN, M., CARVALHO-QUEIROZ, C., ALMEIDA, M., AGUILAR, H., FRANTZ, D. E., HART, P. J., LOVERDE, P. T. & ANDERSON, T. J. 2013. Genetic and molecular basis of drug resistance and species-specific drug action in schistosome parasites. *Science,* 342**,** 1385-9.

VAN DER WERF, M. J., DE VLAS, S. J., BROOKER, S., LOOMAN, C. W., NAGELKERKE, N. J., HABBEMA, J. D. & ENGELS, D. 2003. Quantification of clinical morbidity associated with schistosome infection in sub-Saharan Africa. *Acta Trop,* 86**,** 125-39.

VAN NIEL, G., D'ANGELO, G. & RAPOSO, G. 2018. Shedding light on the cell biology of extracellular vesicles. *Nat. Rev. Mol. Cell Biol.,* 19**,** 213.

VIANA, I. R., CORREA-OLIVEIRA, R., CARVALHO ODOS, S., MASSARA, C. L., COLOSIMO, E., COLLEY, D. G. & GAZZINELLI, G. 1995. Comparison of antibody isotype responses to *Schistosoma mansoni* antigens by infected and putative resistant individuals living in an endemic area. *Parasite Immunol,* 17**,** 297-304.

VIANA, I. R., SHER, A., CARVALHO, O. S., MASSARA, C. L., ELOI-SANTOS, S. M., PEARCE, E. J., COLLEY, D. G., GAZZINELLI, G. & CORREA-OLIVEIRA, R. 1994. Interferon-gamma production by peripheral blood mononuclear cells from residents of an area endemic for *Schistosoma mansoni*. *Trans R Soc Trop Med Hyg,* 88**,** 466-70.

VILLARROYA-BELTRI, C., GUTIÉRREZ-VÁZQUEZ, C., SÁNCHEZ-CABO, F., PÉREZ-HERNÁNDEZ, D., VÁZQUEZ, J., MARTIN-COFRECES, N., MARTINEZ-HERRERA, D. J., PASCUAL-MONTANO, A., MITTELBRUNN, M. & SÁNCHEZ-MADRID, F. 2013. Sumoylated hnRNPA2B1 controls the sorting of miRNAs into exosomes through binding to specific motifs. *Nat Commun,* 4**,** 2980.

VLASSOV, A. V., MAGDALENO, S., SETTERQUIST, R. & CONRAD, R. 2012. Exosomes: Current knowledge of their composition, biological functions, and diagnostic and therapeutic potentials. *Biochimica et Biophysica Acta (BBA) - General Subjects,* 1820**,** 940-948.

WAAIJERS, S., PORTEGIJS, V., KERVER, J., LEMMENS, B. B., TIJSTERMAN, M., VAN DEN HEUVEL, S. & BOXEM, M. 2013. CRISPR/Cas9-targeted mutagenesis in Caenorhabditis elegans. *Genetics,* 195**,** 1187-91.

WAARDENBERG, A. J. & FIELD, M. A. 2019. consensusDE: an R package for assessing consensus of multiple RNA-seq algorithms with RUV correction. *bioRxiv***,** 692582.

WALKER, M., BAZ, A., DEMATTEIS, S., STETTLER, M., GOTTSTEIN, B., SCHALLER, J. & HEMPHILL, A. 2004. Isolation and characterization of a secretory component of *Echinococcus multilocularis* metacestodes potentially involved in modulating the host-parasite interface. *Infect Immun,* 72**,** 527-36.

WANG, L., LI, Z., SHEN, J., LIU, Z., LIANG, J., WU, X., SUN, X. & WU, Z. 2015a. Exosome-like vesicles derived by *Schistosoma japonicum* adult worms mediates M1 type immune-activity of macrophage. *Parasitol Res,* 114**,** 1865-73.

WANG, Q., DA'DARA, A. A. & SKELLY, P. J. 2017. The human blood parasite *Schistosoma mansoni* expresses extracellular tegumental calpains that cleave the blood clotting protein fibronectin. *Sci Rep,* 7**,** 12912.

WANG, R., DING, Q., YAQOOB, U., DE ASSUNCAO, T. M., VERMA, V. K., HIRSOVA, P., CAO, S., MUKHOPADHYAY, D., HUEBERT, R. C. & SHAH, V. H. 2015b. Exosome adherence and internalization by hepatic stellate cells triggers sphingosine 1-phosphate-dependent migration. *J Biol Chem,* 290**,** 30684-30696.

WANG, X.-M., HAMZA, M., WU, T.-X. & DIONNE, R. A. 2009. Upregulation of IL-6, IL-8 and CCL2 gene expression after acute inflammation: Correlation to clinical pain. *Pain* 142**,** 275-283.

WEBBER, J. & CLAYTON, A. 2013. How pure are your vesicles? *J Extracell Vesicles,* 2.

WEERAKOON, K. G., GOBERT, G. N., CAI, P. & MCMANUS, D. P. 2015. Advances in the diagnosis of human schistosomiasis. *Clin Microbiol Rev,* 28**,** 939-67.

WENDT, G. R., COLLINS, J. N., PEI, J., PEARSON, M. S., BENNETT, H. M., LOUKAS, A., BERRIMAN, M., GRISHIN, N. V. & COLLINS, J. J., 3RD 2018. Flatworm-specific transcriptional regulators promote the specification of tegumental progenitors in *Schistosoma mansoni*. *Elife,* 7.

WHITE, I. J., BAILEY, L. M., AGHAKHANI, M. R., MOSS, S. E. & FUTTER, C. E. 2006. EGF stimulates annexin 1-dependent inward vesiculation in a multivesicular endosome subpopulation. *Embo j,* 25**,** 1-12.

WIEBKE MÖBIUS, Y. O. I., ELLY G. VAN DONSELAAR, VIOLA M.J. OORSCHOT & YUKIKO SHIMADA, T. F., HARRY F.G. HEIJNEN, HANS J. GEUZE, AND JAN W. SLOT 2002. Immunoelectron microscopic localization of cholesterol using biotinylated and non-cytolytic perfringolysin O. *J. Histochem. Cytochem.,* 50**,** 43-55.

WIKLANDER, O. P., NORDIN, J. Z., O'LOUGHLIN, A., GUSTAFSSON, Y., CORSO, G., MAGER, I., VADER, P., LEE, Y., SORK, H., SEOW, Y., HELDRING, N., ALVAREZ-ERVITI, L., SMITH, C. I., LE BLANC, K., MACCHIARINI, P., JUNGEBLUTH, P., WOOD, M. J. & ANDALOUSSI, S. E. 2015. Extracellular vesicle in vivo biodistribution is determined by cell source, route of administration and targeting. *J Extracell Vesicles,* 4**,** 26316.

WILSON, H. L., FRANCIS, S. E., DOWER, S. K. & CROSSMAN, D. C. 2004. Secretion of intracellular IL-1 receptor antagonist (type 1) is dependent on P2X7 receptor activation. *J Immunol,* 173**,** 1202-8.

WILSON, M. S., MENTINK-KANE, M. M., PESCE, J. T., RAMALINGAM, T. R., THOMPSON, R. & WYNN, T. A. 2007. Immunopathology of schistosomiasis. *Immuno Cell Biol,* 85**,** 148-154.

WILSON, R. A. 2012. Proteomics at the schistosome-mammalian host interface: any prospects for diagnostics or vaccines? *Parasitology,* 139**,** 1178-94.

WILSON, R. A., COULSON, P. S. & MOUNTFORD, A. P. 1999. Immune responses to the radiation-attenuated schistosome vaccine: what can we learn from knock-out mice? *Immunol Lett,* 65**,** 117-23.

WILSON, R. A., LANGERMANS, J. A. M., VAN DAM, G. J., VERVENNE, R. A., HALL, S. L., BORGES, W. C., DILLON, G. P., THOMAS, A. W. & COULSON, P. S. 2008. Elimination of *Schistosoma mansoni* Adult Worms by Rhesus Macaques: Basis for a Therapeutic Vaccine? *PLoS Negl Trop Dis,* 2**,** e290.

WILSON, R. A., LI, X. H. & CASTRO-BORGES, W. 2017. Schistosome vaccines: problems, pitfalls and prospects. *Emerg Topics Life Sci,* 1**,** 641-650.

WILSON, S., JONES, F. M., VAN DAM, G. J., CORSTJENS, P. L. A. M., RIVEAU, G., FITZSIMMONS, C. M., SACKO, M., VENNERVALD, B. J. & DUNNE, D. W. 2014. Human *Schistosoma haematobium* antifecundity immunity is dependent on transmission intensity and associated with immunoglobulin G1 to worm-derived antigens. *J Infect Dis,* 210**,** 2009-2016.

WU, Z., WANG, L., LI, J., WANG, L., WU, Z. & SUN, X. 2019. Extracellular vesicle-mediated communication within host-parasite interactions. *Front Immunol,* 9**,** 3066.

WUBBOLTS, R., LECKIE, R. S., VEENHUIZEN, P. T., SCHWARZMANN, G., MOBIUS, W., HOERNSCHEMEYER, J., SLOT, J. W., GEUZE, H. J. & STOORVOGEL, W. 2003. Proteomic and biochemical analyses of human B cell-derived exosomes. Potential implications for their function and multivesicular body formation. *J Biol Chem,* 278**,** 10963-72.

WYNN, T. A., JANKOVIC, D., HIENY, S., CHEEVER, A. W. & SHER, A. 1995. IL-12 enhances vaccine-induced immunity to *Schistosoma mansoni* in mice and decreases T helper 2 cytokine expression, IgE production, and tissue eosinophilia. *J Immunol,* 154**,** 4701-9.

XIAO, J., PAN, Y., LI, X. H., YANG, X. Y., FENG, Y. L., TAN, H. H., JIANG, L., FENG, J. & YU, X. Y. 2016. Cardiac progenitor cell-derived exosomes prevent cardiomyocytes apoptosis through exosomal miR-21 by targeting PDCD4. *Cell Death Dis,* 7**,** e2277.

XIAO, S.-H., WU, Y.-L., TANNER, M., WU, W.-M., UTZINGER, J., MEI, J.-Y., SCORNEAUX, B., CHOLLET, J. & ZHAI, Z. 2003. *Schistosoma japonicum*: in vitro effects of artemether combined with

haemin depend on cultivation media and appraisal of artemether products appearing in the media. *Parasitol Res,* 89**,** 459-466.

XU, B. & WANG, T. 2017. Intimate cross-talk between cancer cells and the tumor microenvironment of B-cell lymphomas: The key role of exosomes. *Tumour Biol,* 39**,** 1010428317706227.

XU, X., ZHANG, Y., LIN, D., ZHANG, J., XU, J., LIU, Y. M., HU, F., QING, X., XIA, C. & PAN, W. 2014. Serodiagnosis of *Schistosoma japonicum* infection: genome-wide identification of a protein marker, and assessment of its diagnostic validity in a field study in China. *Lancet Infect Dis,* 14**,** 489-97.

YANG, T., MARTIN, P., FOGARTY, B., BROWN, A., SCHURMAN, K., PHIPPS, R., YIN, V. P., LOCKMAN, P. & BAI, S. 2015. Exosome delivered anticancer drugs across the blood-brain barrier for brain cancer therapy in Danio rerio. *Pharm Res,* 32**,** 2003-14.

YANG, W., GOBERT, G. N. & MCMANUS, D. P. 1997. Oral vaccination of mice with recombinant *Schistosoma japonicum* proteins induces specific anti-parasite antibodies and damage to adult worms after a challenge infection. *Int J Parasitol,* 27**,** 843-53.

YOLE, D. S., PEMBERTON, R., REID, G. D. & WILSON, R. A. 1996. el. *Parasitology,* 112 37-46.

YOUNG, N. D., HALL, R. S., JEX, A. R., CANTACESSI, C. & GASSER, R. B. 2010. Elucidating the transcriptome of *Fasciola hepatica* - a key to fundamental and biotechnological discoveries for a neglected parasite. *Biotechnol Adv,* 28**,** 222-31.

YOUNG, N. D., JEX, A. R., LI, B., LIU, S., YANG, L., XIONG, Z., LI, Y., CANTACESSI, C., HALL, R. S., XU, X., CHEN, F., WU, X., ZERLOTINI, A., OLIVEIRA, G., HOFMANN, A., ZHANG, G., FANG, X., KANG, Y., CAMPBELL, B. E., LOUKAS, A., RANGANATHAN, S., ROLLINSON, D., RINALDI, G., BRINDLEY, P. J., YANG, H., WANG, J., WANG, J. & GASSER, R. B. 2012. Whole-genome sequence of *Schistosoma haematobium*. *Nat Genet,* 44**,** 221-5.

YUAN, C., FU, Y.-J., LI, J., YUE, Y.-F., CAI, L.-L., XIAO, W.-J., CHEN, J.-P. & YANG, L. 2010. *Schistosoma japonicum*: Efficient and rapid purification of the tetraspanin extracellular loop 2, a potential protective antigen against schistosomiasis in mammalian. *Exp Parasitol,* 126**,** 456-461.

ZAMANIAN, M., FRASER, L. M., AGBEDANU, P. N., HARISCHANDRA, H., MOORHEAD, A. R., DAY, T. A., BARTHOLOMAY, L. C. & KIMBER, M. J. 2015. Release of small RNA-containing exosome-like vesicles from the human filarial parasite *Brugia malayi*. *PLoS Negl Trop Dis,* 9**,** e0004069.

ZHANG, H., FREITAS, D., KIM, H. S., FABIJANIC, K., LI, Z., CHEN, H., MARK, M. T., MOLINA, H., MARTIN, A. B., BOJMAR, L., FANG, J., RAMPERSAUD, S., HOSHINO, A., MATEI, I., KENIFIC, C. M., NAKAJIMA, M., MUTVEI, A. P., SANSONE, P., BUEHRING, W., WANG, H., JIMENEZ, J. P., COHEN-GOULD, L., PAKNEJAD, N., BRENDEL, M., MANOVA-TODOROVA, K., MAGALHÃES, A., FERREIRA, J. A., OSÓRIO, H., SILVA, A. M., MASSEY, A., CUBILLOS-RUIZ, J. R., GALLETTI, G., GIANNAKAKOU, P., CUERVO, A. M., BLENIS, J., SCHWARTZ, R., BRADY, M. S., PEINADO, H., BROMBERG, J., MATSUI, H., REIS, C. A. & LYDEN, D. 2018a. Identification of distinct nanoparticles and subsets of extracellular vesicles by asymmetric flow field-flow fractionation. *Nat Cell Biol,* 20**,** 332-343.

ZHANG, J. D. & WIEMANN, S. 2009. KEGGgraph: a graph approach to KEGG PATHWAY in R and bioconductor. *Bioinformatics,* 25**,** 1470-1471.

ZHANG, S., CHU, W. C., LAI, R. C., LIM, S. K., HUI, J. H. & TOH, W. S. 2016. Exosomes derived from human embryonic mesenchymal stem cells promote osteochondral regeneration. *Osteoarthr Cartil,* 24**,** 2135-2140.

ZHANG, W., AHMAD, G., LE, L., ROJO, J. U., KARMAKAR, S., TILLERY, K. A., TORBEN, W., DAMIAN, R. T., WOLF, R. F., WHITE, G. L., CAREY, D. W., CARTER, D., REED, S. G. & SIDDIQUI, A. A. 2014. Longevity of Sm-p80-specific antibody responses following vaccination with Sm-p80 vaccine in mice and baboons and transplacental transfer of Sm-p80-specific antibodies in a baboon. *Parasitol Res,* 113**,** 2239-50.

ZHANG, W., AHMAD, G., MOLEHIN, A. J., TORBEN, W., LE, L., KIM, E., LAZARUS, S., SIDDIQUI, A. J., CARTER, D. & SIDDIQUI, A. A. 2018b. *Schistosoma mansoni* antigen Sm-p80: prophylactic efficacy using TLR4 agonist vaccine adjuvant glucopyranosyl lipid A-Alum in murine and non-human primate models. *J Invest Med,* 66**,** 1124-1132.

ZHANG, W., AHMAD, G., TORBEN, W., NOOR, Z., LE, L., DAMIAN, R. T., WOLF, R. F., WHITE, G. L., CHAVEZ-SUAREZ, M., PODESTA, R. B., KENNEDY, R. C. & SIDDIQUI, A. A. 2010. Sm-p80-based DNA vaccine provides baboons with levels of protection against *Schistosoma mansoni* infection comparable to those achieved by the irradiated cercarial vaccine. *J Infect Dis,* 201**,** 1105-12.

ZHANG, W., MOLEHIN, A. J., ROJO, J. U., SUDDUTH, J., GANAPATHY, P. K., KIM, E., SIDDIQUI, A. J., FREEBORN, J., SENNOUNE, S. R., MAY, J., LAZARUS, S., NGUYEN, C., REDMAN, W. K., AHMAD, G., TORBEN, W., KARMAKAR, S., LE, L., KOTTAPALLI, K. R., KOTTAPALLI, P., WOLF, R. F., PAPIN, J. F., CAREY, D., GRAY, S. A., BERGTHOLD, J. D., DAMIAN, R. T., MAYER, B. T., MARKS, F., REED, S. G., CARTER, D. & SIDDIQUI, A. A. 2018c. Sm-p80-based schistosomiasis vaccine: double-blind preclinical trial in baboons demonstrates comprehensive prophylactic and parasite transmission-blocking efficacy. *Ann N Y Acad Sci,* 1425**,** 38-51.

ZHAO, C., SUN, X. & LI, L. 2019. Biogenesis and function of extracellular miRNAs. *ExRNA,* 1**,** 38.

ZHOU, X., WANG, W., CUI, F., SHI, C., MA, Y., YU, Y., ZHAO, W. & ZHAO, J. 2019. Extracellular vesicles derived from *Echinococcus granulosus* hydatid cyst fluid from patients: isolation, characterization and evaluation of immunomodulatory functions on T cells. *Int J Parasitol,* 49**,** 1029-1037.

ZHOU, Y., ZHENG, H., CHEN, Y., ZHANG, L., WANG, K., GUO, J., HUANG, Z., ZHANG, B., HUANG, W., JIN, K., DOU, T., HASEGAWA, M., WANG, L., ZHANG, Y., ZHOU, J., TAO, L., CAO, Z., LI, Y., VINAR, T., BREJOVA, B., BROWN, D., LI, M., MILLER, D. J., BLAIR, D., ZHONG, Y., CHEN, Z., LIU, F., HU, W., WANG, Z.-Q., ZHANG, Q.-H., SONG, H.-D., CHEN, S., XU, X., XU, B., JU, C., HUANG,

Y., BRINDLEY, P. J., MCMANUS, D. P., FENG, Z., HAN, Z.-G., LU, G., REN, S., WANG, Y., GU, W., KANG, H., CHEN, J., CHEN, X., CHEN, S., WANG, L., YAN, J., WANG, B., LV, X., JIN, L., WANG, B., PU, S., ZHANG, X., ZHANG, W., HU, Q., ZHU, G., WANG, J., YU, J., WANG, J., YANG, H., NING, Z., BERIMAN, M., WEI, C.-L., RUAN, Y., ZHAO, G., WANG, S., SCHISTOSOMA JAPONICUM GENOME, S., SCHISTOSOMA JAPONICUM GENOME, S., FUNCTIONAL ANALYSIS, C., THE SCHISTOSOMA JAPONICUM GENOME, S. & FUNCTIONAL ANALYSIS, C. 2009. The *Schistosoma japonicum* genome reveals features of host-parasite interplay. *Nature,* 460**,** 345-351.

ZHU, L., LIU, J. & CHENG, G. 2014. Role of microRNAs in schistosomes and schistosomiasis. *Front. Cell. Infect. Microbiol.,* 4**,** 165.

ZHU, L., LIU, J., DAO, J., LU, K., LI, H., GU, H., LIU, J., FENG, X. & CHENG, G. 2016a. Molecular characterization of *S. japonicum* exosome-like vesicles reveals their regulatory roles in parasite-host interactions. *Sci Rep,* 6**,** 25885.

ZHU, S., WANG, S., LIN, Y., JIANG, P., CUI, X., WANG, X., ZHANG, Y. & PAN, W. 2016b. Release of extracellular vesicles containing small RNAs from the eggs of *Schistosoma japonicum*. *Parasit Vectors,* 9**,** 574.

ZHU, Y., REN, J., HARN, D. A., SI, J., YU, C., MING, X. & LIANG, Y. 2003. Protective immunity induced with 23 kDa membrane protein DNA vaccine of *Schistosoma japonicum* Chinese strain in infected C57BL/6 mice. *Southeast Asian J Trop Med Public Health,* 34**,** 697-701.

ZHUANG, X., XIANG, X., GRIZZLE, W., SUN, D., ZHANG, S., AXTELL, R. C., JU, S., MU, J., ZHANG, L., STEINMAN, L., MILLER, D. & ZHANG, H. G. 2011. Treatment of brain inflammatory diseases by delivering exosome encapsulated anti-inflammatory drugs from the nasal region to the brain. *Mol Ther,* 19**,** 1769-79.

ZOU, X., GU, D., ZHANG, G., ZHONG, L., CHENG, Z., LIU, G. & ZHU, Y. 2016. NK cell regulatory property is involved in the protective role of MSC-derived extracellular vesicles in renal ischemic reperfusion injury. *Hum Gene Ther,* 27**,** 926-935.

ZWANG, J. & OLLIARO, P. 2017. Efficacy and safety of praziquantel 40 mg/kg in preschool-aged and school-aged children: a meta-analysis. *Parasit Vectors,* 10**,** 47.

# Appendices

**Supplementary Table 2.1. Top 20 surface-exposed proteins released by trypsin treatment of *Schistosoma mansoni* exosome-like vesicles ranked by spectrum counting.**

| Protein name | Accession number | Spectrum counting | Molecular mass (kDa) | Sequence coverage (%) | SP | Matching peptide | TMD |
|---|---|---|---|---|---|---|---|
| histone H4-like | Smp_053300.1 | 1573.84 | 11.36 | 44.66 | N | 6 | N |
| Tegument antigen (I(H)A) | Smp_086480.1 | 1343.91 | 21.67 | 10.33 | N | 2 | N |
| fatty acid binding protein 7, brain | Smp_095360.1 | 1174.57 | 14.84 | 53.38 | N | 7 | N |
| tyrosine 3-monooxygenase/tryptophan 5-monooxygenase activation protein, beta polypeptide | Smp_009760.1 | 1162.99 | 28.35 | 21.43 | N | 4 | N |
| 13 kDa tegumental antigen Sm13 | Smp_195190.1 | 1100.78 | 11.92 | 38.46 | Y | 4 | N |
| Universal stress protein | Smp_043120.1 | 1090.30 | 17.96 | 15 | N | 2 | N |
| enolase | Smp_024110.1 | 1060.90 | 46.96 | 49.77 | N | 33 | N |
| putative dynein light chain | Smp_095520.1 | 926.14 | 10.39 | 30.34 | N | 2 | N |
| putative dynein light chain | Smp_201060.1 | 926.14 | 10.47 | 39.33 | N | 2 | N |
| triosephosphate isomerase 1a | Smp_003990.1 | 821.73 | 28.08 | 22.53 | N | 5 | N |
| Glutathione S-Transferase | Smp_306860.1 | 727.35 | 23.84 | 36.49 | N | 7 | N |
| proteasome (prosome macropain) subunit alpha type 4 | Smp_070930.1 | 681.44 | 27.76 | 19.43 | N | 4 | N |
| Thioredoxin peroxidase | Smp_158110.1 | 629.21 | 21.68 | 14.95 | N | 2 | N |
| arginase type II | Smp_059980.1 | 625.21 | 39.89 | 10.16 | N | 4 | N |
| putative troponin I | Smp_018250.1 | 599.90 | 27.08 | 12.66 | N | 2 | N |
| putative ferritin | Smp_047370.1 | 584.59 | 36.31 | 7.92 | N | 2 | N |
| nucleoside-diphosphate kinase | Smp_092750.1 | 576.41 | 16.06 | 18.18 | N | 2 | N |
| Aldolase | Smp_042160.1 | 559.56 | 39.62 | 44.08 | N | 16 | N |
| Uncharacterised | Smp_309480.1 | 538.74 | 21.05 | 12.43 | N | 2 | N |
| DM9 domain-containing protein | Smp_035560.1 | 528.38 | 17.55 | 21.79 | N | 2 | N |

SP= signal peptide; TMD= Transmembrane domain; Y= yes; N= no

**Supplementary Table 2.2. Top 20 intra-vesicular cargo proteins identified after lysis of *Schistosoma mansoni* exosome-like vesicles cargo ranked by spectrum counting.**

| Protein name | Accession number | Spectrum counting | Molecular mass (kDa) | Sequence coverage (%) | SP | Matching peptide | TMD |
|---|---|---|---|---|---|---|---|
| Saposin B domain-containing protein | Smp_194910.1 | 1332.30 | 21.02 | 14.44 | Y | 2 | N |
| tetraspanin 2 | Smp_335630.1 | 1158.90 | 23.82 | 19.18 | N | 5 | Y |
| putative tetraspanin-CD63 receptor | Smp_140000.1 | 995.55 | 30.59 | 8.27 | N | 3 | Y |
| tetraspanin, putative | Smp_041460.1 | 928.72 | 30.41 | 18.01 | N | 7 | Y |
| putative ferritin | Smp_047650.1 | 898.04 | 19.69 | 18.02 | N | 4 | N |
| DM9 domain-containing protein | Smp_035560.1 | 893.57 | 17.55 | 57.69 | N | 9 | N |
| apoferritin-2 | Smp_063530.2 | 830.72 | 21.90 | 31.05 | Y | 8 | N |
| Mastin precursor | Smp_340060.1 | 748.16 | 42.27 | 10.93 | N | 6 | N |
| Glutathione S-Transferase | Smp_306860.1 | 720.15 | 23.84 | 35.07 | N | 8 | N |
| putative ferritin | Smp_047680.1 | 691.89 | 19.88 | 20.35 | N | 2 | N |
| putative tetraspanin 18, isoform 1 | Smp_344440.1 | 638.26 | 33.07 | 13.22 | N | 4 | Y |
| histone H4-like | Smp_053300.1 | 622.49 | 11.36 | 17.48 | N | 2 | N |
| Uncharacterised | Smp_130100.1 | 607.17 | 14.76 | 15.63 | Y | 3 | N |
| putative ferritin | Smp_311640.1 | 602.57 | 20.92 | 38.12 | N | 7 | N |
| CD63 antigen | Smp_017430.1 | 566.26 | 23.62 | 16.51 | N | 5 | Y |
| Aldolase | Smp_042160.1 | 516.18 | 39.62 | 50.96 | N | 21 | N |
| putative sm29 | Smp_072190.1 | 411.01 | 21.18 | 9.95 | N | 2 | Y |
| Ferritin-1 heavy chain | Smp_087760.1 | 316.79 | 20.16 | 35.26 | N | 8 | N |
| Tegument antigen (I(H)A) | Smp_045200.1 | 296.55 | 22.56 | 13.16 | N | 3 | N |
| Multidrug resistance protein 1 | Smp_053900.1 | 225.89 | 60.90 | 10.88 | Y | 6 | Y |

SP= signal peptide; TMD= Transmembrane domain; Y= yes; N= no

**Supplementary Table 2.3. Top 20 integral membrane proteins identified from *Schistosoma mansoni* exosome-like vesicles ranked by spectrum counting.**

| Protein name | Accession number | Spectrum counting | Molecular mass (kDa) | Sequence coverage (%) | SP | Matching peptide | TMD |
|---|---|---|---|---|---|---|---|
| tetraspanin 2 | Smp_335630.1 | 1914.17 | 23.82 | 19.63 | N | 6 | Y |
| tetraspanin, putative | Smp_041460.1 | 862.76 | 30.41 | 18.01 | N | 9 | Y |
| Saposin B domain-containing protein | Smp_194910.1 | 769.99 | 21.02 | 14.44 | Y | 2 | N |
| putative Cys-rich domain protein | Smp_101970.1 | 736.19 | 13.36 | 29.82 | N | 3 | N |
| putative tetraspanin-CD63 receptor | Smp_140000.1 | 733.85 | 30.59 | 24.46 | N | 7 | Y |
| DM9 domain-containing protein | Smp_035560.1 | 686.95 | 17.55 | 68.59 | N | 16 | N |
| putative tetraspanin 18, isoform 1 | Smp_344440.1 | 632.97 | 33.07 | 22.37 | N | 11 | Y |
| 13 kDa tegumental antigen Sm13 | Smp_331280.1 | 631.93 | 12.70 | 8.04 | Y | 2 | Y |
| histone H4-like | Smp_053300.1 | 538.65 | 11.36 | 38.83 | N | 5 | N |
| transporter, major intrinsic protein family protein | Smp_128110.1 | 497.53 | 31.43 | 6.97 | N | 2 | Y |
| Tegument antigen (I(H)A) | Smp_045200.1 | 475.25 | 22.56 | 34.21 | N | 9 | N |
| ATPase, H+ transporting, lysosomal accessory protein 1 | Smp_267000.1 | 467.47 | 26.31 | 25.91 | Y | 7 | Y |
| putative sm29 | Smp_072190.1 | 439.49 | 21.18 | 25.65 | N | 5 | Y |

| | | | | | | | |
|---|---|---|---|---|---|---|---|
| 13 kDa tegumental antigen Sm13 | Smp_195190.1 | 431.89 | 11.92 | 23.08 | Y | 4 | N |
| vesicle-associated membrane protein 7-like | Smp_055870.1 | 391.27 | 25.37 | 39.91 | N | 11 | Y |
| putative ferritin | Smp_047650.1 | 386.49 | 19.69 | 25.58 | N | 4 | N |
| CD63 antigen | Smp_017430.1 | 368.26 | 23.62 | 25.23 | N | 9 | Y |
| High affinity copper uptake protein 1 | Smp_048230.1 | 364.19 | 22.50 | 11 | N | 2 | Y |
| tetraspanin, putative | Smp_155310.1 | 343.25 | 30.58 | 17.75 | N | 6 | Y |
| Protein lifeguard 3 | Smp_150500.1 | 340.42 | 31.82 | 4.23 | N | 2 | Y |

SP= signal peptide; TMD= Transmembrane domain; Y= yes; N= no

**Supplementary Table 2.4. Top 20 peripheral membrane proteins identified from *Schistosoma mansoni* exosome-like vesicles ranked by spectrum counting.**

| Protein name | Accession number | Spectrum counting | Molecular mass (kDa) | Sequence coverage (%) | SP | Matching peptide | TMD |
|---|---|---|---|---|---|---|---|
| tetraspanin 2 | Smp_335630.1 | 2790.79 | 23.82 | 19.63 | N | 6 | Y |
| tetraspanin, putative | Smp_041460.1 | 1722.45 | 30.41 | 22.79 | N | 7 | Y |
| DM9 domain-containing protein | Smp_035560.1 | 1566.87 | 17.55 | 68.59 | N | 12 | N |
| Saposin B domain-containing protein | Smp_194910.1 | 1455.63 | 21.02 | 14.44 | Y | 2 | N |
| putative ferritin | Smp_311630.1 | 1328.37 | 20.92 | 24.86 | N | 4 | N |
| 13 kDa tegumental antigen Sm13 | Smp_195190.1 | 996.94 | 11.92 | 23.08 | Y | 3 | N |
| putative tetraspanin-CD63 receptor | Smp_140000.1 | 908.58 | 30.59 | 12.95 | N | 4 | Y |
| putative tetraspanin 18, isoform 1 | Smp_344440.1 | 835.09 | 33.07 | 16.61 | N | 6 | Y |
| cathepsin B-like peptidase (C01 family) | Smp_103610.1 | 782.45 | 38.54 | 6.47 | Y | 2 | N |
| CD63 antigen | Smp_017430.1 | 751.37 | 23.62 | 16.51 | N | 5 | Y |
| Mastin precursor | Smp_340060.1 | 725.16 | 42.27 | 11.2 | N | 8 | N |
| putative ferritin | Smp_047650.1 | 717.13 | 19.69 | 18.02 | N | 3 | N |
| histone H4-like | Smp_053300.1 | 676.87 | 11.36 | 38.83 | N | 4 | N |
| apoferritin-2 | Smp_063530.1 | 591.18 | 22.78 | 10.15 | Y | 2 | N |
| Bis(5'-adenosyl)-triphosphatase enpp4 | Smp_104270.1 | 537.55 | 63.29 | 25.96 | N | 19 | Y |
| Cathepsin L-like proteinase precursor | Smp_187140.1 | 529.60 | 40.17 | 13.16 | Y | 5 | N |
| vesicle-associated membrane protein 7-like | Smp_055870.1 | 516.21 | 25.37 | 7.17 | N | 2 | Y |
| protein kiaa0174, putative | Smp_057650.1 | 487.53 | 37.61 | 5.93 | N | 2 | N |
| Dynein light chain 2, cytoplasmic | Smp_201030.1 | 461.97 | 10.22 | 39.33 | N | 3 | N |
| putative Cys-rich domain protein | Smp_101970.1 | 414.20 | 13.36 | 29.82 | N | 3 | N |

SP= signal peptide; TMD= Transmembrane domain; Y= yes; N= no

**Supplementary Table 2.5. Top 20 surface-exposed proteins released by trypsin treatment of *Schistosoma mansoni* microvesicles ranked by spectrum counting.**

| Protein name | Accession number | Spectrum counting | Molecular mass (kDa) | Sequence coverage (%) | SP | Matching peptide | TMD |
|---|---|---|---|---|---|---|---|
| Fatty acid binding protein 7, brain | Smp_095360.1 | 516.29 | 14.84 | 73.68 | N | 2 | N |
| Family C13 non-peptidase homologue | Smp_303330.1 | 477.02 | 16.29 | 9.35 | N | 7 | N |
| Hypothetical protein | Smp_096790.1 | 456.14 | 8.91 | 27.85 | Y | 2 | N |
| Putative universal stress protein | Smp_200240.1 | 450.44 | 19.44 | 8.05 | N | 5 | N |
| 13kDa tegumental antigen Sm 13 | Smp_195190.1 | 444.90 | 11.92 | 46.15 | Y | 4 | N |
| Putative dynein light chain | Smp_095520.1 | 443.76 | 10.39 | 43.82 | N | 2 | N |
| Phosphatase 2A inhibitor I2PP2A | Smp_155060.1 | 415.56 | 29.27 | 26.77 | N | 3 | N |
| Thioredoxin peroxidase 2 | Smp_309480.1 | 399.45 | 21.05 | 30.81 | N | 8 | N |
| Troponin T | Smp_179810.1 | 377.30 | 38.46 | 46.15 | N | 4 | N |
| Actin | Smp_307010.1 | 367.55 | 41.71 | 64.63 | N | 8 | N |
| Tegument antigen (I(H)A) | Smp_086480.1 | 359.94 | 21.67 | 44.02 | N | 2 | N |
| Glutathione S-Transferase | Smp_306860.1 | 308.36 | 23.84 | 46.45 | N | 7 | N |
| Histone H2A | Smp_089870.1 | 299.81 | 13.42 | 36.8 | N | 2 | N |
| Receptor expression-enhancing protein 5 | Smp_099890.1 | 297.81 | 21.42 | 23.28 | N | 2 | Y |
| dynein light chain | Smp_202130.1 | 291.52 | 10.29 | 26.97 | N | 5 | N |
| dynein light chain | Smp_320340.1 | 282.02 | 10.76 | 22.83 | N | 11 | N |
| dynein light chain LC6, flagellar outer arm-like | Smp_174510.1 | 274.56 | 11.88 | 11.54 | N | 4 | N |
| Thioredoxin peroxidase | Smp_158110.1 | 269.73 | 21.68 | 29.9 | N | 3 | N |
| Phosphoglyserate mutase | Smp_096760.1 | 268.61 | 28.41 | 29.6 | N | 2 | N |
| Phosphoglycerate kinase 1 | Smp_214060.1 | 264.43 | 44.48 | 55.53 | N | 5 | N |

SP= signal peptide; TMD= Transmembrane domain; Y= yes; N= no

**Supplementary Table 2.6. Top 20 intra-vesicular cargo proteins identified after lysis of *Schistosoma mansoni* microvesicles cargo ranked by spectrum counting.**

| Protein name | Accession number | Spectrum counting | Molecular mass (kDa) | Sequence coverage (%) | SP | Matching peptide | TMD |
|---|---|---|---|---|---|---|---|
| 23 Kda integral membrane protein | Smp_335630.1 | 2135.62 | 23.82 | 19.63 | N | 6 | Y |
| Tegument antigen | Smp_045200.1 | 1366.22 | 22.56 | 34.21 | N | 9 | N |
| Uncharacterised | Smp_194910.1 | 1175.67 | 21.02 | 19.44 | Y | 3 | N |
| Dynein light chain 2, cytoplasmic | Smp_201030.1 | 1061.04 | 10.22 | 55.06 | N | 10 | N |
| Tegument antigen | Smp_086530.1 | 919.71 | 20.75 | 48.62 | N | 11 | N |
| Histone H4 | Smp_053300.1 | 881.97 | 11.36 | 50.49 | N | 5 | N |
| 13 kDa tegumental antigen Sm-13 | Smp_195190.1 | 852.19 | 11.92 | 23.08 | Y | 3 | N |
| Uncharacterised | Smp_072190.1 | 789.29 | 21.18 | 25.65 | N | 5 | Y |
| Chymotrypsin-like elastase family member 2A | Smp_340060.1 | 577.62 | 42.27 | 28.8 | N | 13 | N |
| Uncharacterised | Smp_130100.1 | 574.94 | 14.76 | 22.66 | Y | 4 | N |
| Ferritin-2 heavy chain | Smp_047680.1 | 562.20 | 19.88 | 50.58 | N | 8 | N |
| Cornifelin | Smp_101970.1 | 511.46 | 13.36 | 29.82 | N | 4 | N |
| Uncharacterised | Smp_331280.1 | 491.16 | 12.70 | 8.04 | Y | 2 | Y |
| Tetraspanin-6 | Smp_140000.1 | 401.54 | 30.59 | 15.83 | N | 5 | Y |
| Receptor expression-enhancing prtein 5 | Smp_099890.1 | 392.39 | 21.42 | 13.76 | N | 2 | Y |
| 23 kDa integral membrane protein | Smp_017430.1 | 372.38 | 23.62 | 21.56 | N | 4 | Y |
| Annexin A8-like protein 1 | Smp_074140.1 | 352.10 | 39.93 | 29.1 | N | 11 | N |
| Aquaporin-3 | Smp_005720.1 | 341.35 | 33.88 | 7.89 | N | 2 | Y |
| Peroxiredoxin 2 | Smp_309480.1 | 338.25 | 21.05 | 37.3 | N | 7 | N |
| Uncharacterised | Smp_035560.1 | 322.18 | 17.55 | 48.72 | N | 7 | N |

SP= signal peptide; TMD= Transmembrane domain; Y= yes; N= no

**Supplementary Table 2.7. Top 20 integral membrane proteins identified from *Schistosoma mansoni* microvesicles ranked by spectrum counting.**

| Protein name | Accession number | Spectrum counting | Molecular mass (kDa) | Sequence coverage (%) | SP | Matching peptide | TMD |
|---|---|---|---|---|---|---|---|
| Tetraspanin 2 | Smp_335630.1 | 1716.55 | 23.82 | 19.63 | N | 7 | Y |
| Saponin B domain-containing protein | Smp_194910.1 | 561.57 | 21.02 | 19.44 | Y | 3 | N |
| Tegument antigen (I(H)A) | Smp_045200.1 | 495.00 | 22.56 | 54.21 | N | 18 | N |
| Putative Cys-rich domain protein | Smp_101970.1 | 466.64 | 13.36 | 29.82 | N | 4 | N |
| Lipopolysaccharide-induced tumor necrosis factor-alpha factor like protein | Smp_203810.1 | 450.36 | 15.06 | 18.38 | N | 2 | Y |
| Histone H-4 like | Smp_053300.1 | 435.88 | 11.36 | 51.46 | N | 7 | N |
| Putative Sm-29 | Smp_072190.1 | 419.00 | 21.18 | 25.65 | N | 5 | Y |
| 13 kDa tegumental antigen Sm-13 | Smp_331280.1 | 410.98 | 12.70 | 8.04 | Y | 2 | Y |
| DM9 domain-containing protein | Smp_035560.1 | 378.99 | 17.55 | 68.59 | N | 18 | N |
| SJCHGC00347 | Smp_181070.1 | 358.90 | 12.99 | 31.58 | Y | 4 | N |
| Putative tetraspanin-CD63 receptor | Smp_140000.1 | 335.27 | 30.59 | 24.46 | N | 8 | Y |
| Cathepsin B-like peptidase (C01 family) | Smp_103610.1 | 323.47 | 38.54 | 30.29 | Y | 18 | N |
| ATPase, H+ transporting, lysosomal acessory protein 1 | Smp_267000.1 | 308.70 | 26.31 | 25.51 | Y | 7 | Y |
| Dynein light chain LC6, flagellar outer arm-like | Smp_174510.1 | 292.07 | 11.88 | 29.81 | N | 3 | N |
| Immunoglobulin like domain-containing protein | Smp_031880.1 | 281.34 | 32.48 | 36.43 | Y | 9 | Y |
| Dynein light chain 2, cytoplasmic | Smp_201030.1 | 258.53 | 10.22 | 55.06 | N | 8 | N |
| Hypoxanthine guanine phosphoribosyltransferase | Smp_103560.1 | 258.47 | 26.04 | 32.03 | N | 7 | N |
| Putative reticulon/nogo | Smp_020370.1 | 256.56 | 23.29 | 29.06 | N | 7 | Y |

| | | | | | | | |
|---|---|---|---|---|---|---|---|
| Putative dynein light chain | Smp_201060.1 | 254.87 | 10.47 | 60.67 | N | 15 | N |
| Phosphoglycerate mutase | Smp_096760.1 | 242.45 | 28.41 | 47.6 | N | 13 | N |

SP= signal peptide; TMD= Transmembrane domain; Y= yes; N= no

**Supplementary Table 2.8. Top 20 peripheral membrane proteins identified from *Schistosoma mansoni* microvesicles ranked by spectrum counting.**

| Protein name | Accession number | Spectrum counting | Molecular mass (kDa) | Sequence coverage (%) | SP | Matching peptide | TMD |
|---|---|---|---|---|---|---|---|
| tetraspanin 2 | Smp_335630.1 | 1461.03 | 23.82 | 19.63 | N | 6 | Y |
| Saponin B domain-containing protein | Smp_194910.1 | 968.10 | 21.02 | 14.44 | Y | 2 | N |
| Dynein light chain 2, cytoplasmic | Smp_201030.1 | 788.71 | 10.22 | 55.06 | N | 7 | N |
| Histone H4 | Smp_305460.1 | 753.73 | 10.86 | 20.65 | Y | 3 | N |
| Hypothetical protein | Smp_096790.2 | 515.16 | 7.15 | 32.26 | Y | 3 | N |
| Saponin containing protein | Smp_130100.1 | 492.50 | 14.76 | 9.38 | Y | 2 | N |
| 13 kDa tegumental antigen Sm13 | Smp_195190.1 | 414.20 | 11.92 | 23.08 | Y | 3 | N |
| Cathepsin L-like proteinase precursor | Smp_187140.1 | 403.57 | 40.17 | 13.16 | Y | 5 | N |
| Flagellar outer dynein arm light chain 8 | Smp_200190.1 | 391.55 | 10.32 | 49.44 | N | 5 | N |
| Mastin precursor | Smp_340060.1 | 379.13 | 42.27 | 42.4 | N | 22 | N |
| Fatty acid binding protein 7, brain | Smp_095360.1 | 356.28 | 14.84 | 35.34 | N | 5 | N |
| 13 kDa tegumental antigen Sm13 | Smp_331280.1 | 326.07 | 12.70 | 7.14 | Y | 1 | Y |
| Putative dynein light chain | Smp_201060.1 | 318.74 | 10.47 | 42.7 | N | 2 | N |
| Hypothetical protein | Smp_096790.1 | 305.89 | 8.91 | 26.58 | Y | 4 | N |
| Actin | Smp_307010.1 | 290.22 | 41.71 | 44.68 | N | 26 | N |
| Tegument antigen | Smp_169200.1 | 280.17 | 21.13 | 7.22 | N | 1 | N |
| Putative Cys-rich domain protein | Smp_101970.1 | 269.07 | 13.36 | 17.54 | N | 2 | N |
| Cytosolic purine 5'-nucleotidase | Smp_147840.1 | 263.23 | 63.02 | 13 | N | 7 | N |
| Putative tetraspapnin-CD63 receptor | Smp_140000.1 | 251.81 | 30.59 | 8.27 | N | 3 | Y |
| Thioredoxin peroxidase | Smp_158110.1 | 227.89 | 21.68 | 25.77 | N | 6 | N |

SP= signal peptide; TMD= Transmembrane domain; Y= yes; N= no